The Role of TNF-α Converting enzyme (TACE: ADAM17) in L-selectin Shedding and Lymphocyte Migration

Emma-Kate Yates

PhD thesis submitted to the

University of London

July 2004

Division of Cellular Immunology

MRC National Institute for Medical Research

Mill Hill,

London

ProQuest LLC
789 East Eisenhower Parkway
P.O. Box 1346
Ann Arbor, MI 48106-1346

Abstract

The leucocyte adhesion molecule L-selectin mediates the tethering and rolling of lymphocytes in high endothelial venules (HEV), which precedes migration across the vessel wall into the lymph node. L-selectin is cleaved by proteolysis in the membrane proximal region, but the physiological role of this shedding is unclear. Studies using hydroxamate-based metalloproteinase inhibitors have implicated metalloproteinase(s) in L-selectin shedding and lymphoid cells lacking in the metalloproteinase TACE (ADAM 17) fail to shed L-selectin, suggesting that it is directly or indirectly involved in cleavage.

Knockout mice in which the catalytic domain of TACE has been targeted (*tace*$^{\Delta Zn/\Delta Zn}$) die *in utero*. To study the role of TACE in leucocytes, irradiated mice were used as hosts for reconstitution with *tace*$^{\Delta Zn/\Delta Zn}$ or wild type (WT) foetal liver stem cells. Phenotypic analysis of the reconstituted chimeric mice determined that there was no significant effect of the TACE mutation on the proportions of cell subsets in the lymph nodes or thymus. The *tace*$^{\Delta Zn/\Delta Zn}$ chimeric spleen was found to be significantly larger than that of mice reconstituted with WT cells and, on further analysis, was shown to have a higher proportion of large granular cells (36% of total cells) in comparison to WT (19%). A higher proportion of large granular cells was also seen in *tace*$^{\Delta Zn/\Delta Zn}$ chimeric bone marrow (70% vs. 59%). Increased L-selectin expression was seen on *tace*$^{\Delta Zn/\Delta Zn}$ B lymphocytes and non-neutrophil myeloid cells in the bone marrow, and on *tace*$^{\Delta Zn/\Delta Zn}$ on neutrophils in the spleen. PMA stimulation of blood lymphocytes and splenocytes confirmed that *tace*$^{\Delta Zn/\Delta Zn}$ T and B lymphocytes are unable to shed L-selectin. However, *tace*$^{\Delta Zn/\Delta Zn}$ peripheral lymph node T lymphocytes undergo constitutive basal shedding *in vitro* suggesting a TACE independent shedding pathway in these cells. TACE independent shedding was confirmed by the presence of wild type levels of soluble L-selectin in the sera of L-selectin$^{-/-}$ mice reconstituted with *tace*$^{\Delta Zn/\Delta Zn}$ foetal liver cells. *tace*$^{\Delta Zn/\Delta Zn}$ cells migrated normally through a cultured high endothelial cell (HEC) monolayer and down-regulated L-selectin upon adhesion to HEC. There was no effect of the TACE mutation on lymphocyte trafficking into peripheral lymph nodes *in vivo*. We conclude that TACE is not the only enzyme

responsible for L-selectin cleavage in T lymphocytes and, that TACE does not regulate lymphocyte interactions with HEC during migration into peripheral lymph nodes.

Acknowledgements

Firstly, thanks to Ann Ager for being a wonderful supervisor, advisor and therapist who made sure that when things went wrong it wasn't the end of the world! In addition, thanks to the rest of the lab, Christelle Faveeuw, Elena Galkina, Alex Ivetic, Stephen Jolles, Lisa Micallef, Rhian Phillips, Graham Preece, Kelly Rember, Kiki Tanousis for all their help, moral support and for being the best group of people you could wish to work with. Particular thanks to Christelle and Graham for teaching me all the techniques, Rhian for help with sequencing, Lena for helping with trafficking experiments and LAM-1.16 ELISAs, Alex for molecular biology help and to Lisa who not only helped when ever she could (particularly with cell culture, LEC-Ig transfection and soluble L-selectin experiments) but has also become a wonderful friend. On a lighter note, thanks to Alex and Stephen for being the funniest people in the world!

Thanks to the BBSRC and Roche who joint funded this project. Particular thanks to John Nixon and Peter Kilby for their support during this study.

Thanks to Victor Tybulewicz and Edina Schweighoffer who taught me how to make irradiation chimeras and were always around to give me any advice I needed.

My thanks go to all the animal staff who have truly been the backbone of this project. There are too many to name individually but thanks to all those who work in Dunkin Blue, Laidlaw blue, Building C, and Laidlaw Red. Particular mention for Marie Caulfield who has always been ready to help with everything (in three different animal houses since I began!) and Hannah Boyes without whom none of the timed matings, and $RAG^{-/-}$ chimeric mice would have ever happened.

Thank you to Dina Patel for her help with sequencing and Kate Sullivan and Stamatis Pagakis for their help with the fluorescent microscopy.

A big thank you must also go to Chris Atkinson, who must have helped with hundreds of FACS runs over the last three years.

Thanks also to Frank Johnson, Joe Brock and Lesley Mc Neill for their help in producing slides and posters for presentations and the diagrams for this thesis whilst never complaining about the number of changes I wanted.

A huge thank you to Mum, Dad, Claire and Louise. To Mum whose support and belief in all her children is so strong it is able to completely carry you through the times when belief in yourself wavers. Also, Claire and Louise for being the best sisters in the world.
Finally, thanks to David, Phoebe and Cassie. Thanks David for managing to live with me during all the madness of the last few months, for pretending you are interested in the ins and outs of L-selectin cleavage, for making me laugh and convincing me it was a good idea to breed a litter of puppies whilst trying to write up! To Phoebe and Cassie (and her brother and sisters), thank you for all your help with the paw print design for the rough drafts of this thesis!

Table of Contents

Table of Figures

List of Tables

Abbreviations

A	Adenine
ADAMs	A Disintegrin and Metalloproteinase
Ag	Antigen
APC	Antigen Presenting Cell
BM	Bone Marrow
bp	base pairs
C	Cytosine
°C	degrees centigrade
CD	Cluster of Differentiation
CFA	Complete Freunds Adjuvant
DC	Dendritic Cells
DNA	Deoxyribonucleic Acid
EGF	Epidermal Growth Factor
FCS	Foetal Calf Serum
FACS	Fluorescence Activated Cell Sorter
G	Guanine
g	G-force/ relative centrifugal force (RCF)
HEV	High Endothelial Venules
HEC	High Endothelial Cells
h	hours
ICAM	Intercellular Adhesion Molecule
Ig	Immunoglobulin
IFA	Incomplete Freunds Adjuvant
KLH	Keyhole Limpet Haemocyanin
l	litre
LFA-1	Lymphocyte Function Associated Antigen-1
LN	Lymph Node

μ	micro
m	milli
M	Molar
mAbs	Monoclonal Antibodies
MAdCAM	Mucosal Addressin Cell Adhesion Molecule
min	minute
MMP	Matrix Metalloproteinase
NMS	Normal Mouse Serum
PBL	Peripheral Blood Lymphocytes
PLN	Peripheral Lymph Nodes
PBS	Phosphate Buffered Saline
PBS-CMF	Calcium and Magnesium Free Phosphate Buffered Saline
%	percent
PMA	Phorbol 12-Myristate Acetate
PNAd	Peripheral Node Addressin
rpm	revolutions per minute
SD	Standard Deviation
T	Thymine
TACE	TNF-α Converting Enzyme
TCR	T Cell Receptor
TGFα	Transforming Growth Factor-α
TIMP	Tissue Inhibitor of Metalloproteinase
TNF-α	Tumour Necrosis Factor-α
WT	Wild Type
Zn	Zinc

Chapter 1: Introduction

1.1: Lymphoid Organs

Development of both the innate and adaptive immune system takes place in the bone marrow and thymus, which are termed primary lymphoid organs. To mount an effective immune response to an invading pathogen, naïve lymphocytes expressing receptors for the pathogen must proliferate and be activated into effector cells. This activation and proliferation takes place in secondary lymphoid organs, such as peripheral lymph nodes, spleen and mucosal lymphoid tissues (Westermann et al., 1989), where cells of the immune system and antigen meet (figure 1.1). The spleen collects antigen from the blood, the mucosal lymphoid tissues, such as Peyer's patches, collect antigen from the epithelial surfaces of the body (e.g. gastrointestinal tract and the respiratory system), and the peripheral lymph nodes drain lymph containing antigen-presenting cells (APC) carrying antigen from infected tissues and cutaneous epithelial surfaces (Haig et al., 1999).

The antigen presenting cells are dendritic cells, macrophages and B cells. Unlike dendritic cells, resting macrophages and B cells do not express the co-stimulatory molecules needed to activate naive T cells. All antigen presenting cells internalize antigen and process it into peptide fragments that are expressed on the cell surface by MHC molecules. Resting macrophages have few or no MHC class II molecules on their surface and do not express co-stimulatory molecules. Macrophages recognize microbial constituents using lipopolysaccaride and peptidoglycan recognizing toll-like receptors and the mannose receptor. Upon binding, the pathogen is engulfed and degraded. This process induces expression of the required co-stimulatory molecules and MHC class II on the surface of the macrophage for T cell activation. It is important that macrophages cannot activate T cells in the absence of the microbe (many foreign proteins do not induce an immune response unless bacterium is present), as macrophages process large quantities of self-peptides, and could therefore elicit an autoimmune response. The majority of antigens will only stimulate B cells if they have the assistance of primed $CD4^+$ T cells. The B cells will process the antigen and present antigenic peptide on its surface in association with MHC class II molecules. The primed T cell recognizes this complex and stimulates the B cells with

subsequent activation, proliferation and maturation. Like macrophages, B cells can be induced by microbial constituents to express co-stimulatory molecules. Immature dendritic cells outside the lymph node (tissue dendritic cells), such as Langerhans cells, only express the co-stimulatory molecules needed for naïve T cell activation upon migration and differentiation in the lymph node (Knight and Stagg, 1993). Dendritic cells expressing processed antigen on their cell surface enter the lymph node via the afferent lymphatics (Steinman, 1991). Lymphocytes enter lymph nodes directly from the blood stream via specialized blood vessels (Gowans and Knight, 1964). As they migrate through the lymph node, naïve T cells bind via adhesion molecules to each dendritic cell that they encounter. This binding enables the T cell to sample the MHC molecules for the presence of its specific peptide. If the T cell recognizes the peptide it will form a stronger stabilizing bond between itself and the APC and will be retained within the lymph node for up to four days. Lymphocytes not recognizing the peptide leave the lymph node via the efferent lymphatics and eventually return to the blood (Bode et al., 1999), (Haig et al., 1999) and continue to recirculate through secondary lymphoid organs until encountering their cognate antigen. Naïve B cells pick up peptides from the same antigen within the lymph node and migrate through the T cell zones. They encounter previously activated CD4 positive T cells and are themselves activated. The majority of activated B cells migrate along with the T cells that activated them into primary follicles within the lymph node and form germinal centres (MacLennan, 1994). The germinal centre is a site of intense proliferation of the specific B lymphocytes and differentiation into antibody-secreting plasma cells and memory B cells (Liu et al., 1997) (MacLennan, 1994). T cells remain in distinct T cell areas within the lymph node (Gutman and Weissman, 1972), Butcher and Picker, 1996) where they proliferate and differentiate into effector cells (Westermann et. al., 1989).

Figure 1.1: Distribution of primary and secondary lymphoid organs. Differentiated T lymphocytes and B lymphocytes leave the thymus and bone marrow respectively, and migrate through the blood stream to the secondary lymphoid organs. Within the secondary lymphoid organs lymphocytes may come in contact with their specific antigen leading to activation and proliferation.

Major Lymphoid Organs and Tissues

primary lymphoid organs	secondary lymphoid organs

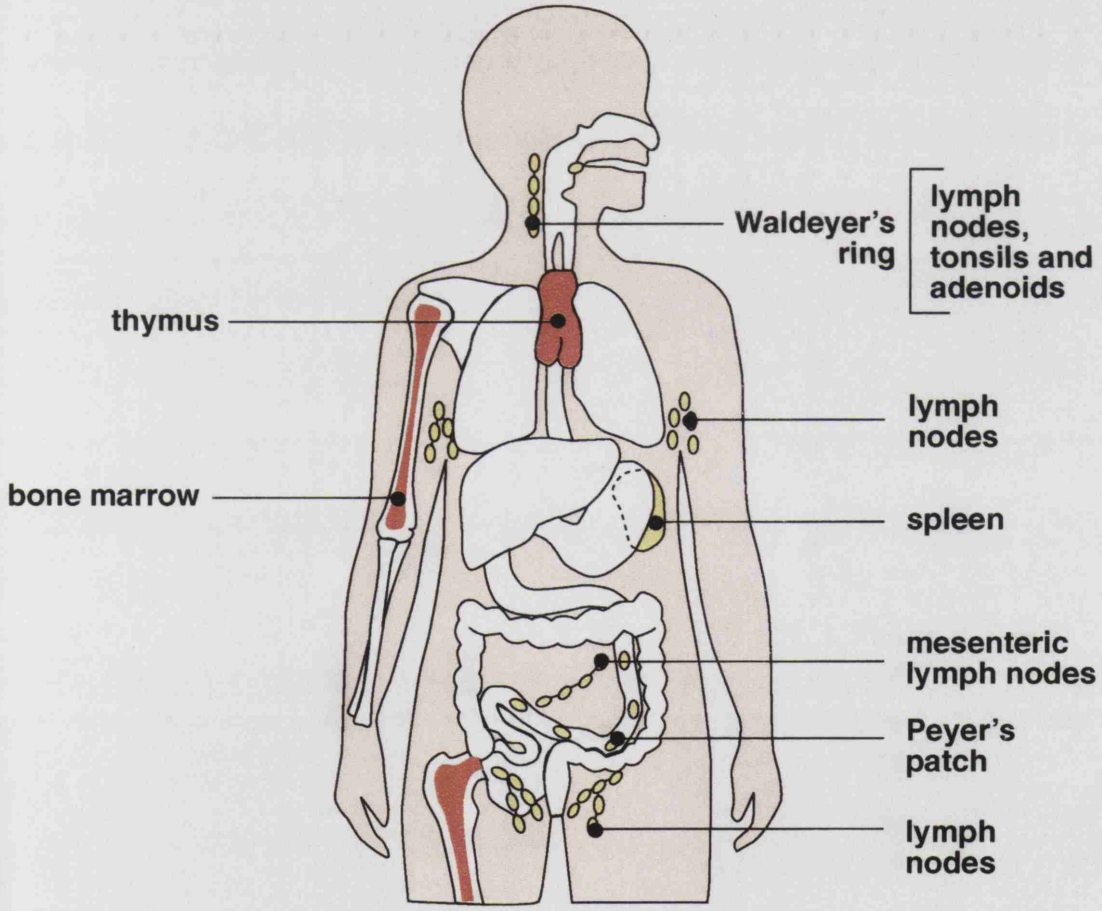

1.2: Migration into Peripheral Lymph Nodes

Lymph nodes have specialized blood vessels termed high endothelial Venules (HEV). The endothelial cells of HEVs have a cuboidal appearance and express ligands for adhesion molecules on the surface of lymphocytes (Girard and Springer, 1995). Stamper and Woodruff (1976) showed that lymphocytes adhere specifically to HEV but not to other vascular structures within the lymph node (Stamper and Woodruff, 1976). Further work (Butcher et al., 1980) suggested that defined populations of lymphocytes recirculate to peripheral tissues or mucosal lymph nodes with lymphocytes that are activated in Peyer's patches selectively migrating to the mucosal tissues and mesenteric lymph nodes of the gut. It was suggested that this preferential migration of cells to particular lymphoid organs was due to organ-specific determinants on the high endothelial cells (HEC) (Kraal et al., 1983), and the demonstration that MAdCAM-1 is essential for lymphocyte homing to mucosal lymphoid tissues (Wagner et al., 1996) supports this hypothesis. L-selectin (CD62L) was identified as a peripheral lymph node homing receptor (Gallatin et al., 1983). Preferential homing is also dependent on the stage of differentiation of the lymphocyte, with memory cells expressing different migration patterns to effector lymphocytes (Bradley et al., 1999). Memory and effector cells can access and recirculate through non-lymphoid organs such as inflamed skin and joints, as well as lymphoid organs (Butcher and Picker, 1996). This tissue-specific homing enables the primed cells to recirculate through the organs in which they are most likely to encounter or reencounter their specific antigen (Butcher and Picker, 1996). Recent work suggests two subsets of T memory cells; one expressing molecules necessary for migration into inflamed tissues to provide an immediate secondary response (effector memory cells), whilst central memory cells recirculate to lymph nodes during infection and stimulate dendritic cells, then finally differentiate into effector cells themselves (Sallusto et al., 1999). Binding of lymphocytes to the endothelial surface is mediated by a sequence of interactions between adhesion molecules on the surface of the lymphocyte and their ligands on the HEC. This sequence of adhesion steps is termed the multistep adhesion cascade (figure 1.2).

Figure 1.2: The Multistep Adhesion Cascade. Interaction of lymphocyte adhesion molecules with their ligands on the surface of HEC in peripheral lymph nodes leads to arrest of the lymphocyte on the HEV wall (modified from Ager, 1997). The stable interactions formed during lymphocyte arrest are mediated by integrin interactions that are stimulated by chemokines. Diapedesis is driven by a chemoattractant gradient.

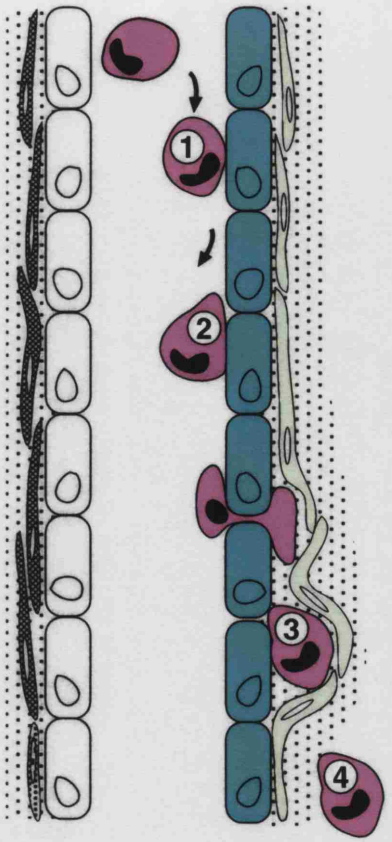

			Lymphocyte	High Endothelial Cells
①	**Rolling**	1 - 3 secs	L-selectin	Peripheral vascular addressin
②	**Stable adhesion**		$\alpha_4\beta_1$ LFA-1 CCR7	VCAM-1, ICAM-1/2 SLC
③	**Transendothelial Migration**	3 min	Metalloproteinase Activity	
④	**Completion of diapedesis**	5 - 10 min	?	Chemoattractants from lymph node stroma

Chemoattractant Gradient

As the lymphocyte enters HEV it is travelling with blood flow. For extravasation into the lymph node, lymphocytes have to adhere to the blood vessel wall, whilst being forced along by the flowing blood. The initial stage of the cascade in peripheral lymph nodes involves a low affinity reversible bond between L-selectin (CD62L) (Gallatin et al., 1983) (and $\alpha 4\beta 7$ integrin in Peyers patches) on the microvilli of the lymphocyte and its ligands (peripheral node addressins) on the high endothelial cells (HEC). This weak interaction acts as an initial brake slowing the cell down against shear force exerted by blood flow and leading to rolling of the lymphocyte along the blood vessel wall.

1.3: L-selectin (CD62L)

The selectin family of adhesion molecules was first identified in 1989. It consists of three structurally similar molecules; P-selectin, also known as CD62P, E-selectin, also known as CD62E, and L-selectin, also known as CD62L. The selectins consist of a C-type lectin domain, an EGF domain, a number of short consensus repeats (SCR) (L-selectin having two SCR and P and E-selectin between 4 and 9), a membrane proximal region, and a transmembrane region (see figure 1.3). The lectin domains are highly conserved between species. The calcium dependent function of the selectins is restricted to the initial weak interaction between leucocytes and endothelium, leading to tethering and rolling of the leucocyte along the blood vessel wall. The role of selectins as the mediators of rolling is probably due to the fast on and off rates of their ligand interactions (Rosen and Bertozzi, 1994). Cloning of the selectins and the discovery of their functioning through a lectin region confirmed reports that carbohydrate recognition plays a role in lymphocyte recirculation (Stoolman and Rosen, 1983). L-selectin is mainly involved in homing to the lymph nodes, whereas P and E-selectin are involved in the recruitment of leucocytes to sites of inflammation.

Figure 1.3: The selectin family of adhesion molecules. Each selectin has a lectin domain, EGF domain, a series of protein repeats, transmembrane domain and a cytoplasmic tail (McEver, 1994).

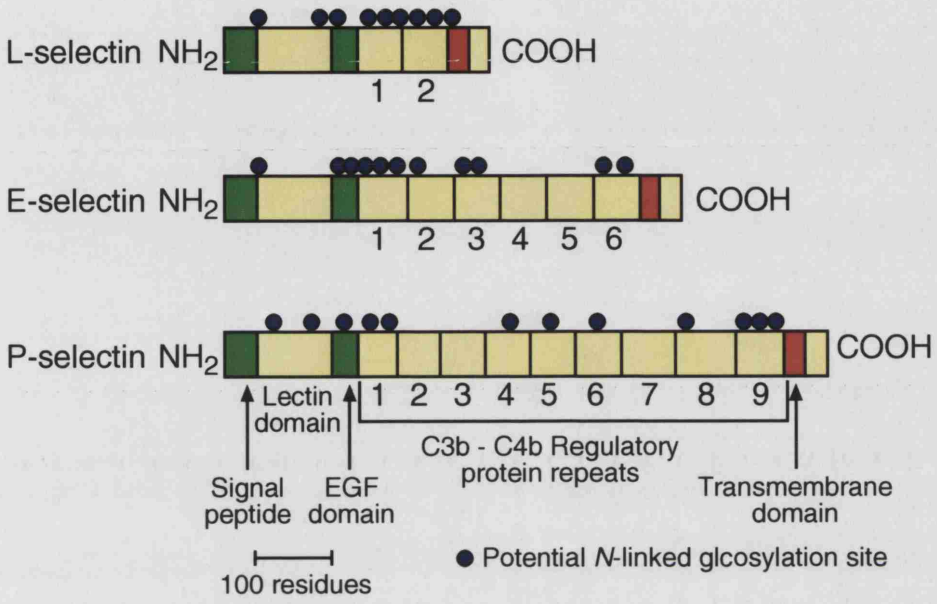
L-selectin NH2
COOH
1 2
E-selectin NH2
COOH
1 2 3 4 5 6
P-selectin NH2
COOH
Lectin domain
1 2 3 4 5 6 7 8 9
C3b - C4b Regulatory protein repeats
Signal peptide
EGF domain
Transmembrane domain
100 residues
Potential N-linked glcosylation site

L-selectin is identified by its cluster of differentiation number CD62L, but is also known as leucocyte adhesion molecule (LAM) and is expressed on the microvilli of monocytes and neutrophils as well as lymphocytes. The distribution of L-selectin on microvilli as opposed to the planar body of the cells increases the efficiency of initiation of tethering but has no role in the maintenance of rolling (Stein et al., 1999). Though the major role of L-selectin is the rolling step of lymphocytes migration to PLN, there is also evidence of a role in the recruitment of granulocytes and monocytes (Ley et al., 1991) (Arbonés et al., 1994) and lymphocytes (Tang et al., 1997) to sites of inflammation. Studies using L-selectin knockout mice have shown initial rolling (mediated by P-selectin) to be unchanged, however a decrease in rolling after 1 hour confirming a role for L-selectin in recruitment to sites of inflammation (Tedder et al., 1995). There is no redundancy between selectins in peripheral lymph nodes with L-selectin being the only selectin involved in lymphocyte homing (Bradley et al., 1994; Ley et al., 1993). L-selectin deficient lymphocytes migrate to the spleen, which recruits cells via an L-selectin independent method (Tang et al., 1998). L-selectin knockout mice have undersized lymph nodes associated with lymphocyte homing deficiency (Arbonés et al., 1994) and are unable to mount a primary immune response (Xu et al., 1996) due to an inability to activate lymphocytes within the lymph node.

Like P and E-selectin, L-selectin recognizes sialylated, fucosylated and sulphated glycoproteins such as sLe^x-like glycoproteins (Sawada et al., 1993) (Paavonen and Renkonen, 1992) via a calcium dependent interaction (Tamatani et al., 1993) through its lectin domain (Imai et al., 1990). However, further reports have suggested that the EGF domain also plays a role in ligand interactions (Imai et al., 1992). L-selectins' known ligands are GlyCAM-1 (Imai et al., 1991), MAdCAM-1 (Berg et al., 1993), CD34 (Imai et al., 1991) (Baumhueter et al., 1993), podocalyxin-like protein (Sassetti et al., 1998), and Sgp150/>200 (Derry et.al., 1999), which contain a complex of sLe^x – like glycoproteins (Hemmerich et al., 1995) and are collectively known as peripheral node addressins (PNAd) (figure 1.4). PNAd is recognized by the lectin domain of L-selectin (Berg et al., 1991). In the absence of inflammation, L-selectins ligands are appropriately glycosylated (Tamatani et.al., 1993) and sulfated ((Hemmerich et al., 1994) (Imai et al., 1993) for L-selectin adhesion only in HEV. GlyCAM-1 (Sgp^{50}) (Brustein et al., 1992) and Sgp200 are secreted

glycoproteins (Hoke et al., 1995), however, Sgp200 is also expressed by HECs. The secretion of GlyCAM-1 and spg200 is decreased during a primary immune response (Hoke et al., 1995) suggesting that the secreted forms may be acting as regulators of lymphocyte migration. CD34 (Sgp^{90}), in contrast, is exclusively found as a transmembrane bound glycoprotein on endothelial cells and is usually only appropriately glycosylated for L-selectin function in HEV. The different ligands have different degrees of importance dependent on their localization. For example, CD34 is the major component of PNAd in the tonsil (Puri et al., 1995), whereas MAdCAM-1 is the major ligand in mucosal lymphoid tissues. Other work has identified the mannose receptor as an additional ligand for L-selectin (Irjala et al., 2001). Although expressed by lymphatic endothelium, the mannose receptor is not expressed in HEV hence its role in lymphocyte recirculation may be restricted to exit from the lymph node. It is probable that this is a further method of regulating the cells that enter the lymph node and that there is L-selectin dependent regulation of later events in the recruitment cascade

There has also been speculation about the role of the selectins as signalling molecules. L-selectin interaction with HEC is thought to act as a signaling molecule upregulating cell-cell adhesion and promoting stable adhesion via integrins (Steeber et al., 1997). T lymphocytes shave been shown to bind to ICAM-1 through the β_2 integrin pathway (Hwang et al., 1996) and fibronectin through the β_1 integrin pathway (Giblin et al., 1997) following treatment with GlyCAM-1. In addition, antibody cross-linking of L-selectin has been shown to increase surface expression of CXCR4 the receptor for the chemokine SDF-1 (Ding et al., 2003). Deletion of part of the cytoplasmic tail of L-selectin abolished rolling of lymphocytes on inflamed venules (Kansas et al., 1993), however, further work suggests that although the truncated L-selectin is still able to form tethers with its ligands, as the tethers are of a shorter duration it is the ability to convert this tethering to persistent rolling that is impaired (Dwir et al., 2001).

Figure 1.4: Known ligands of L-selectin. Mucin-like molecules containing a complex of sLe^x – like glycoproteins and collectively known as peripheral node addressins (PNAd). Ligand expression varies between secondary lymphoid organs, for example, MAdCAM-1 is the major L-selectin ligand in mucosal tissue, whereas CD34 is the major L-selectin ligand in peripheral lymph nodes.

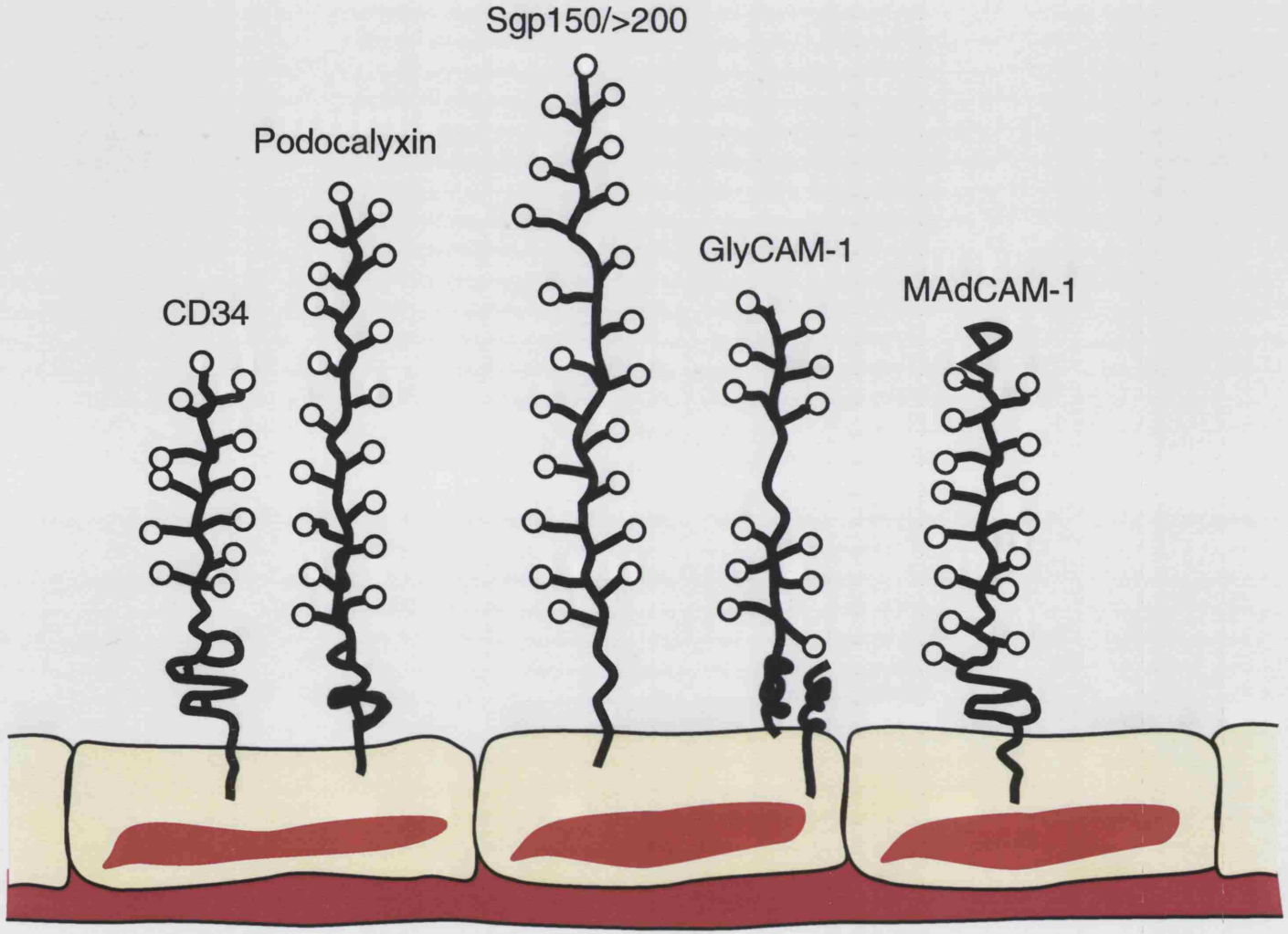
Sgp150/>200
Podocalyxin
GlyCAM-1
CD34
MAdCAM-1

Autoantibodies to L-selectin have been found in murine systemic lupus erythematosus and are thought to relate to the abnormal CD4 T cell response seen in both murine and human lupus (Hattori et al., 1998). Rejection of transplanted organs occurs when there is infiltrate of lymphocytes into the organ (Rosen, 1999). Expression of PNAd has been shown to be associated with transplanted organs (Toppila et al., 1999) implicating L-selectin mediated migration in tissue rejection.

Shear stress on the vessel wall has to be above a critical threshold value (0.6 dyn $cm^{-2)}$ to promote and maintain rolling through L-selectin (Finger et al., 1996). If the stress is below 0.4 dyn cm^{-2} L-selectin bonds cannot be formed and already rolling cells detach from the vessel wall. This critical threshold can be changed by chemical treatment of L-selectin ligands (Puri et al., 1998) suggesting that it is the L-selectin recognition of glycoproteins contained within its ligands that is dependent on the shear stress. Studies using L-selectin with a truncated cytoplasmic tail have shown that a full cytoplasmic tail is essential for effective conversion of tethering into rolling and cytoskeletal anchorage is needed for tethering under shear stress (Dwir et al., 2001). Rolling has been shown to be a series of short fast forward movements, separated by pauses (Alon et al., 1998) relating to the fast formation and subsequent release of the bond between L-selectin and its ligands. Furthermore, it has been shown that levels of L-selectin expression regulate homing to peripheral lymph nodes with those (T cells) expressing higher levels of L-selectin being more efficient at migration over a short time period (Tang et al., 1998). This was also found to be true of neutrophils – reduced levels of neutrophil L-selectin expression correlatng with inhibition of neutrophil accumulation at site of inflammation (Strausberg et al., 1999).

Following rolling is activation of integrins such as lymphocyte function associated antigen-1 (LFA-1) on the lymphocyte, which in turn binds to its ligands, ICAM-1 or 2 on HECs. Work on neutrophils (Von Andrian et al., 1992) proposes that, under shear flow, L-selectin induced rolling (and resistance against flow) is necessary for integrin adhesion. Integrin activation is thought to be due to chemoattractant signalling, as pertussis toxin (an inhibitor of the Giα coupled-chemoattractant receptors) inhibits firm adhesion but not rolling (von Andrian and M'Rini, 1998; Warnock et al., 1998). Integrin interaction mediates firm

adhesion of the lymphocyte to the venule wall and the lymphocyte can now undergo transendothelial migration (diapedesis) into the lymph node.

1.4: Integrins and Chemokines in HEV

The members of the integrin family of adhesion molecules consist of a large α chain non-covalently bonded to a smaller β chain distinguished by characteristic structural repeats. The five major integrins involved in leucocyte migration are: LFA-1 (αLβ2), VLA-4 (α4β1) and LPAM-1 (α4β7) found on lymphocytes, granulocytes and monocytes and Mac-1 (αMβ2) and CR4 (αXβ2) found on myeloid cells. The ligands for these integrins (apart from CR4), ICAM-1, 2,3, VCAM-1, MAdCAM-1, ICAM-1, respectively are all members of the Immunoglobulin superfamily of adhesion molecules.

The integrins are essential in stable adhesion of lymphocytes to the wall of the HEV. Also important is redundancy and overlapping of integrin functions both with other integrins and other adhesion molecules. An example of this redundancy is seen Peyer's patches where lymphocytes can migrate in the absence of L-selectin. The molecule responsible for tethering and rolling in the absence of L-selectin is α4β7 (LPAM-1). Like L-selectin, LPAM-1 is concentrated at the tips of microvilli in lymphocytes and can bind to MAdCAM-1 in the HEV of Peyer's patches and support rolling. Blocking antibodies to α4 integrins, VCAM-1 (VLA-4 ligand) and LFA-1 all inhibit adhesion of both naïve and activated T lymphocytes to HEC, however blocking of ICAM-1 alone had little effect (Faveeuw et al., 2000). There was a more complete inhibition of both adhesion and transmigration if a combination of antibodies against LFA-1 and α4 integrins was used suggesting that combinations of integrins are involved in these processes and redundancy between the molecules can occur (Faveeuw et al., 2000). Studies using LFA-1 deficient mice have confirmed the importance of this molecule in homing to lymph nodes with a marked reduction in homing and possible redistribution of these cells to the spleen (Berlin-Rufenach et al., 1999). These studies also confirmed work suggesting that adhesion and migration involve combinations of integrins as using a blocking antibody to α4 integrins in combination with LFA-1 negative cells completely prevented entry to lymph nodes (Berlin-Rufenach et al., 1999). As ICAM-1 has been shown not to have a crucial role in

lymphocyte adhesion and migration ((Faveeuw et al., 2000; May and Ager, 1992), it is possible that this is not the major ligand for LFA-1 in lymphocyte migration or ICAMs 1 and 2 can undergo some degree of compensation. Interestingly, recent work suggests that ICAM-1 may have an important role in lymphocyte rolling, as opposed to stable integrin arrest (Kadono et al., 2002). It would be interesting to see whether similar results would have been obtained if the endothelial cell line used in this study was transfected with ICAM-2 or 3 instead.

To undergo stable adhesion, integrins on the lymphocyte have to be activated to a high affinity binding state. The stimulus for integrin activation is thought to come from the HEC in the form of chemokines and studies have shown that pre-treatment with pertussis toxin inhibits integrin adhesion but not rolling. Other reports have suggests a role for ligation of L-selectin in the activation of integrins (Giblin et al., 1997; Hwang et al., 1996; Von Andrian et al., 1992) (Steeber et al., 1997).

Chemokines are small secreted or membrane bound proteins (6-14kDa) of which there are defined classes characterized by the arrangement of N-terminal cysteines. Chemokines act on receptors belonging to the Giα-protein coupled receptor superfamily.

Several reports have tried to identify the chemokines responsible for the activation of integrins. A possible candidate expressed by HEV is Stromal Cell-Derived Factor-1 (SDF-1) which is found in both primary and secondary lymphoid organs (Bleu et al., 1998). SDF-1 activates LFA-1 (Soede et al., 2001) and induces actin polymerisation in lymphocytes (Bleul et al., 1996). Further evidence for a role for SDF-1 in lymphocyte migration has been recently described by Ding et al., 2003, who showed that CXCR4 is upregulated at the cell surface by antibody cross linkage of L-selectin. In addition, a recent report (Okada et al., 2002) showed a suppression of homing to lymph nodes in $CXCR4^{-/-}$ B cells. Secondary Lymphoid Organ Chemokine (SLC; CCL21), which is constitutively expressed in HEC and is undetectable in mice with the paucity of lymph node mutation (plt) where naïve T cells fail to home to lymph nodes or to the lymphoid regions of the spleen, has also been shown to have a role both in integrin activation and homing of dendritic cells to T cell zones

(Gunn et al., 1999; Forster et al, 1999).

Directional migration is thought to be driven by a chemokine gradient (Foxman et al., 1997). The most well studied chemokine in terms of directional migration is IL-8, which is involved in the recruitment of neutrophils to sites of inflammation. Furthermore, a recent paper has pieced together the role in which MMP-7, chemokine KC and matrix protein syndecan-1 interact to create a neutrophil chemoattractant gradient (Li et al., 2002b). It was observed that neutrophils deficient in MMP-7 arrested in the interstitial space between the capillaries and epithelial tissue (Li et al., 2002b). On further, investigation it was shown that KC, a chemokine released from injured epithelial cells, binds to syndecan-1 and that this syndecan-1-KC complex is shed from the extracellular matrix by MMP-7. This cleavage forms a chemical gradient of the syndecan-1-KC complex. Chemokines may provide a further filtering stage by the HEV, as although monocytes and granulocytes express L-selectin they do not normally migrate into lymph nodes (Ager, 1994). Neutrophils roll very well in HEV but do not make stable adhesions, suggesting that they are not responding to the integrin activation stimulus. There is also suggestion that the sites of extravasation for T and B lymphocytes may be different, with T cells adhering in parts of Peyer's patch HEV that are high in SLC whereas B lymphocytes will adhere in SLC low areas (Warnock et al., 2000). However, B-lymphocyte chemoattractant (BLC), found on Peyers' Patches HEV (Okada et al., 2002), is strongly chemotactic to B cells but not T cells (Gunn et al., 1998).

1.5: Extravasation

Upon adhesion to HEC lymphocytes lose their spherical shape and surface microvilli and rapidly become polarised. Rapid polarisation can be inhibited by pre-incubation of the lymphocytes with pertussis toxin (Harris, 1991) and blocking of L-selectin adhesion in a static assay also inhibits polarisation (Harris and Miyasaka, 1995), suggesting a further role for chemokines and L-selectin. Polarization of the lymphocytes results in the establishment of two distinct regions: the leading edge and the trailing uropod (Sánchez-Madrid and del Pozo, 1999). A chemoattractant gradient is thought to cause the directional migration into the lymph node (Ager, 1994; Butcher and Picker, 1996). With polarisation of the cell there

is also relocalisation of chemokine receptors and adhesion molecules as well as reorganisation of the cytoskeleton in preparation for diapedesis into the lymph node (Serrador et al., 1998) and towards an APC (Sánchez-Madrid and del Pozo, 1999). The processes occurring during diapedesis into the lymph node are not yet fully understood. It is thought that most leucocyte transmigration occurs at HEC junctions rather than through the cell itself (Bianchi et al., 1997). It is not known whether junctional destabilisation is needed for diapedesis to occur however the junctions of HEC have been shown to differ from those in capillary and arterial endothelium (Anderson and Shaw, 1993). These discontinuous junctions could encourage the migration of lymphocytes between the cells (Girard and Springer, 1995). The localisation of certain Immunoglobulin super family proteins such as PECAM-1 and Junctional adhesion molecule (JAM) to endothelial junctions is associated with successful leucocyte migration. Blockade of both PECAM-1 (Muller et al., 1993) and JAM (Martìn-Padura et al., 1998) inhibited transmigration of monocytes; blockade of PECAM-1 has also been shown to inhibit T lymphocyte migration (Zocchi et al., 1996). In addition, matrix metalloproteinase (MMP) inhibitors block trans-endothelial migration of lymphocytes across PLN HEV (Faveeuw et al., 2001).

After migration through the HEC layer the leucocyte must then migrate through the basement membrane and the underlying connective tissue. Degradation of the matrix compounds by matrix metalloproteinases is thought to play a major role in the migration through these layers (Bianchi et al., 1997) with a suggestion that matrix-metalloproteinase-2 (MMP-2) is upregulated by T lymphocytes upon binding of integrin VLA-4 to its ligand on endothelium (Madri et al., 1996).

For a cell to successfully migrate through an HEV it must go through each stage of the adhesion cascade. The HEV interactions act as a filter enabling only particular cell types to enter the lymph node via the HEV. Granulocytes are able to roll very efficiently within HEVs, however, they rarely undergo stable adhesion thus cannot complete migration (Warnock et al., 1998). In a population of lymphocytes not all cells roll, however the majority of cells that do manage to tether and roll are able to make a stable adhesion and complete migration (Warnock et al., 1998). Multiple lymphocyte–HEC interactions

increase the probability of stable adhesion. Most lymphocytes detach within 3 seconds, those making contact for more than 12 seconds undergo complete arrest on the blood vessel wall (Ager, 1994). Likewise, endothelial cells found elsewhere in the body will resist the migration of certain cells types. For example, blood vessels in the brain restrict the migration of unactivated lymphocytes whilst promoting the entry of activated lymphocytes (Andersson et al., 1992).

1.6: Proteolytic Cleavage of L-selectin

Although there are soluble forms of all the members of the selectin family of adhesion molecules, L-selectin is the only one to be proteolytically cleaved/shed from the lymphocyte surface and a soluble form, retaining functional activity, released into the blood (Schleiffenbaum et al., 1992). It has been demonstrated that soluble L-selectin has a role in the regulation of lymphocyte migration, with a dose dependent inhibition of migration into PLN occurring with increasing concentration of soluble L-selectin (Tu et al., 2002). There is little data investigating the generation of soluble L-selectin from lymphocytes and whether it is the product of shedding of the surface bound molecule rather than secretion from vesicles. However, mice expressing a mutant form of L-selectin (LΔP) that resists shedding on T cells have <5% plasma levels of L-selectin compared with wild type controls suggesting that the majority of soluble L-selectin derived from T cells is generated by ectodomain shedding (Galkina et al., in press). In addition, studies using metalloproteinase inhibitors have shown that shedding is associated with entry into PLN (Faveeuw et al, 2001), which may suggest a physiological relevance for shedding – as opposed to secretion – of L-selectin.

The cleavage site has been identified as between a lysine and serine residue in the membrane proximal region of human L-selectin (Kahn et al., 1994) with the equivalent site in mice being between an arginine and serine residue (figure 1.5) (Zhao et al, 2001). The physiological role of shedding is not known, however structural requirements (Chen et al., 1995), calmodulin (Kahn et al., 1998), anti-CD3 (Büherer et.al.,1992; Chao et.al., 1997), cross-linking and binding of L-selectin (Lepault et al., 1994), protein kinase C activation via phorbol esters (Bührer et al., 1992) and CD45 (Wroblewski and Hamann, 1997)

signalling have been shown to influence cleavage. Stimulation with chemotactic factors (such as Il-8 and TNF) has also been shown to cause down-regulation of L-selectin in neutrophils (Kishimoto et al., 1989). Work on chimeric selectin molecules demonstrated that the length of the membrane proximal region of L-selectin is critical for shedding (Chen et al., 1995).

Further work has shown that there appear to be two separate pathways for L-selectin release. Most studies of shedding in vitro use artificial stimuli, such as PMA. However, it is known that there is also a slower constitutive shedding of L-selectin from unactivated cells (Borland et al., 1999). Disruption of the cleavage region by point mutations has little affect on L-selectin cleavage (Chen et al., 1995; Zhao et al., 2001), however proline substitutions in the membrane proximal region thought to be influencing secondary structure, or deletion of the EGF domain blocked PMA induced cleavage but not constitutive shedding (Zhao et al., 2001). Constitutive shedding was only blocked when the membrane proximal region of L-selectin was shortened by eight amino acids, moving the cleavage site closer to the membrane (Zhao et al., 2001).

Studies stimulating shedding through the TCR receptor via an anti-CD3 antibody have shown maximal downregulation of L-selectin 4 hour after stimulation with re-expression of L-selectin over the following 48 hours (Chao et al., 1997).

Figure 1.5: Domain structure and cleavage site of L-selectin. The cleavage site in murine L-selectin is thought to be between an arginine and serine residue in the extracellular membrane proximal region.

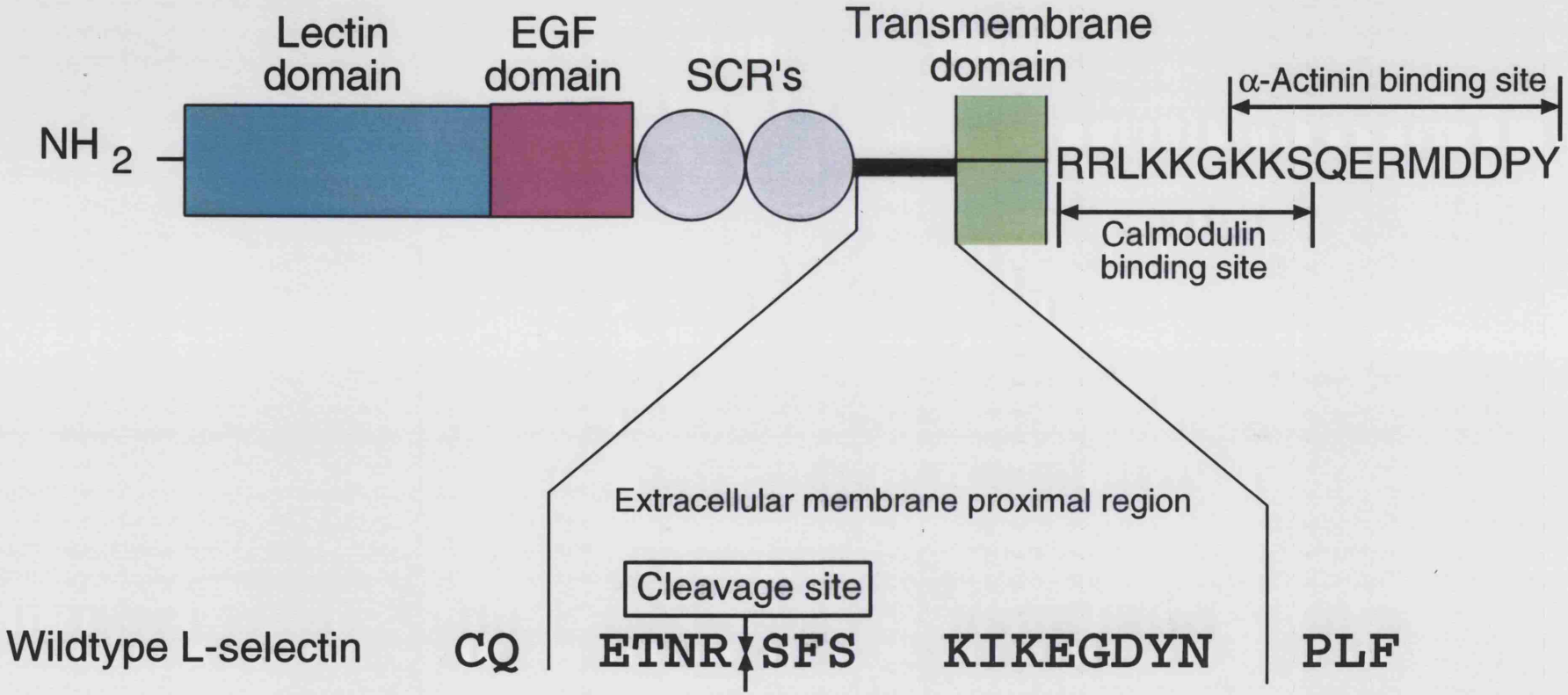
Lectin domain
EGF domain
SCR's
Transmembrane domain
α-Actinin binding site
NH 2
RRLKKGKKSQERMDDPY
Calmodulin binding site
Extracellular membrane proximal region
Cleavage site
Wildtype L-selectin
CQ
ETNR↓SFS
KIKEGDYN
PLF

High levels (1.6μg/ml) of soluble L-selectin are detectable in the serum of healthy people (Schleiffenbaum et al.,1992). Levels are raised in certain diseases such as B-chronic lymphocytic leukaemia and lowered in B-cell immunocytomas and non-Hodgkin's lymphomas (Gu et al., 1998).

Studies using protease inhibitors demonstrate that rapid proteolytic cleavage of L-selectin regulates leucocyte (in particular, neutrophil) rolling. Decreased leucocyte rolling velocity when L-selectin shedding was inhibited was seen for neutrophils *in vivo* (Hafezi-Moghadam and Ley, 1999) and *in vitro* (Walcheck et al., 1996). This is possibly confirmed by the observation that the jerkiness of the rolling motion is also significantly reduced in neutrophils (Hafezi-Moghadam et al., 2001). Lymphocytes treated with protease inhibitors, and viewed with fluorescent microscopy, arrest within the endothelial lining of HEV (Faveeuw et al., 2001). Other reports in neutrophils suggest increased stable adhesion by LFA-1 in neutrophils following blockade of shedding (Hafezi-Moghadam et al., 2001) although inhibition of L-selectin shedding had no effect on rolling or migration in neutrophils when E-selectin was expressed by inflamed endothelial cells (Allport et al., 1997; Hafezi-Moghadam et al., 1999).

It is difficult to assess the role of L-selectin cleavage in regulation of lymphocyte rolling velocity as most studies have been performed on neutrophils. As neutrophils respond to different chemokines/stimuli to lymphocytes, it is difficult to relate these studies to migration in HEVs.

Work using hydroxamate based matrix metalloproteinase (MMP) inhibitors has indicated the enzyme responsible for phorbol ester mediated cleavage of L-selectin is a member of the metzincin metalloproteinase superfamily of enzymes. However, as the cleavage is not inhibited by Tissue Inhibitors of Matrix Metalloproteinase (TIMP) 1 or 2 the enzyme is not a matrix metalloproteinase (Preece et al., 1996) Borland et. al., 1999). Enzymes from related zinc dependent families have been investigated for possible roles in L-selectin cleavage.

1.7: TNF-α-Converting Enzyme (TACE: ADAM 17)

The enzyme responsible for the cleavage of TNF-α was isolated in 1997 (Black et al., 1997; Moss et al., 1997) and given the name TACE (figure 1.6). From the crystal structure of the catalytic domain, it was confirmed that TACE (ADAM 17) is a member of the ADAM family of metalloproteinases (Maskos et al., 1998). The ideal situation to investigate the role of L-selectin shedding would, of course, be to engineer a mouse that was deficient in the enzyme responsible for this proteolytic cleavage. With the identification of TACE as an enzyme that is involved in ectodomain shedding, is not inhibited by TIMP-1 and 2, and is expressed on the surface of lymphocytes; TACE became a potential candidate for the enzyme responsible for L-selectin cleavage. With the development of the TACE knockout further evidence supported this hypothesis.

TACE is a multi-domain transmembrane zinc-dependent protease. TACE mRNA is found in most tissues and expression is largely constitutive. Interestingly, TACE is internalized upon prolonged exposure to phorbol ester. Furthermore, internalization of TACE is inhibited by metalloproteinase inhibitors (Doedens et al., 2000). Therefore, it seems that activation of tace is required for internalization.

Knockout TACE mice with a targeted mutation deleting the Zn^{2+} binding domain (inactivating the metalloproteinase activity) were developed, though the majority die at day 17.5 of gestation (Peschon et al., 1998). Of those surviving some die a few hours after birth with a few surviving for a maximum of two weeks. Studies of $tace^{\Delta Zn/\Delta Zn}$ embryonic lethality show that the developmental stage of eyelid fusion fails to occur, as well as reduced body weights and defective epithelial organisation. As the TNF-α knockout survives to adulthood it was concluded from the tace $^{\Delta Zn/\Delta Zn}$ phenotype that TACE is responsible for the cleavage of more than just TNF-α. The phenotype of the TACE knockout is similar to that of the epidermal growth factor receptor (EGFR) knockout. Werb and Yan, (1998) suggest this may be due to cleavage by TACE making ligands available for the EGF receptor e.g. transforming growth factor-α (TGF-α). Evidence supporting this hypothesis is described by Peschon et al., 1998, who compared amounts of soluble and membrane bound TGF-α in cell cultures of $tace^{WT}$ and tace $^{\Delta Zn/\Delta Zn}$ embryonic fibroblasts

and observed that TGF-α release was reduced by 95%. Recent work has shown that although the transmembrane form of TGF-α can still interact with the EGFR, it does not activate it if proteolytic cleavage is inhibited (Borrell-Pagés et al., 2003). Further evidence to support the hypothesis of TACE making ligands available to the EGFR is demonstrated by Borrell-Pagés et al., (2003). The EGFR has been implicated in the development of malignant tumors (Yarden and Sliwkowski, 2001) and Borrell-Pagés et al., (2003) describe the overexpression of TACE in breast tumours.

Also investigated in the Peschon et al., (1998) study was the cleavage of TNF-α receptor, p75 TNFR, which was ablated in $tace^{\Delta Zn/\Delta Zn}$ cells. The key experiment in this study, in terms of L-selectin cleavage, was the inability of thymocytes deficient in TACE to cleave L-selectin following PMA stimulation. Recombinant TACE was also shown to cleave L-selectin, however, much higher concentrations than those used to cleave TNF-α were needed.

Figure 1.6: Diagrammatic representation of TACE (modified from (Patel et al., 1998). The TACE metalloproteinase consists of an unknown pro domain, which is removed prior to expression on the cell surface, a metalloproteinase domain, disintegrin domain, cysteine –rich region, EGF-like region, transmembrane domain and cytoplasmic tail.

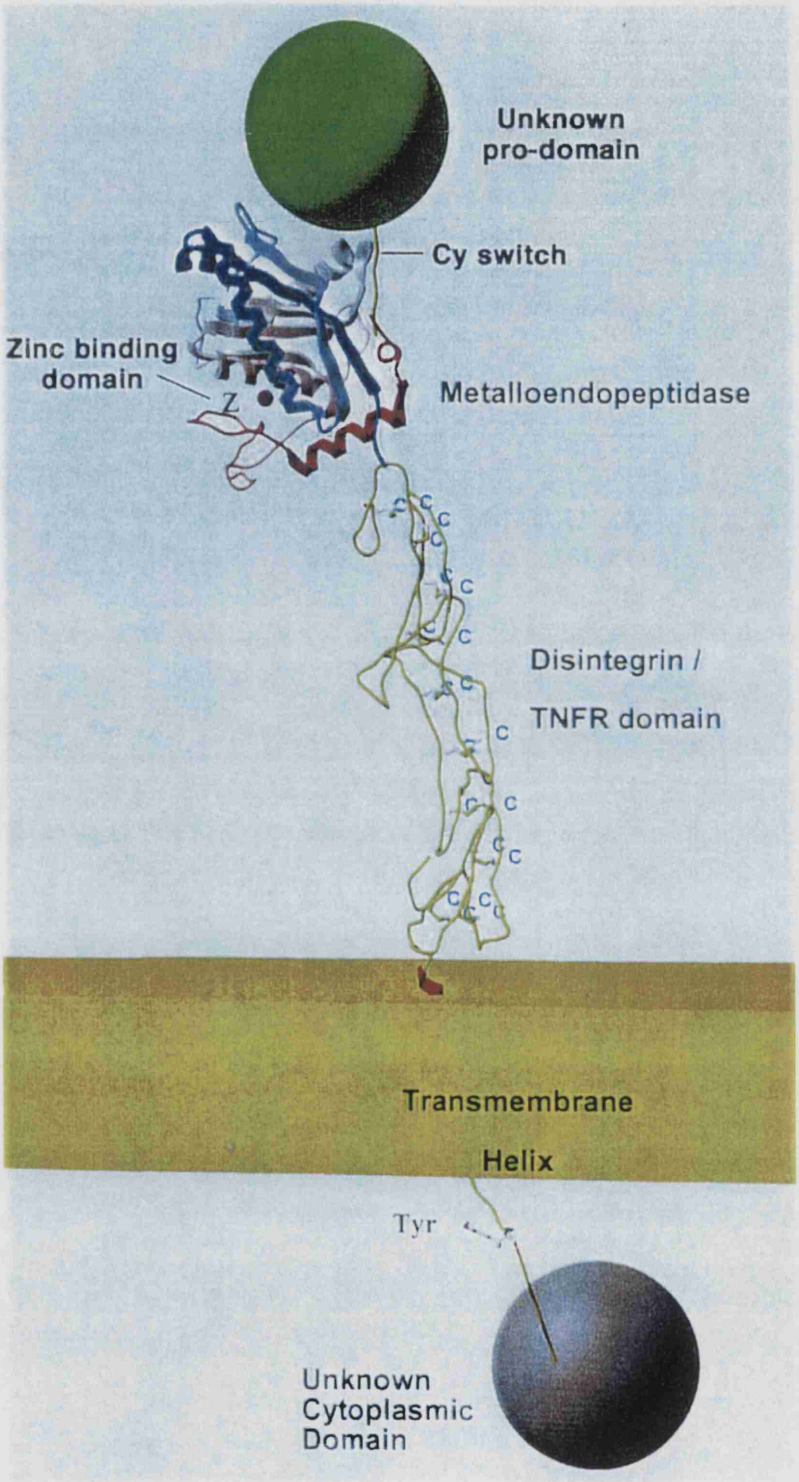
Unknown
pro-domain
Cy switch
Zinc binding
domain
Metalloendopeptidase
Disintegrin /
TNFR domain
Transmembrane
Helix
Tyr
Unknown
Cytoplasmic
Domain

The suggestion that a common enzyme or related enzymes are responsible for the majority of ectodomain shedding (Arribas et al., 1996) (Müllberg et al., 1997) has led to many studies of specific ectodomain shedding in TACE deficient cells. These studies have eliminated TACE as being the enzyme responsible for the shedding of proteins such as angiotensin converting enzyme (ACE) (Sadhukhan et al., 1999). However, it has been implicated as the enzyme responsible for the cleavage of Growth hormone receptor (GHR) into its soluble form growth hormone binding protein (GHBP) (Zhang et al., 2000a) and down regulation of macrophage colony-stimulating factor receptor (M-CSFR) (Rovida et al., 2001). Reports have shown a decrease but not complete loss in shedding of other surface proteins, such as IL-6, suggesting that TACE may have a role in their shedding although other metalloproteinases must also be involved (Althoff et al., 2000).

Both a full-length precursor and a mature form lacking the pro-domain forms of TACE are found within cells. Removal of the pro-domain occurs in a late Golgi compartment. A large proportion of TACE was found localised to the same intracellular compartments as intracellular TNF-α, suggesting that there may be intracellular shedding in addition to that at the cell surface (Schlöndorff et al., 2000). Stimulation of cells with PMA has been shown to induce internalisation of TACE and internalisation can be blocked by a metalloproteinase inhibitor (Doedens and Black, 2000). This suggests that regulation of induced shedding may be achieved by down-regulation of surface TACE. A recent report has shown that the cytoplasmic domain of TACE can interact with mitotic arrest deficient 2 (MAD2), which is a component of the spindle assembly checkpoint mechanism suggesting a further potential mechanism for TACE regulation (Nelson et al., 1999). In addition, work done by Peiretti et al. (2003) demonstrates the interaction of the scaffolding protein synapse associated protein 97 (SAP97) interacting with the cytoplasmic domain of TACE. Furthermore, overexpression of SAP97 altered the proteolytic ability of TACE (Peiretti et al., 2003).

Functional analysis of the domain structure of TACE has shown that structural elements involved in shedding of one substrate may be different to those involved in the shedding of

another. The cytoplasmic domain was shown not to be required for PMA induced shedding of TNF, p75 TNFR and IL-1R-II, with TNF-α and p75 TNFR only needing the catalytic domain of TACE for cleavage, however IL-1R-II required the presence of the cysteine-rich region in addition to the catalytic domain (Reddy et al., 2000).

In recent published literature discussing L-selectin cleavage, it is commonplace to describe TACE as the L-selectin sheddase. However, it should be stressed here that the majority of studies on TACE and L-selectin cleavage, use PMA as the stimulus to induce shedding. Although a convenient experimental technique, the physiological relevance of PMA induced shedding has to be questioned; particularly in light of a study demonstrating that shedding of L-selectin is not diminished by inhibition of PKC (Stoddart et al., 1996). As it is the PKC pathway that is stimulated by PMA, it can be determined that, at most, this is only one pathway that is involved in stimulation of L-selectin shedding. Furthermore, although elevated levels of L-selectin are seen in certain illnesses, there is at present little evidence for acute rapid L-selectin down regulation. In fact, the presence of soluble L-selectin in the sera of healthy individuals suggests a more controlled constitutive shedding. A recent study suggests that although the cleavage sites for PMA induced and basal shedding appear to be identical, there are distinctly different structural requirements for shedding to occur (Zhao et al., 2001). It is therefore possible that TACE does not have the physiological importance in L-selectin shedding that it is currently believed to have. This is further illustrated by the excessive amounts of soluble TACE required to cleave L-selectin, in comparison to the amounts used in TNF-α cleavage (Peschon et al, 1998).

The primary role of TACE is to cleave TNF-α and, thus, is shown to be upregulated in inflammatory conditions, such as inflammatory bowel disease (Brynskov et al., 2002) and upon stimulation by histamine (Wang et al., 2003) and LPS (Li et al., 2002a). It could be hypothesized that the role of TACE in L-selectin shedding is also limited to inflammatory conditions; suggesting an alternative enzyme is responsible for constitutive shedding.

1.8: Zinc Dependent Metalloproteinases

As stated above, TACE is a member of the ADAM family of metalloproteinases, which, in turn, is a member of the zincin superfamily – zinc dependent metalloproteinases. Zincins are grouped by sequence differences, into distinct family groups (figure 1.7) (Hooper, 1994).

Zincins contain a HEXXH zinc-binding motif (Bode et al., 1993) and can be further divided into the Gluzincins (Bode et al., 1993) and the Metzincins each with their own subfamilies.

The gluzincins contains enzymes such as the thermolysin family consisting of related bacterial metalloproteinases, the mammalian endopeptidase-24.11 family, the angiotensin converting enzyme family and the aminopeptidase family consisting of both mammalian and bacterial aminopeptidases (Hooper, 1994).

The metzincin family contains groups of enzymes such as the astacin/tolloid family, which consists of members from a diverse range of sources including a digestive enzyme from crayfish and mammalian endoproteinases e.g. meprin. The serratia family consists of bacterial plant pathogenic proteinases and the matrixins consist of collagenases, gelatinases and stromelysins (Hooper, 1994). The reprolysin/adamalysin family consists of subgroups including snake venom proteases and the ADAM family of metalloproteinases.

Figure 1.7: The zinc dependent metalloproteinase family tree. The zinc metalloproteinase family of enzymes consists of distinct family groups identified by sequence and structure relationships. The largest group of enzymes within the zinc dependent metalloproteinases is the zincins, which is further divided into the gluzincin families and the metzincin families. The ADAM and snake venom proteases belong to the reprolysin/adamalysin subfamily of metzincins.

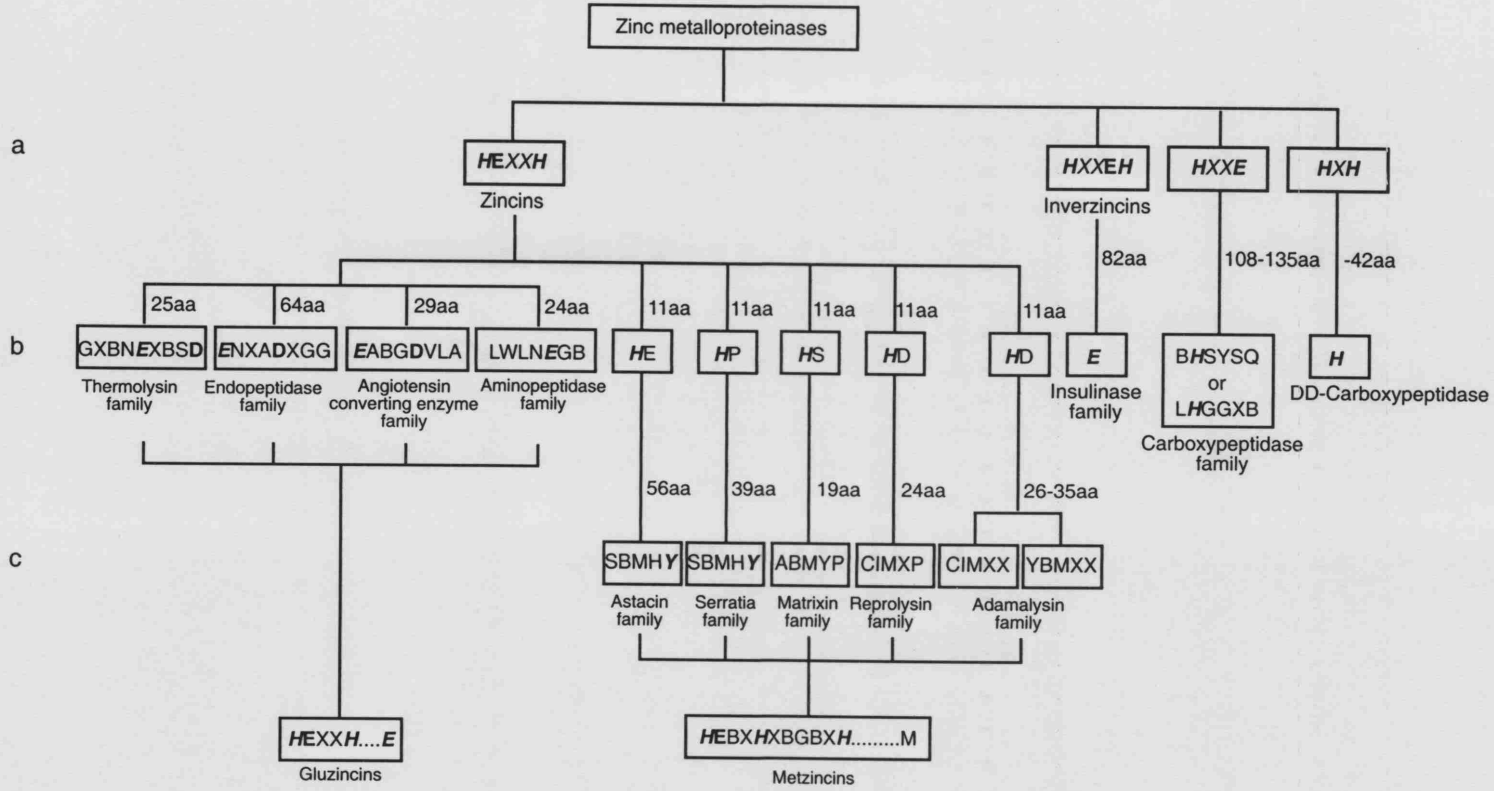
Zinc metalloproteinases
a
b
c
HEXXH
Zincins
HXXEH
Inverzincins
HXXE
HXH
82aa
108-135aa
-42aa
25aa
64aa
29aa
24aa
11aa
11aa
11aa
11aa
11aa
GXBNEXBSD
ENXADXGG
EABGDVLA
LWLNEGB
HE
HP
HS
HD
HD
E
BHSYSQ or LHGGXB
H
Thermolysin family
Endopeptidase family
Angiotensin converting enzyme family
Aminopeptidase family
Insulinase family
Carboxypeptidase family
DD-Carboxypeptidase
56aa
39aa
19aa
24aa
26-35aa
SBMHY
SBMHY
ABMYP
CIMXP
CIMXX
YBMXX
Astacin family
Serratia family
Matrixin family
Reprolysin family
Adamalysin family
HEXXH....E
Gluzincins
HEBXHXBGBXH.....M
Metzincins

The matrixins are commonly referred to as matrix metalloproteinases (MMP). The MMPs are thought to have roles in the migration of cells through the basement membrane as they all have some form of collagenase or gelatinase activity. The ability to break down the extracellular matrix has led to the MMPs being prime targets for drug therapies in diseases where there has been destruction of connective tissues such as rheumatoid arthritis and cancer. Most MMPs are not constitutively expressed in tissues and their function is controlled by natural inhibitors found in the same tissues, known as tissue inhibitors of metalloproteinases (TIMPs).

Many of these families contain members that are further referred to as secretases or sheddases, which are involved in the proteolytic cleavage of membrane proteins. Although these sheddases may share certain common characteristics such activation by phorbol esters and sensitivity to certain inhibitors, there is no apparent common secretory mechanism (Hooper et al., 1997).

1.9: Metalloproteinase Regulation

Regulation of the matrix metalloproteinases is controlled at three different levels. Firstly there is the transcriptional regulation of these enzymes, then an activation step and finally inhibition via specific inhibitors, TIMPS (Apte et al., 1996). There are four known TIMPs, TIMP-1, and 2,3,4. TIMP-1 and 3 are highly inducible by PMA and EGF (Leco et al., 1994). TIMP-3 unlike TIMP-1 and 2 has been shown to have a role in the regulation of shedding of a diverse range of proteins such as L-selectin (Borland et al., 1999), TNF-α (Amour et al., 1998) and Syndecans-1 and 4 (Fitzgerald et al., 2000).

As well as the TIMP inhibitors there are other synthetic inhibitors of enzyme activity. Many of these inhibitors act on more than one ectodomain sheddase, for example, TAPI-2 and 1,10-phenanathroline blocks PMA induced shedding of proTGF-α, L-selectin, IL-6-receptor and β-amyloid precursor protein (Arribas et al., 1996).

The involvement of matrix metalloproteinases and sheddases in diseases such as rheumatoid arthritis, osteoarthritis and cancer, has led to metalloproteinase inhibitors being

entered into clinical trials (Shaw et al., 2000; Coussens et al., 2002).

Studies using these inhibitors showed that the L-selectin sheddase, like the TNF-α sheddase (TACE), is not inhibited by TIMP-1 or 2, however it was sensitive to TIMP-3 (Borland et al., 1999) and other synthetic inhibitors such as Ro 31-9790. As all matrix metalloproteinases are inhibited by TIMP-1 and 2, the inability of L-selectin sheddase to be inhibited by these proteins but inhibited by other metalloproteinase inhibitors suggests that L-selectin sheddase is a metalloproteinase, but not a matrix metalloproteinase (Preece et al., 1996).

1.10: ADAMs

Disintegrin proteins were first discovered by purification of an integrin ligand from snake venom (Huang et al., 1989). When the first members of the ADAM family, were purified and cloned they were found to be membrane bound metalloproteinase disintegrins and included the already known sperm protein, fertilin, which has a role in sperm-egg fusion.

ADAMs are expressed in vertebrates, *Drosphila, Xenopus* and *Caenorhabditis elegans*; although they are not expressed in E. coli or plants (Seals and Courtneidge., 2003).

ADAMs (A Disintegrin and Metalloproteinase) family of metalloproteinases are transmembrane glycoproteins related to snake venom disintegrins (Weskamp and Blobel, 1994) and consist of an N-terminal signal sequence, a prodomain, metalloproteinase domain, disintegrin domain, cysteine-rich region, EGF-like region, transmembrane domain and a cytoplasmic tail. The ADAM family belongs to the adamalysin/reprolysin subfamily of the metzincin superfamily of zinc dependent metalloproteinases and are occasionally referred to by their other name MDC (Metalloprotease/Disintegrin/Cysteine-rich protein) (Blobel, 1997). Other members of the subfamily are a class of snake venom metalloproteinases (SVMPs), which share the same disintegrin/metalloproteinase domain structure (Hooper, 1994). However, unlike the SVMPs not all of the ADAMs are proteolytically active (having no HEXXH sequence present) and functional disintegrin domains have not been demonstrated for some ADAMs. ADAMs have been shown to have

roles in processes such as cell-cell fusion, cell adhesion, protein ectodomain shedding, signalling pathways and integrin interactions. Unlike MMPs, ADAMs are not inhibited by TIMP-1, 2 or 4 (however a recent report suggests *in vitro* inhibition of ADAM10 by TIMP-1 (Amour et al., 2000).

ADAMs, like membrane bound-MMPs, are converted to their active form by intracellular serine proteases from the paired basic amino acid-cleaving enzymes (PACE) family. The converting enzyme removes the pro-domain of the ADAM enzymes, which occurs before the enzyme is expressed on the cell surface (Roghani et al., 1999). As in other metzincins, a thiol group from a cysteine residue in the pro-domain interacts with zinc in the catalytic site and breaking this bond activates the enzyme, in a process termed cysteine-switch (Springman et al., 1990; Park et al., 1991). It is thought that reactive oxygen species (Rajagopalan et al., 1996) and nitrogen radicals (Trachtman et al., 1996) (Zhang et al., 2000b) may be responsible for oxidising the thiol group and thus disrupting the cysteine-zinc bond. Recent work suggests that this may be the mechanism by which PMA activates ADAM17/TACE (Zhang et al., 2000c) and a possible mechanism of ADAM regulation. Like all Zn-dependent metalloproteinases, ADAMs are inhibited by substances that chelate Zn^{2+} ions (Black and White, 1998).

The function of the cysteine-rich and EGF domains of ADAMs is the least known of all the domains. However, Iba et al., (1999, 2000) showed that the cysteine rich domain of ADAM12 acts as a ligand for the cell adhesion molecule syndecan.

The question of why ADAMs have both a metalloproteinase domain and an integrin domain has been addressed in a review by Carl Blobel (1997). He suggests three scenarios involving both domains. Firstly he suggests that the disintegrin domain may be interacting with the integrin on another cell allowing the metalloproteinase to act on substrate in cell membrane other than its own. Secondly, the disintegrin may be working to aid the metalloproteinase by binding to the substrate. Finally it is suggested that removal of the metalloproteinase domain may regulate the function of the disintegrin domain. The suggestion of a role for ADAMs in cell-cell fusion comes from the observation that certain

ADAMs contain features in common with viral fusion proteins such as a potential fusion protein within the cysteine-rich domain (Blobel et al., 1992). Several ADAMs contain potential intracellular signalling domains such as SH3 binding sites.

At present there are 40 known members of the ADAM family (including ADAMTS members) from mammalian and non-mammalian sources. The first two members, ADAM1/fertilin α and ADAM2/fertilin β were cloned in 1992. Antibodies against the integrin region of ADAM2/fertilinβ inhibit fertilisation (Yuan et al., 1997) although direct interaction between an ADAM and an integrin has not yet been shown (Blobel, 1997). A subset of ADAMs are the ADAMTS (A Disintegrin and Metalloproteinase with ThromboSpondin motifs) metalloproteinases that contain a thrombospondin motif and are secreted, rather than membrane bound proteins. ADAMTS, as well as lacking a cytoplasmic domain, also lack cysteine-rich region and an EGF domain. ADAMTS have been implicated in skin development, cancer, vascular development and proteoglycan cleavage (Kaushal and Shah, 2000).

The first sheddase characterised was the TNF-α sheddase named TNF-α converting enzyme (TACE) (Black et al., 1997; Moss et al., 1997), which was found to be a novel member of the ADAM family, ADAM17. Further studies confirmed the roles of other ADAM members as sheddases. For example, MDC9/meltrin-γ/ADAM9 which is involved in the shedding of heparin-binding EGF-like growth factor (HB-EGF). Soluble HB-EGF binds to and stimulates the phosporylation of the EGF receptor, however, it is synthesised as a membrane bound precursor termed proHB-EGF. Shedding of HB-EGF can be induced using an activator of PKC, which has been shown to bind to the cytoplasmic domain of ADAM9 (Izumi et al., 1998). A recent report (Asakura et al., 2002), demonstrated that HB-EGF can also be blocked by inhibition of ADAM12 suggesting, like TACE, other ADAMs are involved in the shedding of the ectodomain of EGFR-like receptor ligands and that there may be redundancy within the ADAM family itself. There have been reports that ADAM10 also has the ability to cleave TNF-α (Rosendahl et al., 1997) (Lunn et al., 1997), however other reports have disputed this claim (Condon et al., 2001). Interestingly ADAM17/TACE and ADAM10/KUZ/SUP-17 protein sequences are closely related to each

other within the ADAM family tree (Black and White, 1998).

	Isolation Source	***Function***
ADAM1/fertilinα/ PH-30α	Testis, placental tissue	Sperm-egg fusion (pseudo gene in humans)
ADAM2/fertilinβ/ PH-30β	Testis	Sperm-egg fusion-interacts with integrin $\alpha_6\beta_1$
ADAM3A/Cyritestin1/ tMDC I	Testis	Sperm protein, sperm-egg fusion
ADAM3B/Cyritestin 2	-	Sperm-egg fusion
ADAM4	Testis	Not known
ADAM5/tMDCII	Testis	Not known
ADAM6/tMDCIV	Testis, Liver	Not known
ADAM7/EAPI	Epididymis	Possible role in sperm maturation
ADAM8/CD156 MS2	Macrophage	Possible role in leucocyte extravasation
ADAM9/MDC9/ Meltrin γ	Widely expressed	Cleavage of HB-EGF, interacts with SH3 proteins binds to $\alpha_6\beta_1$ (Nath et al., 2000)
ADAM10/KUZ/MDAM	Brain,	Notch processing,

	Monocytes, spleen	secretase-TNF, myelin basic protein, type IV collagen
ADAM11	Neural, endocrine	Linked to breast cancer
ADAM12/meltrin α	Muscle, Bone	Myoblast fusion
ADAM13	Mesoderm, neural crest cells	Not known
ADAM14/adm-1	Syncytial organs, Sperm, sheath cells	Not known
ADAM15/metargardin	Placental tissue	Interacts with αvβ3 and $\alpha_5\beta_1$ integrin (Nath et al., 1999)
ADAM16/MDC16	Testis	Role in frog fertilisation
ADAM17/TACE	Monocytes, Spleen, Heart, Placenta, Muscle, Pancreas, Thymus, Prostate, Testis, Ovary	Cleavage of TNF-α, L-selectin, TGF-α and others
ADAM18/MDCIII	Sperm	Not known
ADAM19/meltrinβ	Dendritic Cells, Osteoblasts	Possible role in osteoblast differentiation

ADAM20	Testis	Not known
ADAM21	Testis	Not known
ADAM22/MDC2	Brain	Not known
ADAM23/MDC3	Brain	Not known
ADAM24/testase-1	Testis	Not known
ADAM25/testase-2	Testis	Not known
ADAM26/testase-3	Testis	Not known
ADAM28/MDC-Lm/MDCLs/eMDCII	Lymphocytes	Autocatalytic activity
ADAM29	Testis	Not known
ADAM30	Testis	Not known
ADAM31	Epithelia	Not known

Table 1.1: ADAMs and their functions complied from data in (Wolfsberg and White, 1996) and from R & D systems website.

1.11: Ectodomain Shedding

Many membrane bound proteins have been shown to be released from the cell membrane including cell adhesion molecules, leukocyte antigens, receptor ligands, enzymes and viral proteins (Hooper et al., 1997). The ability to stimulate shedding of many of these proteins by PMA and inhibit shedding with the same metalloproteinase inhibitors has led to the suggestion that the same or a few similar enzymes may be responsible for ectodomain cleavage. As well as PMA stimulation, there are other methods of shedding stimulation that are common to more than one shed ectodomain. For example, as with L-selectin, TNFRI and TNFRII receptors have been shown to undergo cleavage upon contact of receptor expressing cells with endothelial cells (Bjornberg and Lantz, 1998). Also similarly to L-selectin, these same receptors can be downregulated in response to inflammatory mediators, in this case TNF-α (Dri et al., 2000). Many examples of ectodomain shedding have multiple methods of inducing downregulation suggesting that regulation of cleavage is achieved by multiple signalling pathways (Fitzgerald et al., 2000).

1.12: Hypothesis

It is hypothesized that TACE is not the only but one of several enzymes responsible for L-selectin cleavage.

1.13: Aims

The aims of this project were to determine the role of TACE in regulating L-selectin levels on lymphocytes and circulating levels of soluble L-selectin using phenotypic analyses and shedding assays on TACE deficient lymphocytes.

Chapter 2: Materials and Methods

2.1: General Chemicals and Buffers

All general chemicals were obtained from Sigma, Poole, Dorset, UK or BDH/Merck Ltd, Poole, UK unless otherwise stated.

The following buffers were prepared in house at the NIMR:
Ca^{2+} and Mg^{2+} free phosphate buffered saline (PBS-CMF: 137mM NaCl, 2.7mM KCl, 1.4mM KH_2PO_4, 4.3mM $Na_2HPO_4 \cdot 7H_2O$); PBS (PBS-CMF containing 1.2mM $CaCl_2 \cdot 2H_2O$, 1mM $MgCl_2 \cdot 6H_2O$); 50x TAE (Tris base 242g, glacial acetic acid 57.1ml, EDTA (0.5M, pH 8.0) 100ml/l).

2.2: Genotyping of *tace*$^{\Delta Zn/\Delta Zn}$ Mice by PCR (suggested Immunex Method)

Tail tip biopsies were incubated with 100µl of lysis buffer/proteinase K (50 mM KCl, 1.5 mM $MgCl_2$, 10 mM Tris-Cl; pH 8.4, 0.5% Tween 20, 1 mg/ml proteinase K) at 55°C for 1 hour. Following incubation, the mixture was then incubated at 100°C for 15 minutes to inactivate proteinase K (Roche, Welwyn Garden City, Hertfordshire, UK). Mixture was vortexed and centrifuged for 2 minutes at 10,000 x g. The supernatant was kept for use in the PCR (hair pellet was discarded). 15 µl of tail DNA was made up to a reaction volume of 50 µl with 1 x PCR buffer (10 x PCR buffer: 500 mM KCl, 15 mM $MgCl_2$, 100 mM Tris-Cl; pH 8.4), 200 µM each dNTP (Amersham Pharmacia Biotech Inc, Uppsala, Sweden), 25 pmoles of each primer (Oswell DNA service, Southhampton, UK), and 1.25 U Taq polymerase (BDH/Merck Ltd). The reaction underwent 34 cycles of 1 minute at 94°C, 1 minute at 65°C and 30 seconds at 72°C. PCR products were run on a 3% agarose gel (section 2.5).

2.3: Primer Analysis and Design

All primer analysis and design was performed using OLIGO Primer Analysis Software (Molecular Biology Insights Inc, Cascade, USA).

2.4: Genotyping of *tace*$^{\Delta Zn/\Delta Zn}$ Mice by PCR with OLIGO designed primers

Lysis procedure was as described in section 2.1. 15 µl of tail (or earpunch: see section 2.6) DNA was made up to a reaction volume of 50 µl with 1 x PCR buffer (10 x PCR buffer: 500 mM KCl, 15 mM $MgCl_2$, 100 mM Tris-Cl; pH 8.4), 200 µM each dNTP, 25 pmoles of each primer, 1.25 U Taq polymerase and a additional 1.0 mM $MgCl_2$. The reaction underwent 5 minutes hold at 94°C followed by 34 cycles of 1 minute at 94°C, 1 minute at 59°C and 30 seconds at 72°C. PCR products were run on a 3% agarose gel.

2.5: Agarose Gel Electrophoresis

DNA fragments were separarted by electrophoresis on 1% (LEC-Ig analysis and cloning) or 3% (*tace*$^{\Delta Zn/\Delta Zn}$ colony genotyping) w/v in 1 x TAE, agarose (Bio-Rad Ultra Pure DNA Grade Agarose, Bio-Rad Laboratories, Hercules, CA) gels. Ethidium Bromide (0.5µg/ml, Bio-Rad) was added to the agarose gel prior to casting to enable visualisation of DNA bands under UV light (UV transilluminator, UVP Inc., Cambridge, UK).

DNA samples and DNA molecular weight markers (~1µg BSTE II digest and ~1µg 100bp ladder (New England Biolabs) were loaded into separate wells of gel. Photographs of gels were taken usinga Mitsubishi Video Copy Processor (UVP Inc, UK).

2.6: Preparation of Genomic DNA from Earpunches

90 µl of Lysis buffer (1xPCR buffer (described in section 2.1), 0.1 mg/ml proteinase K, 0.5% Tween and 20% Chelex: Bio-Rad) was incubated with the earpunch piece at 56°C for 30 minutes. After the 30 minutes, 10 µl of 25 mM $MgCl_2$ was added to the lysis mixture. The mixture was then incubated at 56°C for 2 hours. Mixture was then incubated at 95°C for 10 minutes to inactivate proteinase K.

2.7: Preparation of Small Tail Tip Biopsies for PCR

0.5mm of tail tip tissue was digested in 100µl of lysis buffer (5 mM KCl, 1 mM Tris-Cl; pH 8.4, 0.15 mM $MgCl_2$, 0.005% v/v Triton X-100, 0.1 mg/ml proteinase K) by incubation at 55°C for 2 hours. Proteinase K was inactivated by incubation at 100°C for 10 minutes.

Lysis mixture was then centrifuged for 10 minutes at 10,000 x g. The supernatant was removed and used in PCR (section 2.3).

2.8: Timed Matings and Foetal Liver Collection

The original breeding pair of *tace*$^{\Delta Zn/+}$ mice was obtained from Immunex, Seattle, USA. Embryos were collected at day 16.5-17 of following the appearance of a vaginal plug (day 0.5) from timed *tace*$^{\Delta Zn/+}$ matings. Heads were fixed in 10% neutral buffered formalin, embedded in paraffin and stained with haematoxylin and eosin. Foetal liver cell suspensions were made by passing the foetal liver through a 70 μm cell strainer (Falcon Becton Dickinson UK Ltd, Oxford, UK). centrifuging (250 x g and suspending in 900 μl serum free RPMI (GIBCO Invitrogen Corporation, Paisley, UK), and 100 μl DMSO (Sigma, Poole, UK) storing at -70°C until needed.

2.9: Generation of *tace*$^{\Delta Zn/\Delta Zn}$ Chimeric Mice

Host mice were fed acid water (concentrated HCl (11.4M) diluted 1 in 8400) for 7 days (unless otherwise stated). The mice were then irradiated with cobalt radiation (2 separate doses of 5 Gy separated by 2 hours in the case of 10 Gy total dose). Foetal liver cell (FLC) suspensions were kindly donated by Immunex, Seattle, USA or collected from *tace*$^{\Delta Zn/+}$ timed matings (section 2.6). If secondary transfers were used, bone marrow from chimeric mice was resuspended in FCS and DMSO (as for FLC, section 2.8) and stored at -70°C. For use, cells were defrosted, washed, filtered, counted and resuspended in RMPI (GIBCO Invitrogen) (no sera). Between 500,000 and 1 million foetal liver cells were intravenously injected into the tail vein of the irradiated mice. The mice received neomycin sulphate (Sigma) (unless otherwise stated) at 1mg/ml in drinking water for four weeks following irradiation and were housed in a clean area.

2.10: Host Mice

129/Sv, SCID and C57BL/10 RAG$^{-/-}$ (RAG-1 knockout) mice were bred in the specific pathogen free unit at the NIMR. L-selectin$^{-/-}$ mice were bred from a redervived line in a clean animal unit at the NIMR. C57BL/6 (Ly 5.2^{+}) mice were obtained from Harlan Olac, Blackthorn, Oxon.

2.11: Cell Suspensions and Yields.

Cervical, brachial, axillary, inguinal and mesenteric lymph nodes were removed and either pooled (all assays unless stated) or separately put into calcium and magnesium free phosphate buffered saline (PBS-CMF) at 4°C. Spleens and thymus' were removed and treated in the same way. Lymph node, spleen and thymus cell suspensions were made by mashing the tissues through a 70μm cell strainer (Falcon) into PBS-CMF. Bone marrow cell suspensions were obtained by removing the femur and tibia, cleaning away all muscle, cutting away the tips of the bone and flushing out the bone marrow with PBS-CMF using a 20 gauge needle. A uniform cell suspension was achieved by gently drawing the marrow in and out of a 25gauge needle. All cell suspensions were then washed and filtered. Resuspending in 0.83% ammonium chloride after the first wash and incubating for 8 minutes at room temperature lysed red cells in the spleen cell suspension. The suspension was then washed and the lysed cells filtered out through a cell strainer (Falcon).

Cell yield was determined by resuspending the cells in 10 ml of PBS-CMF, diluting 1 in 10 and then mixing 1 part suspension to 1 part 0.2% eosin. The stained cells were then loaded into a haemocytometer and viable cells (those that exclude eosin) counted. Alternatively cells were counted using an automated cell counter.

2.12: Biotinylation of antibodies.

Purified antibody was dialysed overnight into carbonate buffer. Biotin *N*-hydroxysuccinimide (Sigma) was dissolved in DMSO (Sigma) to give a concentration of 5mg/ml. 0.15mgs of biotin was added to each mg of antibody and incubated for 2 hours at room temperature. The biotinylated antibody was then dialysed for a minimum of 20 hours in PBS-CMF with 5 changes of buffer.

2.13: Analysis by Flow Cytometry

Normal or chimeric mouse cell suspensions of the primary and secondary lymphoid organs were made (see section 2.11) and resuspended at 5 x 10^7 cells/ml. Antibody mixtures were used to stain aliquots of 2 x 10^7 cells from each organs cell suspension. In brief, cells were incubated for 20 minutes at 4°C with either rat anti-mouse Ly 9.1/S19/8 (Pharmingen),

hamster anti-mouse TCRαβ (Cambridge Bioscience, Cambridge, UK) rat anti-mouse MEL 14 (made on site) and rat anti-mouse CD45R/B220CD4 (Pharmingen) or rat anti-mouse Ly 9.1/S19/8 (Pharmingen), rat anti-mouse CD4 (Caltag, TCS Biologicals, Botolph Claydon,UK), rat anti-mouse MEL 14 (on site) and rat anti-mouse CD8 (Caltag). In the analysis of large cell types an antibody mixture consisting of rat anti-mouse MEL 14 (on site), rat anti-mouse neutrophils (Caltag), rat anti-mouse S19/8 (Pharmingen), Rat anti-mouse Gr-1 (Caltag) was used. Negative controls consisted of FITC, PE and biotinylated rat IgG2a isotype controls (Southern Biotechnology Associates, Inc. Birmingham, UK), PE conjugated hamster IgG isotype control (Southern Biotechnology Associates, Inc) and APC conjugated rat IgG2a isotype control (Cedarlane, Ontario, Canada). The cells were washed extensively and stained with the secondary antibody, RED670 conjugated streptavidin (GIBCO Invitrogen) by incubating for 20 minutes at 4°C. After further washing the stained cells were analysed by flow cytometry using a FACS STAR cell sorter (Becton Dickinson UK Ltd, Oxford, UK). FACS data was analysed using WinMDI, (Joseph Trotter).

2.14: Collection of Blood Samples for FACS and ELISA Analysis

Tail bleeds (~40μl using heprinised capillary tubes: Sigma) were collected from 6 weeks onwards from reconstituting mice. *tace*$^{\Delta Zn/\Delta Zn}$ plasma was kindly donated by Dr. Jacques Peschon (Immunex, Seattle, USA) and MMP-9 knockout plasma by Carl Blobel (Sloan-Kettering Institute, New York, USA). 129/Sv chimeric sera was collected twelve weeks after irradiation by a lethal dose of sagatal (Rhone Merieux) anaesthetic followed by exsangination into heparin from a superficial artery.

2.15: Phorbol 12-Myristrate Acetate (PMA) Stimulation of *tace*$^{\Delta Zn/\Delta Zn}$ Peripheral Blood Lymphocytes (PBL)

Approximately 40μl of blood from tail bleeds of the chimeric mice was incubated with 300μM PMA (Sigma) for 45 minutes at 37°C. Cells were then washed extensively and stained for 20 minutes at 4°C, as described in section 2.13. After primary staining the cells were washed and stained with the secondary antibody, streptavidin conjugated with RED613 (GIBCO Invitrogen) as described in section 2.13. Red blood cells were lysed by adding 1 ml of ACK (8.29g NH_4CL, 1g $KHCO_3$, 37.2g Na_2EDTA and 100ml H2O, pH 7.2-

7.4) and incubating for ~2 minutes until the blood turns to a translucent red. The cells were washed extensively. L-selectin levels of the cells was determined by flow cytometry using a FACS STAR flow cytometer (Becton Dickinson).

2.16: Statistical Analysis

All statistics were performed using unpaired or paired two tailed Students t test in EXCEL (Microsoft Corporation, USA). Where multiple analysis were performed on the same mouse, statistical results were corrected using the Bonferroni analysis.

2.17: Histology

Peripheral lymph nodes were collected, snap frozen and stored at -70°C until cut. 5μm frozen sections were cut and stored at -70°C until stained. Sections were fixed in chilled acetone for 10 minutes and left to air dry. They were washed in PBS for 5 minutes, then drained. Slides were incubated with MECA-79 supernatant (prepared on site) and biotinylated anti-TCR (Pharmingen), or anti-B220 (Pharmingen) diluted in PBS 0.1% BSA for 45 minutes at room temperature. After the incubation slides were washed 3 times in PBS for 5 minutes then incubated with streptavidin conjugated FITC (Vector Laboratories, Burlingame, USA) diluted in PBS 0.1% BSA + 10% normal mouse serum (Sigma) for a further 45 minutes. After further washing, slides were incubated with Texas-RED conjugated goat anti-rat immunoglobulins (Southern Biotechnology Associates Inc, Birmingham, USA). In two further washing and staining cycles cells were additional stained with biotinylated Ly 9.1 (Pharmingen) and Cy5 conjugated anti-rat immunoglobulins (Jackson Immunoresearch Laboratories Inc, West Grove, USA). Fluorescence was detected using an Olympus fluorescent microscope (Olympus, Japan).

Chimeric mouse spleens were fixed overnight in 10% neutral buffer formalin, then embedded in paraffin. 8 μM sections were cut and stained with methyl green and pyronin stain.

Preparation of Methyl Green Pyronin (MGP): 2% Methyl Green
2% Pyronin Y
Distilled water

Acetate buffer pH 4.6 (1.2% Acetic acid, 2.7% sodium acetate (3-hydrate))
Sections were rehydrated in decreasing concentrations of ethanol, then stained with MGP for 30 minutes then rinsed in distilled water. Sections were dehydrate in acetone and histoclear then mounted in depex.

2.18: PMA Titration on *tace*$^{\Delta Zn/\Delta Zn}$ Splenocytes

129/Sv chimeric spleen cell suspensions were incubated in the absence or presence of 1, 3, 10, 30, 100, 300, 1000 or 3000 nM PMA for 1 hour at 37°C. Cells were then washed and stained with antibody and analysed as described in section 2.13. In addition to the antibodies listed in section 2.13, the splenocytes were also stained with rat anti-mouse CD69 (Pharmingen).

2.19: Basal Shedding

C57BL/6 PLN cells were incubated for 2 hours at 37°C in the presence or absence of increasing concentrations of Ro 32-1541, Ro 31-9790 or Ro 32-0526 (all synthetic inhibitors were kindly provided by Roche, Welwyn Garden City, Hertfordshire, UK). Supernatents were collected and analysed by ELISA (section 2.23) for the presence of soluble L-selectin. Cells were washed, stained and analysed as described in section 2.13.

PLN cells from 129/Sv chimeric mice were incubated on ice or at 37°C for 1 hour in the presence or absence of Ro 31-9790 (Roche). Following incubation cells were washed, stained and analysed as described in section 2.13.

PLN cells from C57BL/10 RAG$^{-/-}$ mice were incubated at 4°C or 37°C for 2 hours in the absence or presence of Ro 32-1541 (Roche), Ro 31-9790 (Roche), Ro 32-0526 (Roche), TIMP-1, TIMP-2 or TIMP-3. Supernatents were collected and analysed (section). Cells were washed, stained and analysed as described in section 2.13.

2.20: Cloning of MPΔ

A scrapping from a frozen stock of E.coli (strain DH5α, Life Technologies Ltd, UK) containing the pEE12 vector (Celltech Ltd, Slough, UK) was used to inoculate a starter

culture of 2 ml l-broth containing 100μg/ml of ampicillin (Sigma). The culture was incubated for 8 hours at 37°C with ~ 300rpm shaking. After 9 hours the starter culture was transferred to 250 ml of l-broth containing ampicillin (100μg/ml) and incubated overnight in the same conditions as for the starter culture. The plasmid DNA was prepared using a Qiagen Plasmid Maxi Prep Kit (Qiagen Ltd, UK) according to the manufacturers protocol. Stock vector pEE6 (Celltech) containing the MPΔ mutation was linerised by incubating with restriction enzymes HINDIII (Boehringer Mannhein Ltd, UK) and ECORI (Behringer Mannhein Ltd) for 2 hours at 37°C.

The linerised DNA was then amplified using a PCR method with a total volume of 20μl containing forward primer 5'CCAAGCTTCTAGACCGCCATGGTGTTTCCATGG3' and reverse primer 5'GGCCGTCGACTTGGCAGTTGGCTCTGG3', dNTP (Amersham Pharmacia Biotech Inc) mix and pfu polymerase and 10x pfu buffer (Stratagene). Thermal cycler setting were as follows; Hold for 5 minutes at 95°C initial cycle, denaturing for 45 seconds at 95°C, annealing for 45 seconds at 62°C, extension for 90 seconds at 72 °C and a extension on the last cycle for 7 minutes at 72°C for 35 cycles. The PCR products were run on a 1% agarose gel, illuminated by UV and excised using a fresh razor blade. DNA was purified using Qiagen gel purification kit (Qiagen) according to the manufacturer instructions. Purified DNA was digested by incubating with restriction enzymes HINDIII (Boehringer Mannheim Ltd) and Sal I (Boehringer Mannhiem). The products of digestion were run on a 1% agarose gel then gel purified as before. pEE12 (Celltech) and the digested insert were ligated in a vector: insert ratios of 1:2, 1:8, 1:16. 3:1, 1:1.3, 1:2.3. The vector and insert were incubated with T4 ligase (New England Biolabs) for 2 hours at 37°C. The ligated plasmid was then transformed into ultracompetant bugs (Stratagene) according to the manufacturer protocol. Plates were checked for colonies, Colonies were taken from the plate with the ligation reaction vector to insert 1:1.3 and grown up in 3ml of L-broth containing ampicillin for 4 hours at 37°C and ~300rpm. Minipreps (Bio-Rad) were carried out on each of the colonies according to the manufacturer protocol. 10 μl of the minipreps were digested using restriction enzymes HINDIII (Boehringer Mannheim) and SalI (Boehringer Mannheim) and run on a 1% agarose gel. Two colonies were chosen for further growing up as described above. Cells were then Maxi prepped using the same kit as

previously. DNA was digested using restriction enzymes HINDIII (Boehringer Mannheim) and SalI (Boehringer Mannheim) and run on a 1% agarose gel to ensure there was insert.

2.21: Sequencing

The following primers were purchased from Oswel DNA Service:
1) 5'AAGCTTCCGCCATGGTGTTT3', 2) 5'AAGTCACAACAGAGCAGTGT3', 3) 5'TTTAGTTCGCCATACAAAACA3', 4) 5'GTTTTGTATGGCGACTAAA3', 5) CAAGAGGGAACGAGACTCTGG3', 6) 5'CCAGAGTCTCGTTCCCTCTTG3', 7) 5'TACGGGCCCCAGTGTCAGTAT3', 8) 5'ATACTGACACTGGGGCCCGTA3', 9) 5'TTCAGCTTCCAGTCCAAGTG3' 10) 5'CTCAGAACAGTTGAAAGCA3', 11) 5'TGGGGGGAAGAGGAC3'. Sequencing reactions were performed using ABI PRISM^{TM} Terminator cycle Sequencing Ready Reaction Kit (Perkin Elmer, Warrington, UK). Sequencing and extension product purifications were performed in accordance to the manufacturer instructions. Purified DNA was resuspended in 4 µl of loading buffer and denatured at 90°C for 5 minutes. Samples were loaded onto a polyacrylamide sequencing gel and run for 7 hours. Data was acquired using an ABI PRISM sequencer (Perkin Elmer and analyser using ABI Factura and Autoassembler DNA programmes (Perkin Elmer).

2.22: Transfection of NSϕ Cells (method as provided by Celltech)

The plasmid containing the insert was linearised by digestion with Pvu I (Boehringer Mannheim) that cuts through the ampicillin resistance gene. NSϕ cells were cultured in non-selective medium consisting of Iscoves Modified Dulbecco's Medium (IMDM: GIBCO Invitrogen) (500ml), 200mM L-glutamine (5ml: Sigma) and FCS (50ml: Sigma) at 37°C in an atmosphere of 5% CO_2. Prior to transfection the cells were 90% viable. Cells were centrifuged at 250 x g for 5 minutes and washed in cold PBS by resuspending and recentrifuging. Cells were resuspended at 10^7 cells/ml in PBS and kept on ice. 40µg of linerised plasmid DNA (in 50µl of sterile dH_2O) was added to 10^7 cells (1ml) in an electroporation cuvette on ice. Cells and DNA were gentle mixed with a pipette. The cell/DNA mixture was incubated on ice for 5 minutes. The outside of the cuvette was wiped dry and delivered 2 consecutive pulses of 1500 volts, 3µF from a Gene Pulser (BioRad).

Cuvette was returned to ice for 2-5 minutes. Transfected cells were added to 30ml of non-selective (see above) medium.

20 ml of the cells suspension was distributed between four 96 well (~ 50µl per well) tissue culture plates (Nunc, Life Technologies, Paisley, UK). The remaining 10mls was diluted with a further 30ml of non-selective medium and distributed over five 96 well plates (~ 50µl per well). 10ml of the diluted cell suspension was further diluted by the addition of 40mls of non-selective medium and distributed over five 96 well plates (~ 50µl per well). Plates were incubated at 37°C, 5% CO_2 overnight. 150µl of selective medium, consisting of IMDM (500ml), dialysed FCS (50ml), 5ml of 100x glutamate (Sigma) and asparagine (Sigma) (600 g of each made up to 100ml in dH_2O), 10ml of 50x nucleosides (35mg adenosine, 35mg guanosine, 35mg cytidine, 35mg uridine and 12 mg thymidine all from Sigma, made up to 100ml) was added to each of the wells. 12-18 days later single well colonies were expanded by transfer to one well of a 24 well plate. Confluent 24 wells were then transferred to a 100ml cell culture flask.

Specific production rate (SPR) of the cell lines was calculated by taking a culture at 50-75% confluence, centrifuging and resuspending in fresh selective medium. Cells were incubated overnight, then the medium was sampled and the cells counted. The fusion protein present in the medium was quantitated by ELISA. SPR (µg/10^6 cells/24 hours) = fusion protein concentration (µg/ml)/cell concentration (10^6 cells/ml) x time of incubation (24 hours). High yield transfectants were selected for medium collection.

Medium from the transfectants was purified for expressed product by passing supernatent through HiTrap Protein G column (Amersham Pharmacia Biotech) and collecting eluted fractions. The method in brief: Protein G column was washed with 10x column volumes of molar acetic acid, followed by 10 column volumes of PBS. LEC-Ig supernatant was run through the column. Column was washed with 10x column volumes of PBS. Bound LEC-IG was eluted with molar acetic acid and fraction collected. Collected fractions were neutralised with solid TRIS. Neutralised fractions were dialysed against PBS-CMF.

2.23: Measurement of Soluble L-selectin Using an ELISA

Blood from the knockout mice surviving for up to two weeks after birth was kindly donated by Dr. Jacques Peschon of Immunex, Seattle. Blood from MMP-9 knockout mice was kindly donated by Steve Shapiro and Susan Nourshargh of the Sloan-Ketterin Institute, NY. 10 μg/ml MEL-14 (made on site) or LAM-1.16 (kindly donated by Dr Thomas Tedder, Duke Medical Centre, Durham, USA) in borate buffered saline was used to coat a 96 well Maxisorb plates (Nunc) by incubating overnight at 4°C. Unbound antibody was removed and the plates were blocked using 1% bovine sera albumin (BSA) in PBS and incubating for 1 hour at room temperature (RT). The plates were washed and incubated with the collected sera, a positive control consisting of LEC-Ig or a negative control CTLA-4 for 2 hours at room temperature. After washing, bound L-selectin was detected using biotinylated T28 mAb (produced on site) or biotinylated MEL 14 (produced on site) incubated for 2 hours at RT, washing then incubating with horse radish peroxidase (HRP) labelled streptavidin (DAKO Reagents, Ely, UK) diluted 1/5000 in PBS for 1 hour at RT, washing and adding 1mg/ml of tetramethylbenzidine (TMB: Sigma) in 0.1M citric/acetate buffer. The colour change reaction was quenched with 1M sulphuric acid after 10 minutes and absorbance read at 450 nm. Concentration of soluble L-selectin was determined using a standard curve plotted according to the absorbance reading of the known control.

2.24: Measuring the Reactivity of Anti-Lectin 1 Polysera

Method for raising a polysera against Lectin-1 is decribed in chapter 6. In brief, rabbits were injected with 1ml of 1.5mg/ml Lectin-1 conjugated to ovalubumin in complete Freunds adjuvant (1 mg Mycobacterium tuberculosis, heat killed and dried in 0.85ml paraffin oil, 0.15ml mannide monooleate; Sigma). In a further two sets of injections separated by 28 days rabbits were re-immunised with Lectin-1 conjugated to keyhole limpet haemocyanin in complete Freund adjuvant. Polysera from rabbits were then tested for reactivity. The same incubation times, temperatures and washes as described in section 2.23 were used. The 96 well plates (Nunc) were coated overnight using 5μg/ml of lectin-1 linked to BSA. Wells were blocked as before (section 2.23), then incubated with the doubling dilutions of polysera. Bound antibodies to lectin-1 were detected using swine anti-rabbit conjugated with HRP diluted 1/5000 (DAKO) and TMB (Sigma). The colour change

was quenched with 1M sulphuric acid and absorbance read at 450nm. The same protocol was used to test purified polysera.

2.25: Purifying Anti-Lectin-1 Polysera

Lectin-1 was coupled to a Hi-Trap affinity column (Amersham Pharmacia Biotech Ltd), in accordance with the manufacturers instructions. Polysera was filtered and passed through the affinity column attached to a pump system using the method described by the column manufacturers. Eluted fractions were collected and protein levels determined by spectrometry.

2.26: Staining of C57BL/6 Cells with Anti-Human L-selectin Antibodies

Splenocytes from C57BL/6 mice were incubated with MEL 14, T28, and LAM-1.16 or 1.18 (both kindly donated by Thomas Tedder) and analysed as described in section 2.13.

2.27: Intercellular Cleavage of L-selectin by TACE

$tace^{\Delta Zn/\Delta Zn}$ (and a control population of $tace^{WT}$) cells were incubated with a green cytoplasmic dye, carboxyfluorescein succidimyl ester (CFSE: Molecular Probes, USA) by resuspending the cells at 5 x 10^7 in 2μM of CFSE in PBS-CMF and incubating for 15 minutes at 37°C. $tace^{WT}$ cells were mixed with the fluorescent $tace^{\Delta Zn/\Delta Zn}$ (or control $tace^{WT}$) cells in a ratio of 7:1, respectively and resuspended in a control buffer (NaCl 8.48g/l, KCl 372mg/l, Glucose 1g/l, Sodium Biocarbonate 2g/l, BSA 1g/l, $CaCl_2$ 148mg/l, $MgCl_2$ 204mg/l in RMPI:GIBCO Invitrogen). Cells were incubated for 1 hour at 37°C in the presence or absence of PMA and the analysed for L-selectin expression by incubation with MEL 14 as described in section 2.13.

2.28: Incubation of $tace^{\Delta Zn/\Delta Zn}$ Cells with Soluble TACE

$tace^{WT}$ and $tace^{\Delta Zn/\Delta Zn}$ peripheral lymph node cells (suspended in control buffer described in section 2.25) were incubated with 0.1μM soluble TACE (kindly donated by Dr Gillian Murphy, Norwich, UK) for 1 hour at 37°C in the presence or absence of PMA. Cells were collected and analysed by FACS as described in section 2.13.

2.29: Migration through an HEC Monolayer

A frozen stock of endothelial cells originally isolated from HEV of Louis Rats (Ager, 1987) was thawed and grown up in RMPI (GibcoBRL) supplemented with 1% penicillin/streptomycin and 10% FCS. When confluent, supernatant was tipped off and cells rinsed with 10ml of cold PBS-CMF. Cells were incubated with 10ml of Trypsin –Versene for ~5 minutes and centrifuged at 250 x g for 5 minutes. Cells were resuspended in 10ml of media and counted, recentrifuged and resuspended at $5x10^4$ cells/ml. Cells were plated into a 6 well culture plate (Nunc) at 2ml/well (10^5 cells) and cultured at 37°C, 5% CO_2 until confluent (~72 hours).

PLN cell suspensions from $RAG^{-/-}$ chimeric mice were prepared as in section 2.11 and resuspended at $1x10^7$ cells/ml in assay medium (97ml RPMI, 2ml of 1M Hepes, 1ml heat inactivated FCS, 5ml Penicillin/streptomycin). Medium was removed from confluent endothelial cells and cells washed with assay medium. PLN cells were plated on to the endothelial cells at $2.5x10^7$ cells/well (in 1ml) and incubated for 1 hour at 37°C, 5% CO_2. After incubation, non-adherent cells were collected, the endothelium washed and the washed added to the collected non-adherent cells. 1 ml of assay medium was added back to the endothelium and adherent cells, and photographs taken of the adherent and migrated cells (x 20 magnification; Ocular CK 2 microscope Olympus, Japan). Adherent cells and endothelium were incubated for 5 minutes at room temperature with 0.1% EDTA (1ml/well). Non-adherent cells were also treated with 0.1%EDTA. Adherent cells were collected after the incubation and both the adherent and non-adherent populations were washed twice. Cells were then stained with a B cell, T cell and L-selectin marker and analysed by FACS as described in section 2.13.

2.30: Trafficking of *tace*$^{\Delta Zn/\Delta Zn}$ Lymphocytes

Cell suspensions of $RAG^{-/-}$ chimeric mice PLN were made as described in section 2.11. Cells were washed extensively and stained with either CFSE (section 2.25) or a fluorescent red dye, Rhodamine (Molecular Probes). The results shown in this report were from an experiment where *tace*^{WT} cells were stained with rhodamine and *tace*$^{\Delta Zn/\Delta Zn}$ cells with CFSE, however a small pilot experiment was performed where the dyes were reversed to

ensure that there was no effect of the dye on migration. Cells were then washed extensively and recounted. Cells were then mixed in a 1:1 ratio and resuspended at 200 million cells/ml. 200µl (40 million cells) were then injected into the tail vein of recipient $RAG^{-/-}$ mice. After 1 hour the recipient mice were culled and cell suspensions made of the peripheral lymph nodes and spleens as described in section 2.11. Blood samples were also taken by exsanguinations under Sagatal. Cell suspensions were stained with a T cell and L-selectin marker and analysed by FACS as described in section 2.13.

Chapter 3: Genotyping and Generation of Chimeric Mice

Black et al (1997) engineered an in-frame deletion of the Zn^{2+} binding domain of TACE (see figure 1) and showed that cells homozygous for this mutation failed to efficiently release TNF-α, TGF-α and L-selectin. The majority of mice homozygous for the same deletion (*tace*$^{\Delta Zn/\Delta Zn}$) die between day 17.5 of gestation and a few hours following birth (Peschon et al., 1998). To study L-selectin shedding in TACE deficient cells, chimeric mice containing immune systems derived from *tace*$^{\Delta Zn/\Delta Zn}$ stem cells were generated. In the initial phase of this project, *tace*$^{\Delta Zn/\Delta Zn}$ foetal liver cells were kindly donated by Roy Black, Immunex Corporation, Seattle. *tace*$^{+/+}$ foetal liver cells were initially collected from normal C57BL/6 embryos. It was necessary to establish a *tace*$^{\Delta Zn/+}$ colony at the National Institute for Medical Research to ensure a constant supply of haemopoietic stem cells.

Specific terminology relating to the primers is used in this chapter. The term "neomycin primers" refers to the primers that were used to amplify the neomycin cassette. "Zinc primers" is used to refer to the primers that were used to amplify the zinc binding domain of TACE.

3.1 Establishment of the *tace*$^{\Delta Zn}$ colony

A breeding pair of *tace*$^{\Delta Zn/+}$ mice was transported to the Institute from Immunex. The colony was expanded and rederived into a clean environment. An established Polymerase Chain Reaction (PCR) protocol was originally used to genotype the mice. Immunex suggested using the following primers:

Forward primer: 5′ GCC CTG AAT GAA CTG CAG GAC G

Reverse primer: 5′ CAC GGG TAG CCA ACG CTA TGT C

These primers were designed to recognise the neomycin resistance gene in the PGK-neo cassette replacing the zinc-binding domain in *tace*$^{\Delta Zn/+}$ mice. The intact zinc-binding domain in both WT and *tace*$^{\Delta Zn/+}$ mice was to be amplified with the following primers:

Forward primer: 5′ GAA GCT GAC CTG GTT ACA ACT CAT G 3′

Reverse primer: 5′ CTT ATT ATT ATT CTC GTG GTC ACC GCT 3′

Figure 3.1: Targeted mutation of the Zn^{2+} binding domain of the TACE gene (modified from (Black et al., 1997). Arrows represent the forward and reverse primers used for RT-PCR. Exons are depicted as a solid block on the TACE genetic map and numbered from 1–17. Introns are identified by Roman numerals. The zinc binding domain (exon number 11) was replaced by a neomycin cassette as shown in the smaller TACE map.

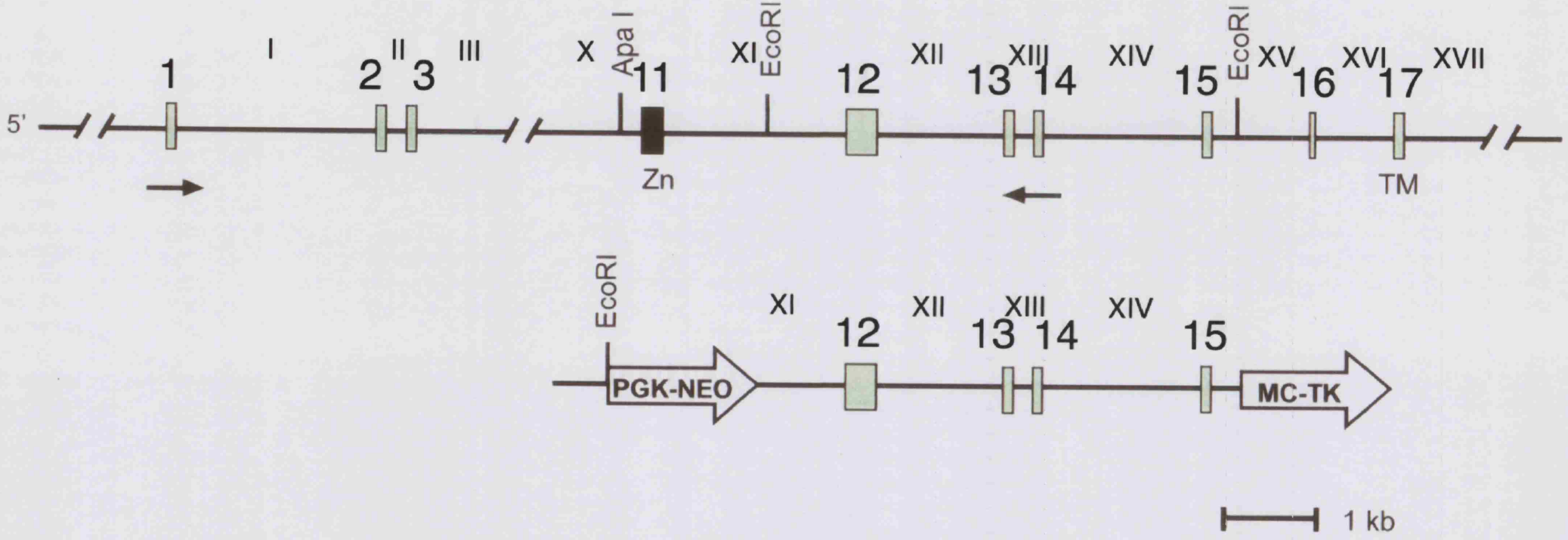
5'
1
I
2
II
3
III
X
Apa I
11
Zn
XI
EcoRI
12
XII
13
XIII
14
XIV
15
EcoRI
XV
16
XVI
17
TM
XVII
EcoRI
XI
12
XII
13
XIII
14
XIV
15
PGK-NEO
MC-TK
1 kb

Primers were used at a concentration of 0.1 μmol/L. PCR conditions were 34 cycles of 1 minute denaturing at 94°C, 1 minute annealing at 65°C, 30 seconds extending at 72°C. The expected PCR products were a band of 152bp relating to the intact zinc domain, thus present in *tace*$^{+/+}$ and *tace*$^{\Delta Zn/+}$ mice and a 520bp product relating to the neomycin region present in the *tace*$^{\Delta Zn/+}$ mice (figure 3.2). Also visible in figure 3.2 are bands of approximately 180bp. This 180bp product did not appear in all reactions and was also referred to as occasional bands in the Immunex method. No explanation was given for these bands.

Although a band of approximately 150bp (the expected size of the zinc domain primer product) could be amplified, a band of ~520bp relating to the neomycin cassette could not be consistently amplified. When the reaction was run with no DNA, the neomycin and zinc primer mixture still yielded a 150bp band (figure 3.3), suggesting that this band was due to dimerism between the primers themselves. Following the suggestion of dimerism between the primers coupled with the occasional presence of a 180bp band, the validity of the results was questioned and the possibility of redesigning the primers (and thus the reaction conditions) was addressed. The neomycin primers were analysed using OLIGO primer design software. This predicted that the primers were prone to forming hairpins and dimers and that the melting temperature of the hairpin and dimer structures was higher than the PCR annealing temperature. The most stable dimer (-6.2 kcal/mol) being between three cytosine residues at the 5′ end of the forward primer with three guanine residues at the 5′ end of the reverse primer (figure 3.4a). The most stable hairpin in the forward primer (-2.4 kcal/mol) is between CCTG at the 5′ end of the primer interacting with GGAC at the 3′ end (figure 3.4b). In the reverse primer the most stable hairpin (-1.2 kcal/mol) is between the TAGC sequence and GCTA sequence four residues later (figure 3.4c).

Figure 3.2: PCR of tail lysates from the TACE colony. DNA from tail lysates from the TACE colony was amplified using primers and conditions suggested by Immunex. Bands of 150bp relating to the intact Zn domain of TACE are visible in all lanes, as would be expected due to the lethality of a homozygous mutation. Bands of 520bp are visible in lanes 1,2,6,8,10 relating to the presence of a neomycin cassette in these *tace*$^{\Delta Zn/+}$ mice. Unexpected bands of approximately 180bp are also visible in lanes 1,2,4, 5, 6 and 8. These bands were also described in the method from Immunex; no explanation was given for these bands.

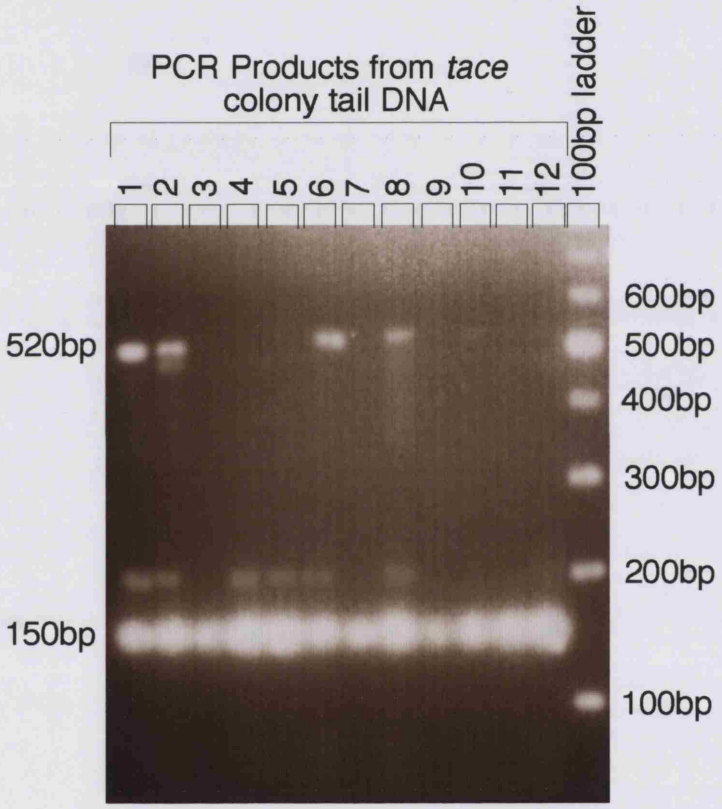
PCR Products from *tace* colony tail DNA
1
2
3
4
5
6
7
8
9
10
11
12
100bp ladder
520bp
150bp
600bp
500bp
400bp
300bp
200bp
100bp

Figure 3.3: Products from a PCR reaction containing primers only (no DNA). There is a visible 150bp product in lane 1. As this reaction contained no DNA, the presence of a band suggested that the primers are themselves being amplified. The 150 bp band is also visible in lane 2, where the products from a PCR amplification of tail DNA from the TACE colony had been loaded. The expected products from the reaction were a band of ~152bp relating to the zinc binding domain.


Primers only - no DNA
Primers and tace colony DNA
100bp ladder
1
2
3
150bp band
500bp
400bp
300bp
200bp
100bp

Figure 3.4 Possible formations of dimers and hairpins by neomycin primers, as predicted by OLIGO software. a) The most stable dimer that could occur between the forward and reverse primers. The interaction is predicted to occur between three cytosine residues in the forward primer and corresponding guanine residues in the reverse primer. The reaction has a stabilization energy value of –6.2 kcal/mol .b) The most stable possible hairpin loop that could occur within the forward primer, consisting of an interaction between a four residue sequence (CCTG) at the 5′ end and the complementary residues at the 3′ end of the primer. The reaction has a stabilization energy value of –2.4 kcal/mol. c) The most stable possible hairpin loop that could occur within the reverse primer, consisting of an interaction between four residues (CGAT) and the complementary sequence (GCTA). The reaction has a stabilization energy value of –1.2 kcal/mol.

a)

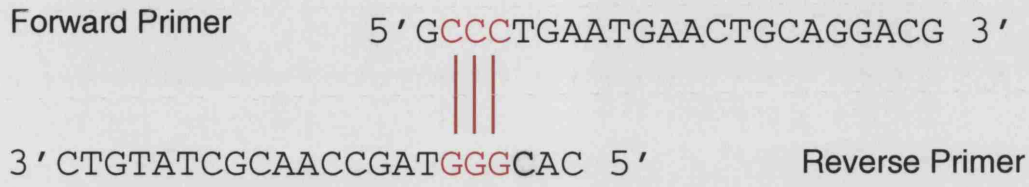
Forward Primer
5′GCCCTGAATGAACTGCAGGACG 3′
3′CTGTATCGCAACCGATGGGCAC 5′
Reverse Primer

b)

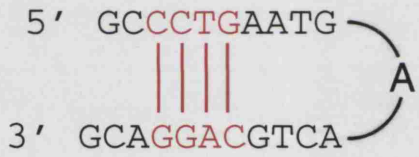
5′ GCCCTGAATG
A
3′ GCAGGACGTCA

c)

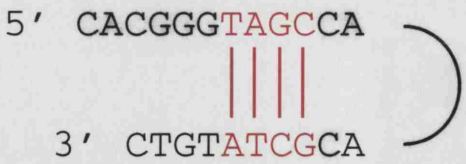
5′ CACGGGTAGCCA
3′ CTGTATCGCA

New primers recognising the neomycin cassette, which were predicted to be less likely to form dimers and hairpins, were designed using the OLIGO software. The resulting primers were as follows:

5′ GGA GAG GCT ATT CGG CTA TG 3′

5′ CAG GAG CAA GGT GAG ATG A 3′

Any possible dimers and hairpins in these sequences were less exothermic than the previous primers. The optimum annealing temperature was calculated to be higher than the melting temperature of the possible dimers and hairpins. The expected PCR product using this primer pair was 281bp in size.

The PCR protocol had to be revised to suit the new primers. A series of PCRs were run using varying concentrations of magnesium chloride ($MgCl_2$) and annealing temperatures around the optimum predicted annealing temperature. The new protocol was established to include the addition of 1 mM of $MgCl_2$ (in addition to that in the PCR buffer) and the following cycle:

5 minute hold at 94°C

Followed by 34 cycles of:

1 minute denaturing at 94°C

1 minute annealing at 59°C

30 seconds extension at 72°C

The Zn primers were also analysed with OLIGO. It was confirmed that the zinc primers were also prone to forming dimers. The most stable dimer (-7.9 kcal/mol) between the forward and reverse primers was a 5bp sequence of TGACC in the upper primer reacting with its complementary residues in the lower primer (figure 3.5a). Although the primers did not form exothermic hairpin stems of longer than 2bp, they were able to form intermolecular dimers. The most stable 3′ dimer (-5.3 kcal/mol) of the forward primer was between the final four residues (GTAC) at the 3′ end, making it particularly vulnerable to extension within the PCR (figure 3.5b). The most stable dimer (-5.3 kcal/mol) overall for the forward primer was a possible interaction between four residues near the 5′ end of the

primer (figure 3.5c). The most stable primer overall (-4.4 kcal/mol) for the reverse primer was between 3bp, GGT, near the 3′ end of the primer (figure 3.5d).

Figure 3.5: Possible formation of dimers by zinc primers, as predicted by OLIGO software. a) The most stable possible dimer between the forward and reverse zinc domain primers. The 5bp bond has a stabilization energy value of –7.9 kcal/mol. b) The most stable 3′ dimer between two strands of the forward primer. The 4bp interaction has a stabilization energy value of –5.3 kcal/mol. c) The most stable intermolecular dimer overall of the forward primer. The 4bp interaction has a stabilization energy value of –6.3 kcal/mol. d) The most stable intermolecular dimer of the reverse primer. The 3bp bond has a stabilization energy value of –4.4 kcal/mol.

a)


5’GAAGCTGACCTGGTTACAACTCATG 3’
3’TCGCCACTGGTGCTCTTATTATTC 5’

b)


5’ GAAGCTGACCTGGTTACAACTCATG 3’
3’ GTACTCAACATTGGTCCAGTCGAAG 5’

c)

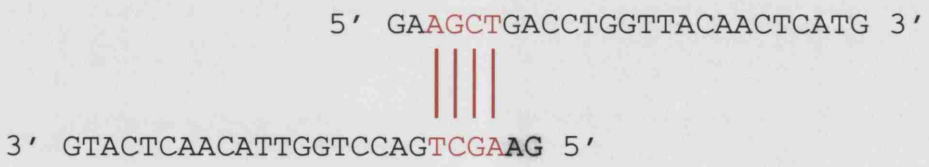
5’ GAAGCTGACCTGGTTACAACTCATG 3’
3’ GTACTCAACATTGGTCCAGTCGAAG 5’

d)

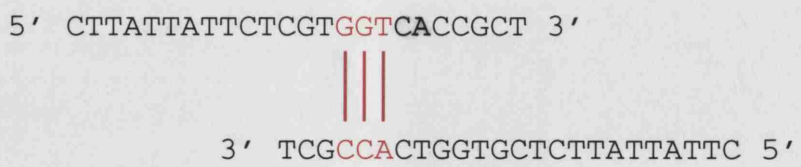
5’ CTTATTATTCTCGTGGTCACCGCT 3’
3’ TCGCCACTGGTGCTCTTATTATTC 5’

Two possible sets of zinc primers were designed to increase the probability of achieving a reproducible PCR reaction. One set of primers had an expected product length of 360bp (set one) and an optimum annealing temperature of 51.7 °C and the other set (set two), an expected product of 292bp and an optimal annealing temperature of 52.4°C. These OLIGO designed primers were tested using the same cycle conditions as described above for the OLIGO designed neomycin primers. Two reactions were run for each primer, one with both the neomycin and the zinc primers in and one with the zinc primers alone. The reactions with both the redesigned neomycin and Zn primers yielded a single band of 281bp relating to the neomycin resistance gene. However, in the reactions with the zinc primers alone there were clear bands of the expected zinc products (product of 360bp and 282bp respectively) in each of the lanes (figure 3.6). Thus, it was decided to run the neomycin and zinc primers in different reactions in future experiments. Although the zinc primers with a 292bp product had the clearest band, it was indistinguishable from the redesigned neomycin primer product (291bp), therefore it was decided to use the primers with the 360bp product. The sequence of the new zinc primers was as follows:
Forward primer 5′ CCA CGA GAA TAA TAA GGT ATG TCT 3′
Reverse primer 5′ AGG AAG AGG AAG GGG ACT A 3′

Genotyping of a series of tail tip biopsies was performed using the new primers, however although the positive controls for these PCRs' consistently worked, the tail reactions were inconsistent. As the positive controls continued to work it was determined that the problem must be in the preparation of the DNA, and hence several different lysis methods were investigated.

Figure 3.6: PCR products from reactions with the OLIGO designed zinc primers. Lane 1 are the products from a reaction where both the redesigned neomycin and zinc primers (set one) were present. There is a band of ~291bp visible – the expected product size for the OLIGO designed neomycin primers – but there is no visible band relating to the size (360bp) of the expected product from the OLIGO designed zinc primers (set one). In lane 2 are the products from a reaction where only the redesigned zinc primers (set one) were present. There is a band of the correct size (360bp) for the expected product for the OLIGO designed zinc primers. Lane 3 are the products from a reaction where both the OLIGO designed neomycin and zinc primers (set two) were present. There is a band of ~291bp visible – the expected product size for the OLIGO designed neomycin primers – but there is no visible band relating to the size (292bp) of the expected product from the OLIGO designed zinc primers (set two). In lane 4 are the products from a reaction where only the redesigned zinc primers (set two) were present. There is a band of the correct size (292bp) for the expected product for the OLIGO designed zinc primers. As the bands present in lane 3 and 4 are indistinguishable from each other, the OLIGO designed zinc primers set two where not used for subsequent reactions. Lanes 5 and 6 are negative controls.

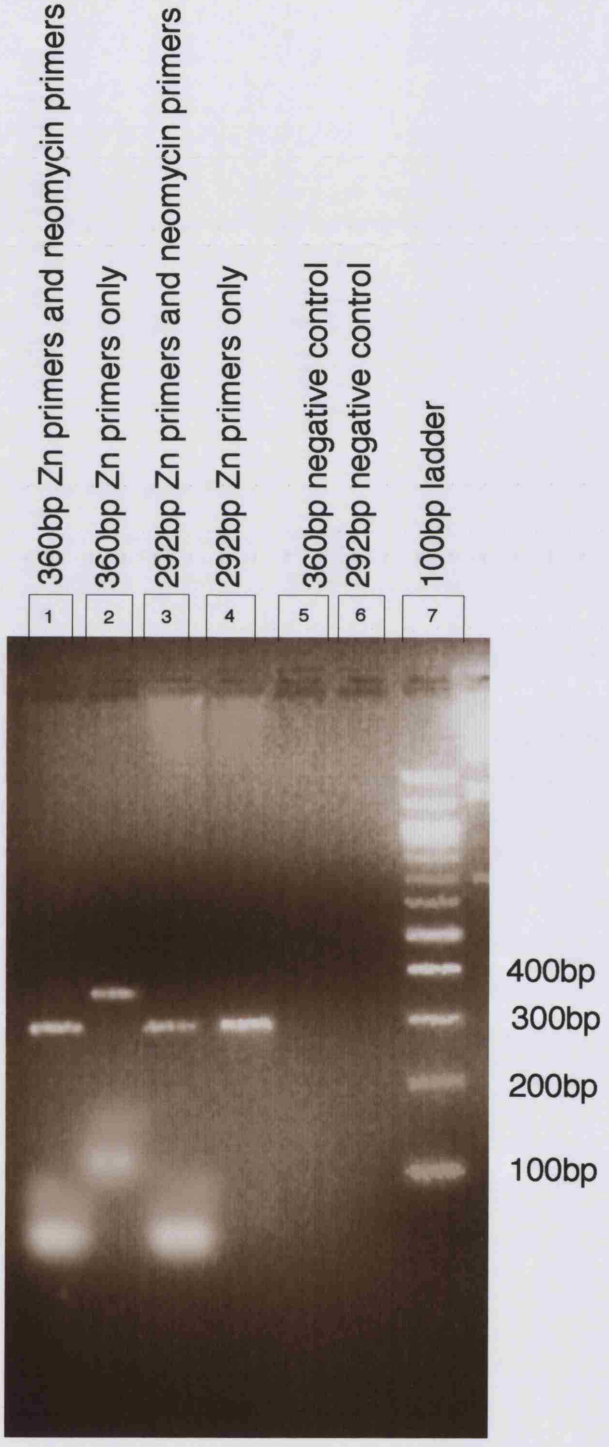
1
360bp Zn primers and neomycin primers
2
360bp Zn primers only
3
292bp Zn primers and neomycin primers
4
292bp Zn primers only
5
360bp negative control
6
292bp negative control
7
100bp ladder
400bp
300bp
200bp
100bp

The first method tested was preparation of DNA from ear punches (chapter 2). The PCR results from the ear punch lysis are shown in figure 3.7. The first batch of ear punches was clear and easy to interpret, however, in later experiments (data not shown) the results were again inconsistent.

It was thought that natural inhibitors within the tissues might be affecting the PCR reactions. A new method was tested that used less than 0.5 mm of tail tip tissue (chapter 2).

Further genotyping was performed using tail tip DNA prepared using the procedure described in Chapter 2: Materials and Methods. Using this method the mice were successfully genotyped (figure 3.8) and heterozygous pairs set up for timed matings. However, as can be seen in the well containing the Zn 360 bp product, there are visible bands under the 360bp band. These bands were present in the majority of the PCR reactions with the new Zn primers. In all reactions the largest of these unexpected bands appears to be slightly smaller than the 281bp neomycin band in the adjacent lane. The presence of unexpected visible bands suggests that, although effective in this investigation, the PCR conditions could be further optimised.

Figure 3.7: PCR products from the ear punch lysis method. Reactions with the OLIGO designed neomycin primers present were run in separate tubes from reactions where the OLIGO designed zinc primers were present. Bands at ~360bp, the size of the expected product of the OLIGO designed zinc primers, is visible from DNA samples (lanes 2,4,6,8,10,12). The absence of a band relating to the neomycin resistance gene from the OLIGO designed neomycin primer reactions of samples 43, 44 and 47 (lanes 1,3, 9), demonstrate that these mice are TACE homozygous ($tace^{+/+}$). The presence of a band of ~281bp from the OLIGO designed neomycin primer reactions of samples 45, 46 and 48 (lanes 5,7,11) indicate the presence of a neomycin cassette and determines that these mice are TACE heterozygous ($tace^{\Delta Zn/+}$). Negative controls (lanes 13,14) and positive controls (lanes 15,16) are also shown.

43 tace colony earpunch DNA
44 tace colony earpunch DNA
45 tace colony earpunch DNA
46 tace colony earpunch DNA
47 tace colony earpunch DNA
48 tace colony earpunch DNA
negative controls
positive controls
100bp ladder
1 2 3 4 5 6 7 8 9 10 11 12 13 14 15 16 17
+ + + + - + - + + + - + – - + –
Zn band 360bp
neomycin band 281bp
500bp
400bp
300bp
200bp
100bp

Figure 3.8: PCR products from the tail lysis method using OLIGO designed primers. In lane 1 there is a band of the expected size (~281bp) of the product from the OLIGO design neomycin primers. In lane 2 there is a band relating to an intact zinc binding domain (~360bp). The presence of both an intact zinc binding domain and a neomycin cassette, determined that this mouse was a TACE heterozygous mouse (*tace*$^{\Delta Zn/+}$). Also present in the lane containing the Zn primer PCR products are unexpected smaller bands suggesting the PCR conditions could be further optimised. Negative controls (lanes 3,4), consisting of a reaction run with no DNA, and a positive control (lanes 5,6), consisting of known heterozygous DNA, are also shown.

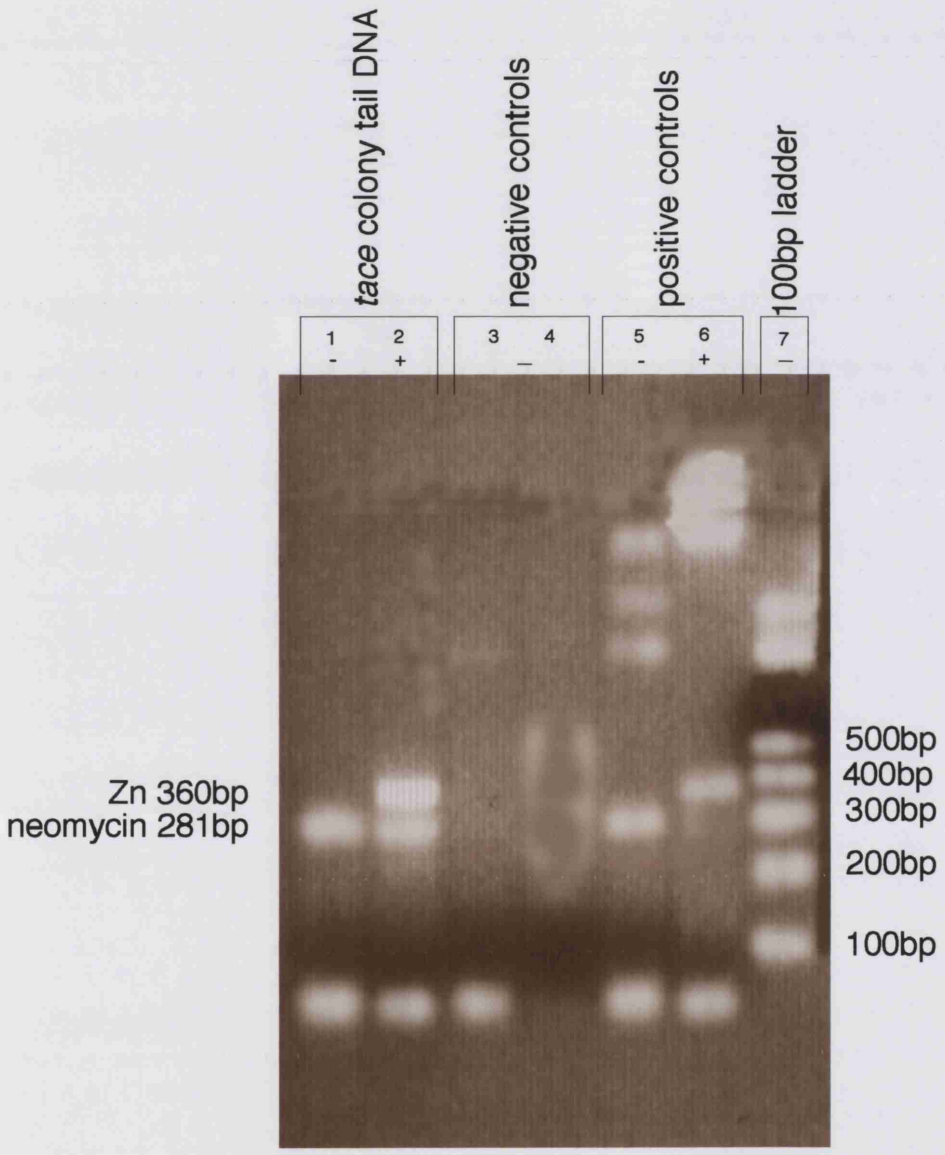
tace colony tail DNA
negative controls
positive controls
100bp ladder
1 -
2 +
3 –
4
5 -
6 +
7 –
Zn 360bp
neomycin 281bp
500bp
400bp
300bp
200bp
100bp

3.2: Timed matings and collection of foetal liver cells

The *tace*$^{\Delta Zn/\Delta Zn}$ embryos die from day 17.5 of gestation (Peschon et al., 1998) and can be distinguished from their littermates by the lack of fused eyelids. Eyelid fusion normally occurs at about day 16.5 of gestation and pup's eyes do not open until approximately 14 days after birth.

Initially, the brain tissue of the collected embryos was genotyped using OLIGO designed neomycin and zinc primers (figure 3.9). Similarly to the results from PCR performed on tail tip DNA, although the embryos could be successfully genotyped, there were a number of smaller bands present in the Zn primer reaction in addition to the expected product of 360bp. However, as brain tissue DNA was analysed, the extraction procedure was far lengthier and the resulting gels were often difficult to interpret. Thus, due to time constraints, embryos were not routinely genotyped and phenotypic selection was used. The disadvantage of phenotypic analyses was that *tace*$^{+/+}$ and *tace*$^{+/\Delta Zn}$ embryos could not be distinguished from each other. Where it had not been distinguished whether the positive control was a heterozygous (*tace*$^{+/\Delta Zn}$) or homozygous (*tace*$^{+/+}$) embryo, the terminology *tace*^{WT} has been used in this report.

The original TACE colony was expanded by mating mice heterozygous for the TACE gene with *tace*$^{+/+}$ mice. Live young from these mating pairs were genotyped. Approximately 50% of live offspring were *tace*$^{+/\Delta Zn}$ and 50% *tace*$^{+/+}$ (as demonstrated in the litter genotyped in figure 3.7: 3/6 *tace*$^{+/\Delta Zn}$ and 3/6 *tace*$^{+/+}$). This was the expected ratio of heterozygous to homozygous offspring from a mating pair of *tace*$^{+/\Delta Zn}$ to *tace*$^{+/+}$. Heterozygous mating pairs identified by genotyping were set up to supply *tace*$^{\Delta Zn/\Delta Zn}$ and control embryos identified phenotypically by eyelid fusion.

Expected ratios of ~25% *tace*$^{\Delta Zn/\Delta Zn}$ embryos were phenotypically identified from collected litters produced from heterozygous mating pairs (actual numbers were 16 out of 77 or 21%).

Embryos were collected at day 16.5 - 17 following the appearance of a vaginal plug (day 0.5). The collected *tace*$^{\Delta Zn/\Delta Zn}$ embryos were identified by phenotypic selection according to the presence of open eyelids – later confirmed by histology (figure 3.10). Littermates of the selected embryos were used as a source of *tace*$^{+/\Delta Zn}$ or *tace*$^{+/+}$ control foetal liver cells. The reliability of phenotypic selection was confirmed by PMA analysis of cells from mice reconstituted with the foetal liver cells. All lymphocytes derived from the foetal liver cells of embryos identified as *tace*$^{\Delta Zn/\Delta Zn}$ either by genotyping and phenotype (n=6) or by phenotype due to the presence of open eyelids only (n=12), failed to shed L-selectin in response to stimulation with PMA. Lymphocytes derived from foetal livers of embryos selected as *tace*^{WT} (*tace*$^{+/\Delta Zn}$ or *tace*$^{+/+}$) responded to stimulation with PMA with rapid shedding of L-selectin –the *tace*$^{+/\Delta Zn}$ response was not distinguishable by this method.

Figure 3.10 shows haematoxylin and eosin (H and E) staining of paraffin embedded sections through the eye of a *tace*$^{+/+}$, tace$^{+/\Delta Zn}$ and *tace*$^{\Delta Zn/\Delta Zn}$ embryo (identified by the genotyping). Peschon et al (1998) described a failure of fusion between the upper and lower eyelids, as well as an attenuated cornea in a 17.5 day *tace*$^{\Delta Zn/\Delta Zn}$ embryo. At 16.5-17 days, there was a failure of eyelid fusion, however, there was no evidence of an attenuated cornea (figure 3.10c). There was no evidence of any phenotypic difference between *tace*$^{+/+}$ and *tace*$^{+/\Delta Zn}$ embryos.

Foetal liver cell suspensions were prepared from the livers removed from the collected embryos and stored in foetal calf serum (FCS) and DMSO at -70°C (chapter 2).

Figure 3.9: Genotypic analysis of DNA from TACE colony embryos. PCR using the OLIGO designed neomycin primers present were run in separate tubes from reactions where OLIGO designed zinc primers were present. Embryos 1 and 5 have a visible reaction product of ~281bp relating to the presence of a neomycin resistance cassette (lanes 1 and 9 respectively). The absence of a band relating to the presence of an intact zinc binding region in lanes 2 and 10 of these samples (embryo 1 and 5 respectively), identified these embryos as *tace*$^{\Delta Zn/\Delta Zn}$. The presence of a band (~281bp) relating to amplification of a neomycin resistance cassette in lane 3, and a band (~360bp) in lane 4 relating to an intact zinc binding domain identified embryo 2 as being of a genotype *tace*$^{\Delta Zn/+}$. The absence of bands (~281bp) relating to amplification of neomycin resistance cassettes in lanes 5 and 7, in addition to the presence of bands (360bp) in lanes 6 and 8, identified embryos 3 and 5, respectively, as being of a *tace*$^{+/+}$ phenotype. Negative controls (lanes 11) are also shown.

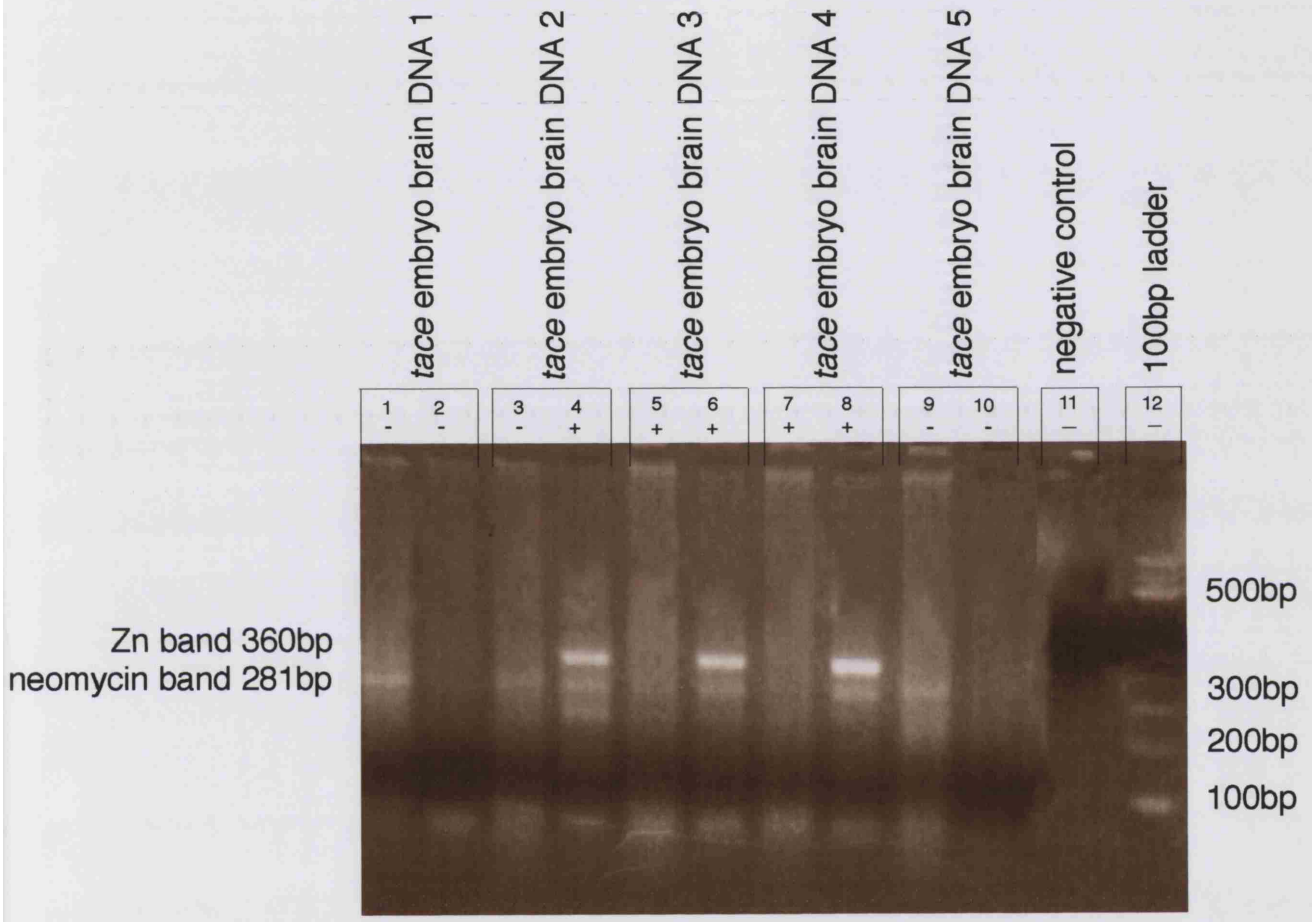
tace embryo brain DNA 1
tace embryo brain DNA 2
tace embryo brain DNA 3
tace embryo brain DNA 4
tace embryo brain DNA 5
negative control
100bp ladder
1 2 3 4 5 6 7 8 9 10 11 12
- - - + + + + + - - - -
Zn band 360bp
neomycin band 281bp
500bp
300bp
200bp
100bp

Figure 3.10: Haematoxylin and eosin stained paraffin embedded sections of eyes from *tace*$^{+/+}$ (a), tace$^{+/\Delta Zn}$ (b), *tace*$^{\Delta Zn/\Delta Zn}$ (c) embryos ($_e$16.5-17). Both *tace*$^{+/+}$ (a) and tace$^{+/\Delta Zn}$ (b) have fused eyelids. Eyelids fuse at approximately 16.5 days of gestation and remain closed until ~14 days after birth. There was a failure in the fusion between upper and lower eyelids (L) in the *tace*$^{\Delta Zn/\Delta Zn}$ embryo (c). Unlike the findings of Peschon et al., (1998) there was no apparent attenuation of the cornea (C).

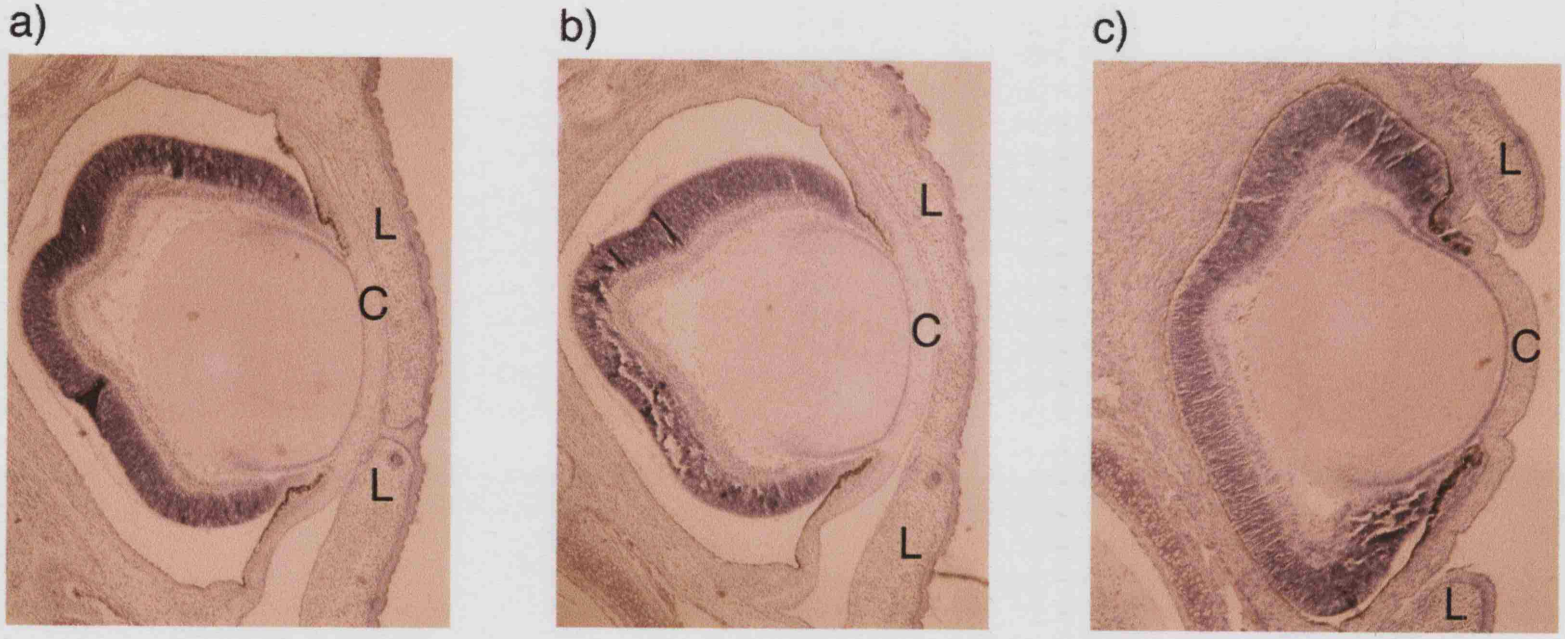
a)
L
C
L
b)
L
C
L
c)
L
C
L

3.3: Production of chimeric mice

The production of chimeric mice involved irradiation of a host mouse followed by intravenous injection of foetal liver or bone marrow cells from the *tace*$^{\Delta Zn/\Delta Zn}$ line (C57BL/6 background) (figure 3.11). The amount of radiation used, and whether they received acid water treatment, depended on the strain of the host. Irradiation is used to destroy the host's own immune system (although some host cells may survive irradiation) and to provide 'niches' within the primary lymphoid organs to enable full reconstitution. Several strains of 'empty' mice (devoid of T and B lymphocytes) were investigated as potential hosts. These 'empty' mice were also irradiated following procedures used by other labs at the NIMR, where it was found that there was incomplete reconstitution if irradiation was not performed; incomplete reconstitution of unirradiated SCID mice was also reported by Fulop and Phillips (1986). Acid water was used, in certain cases, to limit the chance of infection from the water. If acid water was used it was administered for one week prior to irradiation. In most strains neomycin was added to the drinking water for four weeks following irradiation. The administration of this antibiotic, serves to decrease the risk of opportunistic infection whilst the transplanted immune system is reconstituting. For the purpose of this study various strains of host mice were investigated.

Figure 3.11: Generation of chimeric mice. Chimeric mice were generated by irradiaion of a host mouse. The hosts were then intravenously injected with haemopoietic stem cels from TACE colony embryos (C57BL/6 background).

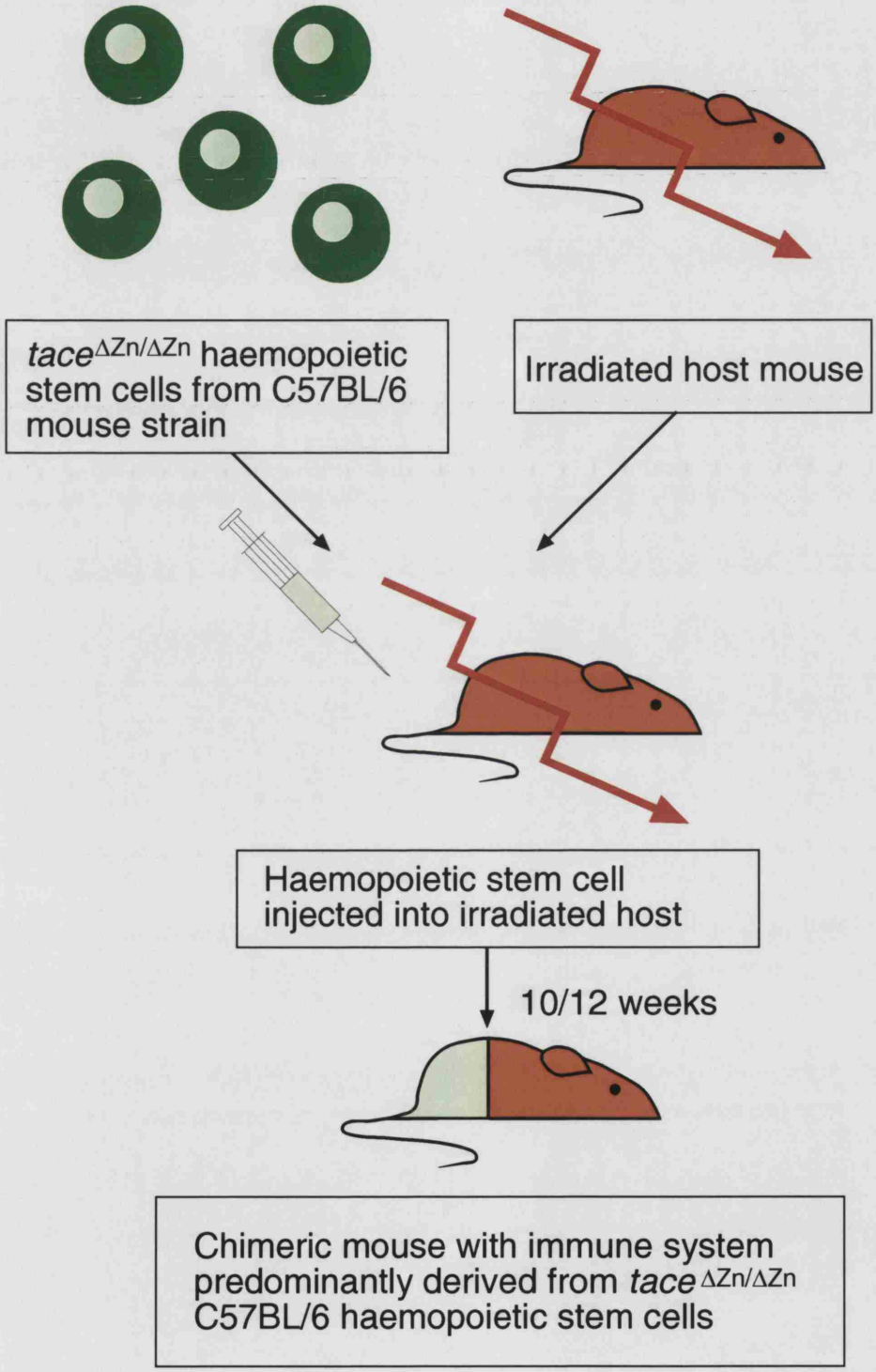
tace$^{\Delta Zn/\Delta Zn}$ haemopoietic stem cells from C57BL/6 mouse strain
Irradiated host mouse
Haemopoietic stem cell injected into irradiated host
10/12 weeks
Chimeric mouse with immune system predominantly derived from *tace*$^{\Delta Zn/\Delta Zn}$ C57BL/6 haemopoietic stem cells

3.4: Host mice strains

The severe combined immunodeficiency (SCID) mouse was investigated to eliminate the presence of any residual T or B lymphocytes following irradiation. The SCID mutation in mice was first described in 1983 (Bosma et al., 1983). SCID mice have a defect in the enzyme DNA-dependent kinase, which binds to double stranded DNA breaks. These occur during antigen receptor gene rearrangement, as well as a consequence of naturally occurring DNA damage. DNA-dependent kinase has a critical role in ligation between the variable, joining and diversity gene segments of immunoglobulin and the TCR chains. Mice with the SCID mutation are unable to undergo antigen receptor rearrangement making them devoid of mature T and B lymphocytes. As the irradiation procedure may not completely remove all host lymphocytes, SCID mice were tested as potential hosts. Although, SCID mice are deficient in T and B lymphocytes, to act a viable host they must undergo some irradiation to reduce the risk of host versus graft reaction mediated by natural killer cells, and to provide niches for developing donor cells. SCID mice, therefore, underwent a reduced rate of irradiation (6 Gy) and were intravenously injected with normal C57BL/6 foetal liver cells. The SCID mutation means that the mice are abnormally sensitive to ionising radiation and this was born out in our studies by excessive mortality rates. It was therefore decided to use other mice as hosts for this procedure.

Due to the possibility of residual host cell populations in the chimeric mice, it is important to have markers that distinguish between host and donor cells. It was therefore decided to investigate the possibility of using a type of C57BL/6 mouse that could be distinguished from donor cells by the presence or absence of two markers, Ly 5.1 and Ly 5.2 (table 3.1).

	Ly 9.1$^+$	*Ly-m11*$^+$ *(S19/8)*	*Ly 5.1*$^+$ *(CD45.1*$^+$*)*	*Ly 5.2*$^+$ *(CD45.2*$^+$*)*
Donor Strain (C57BL/6)	No	Yes	No	Yes
129/Sv	Yes	No	-	-
C57BL/6 (as host)	No	Yes	Yes	No

Table 3.1: Epitope expression in donor and host mice.

Donor cells are Ly 5.2$^+$. C57BL/6 (H2^b) mice positive for the Ly 5.1 epitope were tested as potential hosts, as there is an excellent range of antibodies commercially available to distinguish between the Ly 5.1 and 5.2 epitopes. As these mice have a full immune system, they need to undergo a potentially lethal dose of irradiation (10 Gy) to ensure complete reconstitution. However, the mice died between day 9 and day 14 following irradiation, despite injection of normal C57BL/6 foetal liver cells. Post mortems on the bodies of the dead mice revealed that they had died from severe haemorrhaging and anaemia, symptoms to which the strain are susceptible (Altman and Katz, 1979), and which were probably initiated by the radiation. Due to the sensitivity of these mice, it was decided not to use them as hosts for this study.

129/Sv mice are haplotype matched to the donor cells, H2^b, and encountered few problems associated with irradiation. They are a particularly docile mouse strain making them ideal for tail vein injections. Residual host cells in this strain can be identified by the presence of the Ly 9.1 marker of which donor cells are negative. 129/Sv mice were irradiated with 10 Gy of irradiation given in a split dose of two batches of 5 Gy to minimise gut problems associated with high dose of irradiation, and reconstituted with the C57BL/6 stem cells (either foetal liver or at a later stage, secondary bone marrow transfer), and all data presented in the phenotypic analysis section of this report arose from analysis of the first colony of these chimeric mice. However, the problem with this system is that Ly 9.1, used

to distinguish between the two strains, stains the host 129/Sv cells. Hence, during analysis of the reconstituted mice the donor cells are the negative population in terms of the strain marker.

To improve on the 129/Sv chimera and to eliminate the problem arising from contaminating host cells, the possibility of using immunocompromised mice was again approached. C57BL/10 RAG knockout mice are $H2^b$ matched and have a mutation in the recombination activation gene RAG-1. The enzymes encoded by these genes mediate the rearrangement of the TCR genes and immunoglobulin genes. Like SCIDs, mice with the RAG mutation are deficient in mature T and B lymphocytes due to the inability to successfully rearrange the antigen receptor genes. However, unlike SCID mice the mutation does not affect DNA repair and the mice are not as sensitive to ionising radiation. As the mice have no T and B lymphocytes the dose of radiation does not need to be potentially lethal. The mice were, therefore, irradiated with a sub lethal dose of 5 Gy. They were then injected with foetal liver cells and reconstitution was monitored over 12 weeks. These mice did not receive acid water or neomycin in accordance with the protocol used by other groups at the NIMR reconstituting $RAG^{-/-}$ mice.

L-selectin knockout mice were also used as host mice. The L-selectin knockout is on a C57BL/6 background, thus like the C57BL/6 Ly 5.1^+ mice the strain was prone to haemorrhage and anaemia. To use the L-$selectin^{-/-}$ mice as hosts for the $tace^{\Delta Zn/\Delta Zn}$ foetal liver cells, they were irradiated with a sub lethal dose of 6 Gy and reconstituted for a period of 12 weeks. The L-selectin mutation in these mice makes them ideal for monitoring the role of TACE in L-selectin shedding *in vivo,* as any circulating soluble L-selectin must have originated from the donor cells.

3.5: Summary

Mice heterozygous for the *tace* mutation were set up in timed matings. The appearance of a vaginal plug was taken as day 0.5 and embryos were collected at day 16.5-17 and identified by genotyping or phenotyping. Foetal liver cells from these embryos were intravenously injected into irradiated host mice of various strains. Reconstitution was monitored over 12 weeks, which was followed by a complete phenotypic analysis of 129/Sv chimeric mice.

Chapter 4: Phenotypic Analysis of *tace*$^{\Delta Zn/\Delta Zn}$ Chimeric Mice

The effect of the *tace*$^{\Delta Zn/\Delta Zn}$ mutation on lymphocyte development and function was studied using 129/Sv and RAG$^{-/-}$ chimeric mice. For controls, initial studies utilised 129/Sv mice reconstituted with *tace*$^{+/+}$ or *tace*$^{\Delta Zn/\Delta Zn}$ stem cells identified by genotyping of embryos. In all other studies, where the genotype of the stem cells was not known (see chapter 3), the term *tace*^{WT} has been used to encompass in both *tace*$^{+/+}$ and *tace*$^{+/\Delta Zn}$. *tace*$^{+/+}$ and *tace*$^{+/\Delta Zn}$ are not distinguishable by PMA induced shedding.

The yield and subset composition of lymphocytes harvested from primary and secondary lymphoid organs were determined 12 weeks after reconstitution.

4.1: Cell Yields from Reconstituted Chimeric Mice

Table 4.1 shows the splenic weight and total cell yield from primary and secondary lymphoid organs of 129/Sv and RAG$^{-/-}$ chimeric mice. The TACE mutation had no significant effect on cell yields from the bone marrow, thymus or pooled lymph nodes of 129/Sv chimeric mice. Cell yields were found to be consistent with those of normal 129/Sv and C57BL/6 mice. Pooled lymph node and splenic cell yields from RAG$^{-/-}$ *tace*^{WT} and RAG$^{-/-}$ *tace*$^{\Delta Zn/\Delta Zn}$ chimeric mice were collected and found to be of similar levels to those of the 129/Sv chimeric mice.

	tace$^{+/+}$ *129/Sv Host Cell Yield*	*tace*$^{\Delta Zn/\Delta Zn}$ *129/Sv Host Cell Yield*	*tace*^{WT} *RAG*$^{-/-}$ *Host Cell Yield*		*tace*$^{\Delta Zn/\Delta Zn}$ *RAG*$^{-/-}$ *Host Cell Yield*	
Pooled Lymph Nodes	34 ± 5.0	25 ± 12	22	30	25	29
Thymus	28 ± 4.0	30 ± 7.0	-		-	
Bone Marrow	28 ± 7.0	28 ± 4	-		-	
Spleen	65 ±25	73 ±20	32	48	50	70
Splenic weight (mg± SD)	101 ±22 (n=5)	138 ±36 (n=5)	136 ± 1 (n=4)		104 ± 1 (n=4)	

Table 4.1: The total number of cells in primary and secondary lymphoid organs of 129/Sv and RAG$^{-/-}$ chimeric mice. Cell yields and splenic weights from the reconstituted chimeras were compared. No statistically significant differences were seen between the two groups. Results are average number of cells (donor and host derived) x 10^6 ± SD (n=4-5). Also shown are the average splenic weights in mg ± SD (n=4-5). 129/Sv chimeric mice were reconstituted with stem cells from genotyped embryos. RAG$^{-/-}$ chimeric mice were reconstituted with cells from phenotypically selected embryos. The RAG$^{-/-}$ cell yields shown are two separate experiments.

If L-selectin cleavage is required for effective migration into lymph nodes, and TACE is the enzyme responsible for this cleavage, a decrease in cell yield in the lymph nodes would be expected. However, there are different mechanisms for the migration of cells into different types of lymph nodes. It is possible that lymphocytes, unable to migrate into a particular lymph node, may reroute into a lymph node where L-selectin cleavage is not required. Therefore, although the pooled cell yield may show no effect of the TACE mutation, separate analysis of lymph nodes may show increase yields in certain lymph nodes and reduced yields in others. Thus, cell yields from cervical, axillary, brachial, inguinal, mesenteric lymph nodes and Peyers' patches from the two groups of reconstituted mice were compared. The results from this analysis are shown in table 4.2. From the results it was concluded that there is no effect of the TACE mutation on cell yield from peripheral or gut associated lymphoid organs.

	tace^{WT} *129/Sv Host Cell Yield*	*tace*$^{\Delta Zn/\Delta Zn}$ *129/Sv Host Cell Yield*
Cervical Lymph Node	3.6 ±1.0	5.5 ±0.5
Axillary Lymph Node	2.0 ±0.7	3.0 ±0.7
Brachial Lymph Node	3.8 ±1.3	3 ±1.2
Inguinal Lymph Node	2.0 ±0.7	1.8 ±0.4
Mesenteric Lymph Node	6.0 ±1.0	8.5 ±2.6
Peyer's Patches	2.6 ±1.3	3.5 ±0.3

Table 4.2: Comparison of cell yield in separate lymph nodes in the reconstituted mice. There was no effect of the TACE mutation on cell yield from cervical, axillary, brachial, inguinal, mesenteric lymph nodes or Peyer's Patches. Results are average number of cells (donor and host derived) x 10^6 ± SD (n=4-5).

Splenic weights were recorded because the spleens of mice reconstituted with *tace*$^{\Delta Zn/\Delta Zn}$ foetal liver cells appeared to be visibly larger than those reconstituted with either *tace*$^{+/+}$ or *tace*^{WT} cells. As initial studies showed no significant difference between the splenic weights of the two mice groups (table 4.1), further analysis was performed on a larger number of mice (table 4.3). Results from this analysis showed that the spleens from mice reconstituted with *tace*$^{\Delta Zn/\Delta Zn}$ foetal liver cells where significantly larger than those of the control group.

	tace^{WT}*129/Sv Chimeric Mouse*	*tace*$^{\Delta Zn/\Delta Zn}$*129/Sv Chimeric Mouse*
Splenic weight (mg±SD)	79±22 (p=0.0055)	119±44

Table 4.3: Comparison of splenic weight in mice reconstituted with *tace*^{WT} and *tace*$^{\Delta Zn/\Delta Zn}$ foetal liver cells. The splenic weights of mice reconstituted with *tace*$^{\Delta Zn/\Delta Zn}$ were significantly larger than those of the control *tace*^{WT} group. The p value is the result of a student t test analysis between the two groups of mice. Results are mean weights in mg ± SD (n=23).

4.2: Phenotypic Analysis of Lymphoid Organs in 129/Sv Chimeric Mice

Staining with Ly 9.1 (Lpg100) antibody distinguishes between host (129/Sv) and donor (C57BL/6) mouse strains in the 129/Sv chimeras. The Ly 9.1 epitope is present on 129/Sv lymphocytes but does not stain most myeloid cells (Ledbetter and Herzenberg, 1979). The C57BL/6 strain is negative for Ly 9.1(Ledbetter and Herzenberg, 1979). Primary and secondary lymphoid organs from 129/Sv and C57BL/6 mice were stained with Ly 9.1 (figure 4.1). Greater than 95% of cells in the 129/Sv thymus, lymph nodes and spleen were positive for Ly 9.1 with less cells (~45%) expressing this epitope in the bone marrow. These figures correspond to those found in previous work (Ledbetter et al., 1979; Ledbetter and Herzenberg, 1979). The lower expression seen in the bone marrow is due to the diverse range of cell types found. Ly 9.1 is expressed on all haemopoietic stem cells in the bone marrow and persists during lymphoid development, but is lost during haemopoietic differentiation (Miller et al., 1985).

The primary lymphoid organs (bone marrow and thymus) of the reconstituted mice comprised an average of greater than 97% donor-derived (Ly 9.1$^-$) lymphocytes (figure 4.2a and b). However, lymph nodes and spleen had significant proportions of host derived (Ly 9.1$^+$) cells; on average 22% in lymph nodes and 13% in spleen (figure 4.2c and d).

Figure 4.1: Ly 9.1 staining in 129/Sv and C57BL/6 primary and secondary lymphoid organs. Percentages shown refer to the 129/Sv Ly 9.1^+ cell population. a) FACs analysis of Ly 9.1 staining of 129/Sv and C57BL/6 bone marrow cells. Only 46% of bone marrow cells from the 129/Sv stain positive for Ly 9.1. This is thought to be due to the diverse range of cells found in the bone marrow, whereas in all other organs tested the primary cell type in lymphoid. b) FACs analysis of Ly 9.1 staining of 129/Sv and C57BL/6 thymocytes. Approximately 97% of thymocytes in 129/Sv mice are positive for Ly 9.1. c) FACs analysis Ly 9.1 staining of 129/Sv and C57BL/6 lymph node cells. All 129/Sv lymph node cells are positive for Ly 9.1. d) Ly 9.1 staining of 129/Sv and C57BL/6 splenocytes. Approximately 98% of cells in the 129/Sv spleen are positive for Ly 9.1. There was no Ly 9.1 staining of C57BL/6 cells in any lymphoid organs.

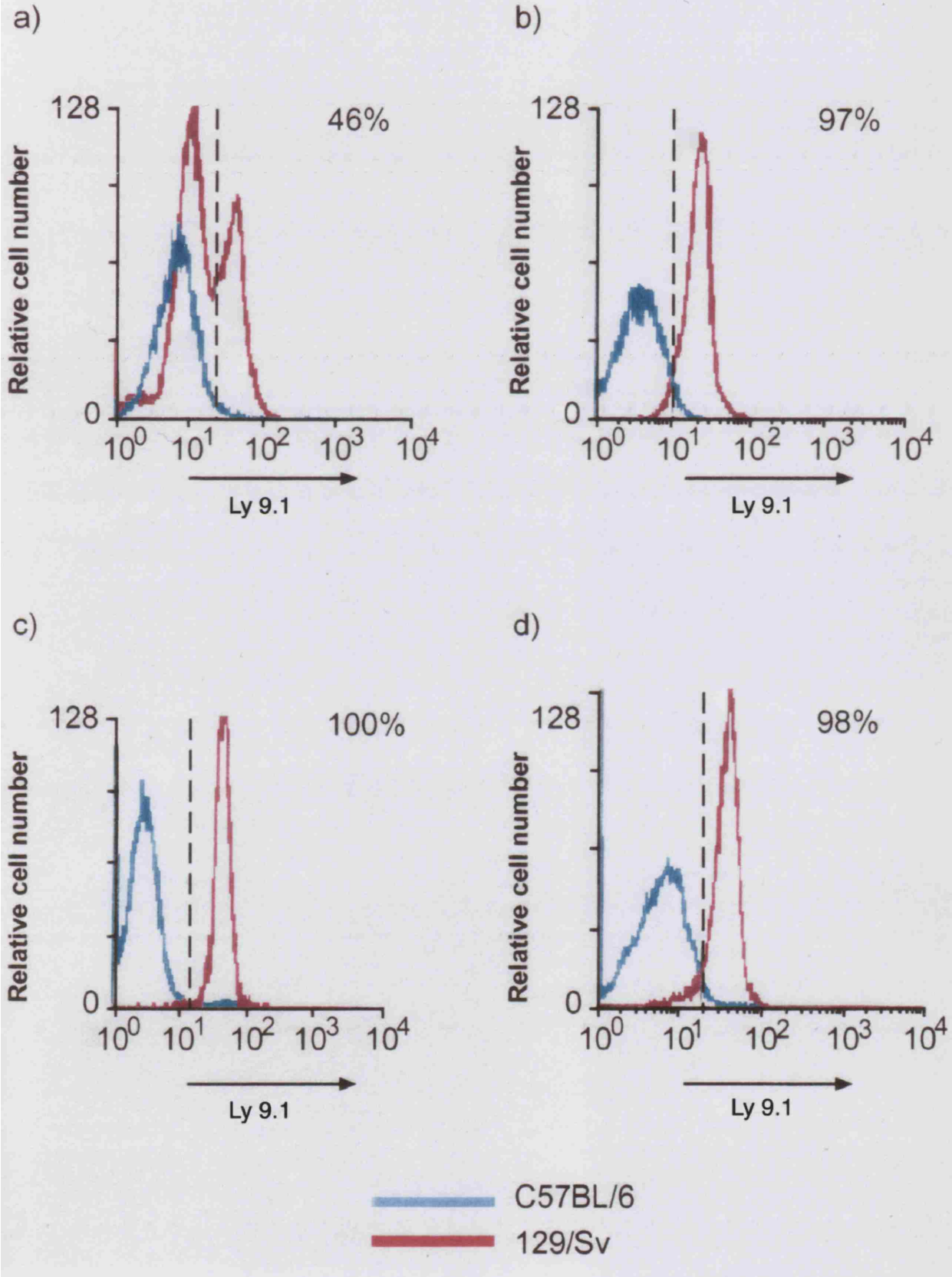
a)
b)
c)
d)
128
0
46%
97%
100%
98%
Relative cell number
10^0 10^1 10^2 10^3 10^4
Ly 9.1
C57BL/6
129/Sv

Figure 4.2: Ly 9.1^+ cells in lymphoid organs from 129/Sv chimeras. Data from one mouse representative of 4 chimeric mice analysed. Percentages refer to FACs analysis of the 129/Sv Ly 9.1^+ cell population. a) Example of Ly 9.1 staining in bone marrow. b) Example of Ly 9.1 staining in the thymus. c) Example of Ly 9.1 staining in pooled lymph nodes. d) Example of Ly 9.1 staining in the spleen. The results indicate that there are few residual host-derived cells in the primary organs of the reconstituted mice, however, there are significant populations of residual host-derived cells in the secondary organs from these mice.

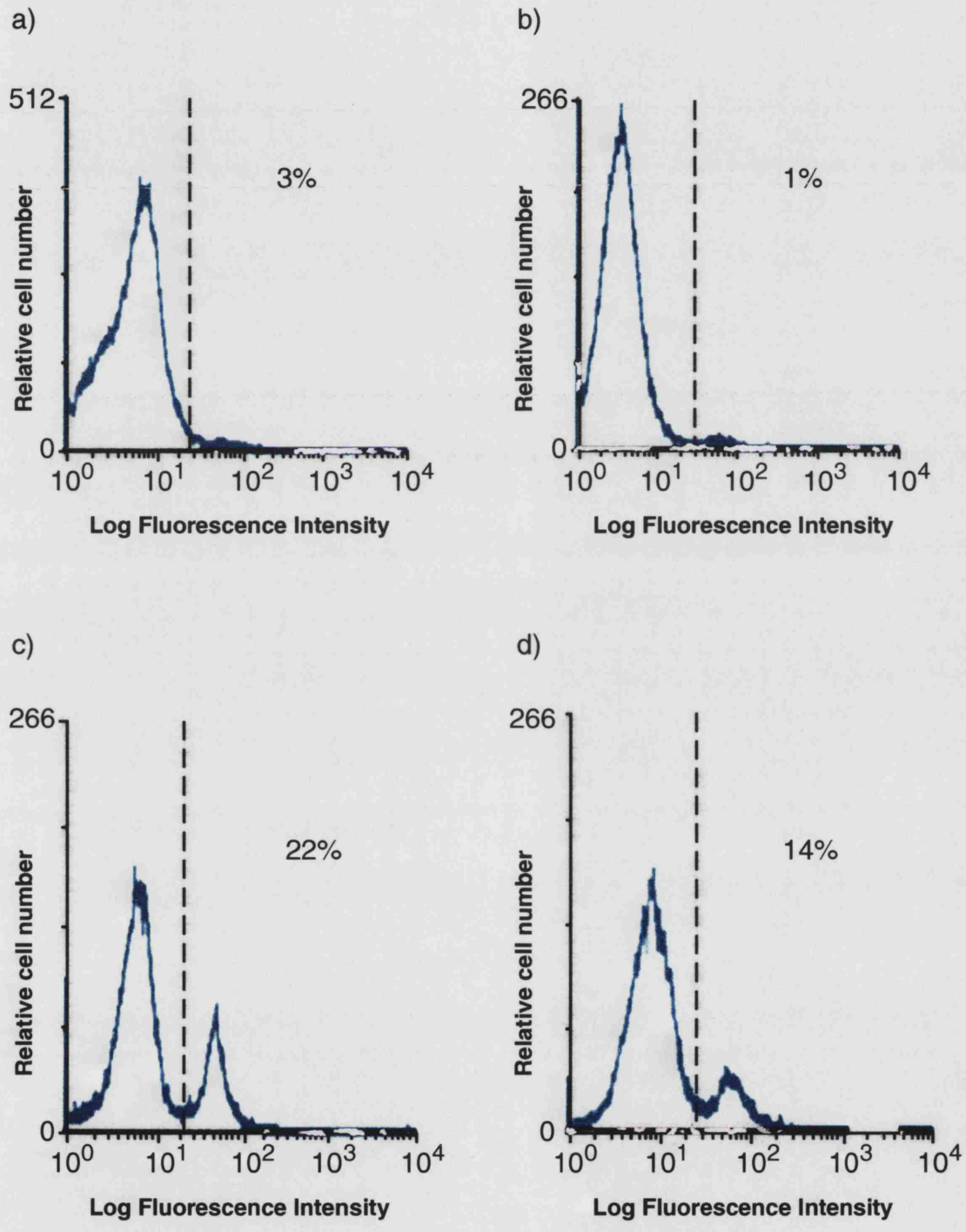
a)
512
3%
Relative cell number
0
10^0 10^1 10^2 10^3 10^4
Log Fluorescence Intensity
b)
266
1%
Relative cell number
0
10^0 10^1 10^2 10^3 10^4
Log Fluorescence Intensity
c)
266
22%
Relative cell number
0
10^0 10^1 10^2 10^3 10^4
Log Fluorescence Intensity
d)
266
14%
Relative cell number
0
10^0 10^1 10^2 10^3 10^4
Log Fluorescence Intensity

Further analysis of lymph node and splenic host derived cells (Ly 9.1^{+}) determined that the majority were T lymphocytes, with almost half the total splenic population of T cells being host derived (figure 4.3). There was no difference between the proportions of host-derived cells in the $tace^{+/+}$ and $tace^{\Delta Zn/\Delta Zn}$ 129/Sv chimeric mice.

Figure 4.3: Proportions of host-derived T and B cells in secondary lymphoid organs of chimeric mice. Each bar is divided to show the fraction of donor (above) and host (below)-derived lymphocytes. Values give the percentage of donor-derived lymphocytes. The results indicate that the majority of the residual host cells were of a T cell phenotype. In the case of the *tace*$^{+/+}$ spleen, 49% of the T cell population was host derived.

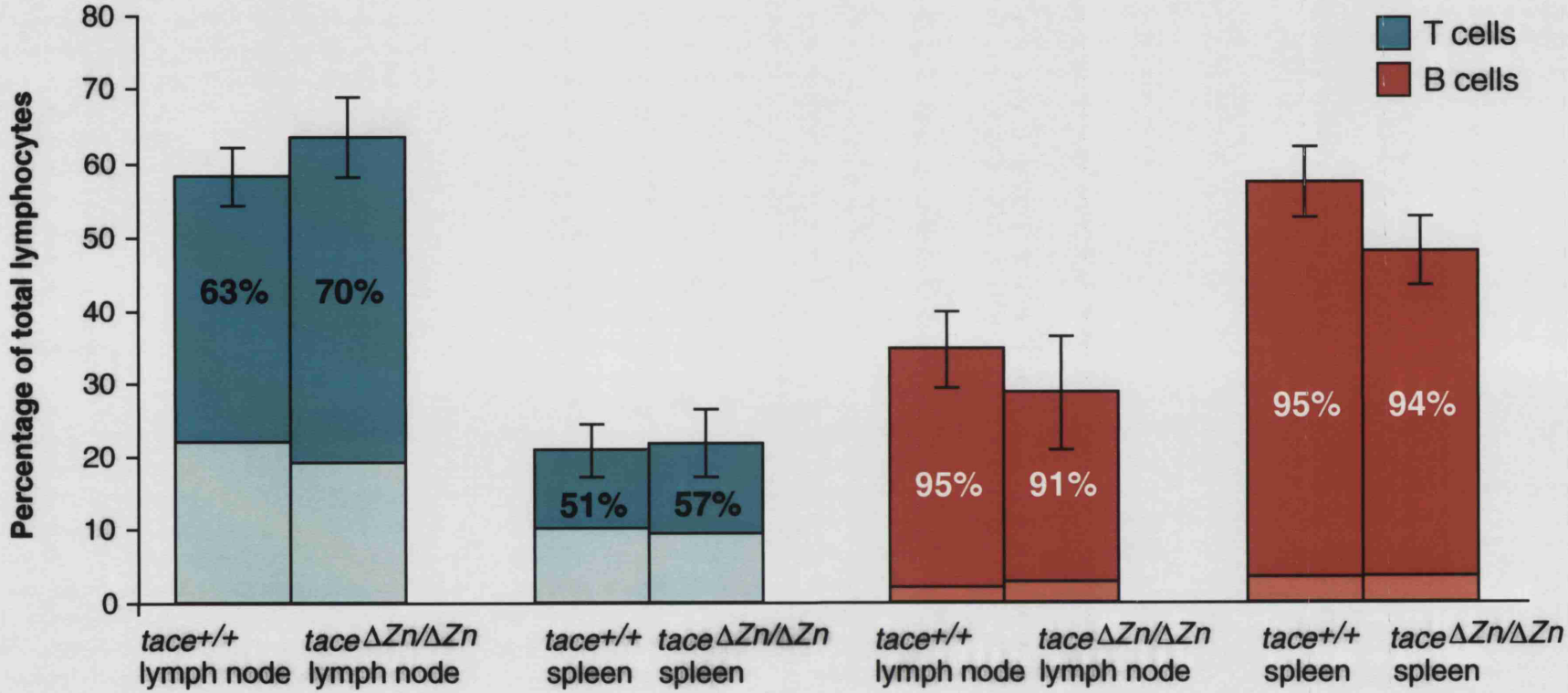
Percentage of total lymphocytes
80
70
60
50
40
30
20
10
0
T cells
B cells
63%
70%
51%
57%
95%
91%
95%
94%
tace+/+ lymph node
tace ΔZn/ΔZn lymph node
tace+/+ spleen
tace ΔZn/ΔZn spleen
tace+/+ lymph node
tace ΔZn/ΔZn lymph node
tace+/+ spleen
tace ΔZn/ΔZn spleen

Donor-derived lymphocytes in *tace*$^{\Delta Zn/\Delta Zn}$ and *tace*$^{+/+}$ reconstituted 129/Sv chimeric mice were analysed for the expression of subset markers and L-selectin (tables 4.4 and 4.5, figures 4.4-4.8). Analyses showed that the proportions of cell subsets in 129/Sv chimeric mice were consistent with those of normal 129/Sv and C57BL/6 mice (data not shown). The percentages of B cells in the bone marrow, T cells subsets in the thymus and T and B cells in the lymph node and spleen showed no significant differences due to the TACE mutation. The number of lymphocytes in each subset expressing L-selectin and the level of expression were not affected by the TACE mutation in lymph node, thymus or spleen (table 4.3). However, subpopulations of total and B220^{+} cells in bone marrow expressed a higher level of L-selectin in all four experiments performed (figure 4.5). When the percentages of B220^{+} cells expressing L-selectin in *tace*$^{+/+}$ and *tace*$^{\Delta Zn/\Delta Zn}$ chimeric mice (table 4.3) were compared using Student t test they were statistically significant with a p value of 0.008. However, this value needs to be adjusted since a total of 16 measurements were made in this analysis. Using the Bonferroni correction a p value of (0.008 x 16) 0.128 is obtained, which is not significant.

	tace$^{+/+}$				*tace*$^{\Delta Zn/\Delta Zn}$			
	BM	***T***	***LN***	***S***	***BM***	***T***	***LN***	***S***
TCR^{+}	2±0.9	22±5	50±3	14±1	4±2	20±2	58±2	15±2
B220^{+}	20±11	0.6±0.3	45±2	67±2	15±4	0.5±0.3	36±8	56±7
CD4^{+}	1±0.2	10±2	26±3	9±0.6	2±1	11±0.8	34±2	9±3
CD8^{+}	1±0.4	14±1	23±2	7±0.8	1±0.3	16±1	24±3	6±1

Table 4.4: Phenotypic analysis of Ly 9.1^{-} lymphocytes in the 129/Sv chimeric mice. Results are average percentage ± S.D (n=4-5). There was no statistically significant phenotypic difference between the mice reconstituted with *tace*$^{+/+}$ cells and those reconstituted with *tace*$^{\Delta Zn/\Delta Zn}$.

	tace$^{+/+}$				*tace*$^{\Delta Zn/\Delta Zn}$			
	BM	***T***	***LN***	***S***	***BM***	***T***	***LN***	***S***
TCR^{+} ***CD62L***$^{+}$	61±13	66±4	90±6	57±30	67±26	74±8	95±2	88±2
B220^{+} ***CD62L***$^{+}$	48±27	62±17	88±2	85±4	76±15	57±24	91±4	90±6
CD4^{+} ***CD62L***$^{+}$	41±37	90±2	87±6	70±4	88±30	95±2	95±5	77±7
CD8^{+} ***CD62L***$^{+}$	43±5	93±3	89±10	83±5	64±30	92±4	97±1	89±3

Table 4.5: L-selectin expression on Ly 9.1^{-} lymphocyte subsets in the 129/Sv chimeric mice. Results are average percentage of cells positive for L-selectin ± S.D (n=4-5). There was no statistically significant difference in L-selectin expression between the mice reconstituted with *tace*$^{+/+}$ cells and those reconstituted with *tace*$^{\Delta Zn/\Delta Zn}$.

Figure 4.4: Phenotypic analysis of 129/Sv chimeric bone marrow Ly 9.1$^-$ cells. Results are shown as FACs plots. i) B220$^+$ Lymphocyte population in *tace*$^{+/+}$ bone marrow. ii) B lymphocyte population in *tace*$^{\Delta Zn/\Delta Zn}$ bone marrow. iii) L-selectin expression on total bone marrow cells. iv) L-selectin expression on B220$^+$ cells in bone marrow. Higher levels of L-selectin expression on B220$^+$ Ly 9.1$^-$ cells in the reconstituted bone marrow are apparent from the histogram.

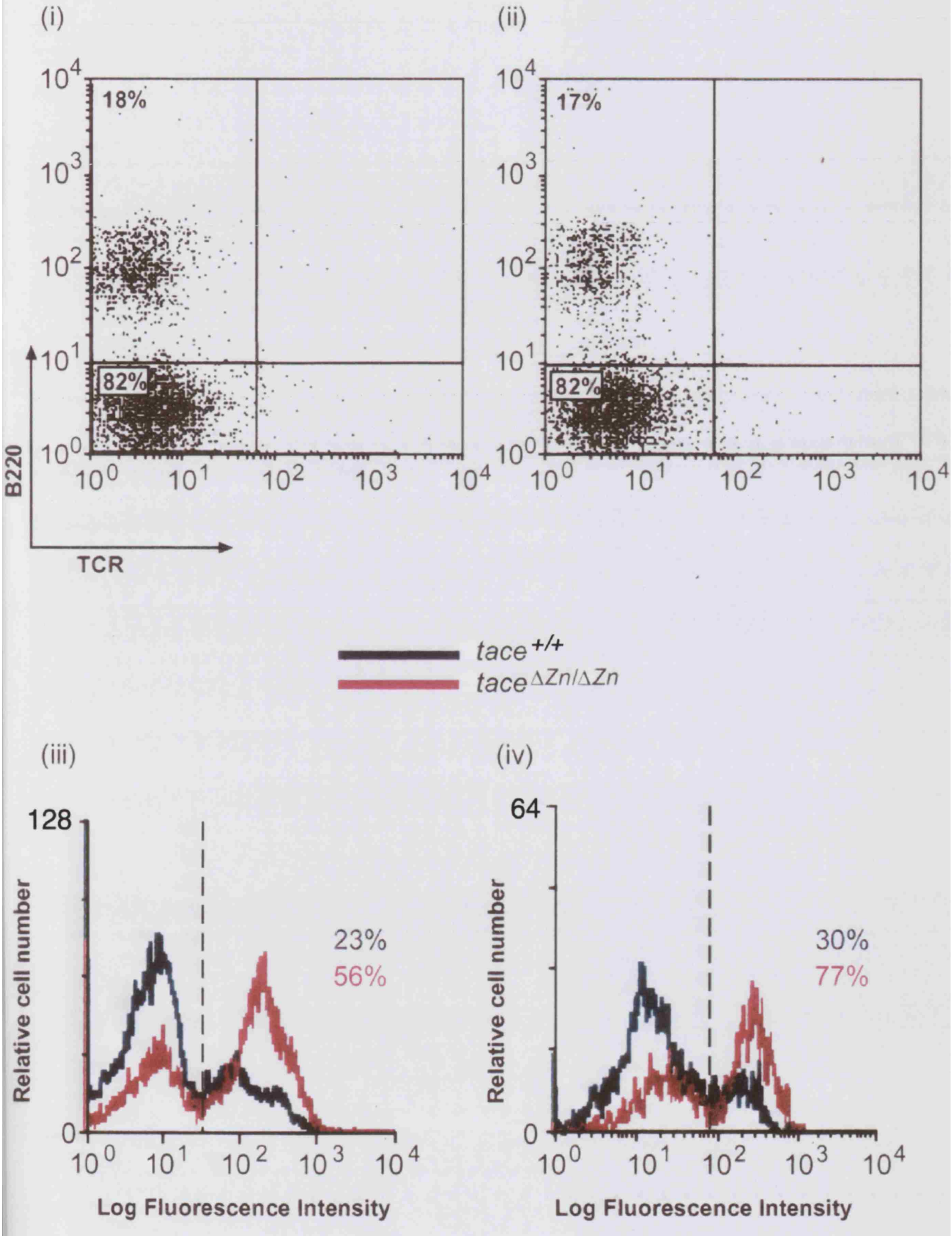
(i)
(ii)
18%
17%
82%
82%
B220
TCR
tace+/+
taceΔZn/ΔZn
(iii)
(iv)
128
64
Relative cell number
23%
56%
30%
77%
Log Fluorescence Intensity

Figure 4.5: Expression of L-selectin on $B220^+$ Ly 9.1^- bone marrow cells from chimeric mice. Histograms show the levels of L-selectin expression on the $B220^+$ Ly 9.1^- cells in the reconstituted mice. Although not statistically significant following Bonferroni correction, the histogram profiles from all 4 experiments suggest that there is higher expression of L-selectin on $tace^{\Delta Zn/\Delta Zn}$ $B220^+$, Ly 9.1^- bone marrow cells than $tace^{+/+}$ cells.

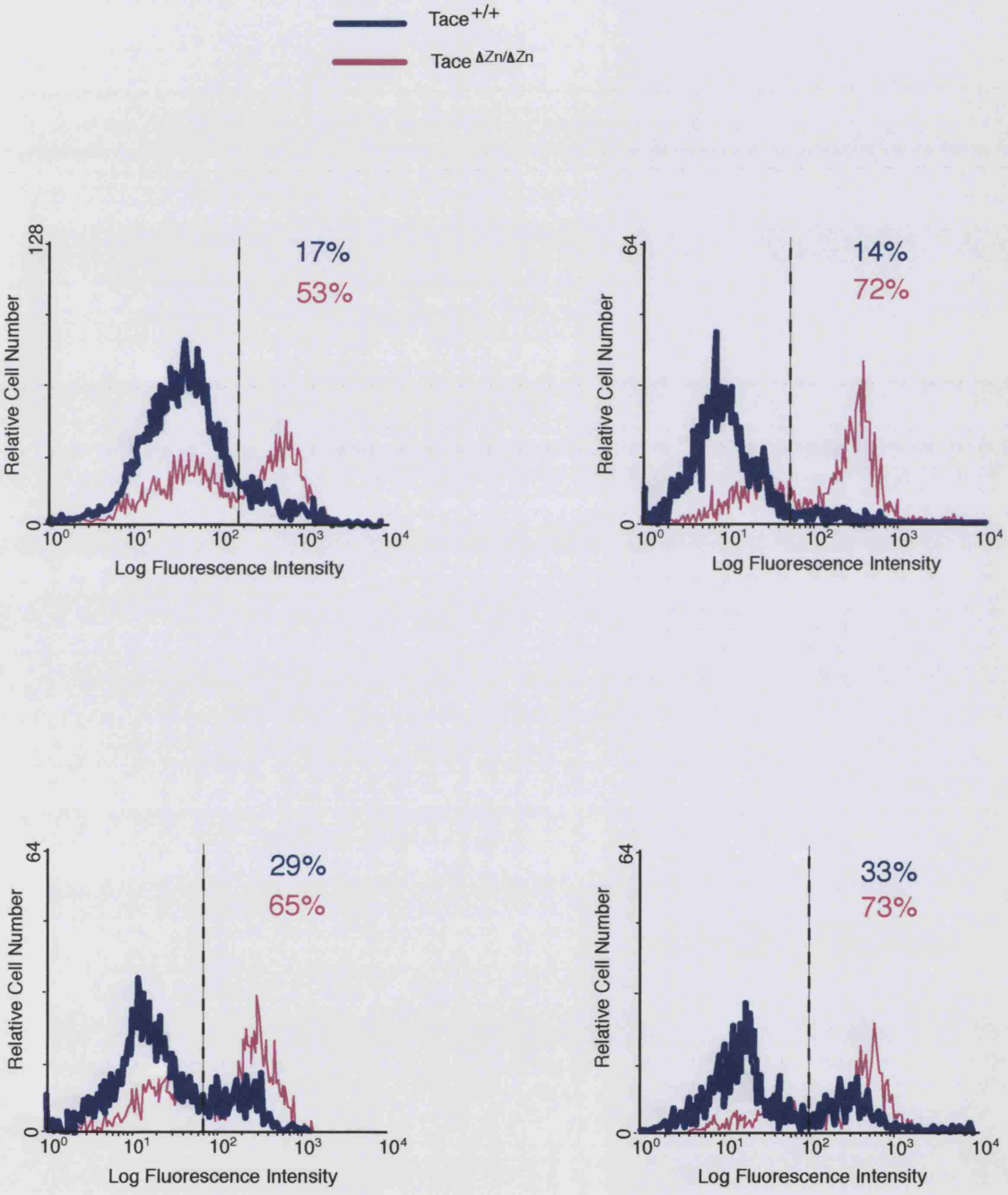
Tace +/+
Tace ΔZn/ΔZn
17%
53%
14%
72%
29%
65%
33%
73%
Relative Cell Number
Log Fluorescence Intensity
0
64
128
10^0
10^1
10^2
10^3
10^4

Figure 4.6: Phenotypic analysis of Ly 9.1$^-$ (donor-derived) thymocytes from129/Sv chimeric mice.Results are shown as FACs analysis plots. i) CD4 and CD8 expression on *tace*$^{+/+}$ thymocytes. ii) CD4 and CD8 expression on *tace*$^{\Delta Zn/\Delta Zn}$ thymocytes. iii) L-selectin expression on CD8 single positive lymphocytes. iv) L-selectin expression on double positive thymocytes. v) L-selectin expression on double negative (CD4$^-$CD8$^-$) thymocytes. vi) L-selectin expression on CD4 single positive thymocytes.

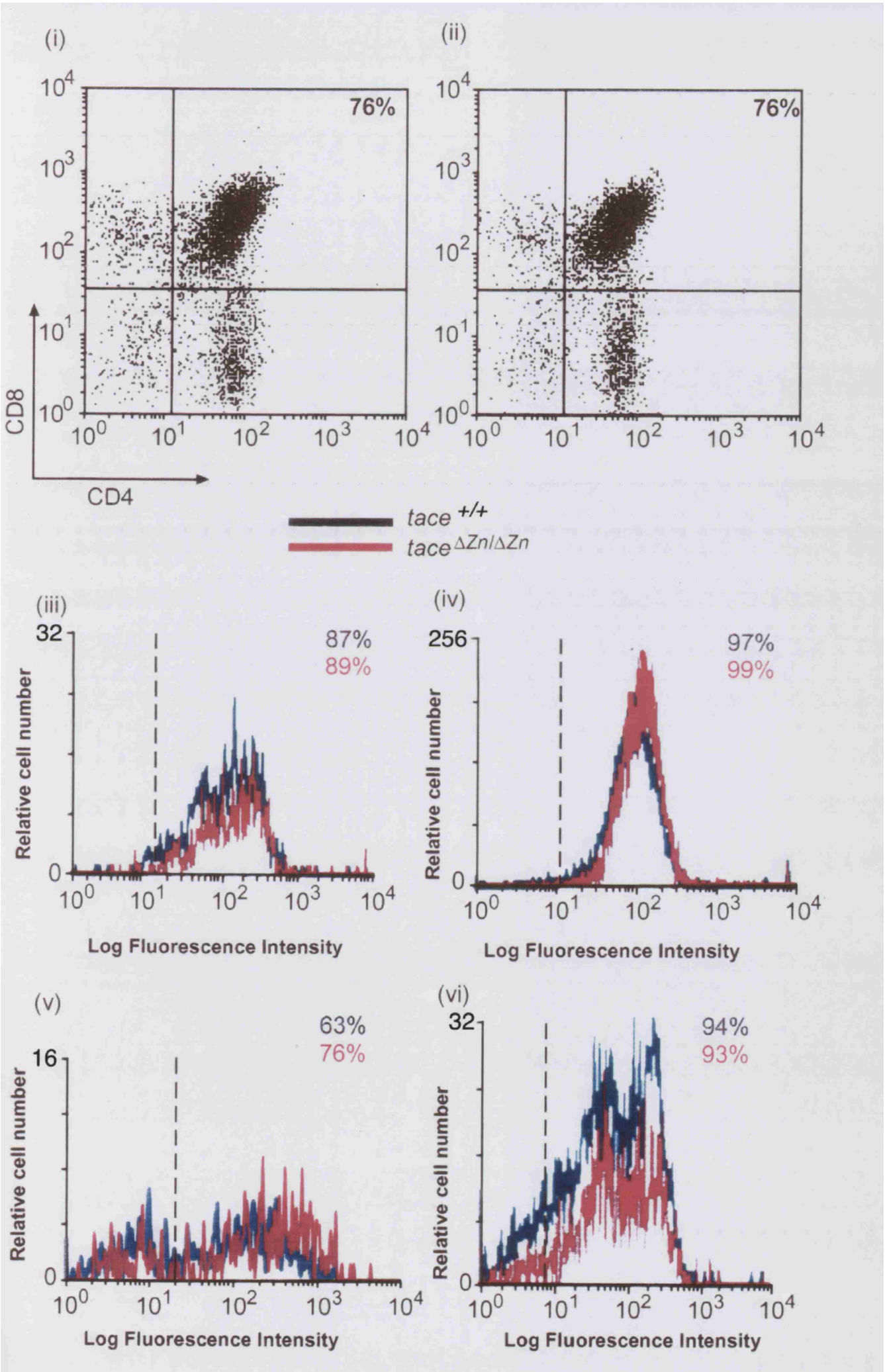
(i)
(ii)
76%
76%
CD8
CD4
tace +/+
tace ΔZn/ΔZn
(iii)
(iv)
87%
89%
97%
99%
Relative cell number
Log Fluorescence Intensity
(v)
(vi)
63%
76%
94%
93%

Figure 4.7: Phenotypic analysis of lymph nodes from 129/Sv chimeric mice. i) CD4 and CD8 expression on *tace*$^{+/+}$ lymph node cells. ii) CD4 and CD8 expression on *tace*$^{\Delta Zn/\Delta Zn}$ lymph node cells. iii) L-selectin expression on total lymph nodes cells. iv) L-selectin expression on B lymphocytes. v) L-selectin expression on CD4 positive lymphocytes. vi) L-selectin expression on CD8 positive lymphocytes.

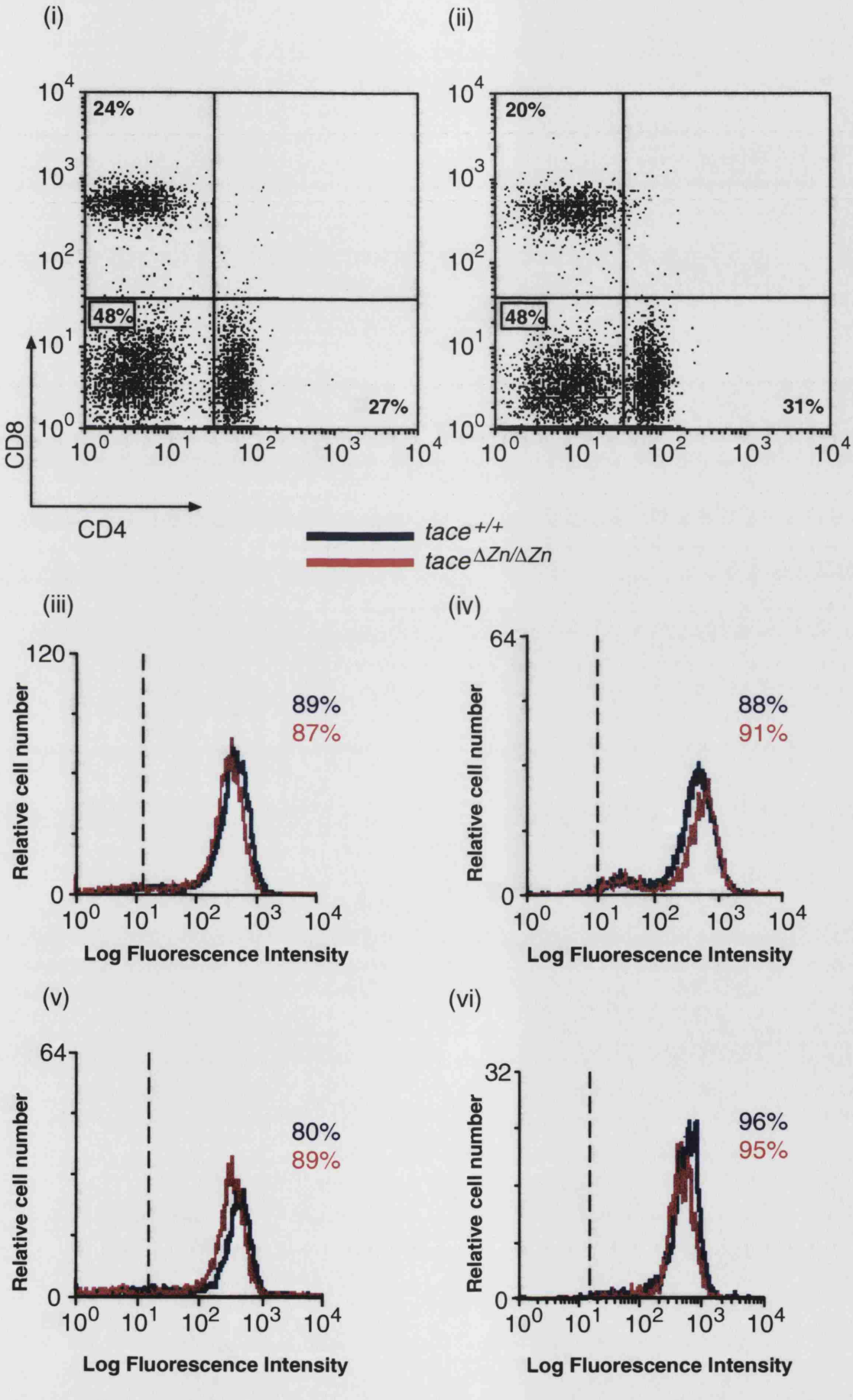
(i)
(ii)
24%
48%
27%
20%
48%
31%
CD8
CD4
tace+/+
taceΔZn/ΔZn
(iii)
(iv)
89%
87%
88%
91%
Relative cell number
Log Fluorescence Intensity
(v)
(vi)
80%
89%
96%
95%

Figure 4.8: Phenotypic analysis of Ly 9.1$^-$ splenic cells from 129/Sv chimeric mice i) CD4 and CD8 expression on *tace*$^{+/+}$ splenocytes. ii) CD4 and CD8 expression on *tace*$^{\Delta Zn/\Delta Zn}$ splenocytes. iii) L-selectin expression on total splenocytes. iv) L-selectin expression on B splenocytes. v) L-selectin expression on CD4 positive splenocytes. vi) L-selectin expression on CD8 positive splenocytes.

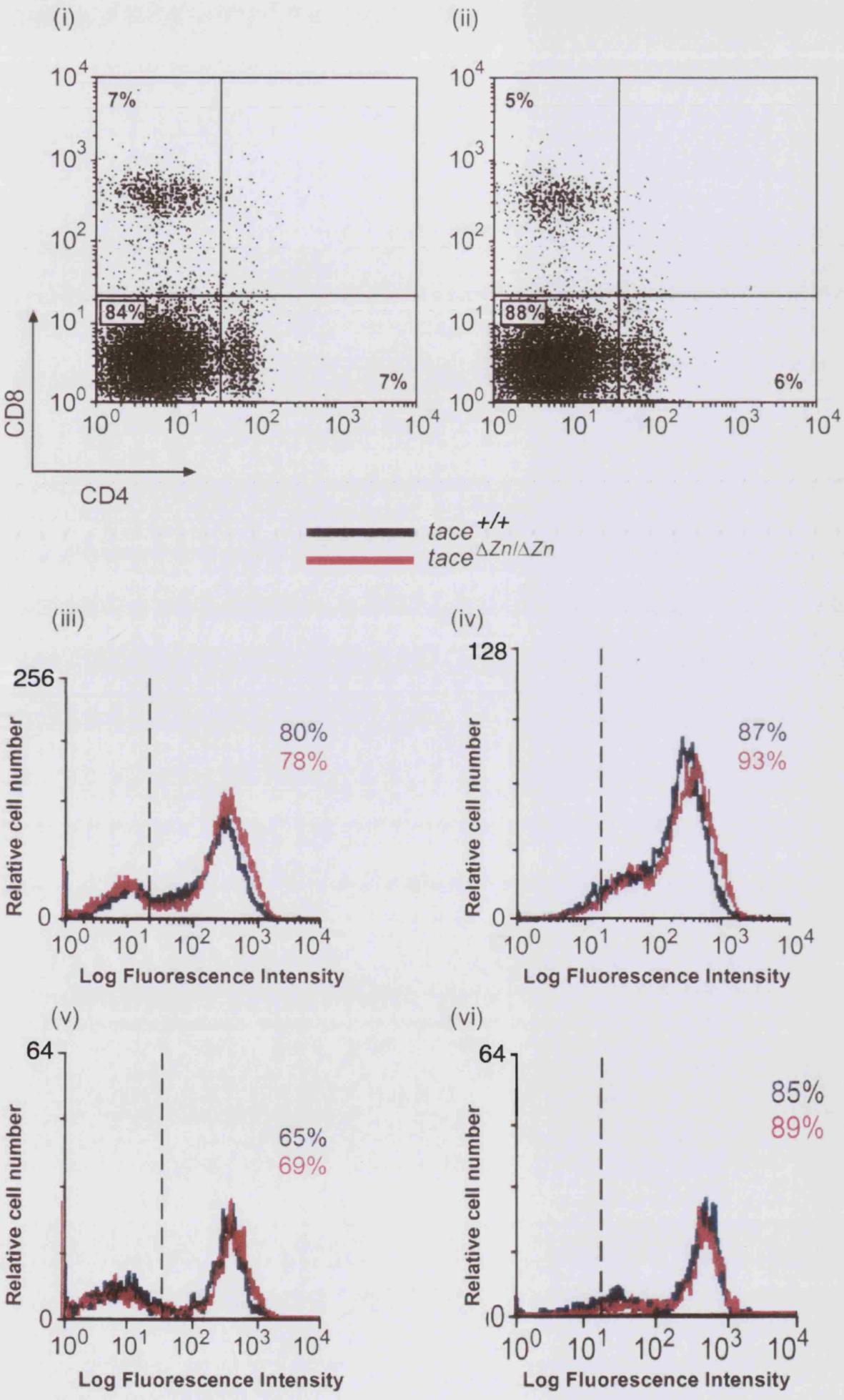
(i)
(ii)
7%
84%
7%
5%
88%
6%
CD8
CD4
tace+/+
taceΔZn/ΔZn
(iii)
(iv)
(v)
(vi)
Relative cell number
Log Fluorescence Intensity
80%
78%
87%
93%
65%
69%
85%
89%

Peripheral lymph node sections were stained using fluorescently labelled anti-TCR and anti-B220 antibodies to determine the localization of T and B cells in chimeric mice. Lymph node structure and morphology within T and B cell areas showed no obvious differences between the *tace*$^{+/+}$ and *tace*$^{\Delta Zn/\Delta Zn}$ chimeric mice (figure 4.9). In both cases there was evidence of good reconstitution of the lymph nodes following the irradiation process.

Figure 4.9: Fluorescent staining of peripheral lymph nodes from *tace*$^{+/+}$ and *tace*$^{\Delta Zn/\Delta Zn}$ 129/Sv chimeric mice. Sections were stained for HEV using MECA-79 (red), T and B cells using anti-TCR and anti-B220 respectively (green). a) Anti-TCR staining of *tace*$^{+/+}$ lymph node section showing two HEV within the T cell area. b) Anti-TCR staining of *tace*$^{\Delta Zn/\Delta Zn}$ lymph node section showing an HEV running through a T cell area. c) Anti- B220 staining of a *tace*$^{+/+}$ lymph node section. B lymphocytes can be seen inside HEV and scattered throughout the paracortex. d) Anti-B220 staining of a *tace*$^{\Delta Zn/\Delta Zn}$ lymph node. HEV at the edge of a B cell area is visible.

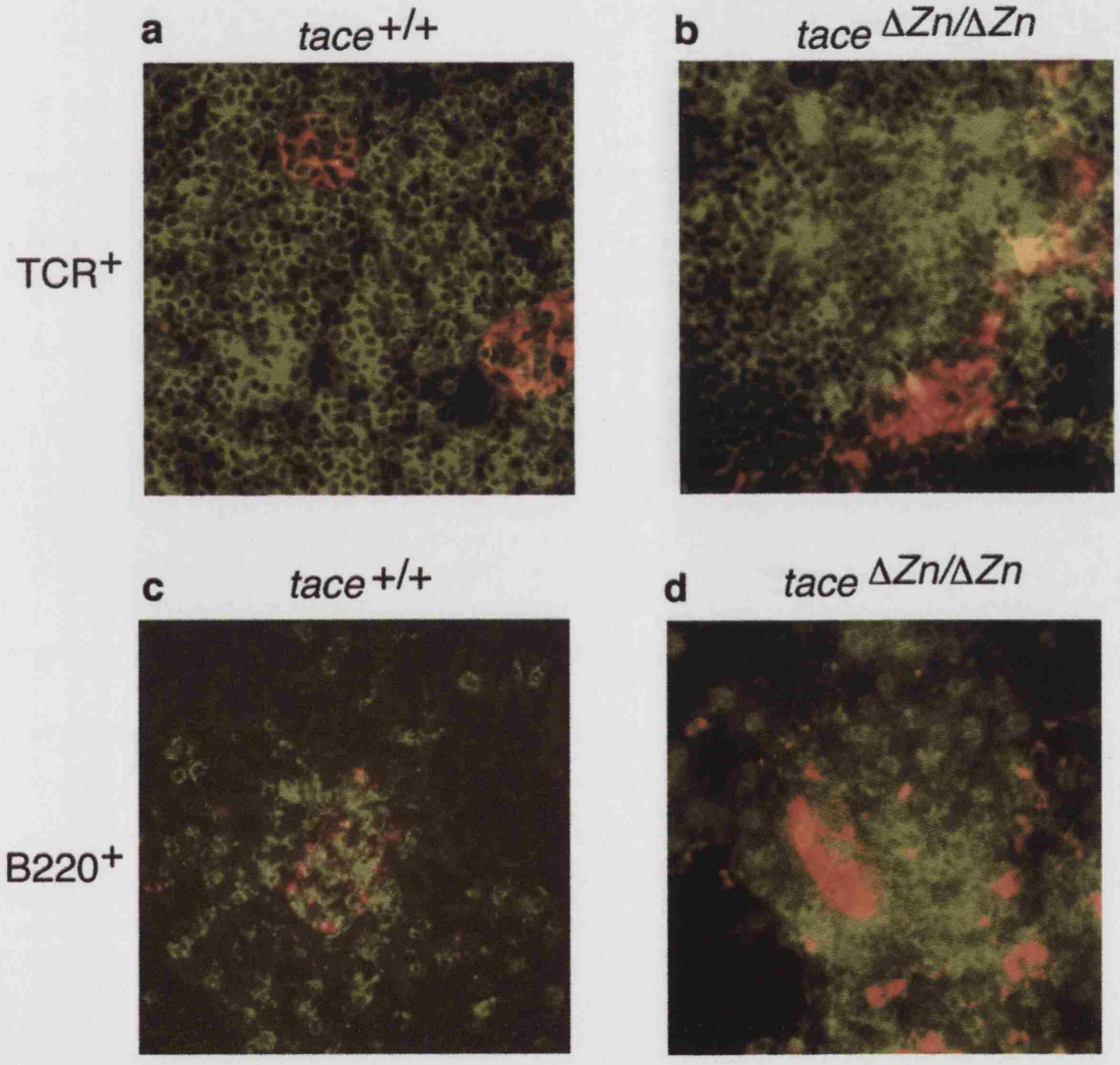
a
tace+/+
b
tace ΔZn/ΔZn
TCR+
c
tace+/+
d
tace ΔZn/ΔZn
B220+

4.3: β_2 Microglobulin Analysis of Spleen and Bone Marrow

Results of the phenotypic analysis suggested that the TACE mutation affected the spleen and bone marrow of reconstituted 129/Sv mice. It was decided to perform further analysis of these organs by looking at the distribution of non-lymphoid cells. As discussed previously, the Ly 9.1 marker does not stain myeloid cells, hence a new marker had to be found to distinguish donor-derived myeloid cells from host-derived cells.

The S19/8 anti-mouse β_2- microglobulin monoclonal antibody recognizes an epitope (Ly-m11) present in certain mouse strains (Tada et al., 1980). β_2-microglobulin in the C57BL/6 mouse strain is positive for Ly-m11, whereas the 129/Sv mouse strain is negative (Kurtz et al., 1985; Tada et al., 1980). β_2-microglobulin is a polypeptide chain, non-covalently associated with the MHC Class I molecule. As MHC Class I is expressed on almost all nucleated cells, it was expected to positively stain all donor-derived cells within the lymphoid organs of 129/Sv chimeras, including myeloid derived cells.

Total cells from lymph node, spleen and bone marrow of normal 129/Sv and C57BL/6 mice were stained with anti-Ly-m11 (figure 4.10). Greater than 95% of cells in the C57BL/6 lymph node and spleen stained positively for Ly-m11 (figure 4.10a-b). Greater than 87% of cells in the C57BL/6 bone marrow stained positively for Ly-m11 (figure 4.10c). As expected, cells from all three lymphoid organs of 129/Sv mice did not express the Ly-m11 epitope.

Figure 4.10: Anti-Ly-m11 (S19/8) staining of 129/Sv and C57BL/6 bone marrow, spleen and lymph node. a) Total bone marrow cells in the C57BL/6 mouse positively stain for the β_2-microglobulin epitope Ly-m11. The expression of β_2-microglobulin varies across the population with a small proportion of cells having lower fluorescence intensity crossing into the 129/Sv negative peak. b) Total C57BL/6 splenocytes positively stain for Ly-m11. The fluorescence intensity peak is distinct from the negative peak of 129/Sv splenocytes. c) Total cells from C57BL/6 lymph nodes have a high level of β_2-microglobulin fluorescence intensity clearly distinct from that of the negative 129/Sv cells.

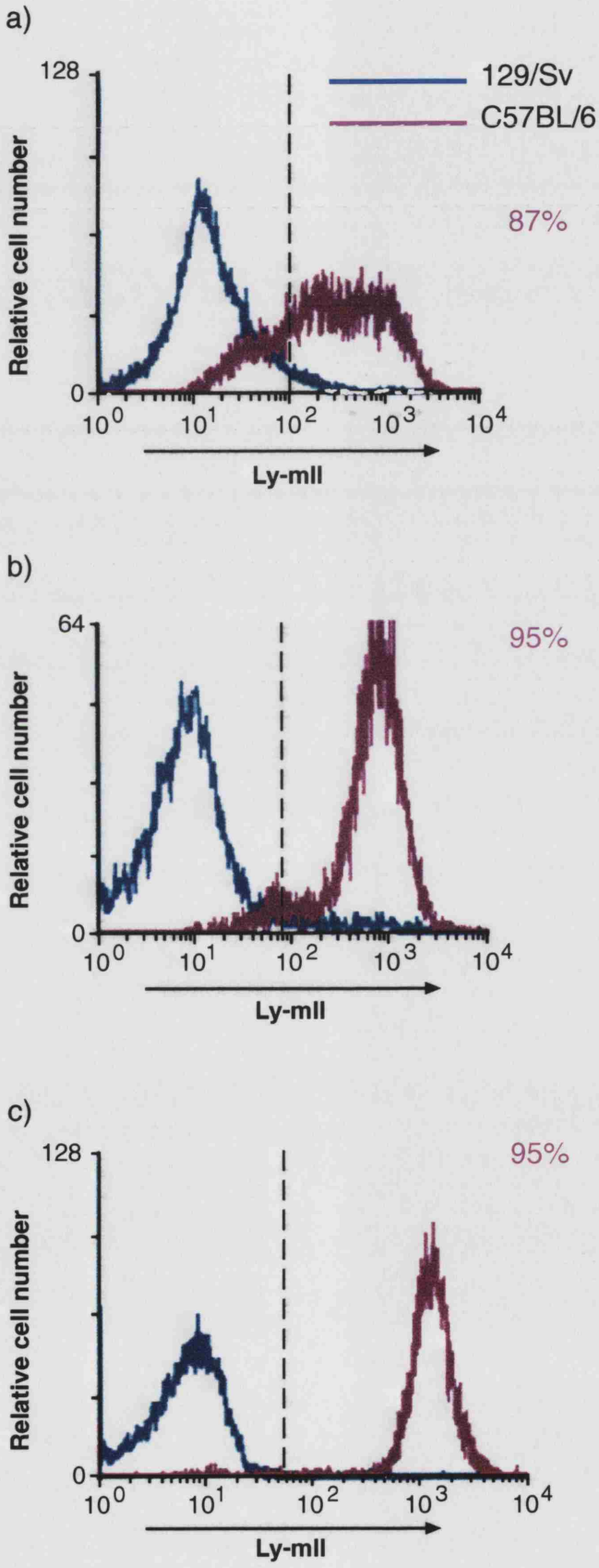
a)
128
129/Sv
C57BL/6
87%
Relative cell number
0
10^0 10^1 10^2 10^3 10^4
Ly-mII
b)
64
95%
Relative cell number
0
10^0 10^1 10^2 10^3 10^4
Ly-mII
c)
128
95%
Relative cell number
0
10^0 10^1 10^2 10^3 10^4
Ly-mII

The bone marrow of reconstituted 129/Sv mice comprised of an average of 59% Ly-m11 positive cells (figure 4.11a). Secondary lymphoid organs (lymph nodes and spleen) comprised of greater than 84% Ly-m11 positive (donor-derived) cells (figure 4.11b and c).

Figure 4.11: Ly-m11$^+$ cells in lymphoid organs from 129/Sv chimeras. Data from one mouse representative of 5 chimeric mice analysed. Percentages refer to 129/Sv Ly-m11$^+$ cell population. a) Example of Ly-m11 staining in bone marrow. b) Example of Ly-m11 staining in the thymus. c) Example of Ly-m11 staining in pooled lymph nodes. d) Example of Ly-m11 staining in the spleen. The results indicate that both primary and secondary lymphoid organs have both donor-derived (Ly-m11$^+$) and host-derived (Ly-m11) cell populations.

a)

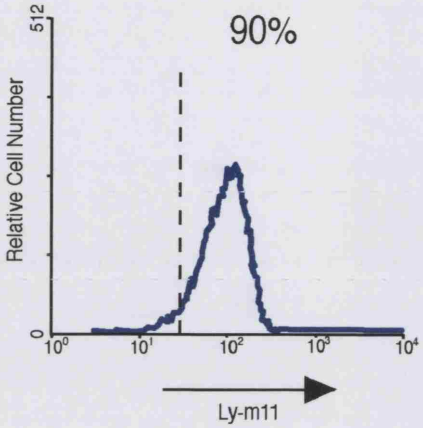
90%
512
Relative Cell Number
0
10^0
10^1
10^2
10^3
10^4
Ly-m11

b)

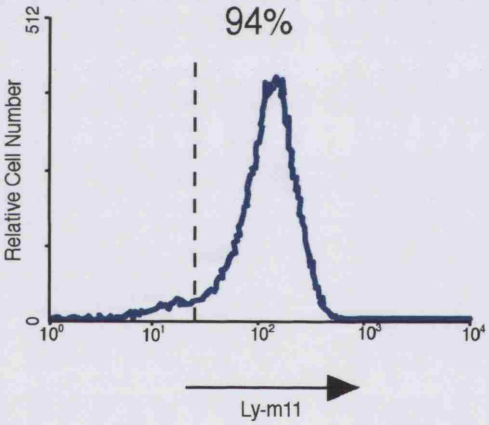
94%
512
Relative Cell Number
0
10^0
10^1
10^2
10^3
10^4
Ly-m11

c)

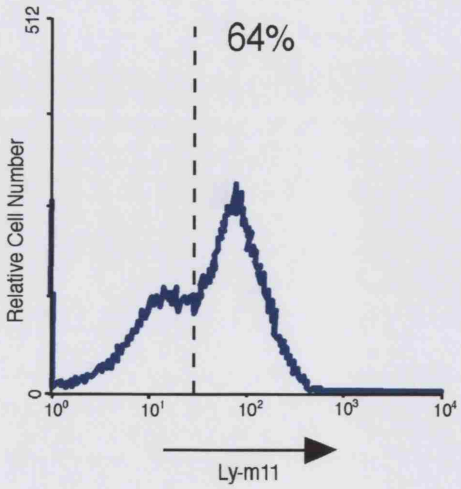
64%
512
Relative Cell Number
0
10^0
10^1
10^2
10^3
10^4
Ly-m11

4.4: Ly-m11 Analysis of Bone Marrow Cells from 129/Sv Chimeras

The increased number of L-selectin positive cells seen in the *tace*$^{\Delta Zn/\Delta Zn}$ bone marrow has previously been shown to be due, in part, to an increase in L-selectin expression on the B220^{+} population. Further analysis was carried to determine if the TACE mutation affected L-selectin expression on other subpopulations including cells of myeloid linage.

The morphology of total cells within the bone marrow of *tace*^{WT} and *tace*$^{\Delta Zn/\Delta Zn}$ 129/Sv chimeric mice was analysed (figure 4.11). A higher proportion of *tace*$^{\Delta Zn/\Delta Zn}$ cells were of a larger more granular cell type (increased side scatter). Previous analyses described in this report were performed on samples gated on the small cell (lower levels of side scatter) population, as this gate was thought to contain mostly lymphocytes. The larger cell population contains most of the myeloid-derived cells with a small number of lymphocytes (table 4.4). An average of 59% of cells in the *tace*^{WT} bone marrow were of a large cell type and 70% of cells in the *tace*$^{\Delta Zn/\Delta Zn}$. When the percentages of cells of a large cell type cells in *tace*$^{+/+}$ and *tace*$^{\Delta Zn/\Delta Zn}$ chimeric mice (table 4.6) were compared using Student t test they were statistically significant with a p value of 0.02. However, this value needs to be adjusted since a total of 4 measurements were made in this analysis. Using the Bonferroni correction a p value of (0.02 x 4) 0.08 is obtained, which is not significant.

Figure 4.12: Cell distribution in *tace*^{WT} and *tace*$^{\Delta Zn/\Delta Zn}$ 129/Sv chimeric bone marrow. a) Example of cell distribution in *tace*^{WT} bone marrow. Approximately, 60% of cells within the chimeric bone marrow were of a "large cell" type (i.e. increased side scatter). b) Example of cell distribution in *tace*$^{\Delta Zn/\Delta Zn}$ bone marrow. Approximately, 70% of cells within the chimeric bone marrow were of a "large cell" type (i.e. increased side scatter).

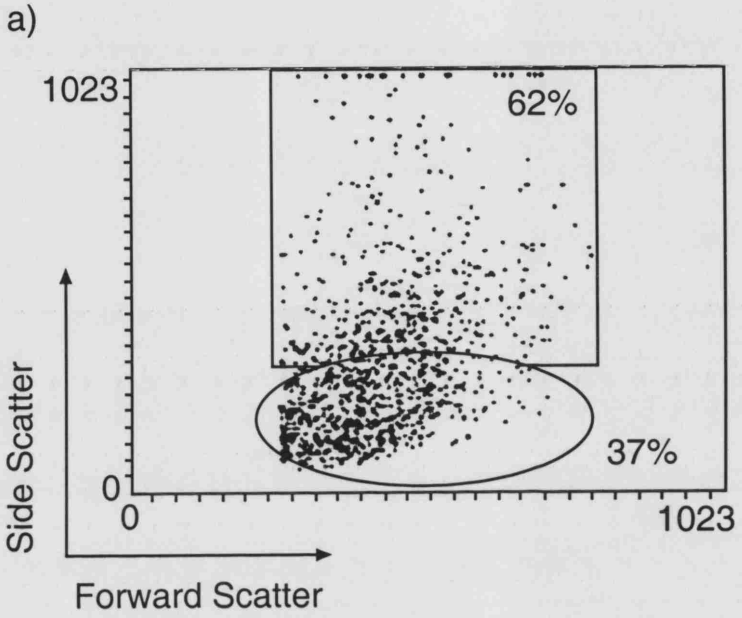
a)
1023
62%
37%
0
0
1023
Side Scatter
Forward Scatter

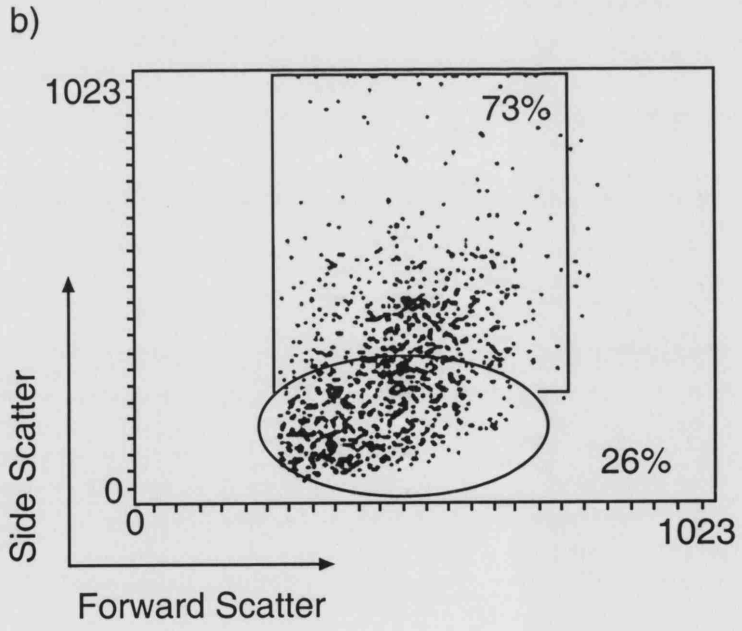
b)
1023
73%
26%
0
0
1023
Side Scatter
Forward Scatter

Further analysis of donor-derived (S19/8$^+$) bone marrow cells was performed using the neutrophil marker 7/4, and a granulocyte marker, Gr.1 (against myeloid differentiation epitope Ly-6G). As Gr.1 stains all granulocytes, including neutrophils, Gr.1 positive but neutrophil marker 7/4 negative cells were studied for expression levels of L-selectin in addition to total Gr.1 positive and neutrophil marker positive cells. The Gr.1 positive but 7/4 negative population of cells was assumed to comprise mainly of monocytes.

There was no difference in the proportion of myeloid cell types within the large cell subpopulation of the bone marrow due to the TACE mutation (table 4.6 and figure 4.13a-b). However, there were significantly more L-selectin positive S19/8$^+$ Gr.1 positive *tace*$^{\Delta Zn/\Delta Zn}$ cells (Bonferroni corrected p=0.003) (table 4.7 and figure 4.13c). However, the number of L-selectin positive S19/8$^+$ donor-derived *tace*$^{\Delta Zn/\Delta Zn}$ neutrophils, identified using the 7/4 marker, was not increased. Increase in the Gr.1$^+$ population was due to donor-derived *tace*$^{\Delta Zn/\Delta Zn}$ non-neutrophil myeloid cells. This was confirmed by a significant increase in L-selectin positive monocytes (Gr.1 positive, 7/4 negative) (Bonferroni corrected p=0.0015) (table 4.7 and figure 4.13d).

	$tace^{WT}$	$tace^{\Delta Zn/\Delta Zn}$
Cells of a large cell type	59 ± 8	70 ± 6 (p=0.08)
$Gr.1^+$	88 ± 4	89 ± 3
$Gr.1^+$ $7/4^-$	15 ± 2	15 ± 4
$7/4^+$	73 ± 4	73 ± 8

Table 4.6: Phenotypic analysis of donor-derived myeloid cells in the bone marrow large cell population. Results are average percentage ± S.D (n=5). After applying the Bonferroni correction to the student t test, there was no statistically significant effect of the TACE mutation on total cell distribution or donor-derived non-myeloid cells.

	$tace^{WT}$	$tace^{\Delta Zn/\Delta Zn}$
$Gr.1^+$ $CD62L^+$	90 ± 5	99 ± 0.7 (p=0.03)
$Gr.1^+$ $7/4^-$ $CD62L^+$	81 ± 5	94 ± 3 (p=0.0015)
$7/4^+$ $CD62L^+$	90 ± 5	97 ± 4

Table 4.7: L-selectin expression on myeloid subsets within the bone marrow large cell population. Increased expression of L-selectin was seen on $S19/8^+$ non-neutrophil myeloid $tace^{\Delta Zn/\Delta Zn}$ cells. Results are average percentage of cells positive for L-selectin ± S.D (n=5). The student t Test p values shown are a comparison between $tace^{WT}$ and $tace^{\Delta Zn/\Delta Zn}$. P values were adjusted in accordance with the Bonferroni correction.

Figure 4.13: Example of analysis of large non-lymphoid S19/8^{+} bone marrow cells in 129/Sv chimeric mice (representative of n=5). a) Gr.1 and neutrophil marker expression on *tace*^{WT} cells. b) Gr.1 and neutrophil marker expression on *tace*$^{\Delta Zn/\Delta Zn}$ cells. No effect of the TACE mutation was seen on myeloid linage cells within the bone marrow of the reconstituted mice. c) L-selectin expression on neutrophil marker positive cells. There was no significant difference seen between L-selectin expression on donor-derived neutrophils from mice reconstituted with *tace*^{WT} or *tace*$^{\Delta Zn/\Delta Zn}$ foetal liver cells. d) L-selectin expression on Gr.1 positive cells. Increased L-selectin expression on donor-derived *tace*$^{\Delta Zn/\Delta Zn}$ cells, is consistent with the increased levels seen on donor-derived *tace*$^{\Delta Zn/\Delta Zn}$ non-neutrophil myeloid cells. e) L-selectin expression on Gr.1 positive, neutrophil marker negative cells. Significantly higher levels of L-selectin expression were observed on donor-derived *tace*$^{\Delta Zn/\Delta Zn}$ non-neutrophil myeloid cells.

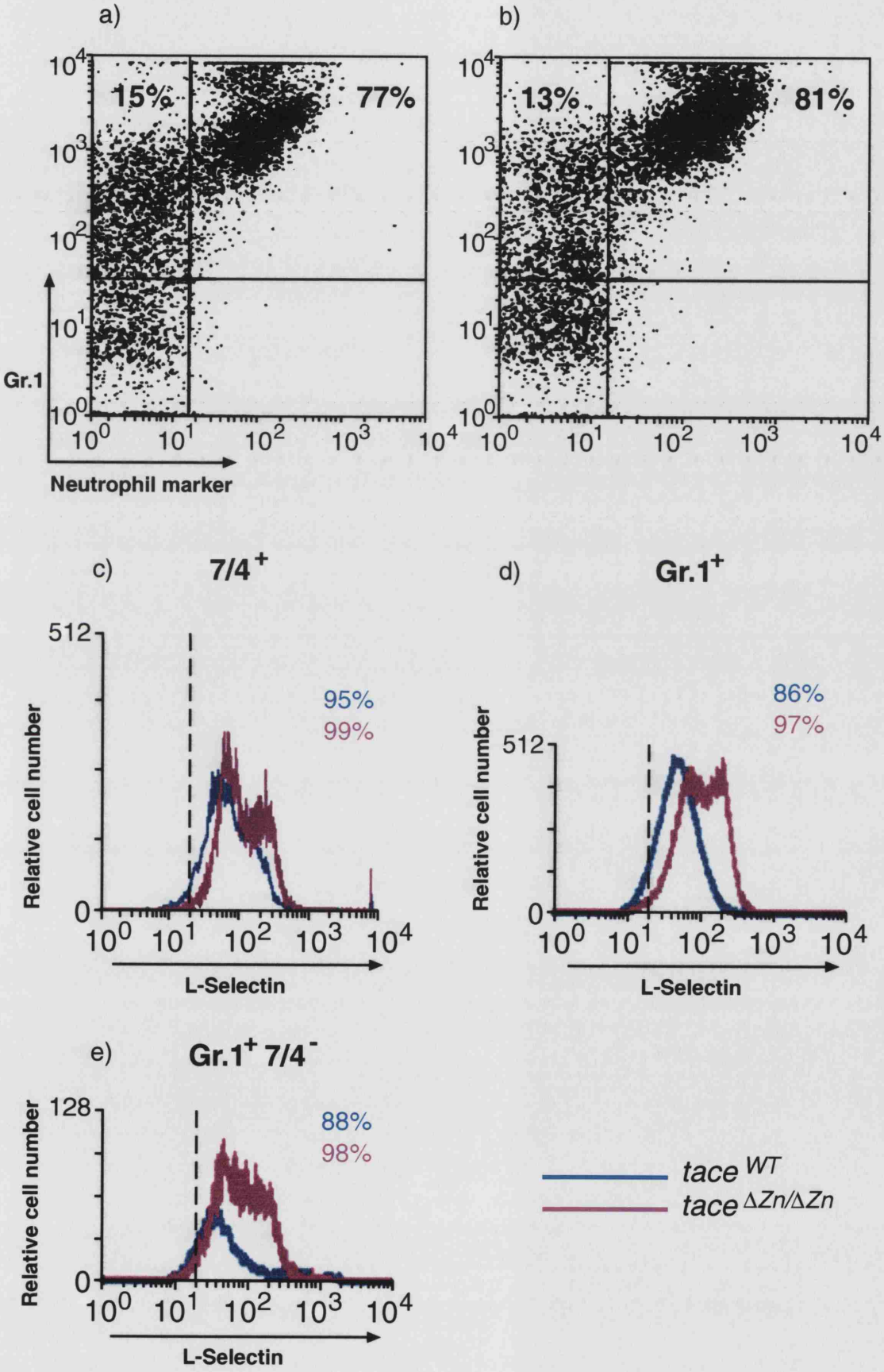
a)
b)
15%
77%
13%
81%
Gr.1
Neutrophil marker
c)
7/4+
d)
Gr.1+
95%
99%
86%
97%
Relative cell number
L-Selectin
e)
Gr.1+ 7/4-
88%
98%
tace WT
tace ΔZn/ΔZn

4.5: Ly-m11 Analysis of Splenocytes from 129/Sv Chimeric Mice

The spleens in *tace*$^{\Delta Zn/\Delta Zn}$ 129/Sv chimeric mice have been shown to be significantly larger than those *tace*$^{+/+}$ mice. Histological analysis of spleen sections was carried out to determine if there were any structural changes associated with the enlarged spleen (Figure 4.13). Clearly defined white pulp areas were distinguishable from the red pulp in *tace*^{WT} mice. There were no effects of the TACE mutation on the structure of the spleen.

Previous analysis of T and B subsets within the small cell population showed no differences between donor-derived *tace*^{WT} and *tace*$^{\Delta Zn/\Delta Z}$ splenocytes. Hence, further analysis of splenocytes was carried out to determine if the TACE mutation affected distribution of cells other than lymphocytes, such as the myeloid cell populations.

Cell morphology within the spleen of *tace*^{WT} and *tace*$^{\Delta Zn/\Delta Zn}$ 129/Sv chimeric mice was analysed (table 4.6 and figure 4.14). An average of 19% of total live cells in the *tace*^{WT} spleen were of a large more granular cell type (increase side scatter). An average of 36% of live cells in the *tace*$^{\Delta Zn/\Delta Zn}$ were of a large cell type. Like the bone marrow, however, after adjustment of student's t test p value using the Bonferroni correction, this was not significantly different.

Figure 4.14: Methyl green pyronin staining of spleens of *tace*^{WT} and *tace*$^{\Delta Zn/\Delta Zn}$ 129/Sv chimeric mice. a) *tace*^{WT} spleen with defined white (WP) and red pulp (RP) areas. Central arterioles (CA) can also be seen. b) *tace*$^{\Delta Zn/\Delta Zn}$ spleen with defined white (WP) and red pulp (RP) areas. Central arterioles (CA) can also be seen.

a)

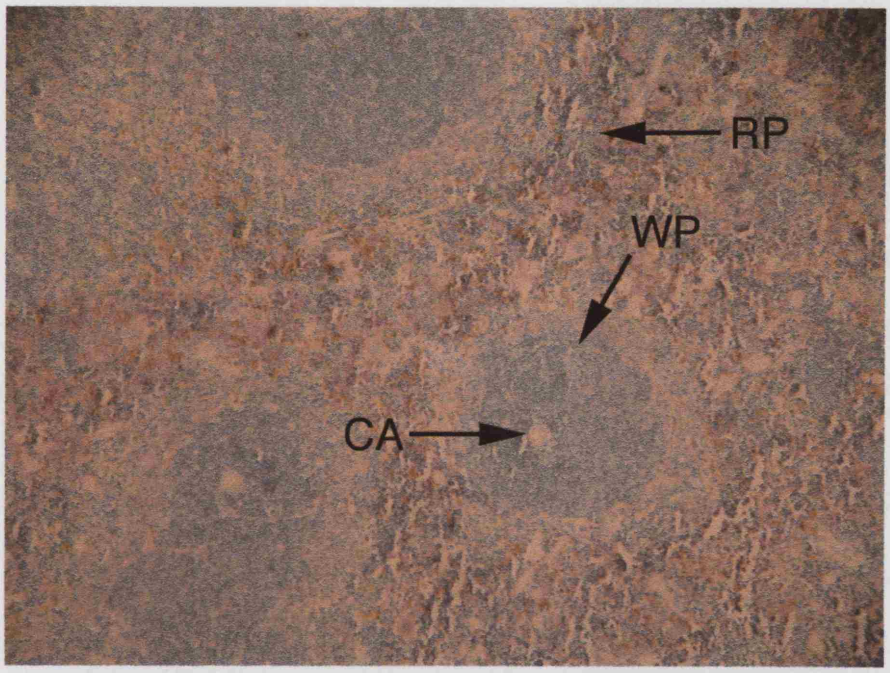

b)

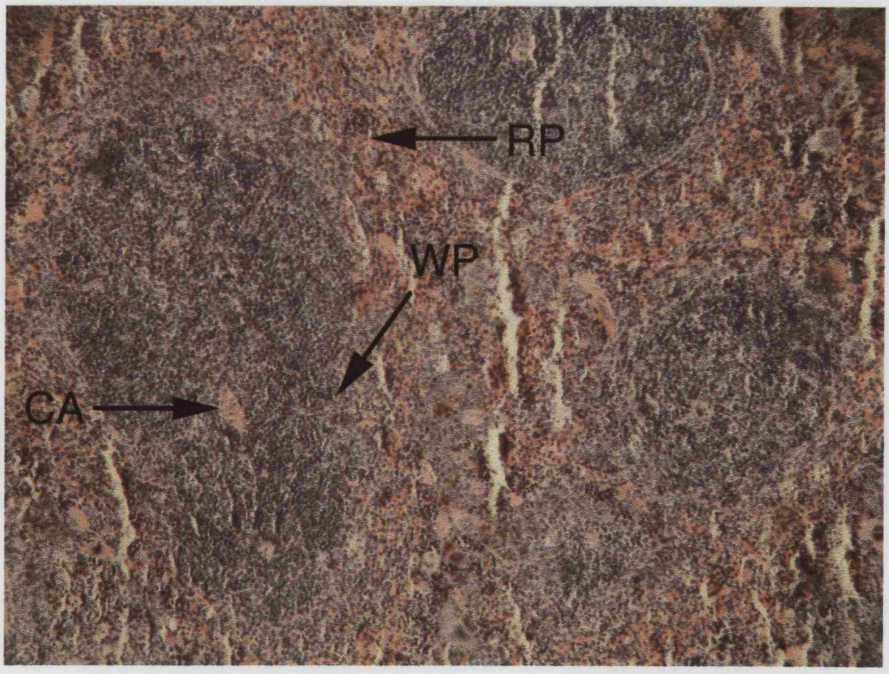

Figure 4.15: Cell size distribution in *tace*^{WT} and *tace*$^{\Delta Zn/\Delta Zn}$ 129/Sv S19/8^{+} chimeric splenocytes. a) Cell distribution (total live cells) in *tace*^{WT} spleen. Approximately 20% of total cells in the reconstituted spleen were of a "large cell type" i.e. increased side scatter. b) Cell distribution (total live cells) in *tace*$^{\Delta Zn/\Delta Zn}$ spleen. Approximately 35% of total cells in the reconstituted spleen were of a "large cell type" i.e. increased side scatter.

a)

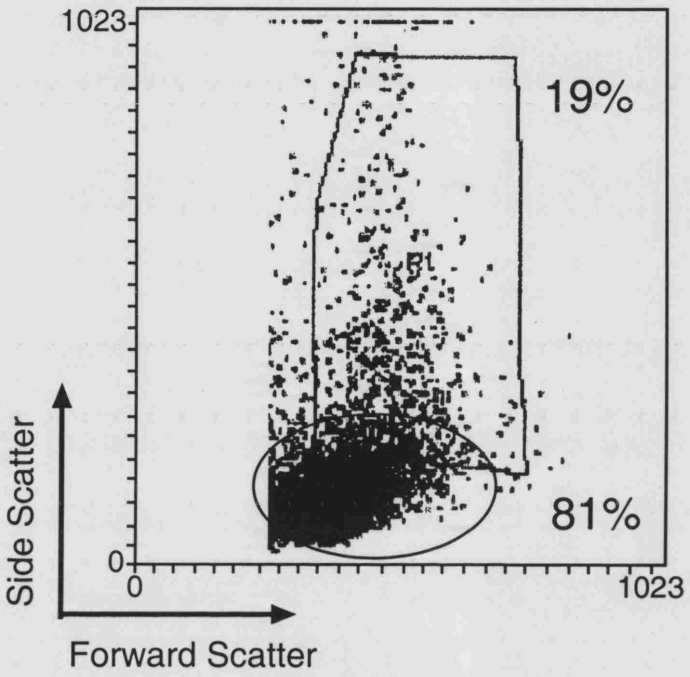
1023
19%
R1
81%
0
0
1023
Side Scatter
Forward Scatter

b)

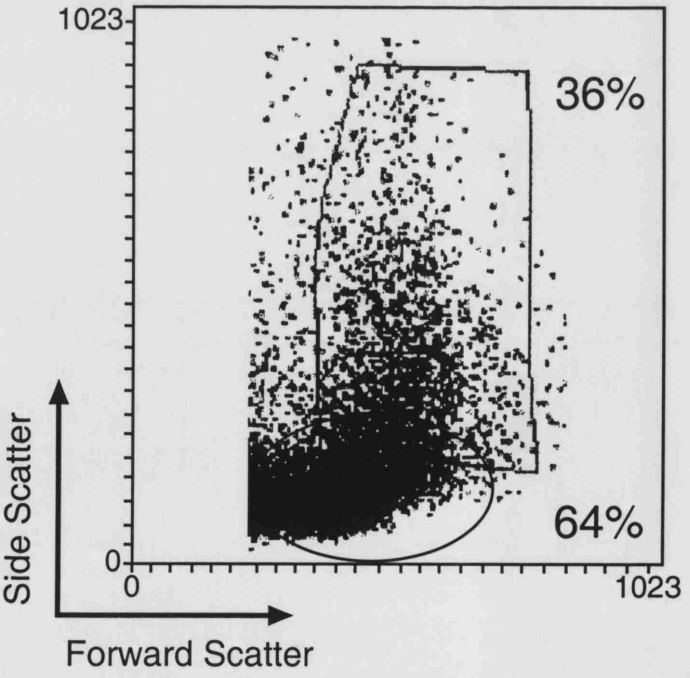
1023
36%
64%
0
0
1023
Side Scatter
Forward Scatter

Further analysis of the spleen was carried out on donor-derived non-lymphoid cells within the large cell gate, using the Gr.1 and neutrophil (7/4) markers.

There was no difference in the proportion of myeloid cell types within the large cells of the spleen due to the TACE mutation (table 4.8 and figure 4.16a and b). However, there was a significance increase ($p<0.005$) in the number of L-selectin positive neutrophil marker positive cells in the *tace*$^{\Delta Zn/\Delta Zn}$ spleen (table 4.9 and figure 4.16c). There was also a significant increase ($p<0.001$) in the number of L-selectin positive Gr.1 positive cells, but no increase in the Gr.1 positive, neutrophil marker negative cells. As seen in the bone marrow, mean fluorescence intensity was increased on all three populations studied (figure 4.16).

	$tace^{WT}$	$tace^{\Delta Zn/\Delta Zn}$
Cells of a large cell type	19 ± 6	36 ± 11 (p=0.12)
$Gr.1^+$	69 ± 14	68 ± 11
$Gr.1^+ 7/4^-$	36 ± 9	27 ± 9
$7/4^+$	37 ± 6	42 ± 15

Table 4.8: Phenotypic analysis of donor-derived myeloid cells in the splenic large cell population. Results are average percentage ± S.D (n=5). After applying the Bonferroni correction to the student t test, there was no statistically significant effect of the TACE mutation on total cell distribution or donor-derived non-myeloid cells.

	$tace^{WT}$	$tace^{\Delta Zn/\Delta Zn}$
$Gr.1^+ CD62L^+$	86 ± 2	99 ± 1 (p=0.0018)
$Gr.1^+ 7/4^- CD62L^+$	93 ± 4	96 ± 2
$7/4^+ CD62L^+$	82 ± 5	98 ± 1 (p=0.006)

Table 4.9: L-selectin expression on donor-derived myeloid subsets within the splenic large cell population. The number of L-selectin positive cells was increased in donor-derived $tace^{\Delta Zn/\Delta Zn}$ neutrophils and $Gr.1^+$ cell populations. Results are average percentage ± S.D (n=5). The student t Test p values shown are a comparison between $tace^{WT}$ and $tace^{\Delta Zn/\Delta Zn}$. P-values have been adjusted using the Bonferroni correction.

Figure 4.16: Example of analysis of large non-lymphoid cells from 129/Sv chimeric spleen (representative of n=5). a) Gr.1 and neutrophil marker expression on *tace*^{WT} splenocytes. b) Gr.1 and neutrophil expression on *tace*$^{\Delta Zn/\Delta Zn}$ splenocytes. There was no effect of the TACE mutation on donor-derived myeloid cell subsets in the spleen. c) L-selectin expression on neutrophil marker positive splenocytes. There was a statistically significant increase in the number of L-selectin positive donor-derived neutrophils from mice reconstituted with *tace*$^{\Delta Zn/\Delta Zn}$ foetal liver cells, in comparison with those reconstituted with *tace*^{WT} foetal liver cells. d) L-selectin expression on Gr.1 positive splenocytes. There was a statistically significant increase in the number of L-selectin positive donor-derived Gr.1^{+} cells from mice reconstituted with *tace*$^{\Delta Zn/\Delta Zn}$ foetal liver cells, in comparison with those reconstituted with *tace*^{WT} foetal liver cells. e) L-selectin expression on Gr.1 positive, neutrophil negative splenocytes. There was no significant difference seen between the numbers of donor-derived non-neutrophil myeloid cells expressing L-selectin in mice reconstituted with *tace*^{WT} foetal liver cells compared to those reconstituted with *tace*$^{\Delta Zn/\Delta Zn}$ foetal liver cells.

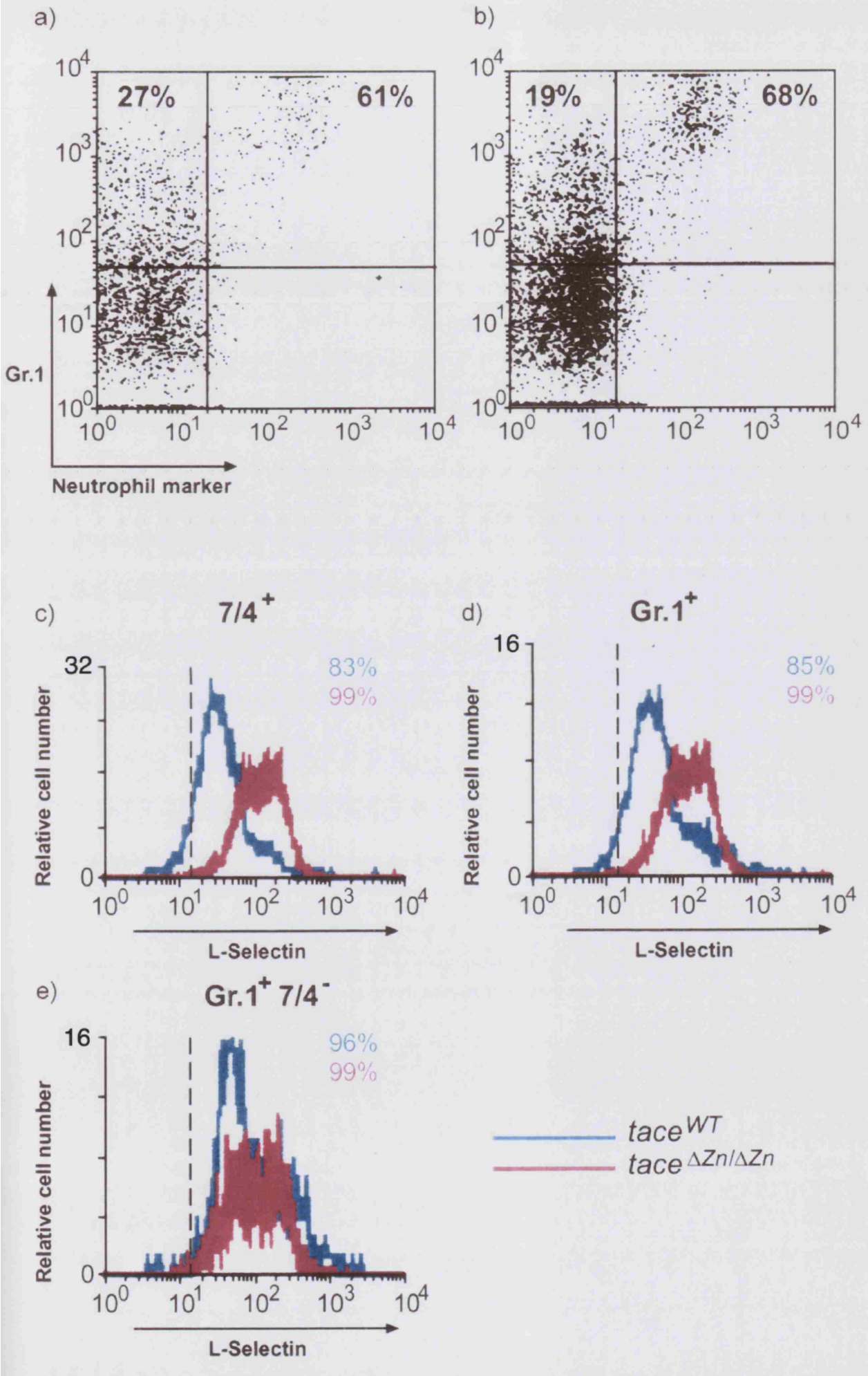
a)
b)
27%
61%
19%
68%
Gr.1
Neutrophil marker
c)
7/4+
d)
Gr.1+
83%
99%
85%
99%
Relative cell number
L-Selectin
e)
Gr.1+ 7/4-
96%
99%
tace WT
tace ΔZn/ΔZn

4.6: Summary

Initial phenotypic analyses were performed on *tace*$^{+/+}$ and *tace*$^{\Delta Zn/\Delta Zn}$ 129/Sv chimeric mice reconstituted with foetal livers from TACE deficient mice, kindly donated by Dr Jacques Peschon, and wild-type foetal livers from C57BL/6 mice bred at NIMR. Comparisons of total cell yields showed no effect of the TACE mutation in any of the lymphoid organs. Splenic weights were significantly increased in the *tace*$^{\Delta Zn/\Delta Zn}$ mice, however, histological analysis of peripheral lymph node and spleen sections demonstrated no effect of the TACE mutation on secondary lymphoid organ structure.

Ly 9.1 analysis of reconstituted lymphoid organs showed significant populations of host-derived cells in secondary lymphoid organs. Further analysis showed that the majority of the host-derived cells were of a T lymphocyte phenotype. Phenotypic analysis of donor-derived cells for T, B, CD4 and CD8 markers in the chimeric mice showed no effect of the TACE mutation on proportions of cell subsets. However, although not statistically significant, there were increased levels of L-selectin expression on B220 positive cells in the bone marrow of *tace*$^{\Delta Zn/\Delta Zn}$ mice.

Donor-derived non-lymphoid cells in bone marrow and spleen were analysed using the Ly-m11 epitope present on C57BL/6 β-microglobulin. Greater than 95% of cells in C57BL/6 lymph node and spleen stained positively for Ly-m11. Greater than 87% of cells in C57BL/6 bone marrow stained positively for Ly-m11. 129/Sv lymphoid organs were all negative for the Ly-m11 epitope. Lymphoid organs from the reconstituted chimeric mice consisted of both donor-derived (Ly-m11^{+}) and host derived (Ly-m11^{-}) cell populations. Cell distribution in bone marrow of reconstituted mice showed a higher proportion of large cells (increased side scatter) in *tace*$^{\Delta Zn/\Delta Zn}$ chimeric mice, although this was not statistically significant. The majority of these cells expressed myeloid markers (89%). There was no effect due to the TACE mutation on donor-derived myeloid cell proportions in the large cell population of the bone marrow. However, there was increased expression of

L-selectin on donor-derived monocytes (non-neutrophil granulocytes) in the bone marrow of $tace^{\Delta Zn/\Delta Zn}$ chimeric mice.

Cell distribution analysis of $tace^{WT}$ and $tace^{\Delta Zn/\Delta Zn}$ chimeric spleen showed a higher proportion of large cells (increased side scatter) in the $tace^{\Delta Zn/\Delta Zn}$ chimeric spleen, although this was not statistically significant. The majority of these cells expressed myeloid markers (69%). There was no effect of the TACE mutation on proportion of donor-derived myeloid cell types within the large cell population. There was a significant increase in L-selectin expression on donor-derived neutrophils within the splenic large cell population.

Chapter 5: Regulation of L-Selectin Shedding

L-selectin shedding can be induced by a variety of stimuli including chemoattractants, phorbol esters and L-selectin cross-linking. Most studies have used phorbol esters, particularly Phorbol 12-Myristrate Acetate (PMA), to induce rapid down-regulation of surface L-selectin. PMA induced shedding can be inhibited using hydroxamate based synthetic MMP inhibitors Ro 31-9790 and Ro 32-0526, which have a hydroxamic acid side chain that binds to the zinc molecule in the catalytic site of the enzyme responsible for L-selectin cleavage (table 5.1). Naturally occurring inhibitors, the TIMPs, of which four are known, inhibit MMP activity by forming non-covalent interactions with them. TIMP-2, 3 and 4 inhibit all membrane bound MMPs (MT-MMPs), while TIMP-1 inhibits most MT-MMPs. TIMP-1 and TIMP-3 have been shown to inhibit some members of the ADAMs family. PMA induced shedding is not inhibited by TIMP 1 or 2 but is inhibited by TIMP-3 (Borland et al., 1999).

L-selectin also undergoes constitutive or basal shedding in resting cells at 37°C. Like PMA induced shedding, basal shedding is inhibited by the metalloproteinase inhibitor Ro-31-9790 (Zhao et al., 2001). A recent study suggests that although the cleavage sites for PMA induced and basal shedding appear to be identical, there are distinctly different structural requirements for shedding to occur (Zhao et al., 2001).

As in the previous chapter, if it was not known if the controls cells (i.e. those that shed L-selectin in response to PMA stimulation) were $tace^{+/+}$ or $tace^{+/\Delta Zn}$ they are designated as $tace^{WT}$. PMA mediated shedding was indistinguishable between $tace^{+/+}$ or $tace^{+/\Delta Zn}$ derived lymphocytes.

Table 5.1: Properties of hydroxamate based synthetic MMP inhibitors. IC_{50} refers to the concentration of inhibitor that inhibits PMA-induced L-selectin shedding by 50%. Ro 32-0526 is the most effective at low concentrations of all of the three inhibitors. Ro 32-1541 is the least effect of the three inhibitors.

Compound	Structure	IC_{50} L-selectin Shedding (μM)	IC_{50} Stromelysin MMP3 (nM)	IC_{50} gelatinase MMP9 (nM)	IC_{50} collagenase MMP1 (nM)
Ro 32-1541	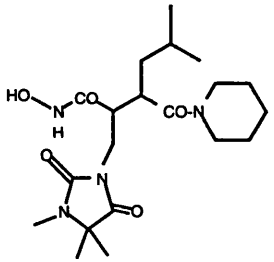	No inhibition at 50μM	2175	237	10.1
Ro 31-9790	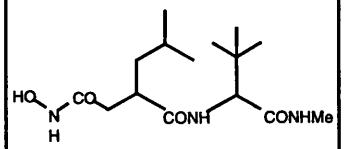	2	160	10	5
Ro 32-0526	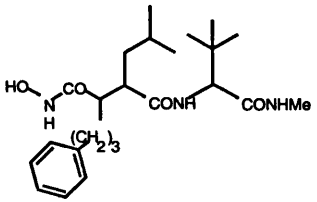	0.5 (pers comm A. Ager)	8	2.6	1.5

5.1: PMA Induced Shedding from *tace*$^{\Delta Zn/\Delta Zn}$ Peripheral Blood Lymphocytes

To investigate the role of TACE in shedding, expression of L-selectin on peripheral blood lymphocytes was measured following stimulation with PMA. PMA stimulation was carried out on lymphocytes from tail bleeds of 129/Sv mice reconstituted with foetal liver cells. L-selectin expression on the surface of Ly 9.1 negative *tace*$^{+/+}$ and *tace*$^{\Delta Zn/\Delta Zn}$ T and B lymphocytes before PMA stimulation are of similar levels (figure 5.1a and c). Figure 5.1b and d show the cells following PMA stimulation. *tace*$^{+/+}$ lymphocytes downregulated L-selectin in response to PMA stimulation. There was no effect of PMA on the number of *tace*$^{\Delta Zn/\Delta Zn}$ T lymphocytes expressing L-selectin. *tace*$^{\Delta Zn/\Delta Zn}$ B cells did not shed L-selectin. Also shown are the starting and post stimulation levels of L-selectin on non-lymphoid (TCR$^-$ B220$^-$) cells, which comprise approximately 19% of the peripheral blood cell population. As described in the previous chapter, there were higher starting levels of L-selectin on *tace*$^{\Delta Zn/\Delta Zn}$ non-lymphoid cells. The *tace*$^{+/+}$ non-lymphoid cells downregulated L-selectin in response to PMA. There was no downregulation of L-selectin on *tace*$^{\Delta Zn/\Delta Zn}$ non-lymphoid cells.

In the case of all the *tace*$^{\Delta Zn/\Delta Zn}$ cell populations investigated, mean fluorescence intensity (MFI) actually increased with incubation in the presence of PMA. This suggests that PMA may be stimulating L-selectin expression, as well as inducing shedding.

Figure 5.1: PMA stimulation of peripheral blood cells. Numbers refer to MFI of the L-selectin positive cell population. Cells were incubated with PMA for 1 hour at 37°C. a) Starting levels of L-selectin on T lymphocytes. b) L-selectin expression on T lymphocytes following PMA stimulation. There was downregulation of L-selectin on *tace*$^{+/+}$ T cells but not from *tace*$^{\Delta Zn/\Delta Zn}$ cells. c) Starting levels of L-selectin on B lymphocytes. d) L-selectin expression on B lymphocytes following PMA stimulation, showing downregulation of L-selectin from *tace*$^{+/+}$ cells but not from *tace*$^{\Delta Zn/\Delta Zn}$ cells. e) Starting levels of L-selectin on non-lymphocytes. f) L-selectin expression on non-lymphoid cells (TCR$^-$ B220$^-$) following stimulation with PMA. There was downregulation of L-selectin from the *tace*$^{+/+}$ cells but not from the *tace*$^{\Delta Zn/\Delta Zn}$ cells. All analyses were performed on Ly 9.1$^-$ (donor-derived) cells.

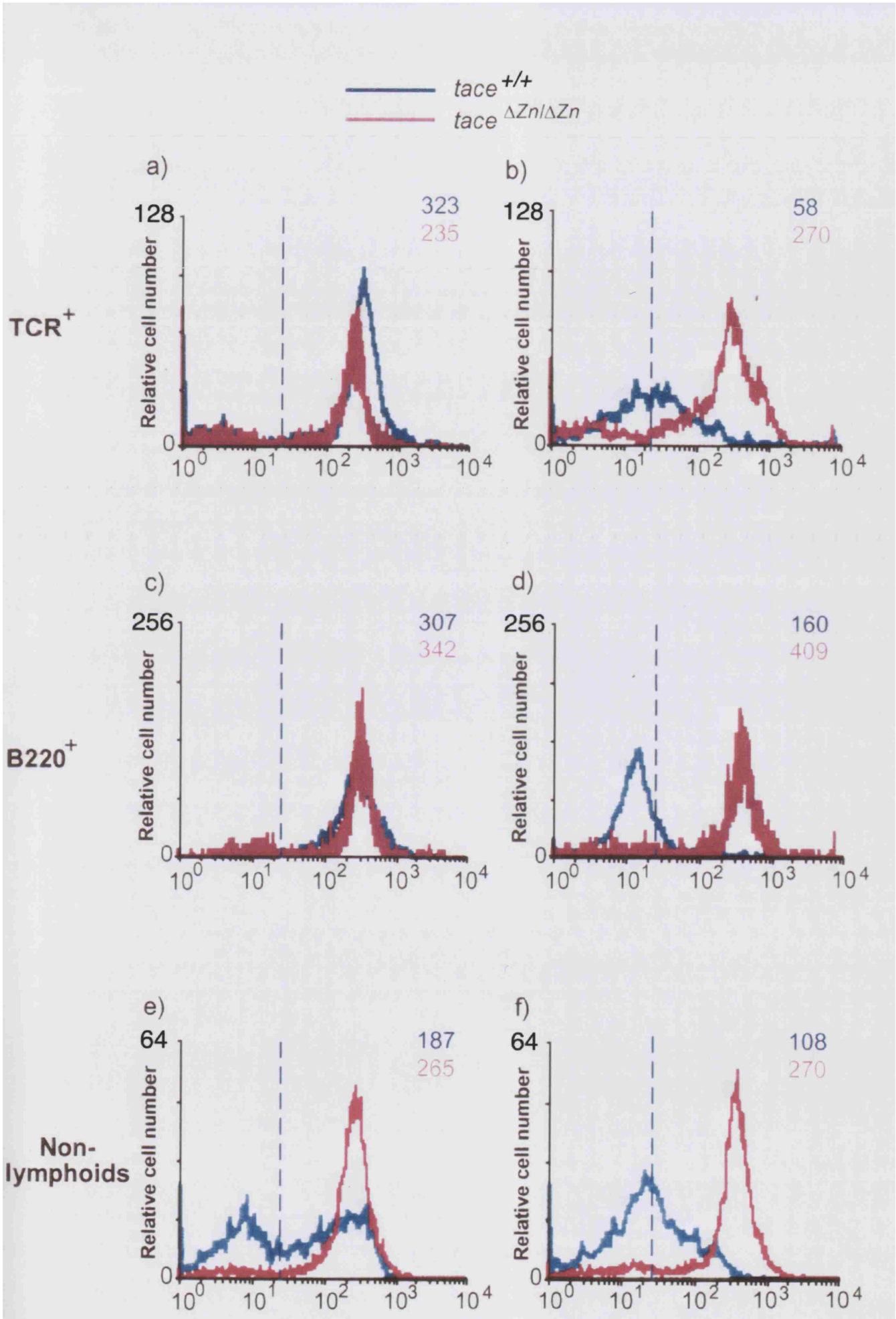
tace +/+
tace ΔZn/ΔZn
a)
b)
c)
d)
e)
f)
TCR+
B220+
Non-lymphoids
Relative cell number
128
64
256
0
323
235
58
270
307
342
160
409
187
265
108
270
10^0
10^1
10^2
10^3
10^4

5.2: PMA Titration and L-Selectin Expression on *tace*$^{\Delta Zn/\Delta Zn}$ Splenocytes

Following the observation that there was no down-regulation of L-selectin following PMA stimulation of *tace*$^{\Delta Zn/\Delta Zn}$ peripheral blood lymphocytes, a PMA titration was carried out on *tace*$^{\Delta Zn/\Delta Zn}$ splenocytes.

As the Ly 9.1 epitope is only expressed by cells from the lymphoid lineage, there is a possibility that host-derived myeloid cells may be included in the Ly 9.1$^-$ total cell population. To study the response of cell subsets within this population of splenocytes and ensure that the population includes no host cells, T and B Ly 9.1 negative lymphocytes were gated on independently.

tace$^{\Delta Zn/\Delta Zn}$ T lymphocytes did not shed L-selectin in response to PMA. Increased shedding of L-selectin from the surface of *tace*^{WT} T lymphocytes was observed with increasing concentration of PMA. At maximal shedding (3000 nM), cells positive for L-selectin are reduced to 20% of starting numbers (figure 5.2b).

tace$^{\Delta Zn/\Delta Zn}$ B lymphocytes did not shed L-selectin in response to PMA stimulation. *Tace*^{WT} B lymphocytes show dose-dependent loss of L-selectin in response to PMA. At maximal shedding, B- lymphocytes positive for L-selectin are reduced to 10% of starting number (figure 5.2b).

Splenocytes were collected from reconstituted 129/Sv mice, hence there is a residual population of *tace*$^{+/+}$ Ly 9.1$^+$ host derived lymphocytes present. To confirm the lack effect of PMA acting on the *tace*$^{\Delta Zn/\Delta Zn}$ cells, L-selectin expression on gated host-derived cells was monitored following PMA stimulation. There was a dose dependent downregulation of L-Selectin in Ly 9.1$^+$ cells in both the *tace*$^{\Delta Zn/\Delta Zn}$ and *tace*^{WT} chimeric mice (Figure 5.2c). The numbers of L-selectin positive host-derived lymphocytes are reduced to 42% and 30% of starting levels in *tace*^{WT} and *tace*$^{\Delta Zn/\Delta Zn}$ cells respectively.

Figure 5.2: PMA titration on lymphocytes from 129/Sv chimeric mice. Cells were incubated in the presence of increasing concentrations of PMA for 1 hour at 37°C. Results are the means of two experiments. a) L-selectin levels on Ly 9.1 negative T lymphocytes following stimulation with PMA. *tace*$^{\Delta Zn/\Delta Zn}$ T lymphocytes do not down regulate L-selectin. Instead there is an increase in the percentage of L-selectin positive lymphocytes. The percentage of L-selectin positive *tace*^{WT} cells decreases with increasing concentration of PMA. b) *tace*$^{\Delta Zn/\Delta Zn}$ B cells do not shed or increase expression of L-selectin in response to PMA. *Tace*^{WT} B lymphocytes positive for L-selectin decrease in number in response to increasing concentrations of PMA. c) Effect of PMA stimulation on host-derived lymphocytes (Ly 9.1^{+}) from the *tace*$^{\Delta Zn/\Delta Zn}$ and *tace*^{WT} chimeric mice. Both L-selectin positive populations decrease in number with increasing concentrations of PMA.

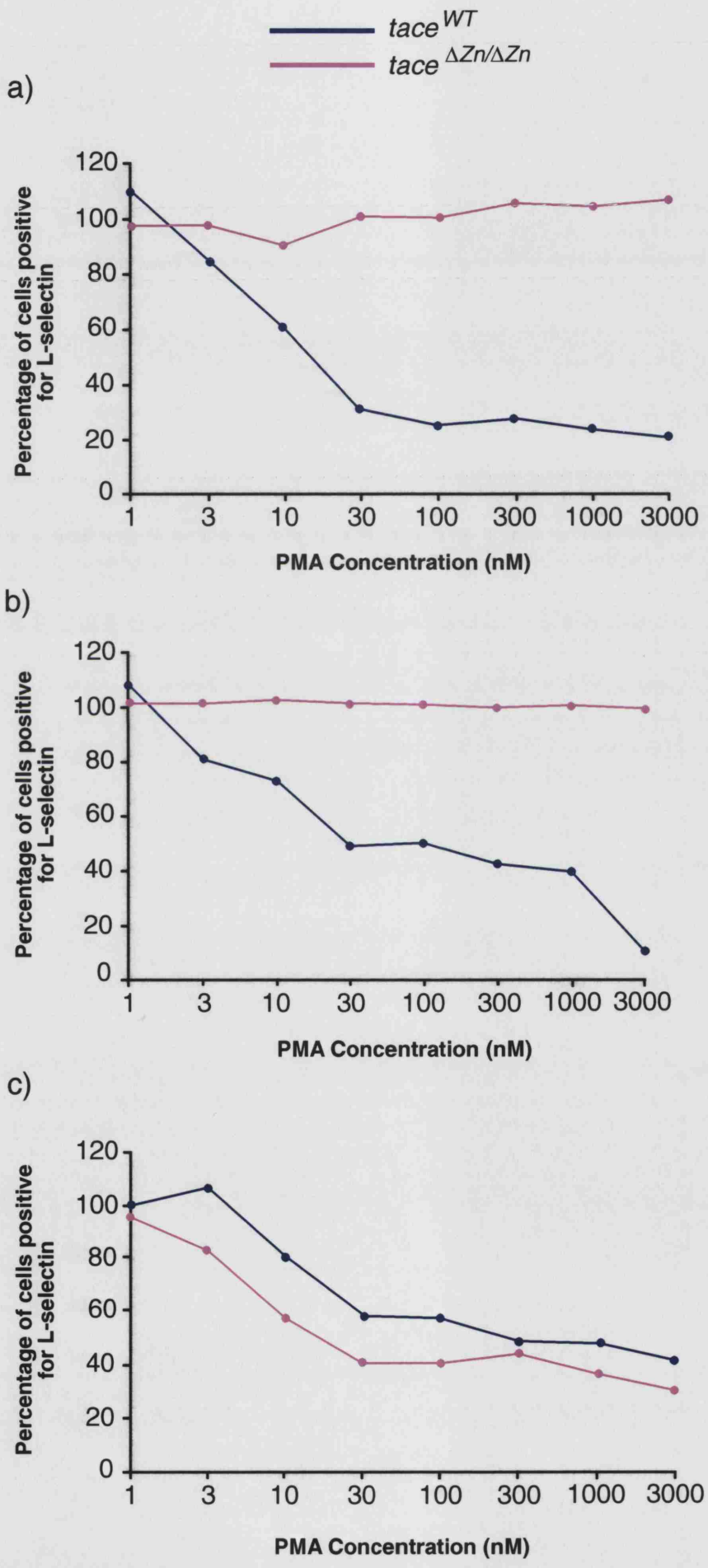
tace WT
tace ΔZn/ΔZn
a)
Percentage of cells positive for L-selectin
120
100
80
60
40
20
0
1
3
10
30
100
300
1000
3000
PMA Concentration (nM)
b)
Percentage of cells positive for L-selectin
120
100
80
60
40
20
0
1
3
10
30
100
300
1000
3000
PMA Concentration (nM)
c)
Percentage of cells positive for L-selectin
120
100
80
60
40
20
0
1
3
10
30
100
300
1000
3000
PMA Concentration (nM)

The inability of *tace*$^{\Delta Zn/\Delta Zn}$ cells to down-regulate L-selectin following incubation with PMA may have been due to the TACE mutation affecting the ability of the cell to respond to stimulation. To determine whether this was the case, expression of CD69 on both *tace*^{WT} and *tace*$^{\Delta Zn/\Delta Zn}$ cells was compared in the absence and presence of PMA. CD69 is an early activation marker upregulated upon stimulation with PMA.

There was normal upregulation of CD69 following stimulation with PMA in *tace*$^{\Delta Zn/\Delta Zn}$ T and B lymphocytes (Figures 5.3b and d). Normal upregulation of CD69 was also seen on residual host cells from the *tace*^{WT} and *tace*$^{\Delta Zn/\Delta Zn}$ chimeric mice.

Figure 5.3: Upregulation of CD69 on PMA stimulated lymphocytes. Starting levels of L-selectin refers to levels on cell kept at 4°C for the duration of the experiment. a) Starting levels of CD69 on *tace*^{WT} and *tace*$^{\Delta Zn/\Delta Zn}$ T lymphocytes. Both *tace*^{WT} and *tace*$^{\Delta Zn/\Delta Zn}$ resting T lymphocytes do not express CD69. b) T lymphocyte CD69 levels following stimulation with PMA (1000 nM) for 1 hour at 37°C. Both *tace*^{WT} and *tace*$^{\Delta Zn/\Delta Zn}$ T lymphocytes upregulate CD69 in response to PMA. c) Starting levels of CD69 on *tace*^{WT} and *tace*$^{\Delta Zn/\Delta Zn}$ B lymphocytes. Both *tace*^{WT} and *tace*$^{\Delta Zn/\Delta Zn}$ resting B lymphocytes do not express CD69. d) B lymphocyte CD69 levels following stimulation with PMA (1000nM) for 1 hour at 37°C. Both *tace*^{WT} and *tace*$^{\Delta Zn/\Delta Zn}$ B lymphocytes upregulate CD69 in response to PMA.

e) Starting levels of CD69 on host-derived lymphocytes (Ly 9.1^{+}) in *tace*^{WT} and *tace*$^{\Delta Zn/\Delta Zn}$ chimeras. Both *tace*^{WT} and *tace*$^{\Delta Zn/\Delta Zn}$ resting host-derived lymphocytes do not express CD69. f) Host cell CD69 levels following stimulation with PMA (1000nM) for 1 hour at 37°C. Host-derived lymphocytes, in both *tace*^{WT} and *tace*$^{\Delta Zn/\Delta Zn}$ chimeras, upregulate CD69 in response to PMA.

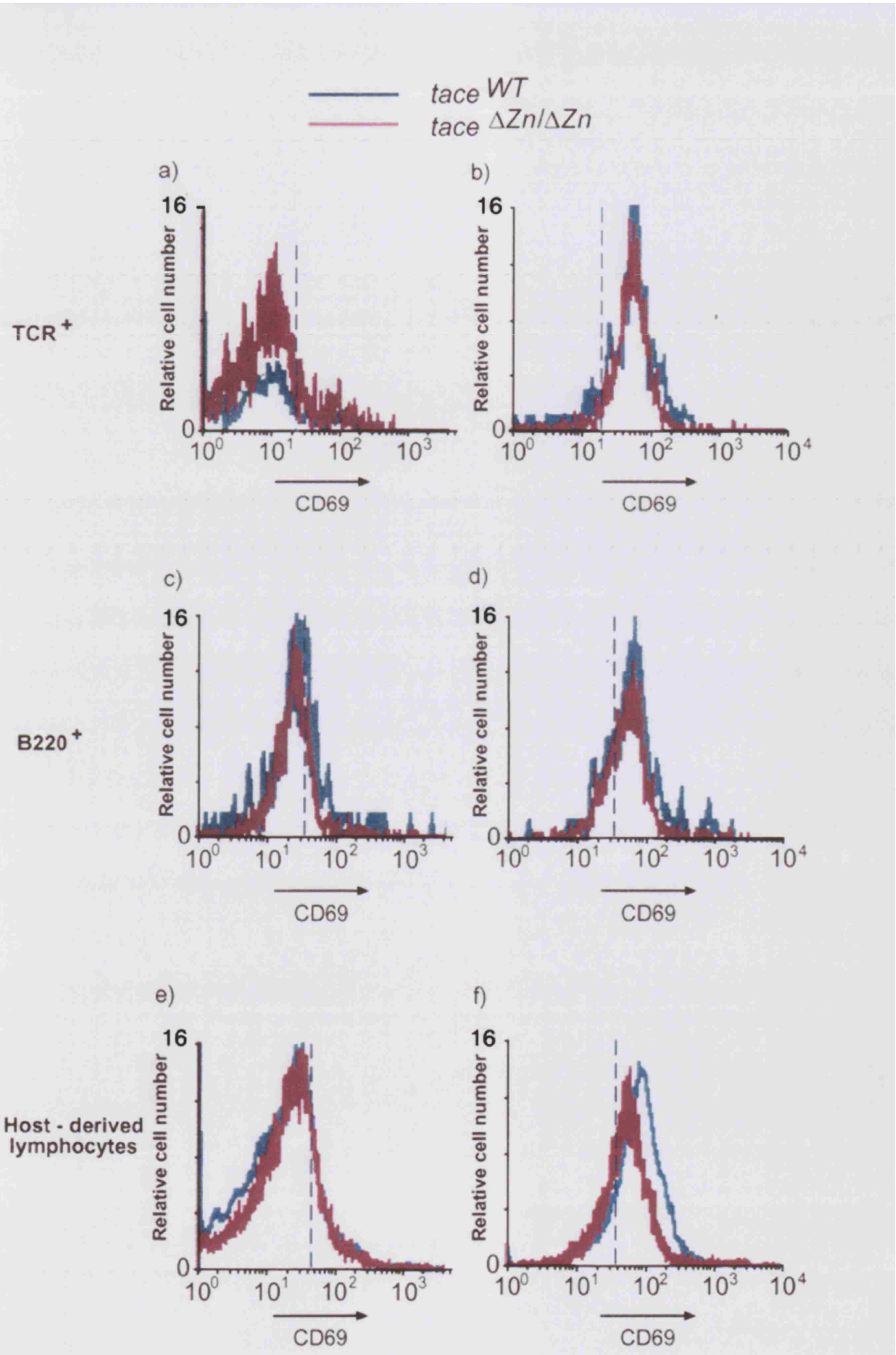
tace WT
tace ΔZn/ΔZn
a)
b)
c)
d)
e)
f)
TCR+
B220+
Host - derived lymphocytes
Relative cell number
16
0
CD69
10^0
10^1
10^2
10^3
10^4

5.3: Basal Shedding from TACE Chimeric Mice Peripheral Lymph Node Cells

Although PMA is a useful tool for studying *in vitro* down-regulation of L-selectin, more physiologically relevant stimuli such as chemokines and TCR (anti-CD3) activation were considered. However, no effects of these alternative stimuli – such as SDF-1α, SLC (CXCR4or CCR7 engagement respectively) – were seen. Basal shedding of L-selectin has been reported to occur by a different mechanism to PMA induced shedding (Zhao et al., 2001). It was decided to study basal shedding in $tace^{\Delta Zn/\Delta Zn}$ lymphocytes.

Basal shedding was monitored in peripheral lymph node (PLN) cells. L-selectin levels were measured on T and B cells that had been kept on ice (4°) and compared with cells incubated at 37°C for 1 hour. Basal shedding was observed in $tace^{\Delta Zn/\Delta Zn}$ T lymphocytes as well as $tace^{WT}$ T lymphocytes (table 5.2). Basal shedding in $tace^{WT}$ and $tace^{\Delta Zn/\Delta Zn}$ B cells was variable (Table 5.2) so it was decided to concentrate on T lymphocytes. These observations suggest a TACE independent pathway for L-selectin shedding in T lymphocytes.

	$tace^{WT}$ **Peripheral lymphocytes**	$tace^{\Delta Zn/\Delta Zn}$ **Peripheral lymphocytes**
T(αβTCR$^+$) Lymphocytes	23.6±9	15±6
B (B220$^+$) Lymphocytes	14.5±17	5±8

Table 5.2: Decreases in number of L-selectin positive peripheral lymph nodes T and B lymphocytes, following incubation at 37°C for 1 hour. Results are mean percentage of cells positive for L-selectin ± SD (n=5).

5.4: Inhibition of Basal Shedding

As described previously, PMA induced shedding can be inhibited using hydroxamate inhibitors. A titration curve of the inhibitors on PMA stimulated C57BL/6 peripheral lymph node cells was compared to that of cells incubated for 2 hours at 37°C to determine if basal shedding was also blocked.

Ro 32-0526 inhibited L-selectin shedding from T lymphocytes even at very low concentrations. Consistent with previously published work, (Preece et al., 1996; Borland et al., 1999) the inhibitory effectiveness of Ro 31-9790 on T lymphocytes increased with increasing concentrations with complete inhibition reached at approximately 30μM. There was no inhibition of L-selectin shedding from T lymphocytes by Ro 32-1541 until a concentration of 100μM was reached and this was a very slight inhibition of approximately 10%. (figure 5.4a). As seen with T lymphocytes, Ro 32-0526 inhibited L-selectin shedding from B lymphocytes even at very low concentrations. Consistent with previously published work, (Preece et al., 1996; Borland et al., 1999) the inhibitory effectiveness of Ro 31-9790 on B lymphocytes increased with increasing concentrations with complete inhibition reached at approximately 30μM. There was no inhibition of L-selectin shedding from B lymphocytes by Ro 32-1541 until a concentration of 100μM was reached and this was a very slight inhibition of approximately 10%. (Figure 5.4b). The supernatants from the incubations were collected and levels of soluble L-selectin determined (Figure 5.4c). The levels of soluble L-selectin differ from those of surface expression of L-selectin in that Ro 32-0526 did not completely inhibit L-selectin release into the supernatant until it was added at a concentration of 10μM; Ro 31-9790 had a dose dependent response but did not achieve complete blockage of L-selectin release at 30μM, and Ro 32-1541 also had a dose dependent response, although not to the extent of Ro 31-9790. (Figure5.4c).

Figure 5.4: Inhibition of PMA induced shedding of L-selectin from C57BL/6 PLN cells using hydroxamate based MMP inhibitors. Results are from a single experiment a) Effect of increasing concentrations of inhibitors Ro 32-1541, Ro 31-9790 and Ro 32-0526 on the proportion of L-selectin positive peripheral lymph node T lymphocytes following incubation at 37°C for 2 hours in the presence of 300 nM PMA. b) Effect of increasing concentrations of inhibitors Ro 32-1541, Ro 31-9790 and Ro 32-0526 on the proportion of L-selectin positive peripheral lymph node B lymphocytes following incubation at 37°C for 2 hours in the presence of 300 nM PMA. c) Amount (ng/ml) – determined by ELISA – of soluble L-selectin present in the supernatant of cells incubated in the presence of increasing concentrations of inhibitors Ro 32-1541, Ro 31-9790 and Ro 32-0526 and 300 nM PMA.

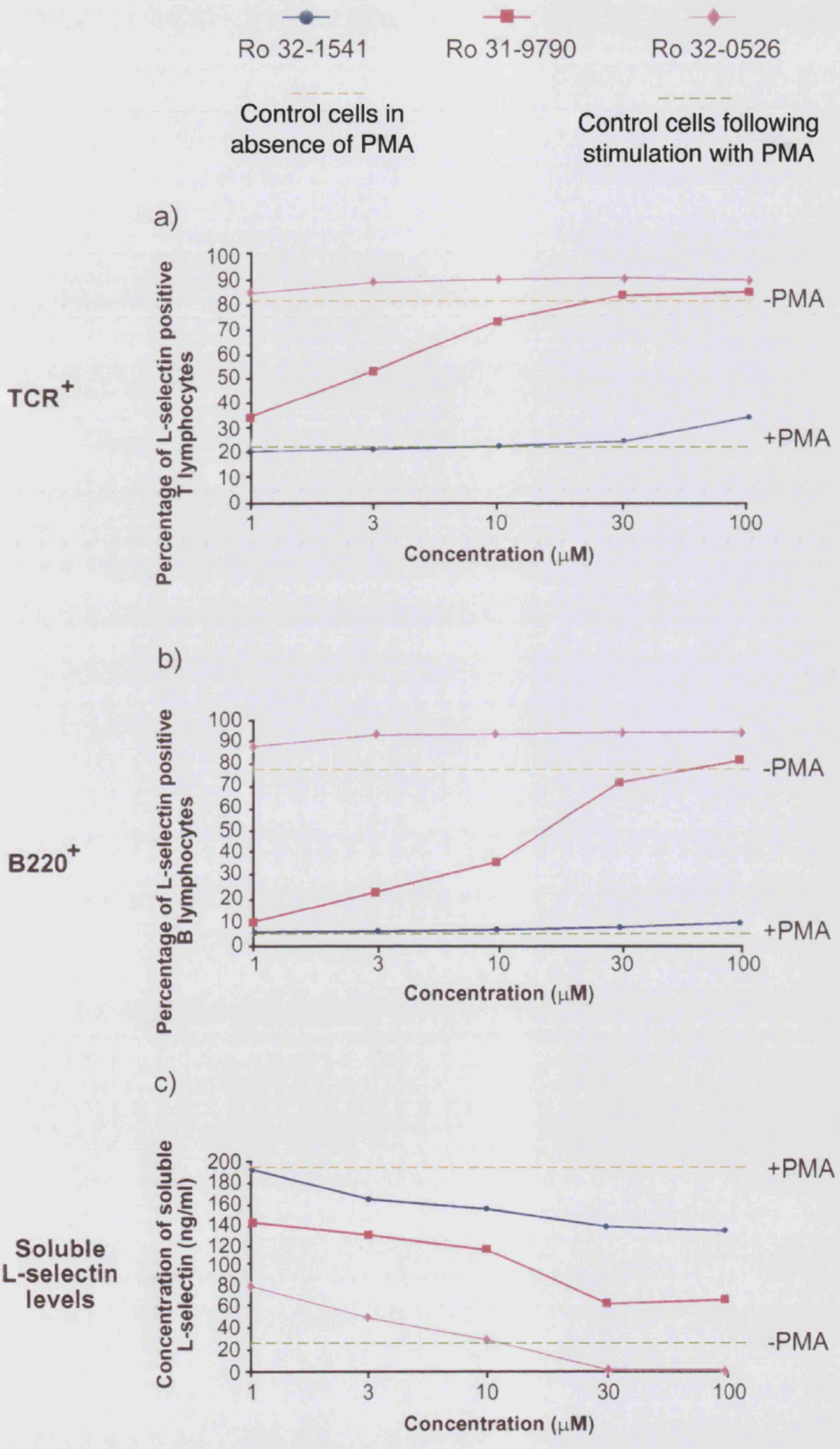
Ro 32-1541
Ro 31-9790
Ro 32-0526
Control cells in absence of PMA
Control cells following stimulation with PMA
a)
TCR+
Percentage of L-selectin positive T lymphocytes
-PMA
+PMA
Concentration (μM)
b)
B220+
Percentage of L-selectin positive B lymphocytes
-PMA
+PMA
Concentration (μM)
c)
Soluble L-selectin levels
Concentration of soluble L-selectin (ng/ml)
+PMA
-PMA
Concentration (μM)

As with PMA induced shedding, the most potent inhibitor of basal shedding from both T and B lymphocytes was Ro 32-0526 (blocked shedding from ~20 and 24% of T and B lymphocytes respectively). Similar to the effect seen on PMA stimulated cells, Ro 32-0526 inhibits L-selectin shedding from T lymphocytes even at very low concentrations. The inhibitory effectiveness of Ro 31-9790 on shedding from T lymphocytes increased with increasing concentrations with complete inhibition reached at approximately 30μM. There was no inhibition of L-selectin from T lymphocytes shedding by Ro 32-1541 (figure 5.5a). Ro 32-0526 inhibited L-selectin shedding from B lymphocytes even at very low concentrations. Ro 31-9790 inhibition of shedding from B lymphocytes increased with increasing concentrations with complete inhibition reached at approximately 30μM. However, a less effective inhibitory response on B lymphocytes was observed with Ro 32-1541 (figure 5.5b). Like the response with PMA stimulated cells, the levels of soluble differ from those of surface expression of L-selectin in that Ro 32-0526 did not completely inhibit L-selectin release into the supernatant until it was added at a concentration of 10μM; Ro 31-9790 had a dose dependent response but did not achieve complete blockage of L-selectin release at 30μM, although Ro 32-1541 had no inhibitory effect (figure 5.5c).

Figure 5.5: Inhibition of basal shedding of L-selectin from C57BL/6 PLN lymphocytes using hydroxamate based MMP inhibitors. Results are means of two experiments. a) Effect of increasing concentrations of inhibitors Ro 32-1541, Ro 31-9790 and Ro 32-0526 on the percentage of L-selectin positive peripheral lymph node T lymphocytes following incubation at 37°C for 2 hours. b) Effect of increasing concentrations of inhibitors Ro 32-1541, Ro 31-9790 and Ro 32-0526 on the percentage of L-selectin positive peripheral lymph node B lymphocytes following incubation at 37°C for 2 hours. c) Amount (ng/ml) – determined by ELISA – of soluble L-selectin present in the supernatant of cells incubated in the presence of increasing concentrations of inhibitors Ro 32-1541, Ro 31-9790 and Ro 32-0526 at 37°C for 2 hours.

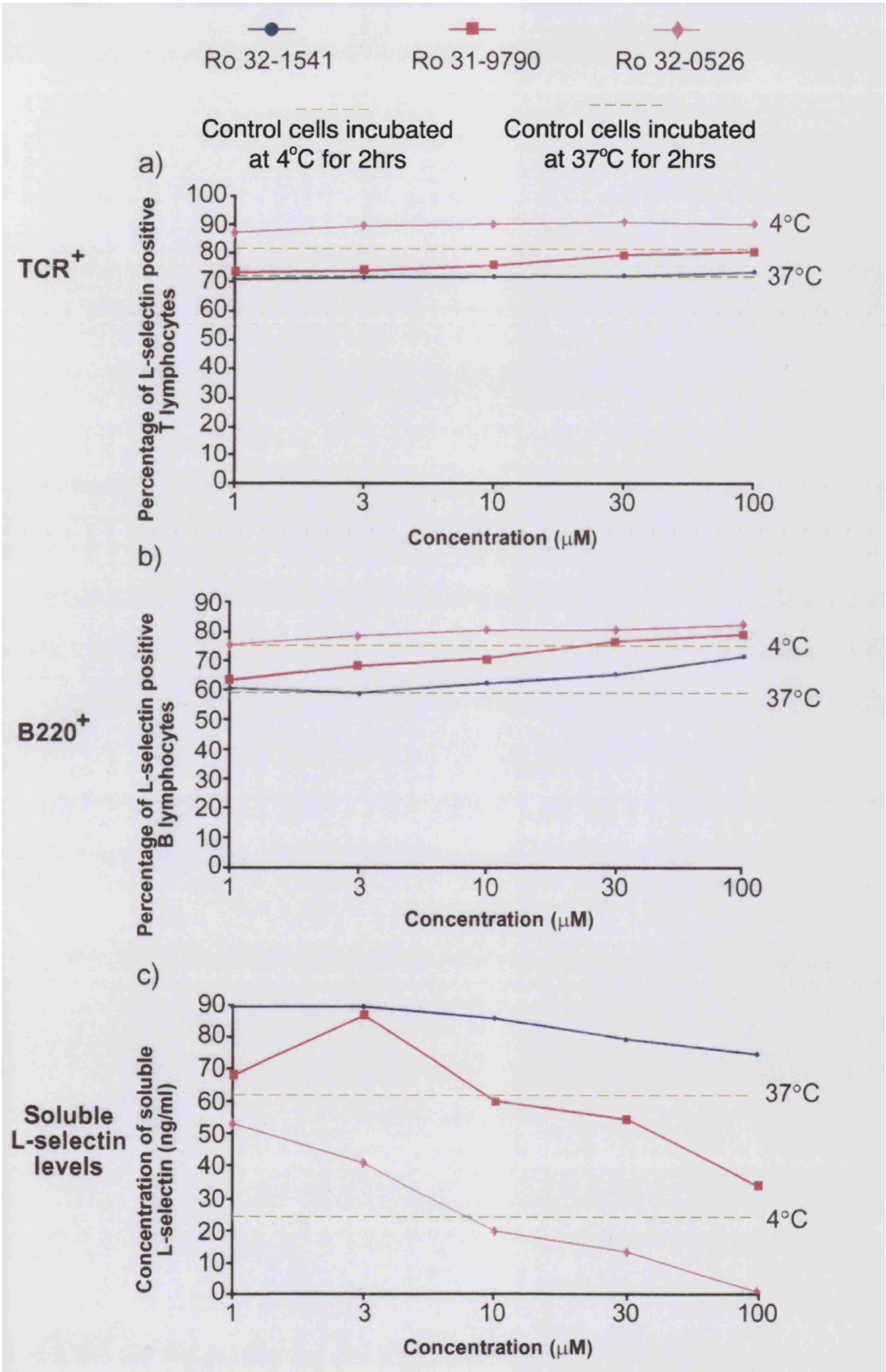
Ro 32-1541
Ro 31-9790
Ro 32-0526
Control cells incubated at 4°C for 2hrs
Control cells incubated at 37°C for 2hrs
a)
TCR+
Percentage of L-selectin positive T lymphocytes
4°C
37°C
Concentration (μM)
b)
B220+
Percentage of L-selectin positive B lymphocytes
4°C
37°C
Concentration (μM)
c)
Soluble L-selectin levels
Concentration of soluble L-selectin (ng/ml)
37°C
4°C
Concentration (μM)

5.5: Inhibition of Basal Shedding from 129/Sv Chimeric Mice Peripheral Lymph Node Lymphocytes with Ro 31-9790

To investigate basal shedding from $tace^{\Delta Zn/\Delta Zn}$ cells, PLN cell suspensions were split into four samples. Two samples were kept on ice for 1 hour, one in the presence and the other in the absence of hydroxamate based MMP inhibitor Ro-31-9790. The remaining two samples were incubated for 1 hour at 37°C, one in the presence and one in the absence of Ro-31-9790. L-selectin expression on T lymphocytes was measured. The results of this assay are shown in figure 5.6.

Both $tace^{WT}$ and $tace^{\Delta Zn/\Delta Zn}$ PLN T lymphocytes undergo basal shedding of L-selectin following incubation at 37°C (20 and 14% decrease in L-selectin positive cells respectively). The P values using a students t test to compare L-selectin expression at 4°C with that at 37°C are p=0.012 for $tace^{WT}$ cells and p=0.011 for $tace^{\Delta Zn/\Delta Zn}$ cells. The basal shedding is inhibited in $tace^{WT}$ cells with the inhibitor Ro 31-9790 ($p<0.05$), however, it is not significantly inhibited by Ro 31-9790 in $tace^{\Delta Zn/\Delta Zn}$ lymphocytes (p=0.6).

Figure 5.6: Basal shedding from Ly 9.1$^-$ PLN T lymphocytes from 129/Sv chimeric mice. L-selectin levels on lymphocytes kept on ice for 1 hour (in the absence or presence of Ro 31-9790), were compared to those of lymphocytes incubated at 37°C for 1 hour (in the absence or presence of Ro 31-9790). a) Basal shedding from *tace*^{WT} T lymphocytes. There was significant basal shedding from *tace*^{WT} T lymphocytes (p=0.012). The basal shedding was inhibited by Ro-31-9790, a hydroxamate based metalloproteinase inhibitor in *tace*^{WT} cells (p=0.038). b) Basal shedding from *tace*$^{\Delta Zn/\Delta Zn}$ T lymphocytes. There was significant basal shedding from *tace*$^{\Delta Zn/\Delta Zn}$ T lymphocytes (p=0.011). Basal shedding occurs by a TACE independent pathway in PLN T lymphocytes. Results are shown as percentage of L-selectin positive T lymphocytes ± SD (n=5).

a)

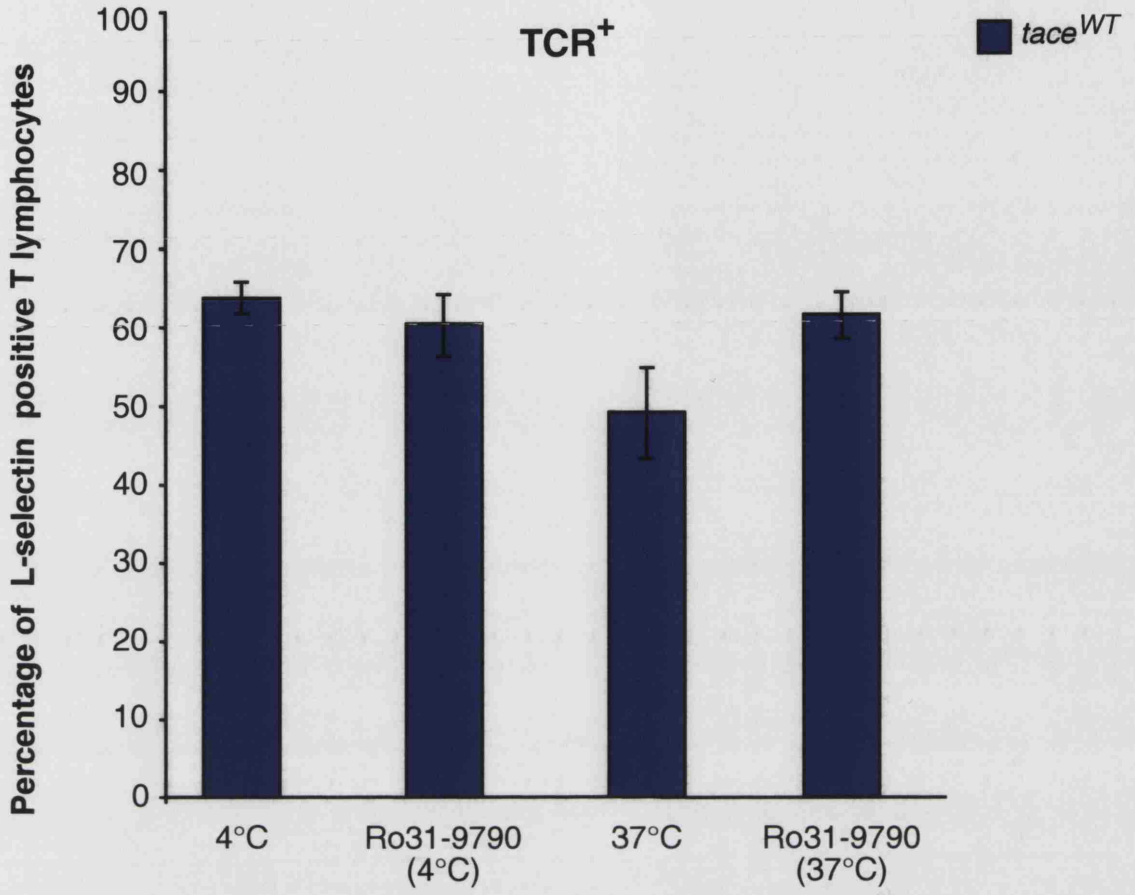
TCR+
tace WT
Percentage of L-selectin positive T lymphocytes
100
90
80
70
60
50
40
30
20
10
0
4°C
Ro31-9790 (4°C)
37°C
Ro31-9790 (37°C)

b)

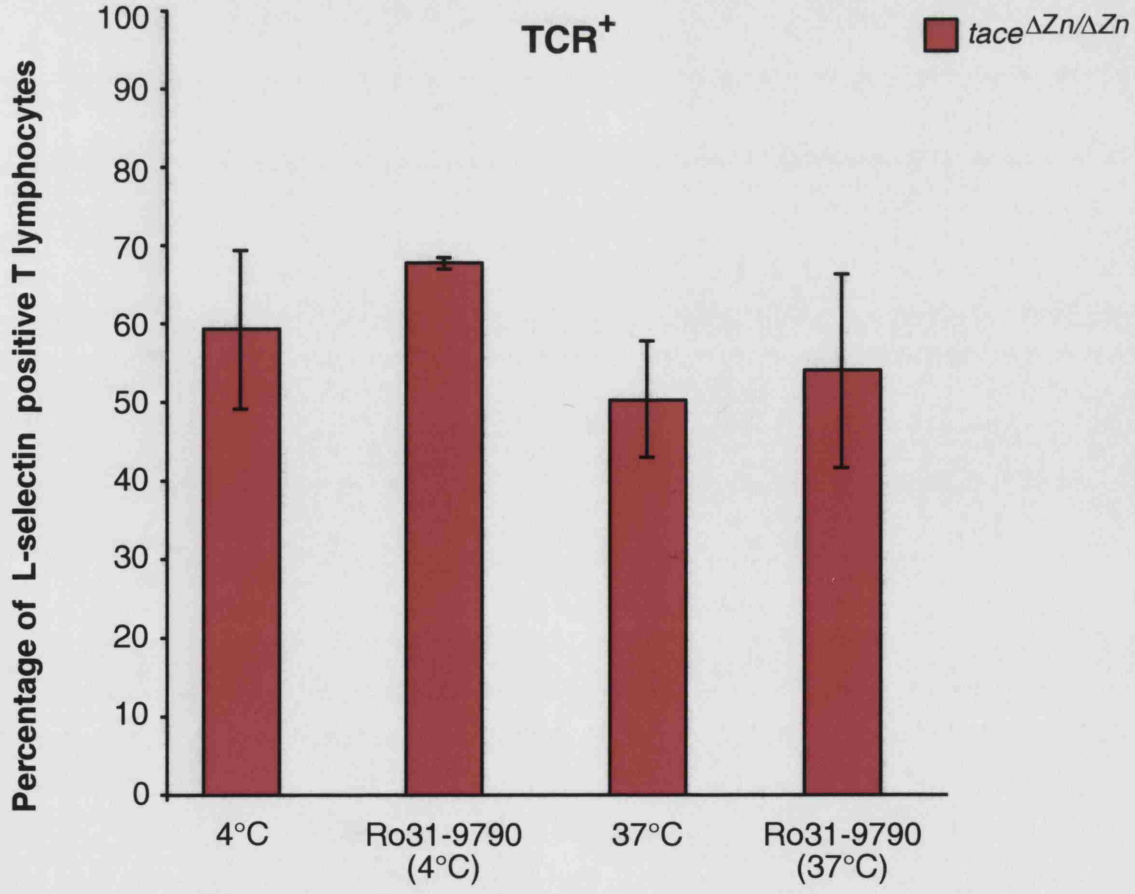
TCR+
tace ΔZn/ΔZn
Percentage of L-selectin positive T lymphocytes
100
90
80
70
60
50
40
30
20
10
0
4°C
Ro31-9790 (4°C)
37°C
Ro31-9790 (37°C)

5.6: Inhibition of Basal Shedding from C57BL/10 RAG$^{-/-}$ Chimeric Mice Lymphocytes

Basal shedding of L-selectin cannot be assessed in 129/Sv chimeric mice by measuring levels of soluble L-selectin due to the presence of residual host cells, particularly T lymphocytes. Hence, basal shedding inhibition assays were also performed on PLN cells from reconstituted C57BL/10 RAG$^{-/-}$ mice. As these mice are devoid of host-derived lymphocytes and the proportion of myeloid cells within PLNs is very small, supernatants from these cells were analysed for the presence of soluble L-selectin derived from *tace*$^{\Delta Zn/\Delta Zn}$ lymphocytes.

There was very little surface basal shedding seen from the surface of C57BL/10 RAG$^{-/-}$ PLN T lymphocytes (figure 5.7a and b). Ro 32-1541 did not inhibit what basal shedding there was in *tace*^{WT} or *tace*$^{\Delta Zn/\Delta Zn}$ PLN T lymphocytes. Addition of the metalloproteinase inhibitor Ro 31-9790 inhibited all shedding, in fact the surface levels of both *tace*^{WT} and *tace*$^{\Delta Zn/\Delta Zn}$ appeared to be higher in its presence than at 4°C. This was also true of Ro 32-0526. The percentage of L-selectin positive *tace*^{WT} and *tace*$^{\Delta Zn/\Delta Zn}$ cells in the Ro 32-0526 inhibited samples, were 9% and 3% (respectively) higher than the equivalent samples incubated on ice.

Although there was little change in cell surface expression, soluble L-selectin was detected and its release was metalloproteinase dependent. There was no effect of the Ro 32-1541 inhibitor on soluble L-selectin levels in the supernatants from both *tace*$^{\Delta Zn/\Delta Zn}$ cells when compared with those at 37°C. Ro 31-9790 and Ro 32-0526 partially blocked the release of L-selectin from *tace*^{WT} PLN cells, however completely blocked L-selectin release from *tace*$^{\Delta Zn/\Delta Zn}$ cells (0 ng/ml of selectin released) into the supernatant (table 5.4 and figure 5.7d). Inhibition of soluble L-selectin release by Ro 31-9790 was statistically significant ($p<0.002$).

As seen in the basal shedding from C57BL/6 peripheral lymph node cell data, there was soluble L-selectin present in the supernatant of *tace*^{WT} cells

kept on ice. This suggests that TACE dependent shedding can occur at very low temperatures. In addition, there was soluble L-selectin present in the supernatants of *tace*^{WT} cells incubated with Ro 31-9790 and Ro 32- 0526. It can be concluded that TACE independent shedding is completely blocked at low temperatures and in the presence of hydroxamate based metalloproteinase inhibitors Ro 31-9790 and Ro 32-0526, whereas TACE dependent shedding is only partially blocked under the same conditions.

Figure 5.7: Surface and soluble levels of L-selectin on PLN cells from $RAG^{-/-}$ chimeric mice following inhibition of basal shedding by hydroxamate based MMP inhibitors for 2 hours at 37°C. a) Inhibition of basal shedding from $tace^{WT}$ PLN T lymphocytes with hydroxamate inhibitors (100 μM). b) Inhibition of basal shedding in $tace^{\Delta Zn/\Delta Zn}$ cells by Ro 31-9790 was statistically significant (p=0.0018). c) Soluble levels of L-selectin in the supernatant of $tace^{WT}$ cells incubated in the presence of hydroxamate based inhibitors (100 μM). d) Soluble levels of L-selectin in the supernatant of $tace^{\Delta Zn/\Delta Zn}$ cells incubated in the presence of hydroxamate based inhibitors (100 μM). Soluble results (determined by ELISA) are a mean of two experiments with the exception of 4°C, absence of inhibitor and Ro 31-9790, which are a mean of four experiments.

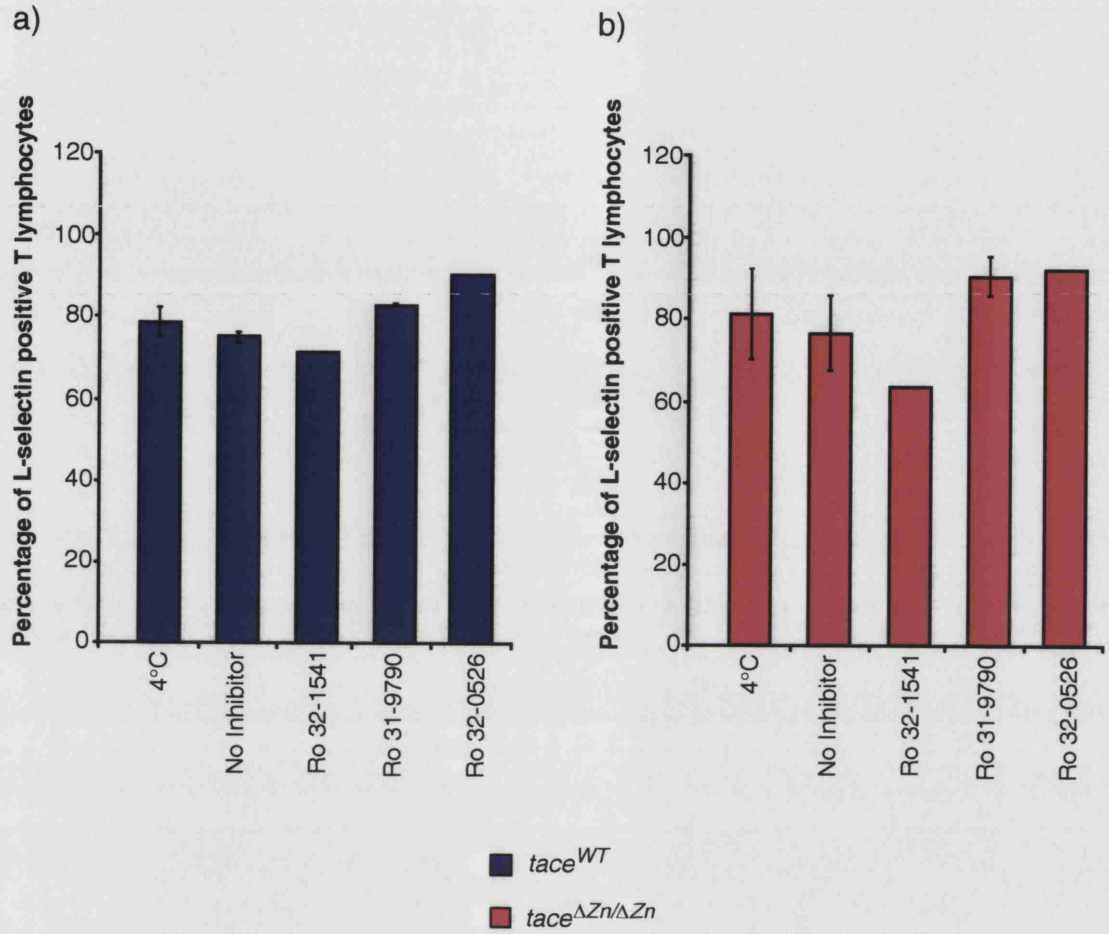
a)
b)
Percentage of L-selectin positive T lymphocytes
120
100
80
60
40
20
0
4°C
No Inhibitor
Ro 32-1541
Ro 31-9790
Ro 32-0526
tace^WT
tace^ΔZn/ΔZn

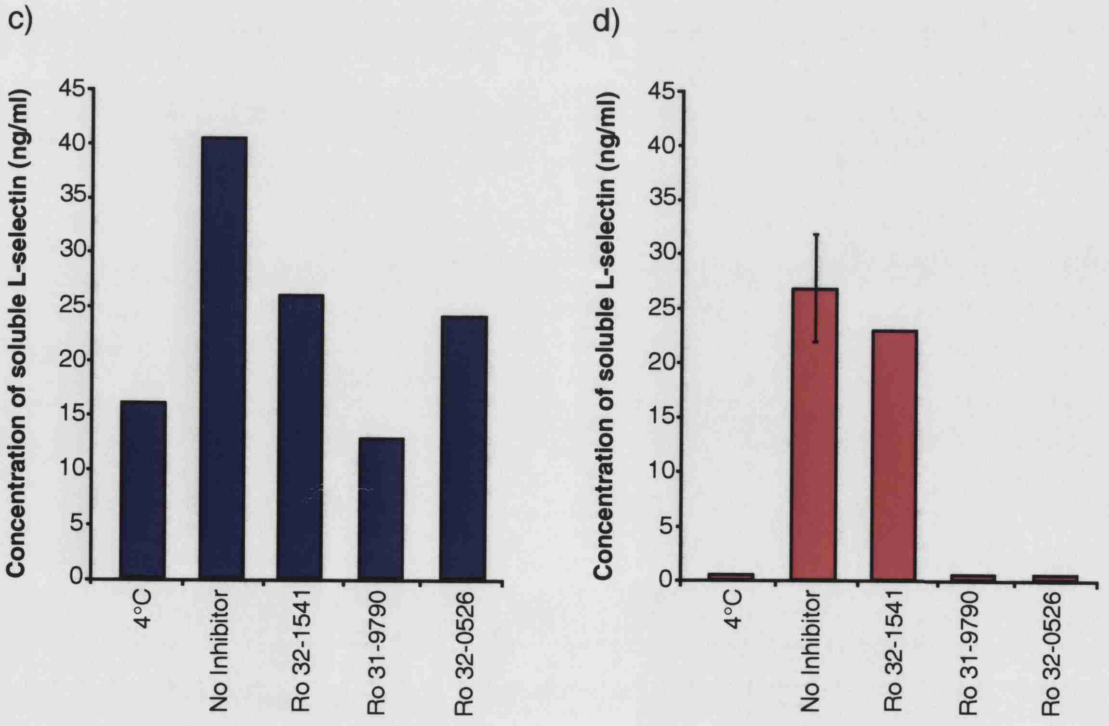
c)
d)
Concentration of soluble L-selectin (ng/ml)
45
40
35
30
25
20
15
10
5
0
4°C
No Inhibitor
Ro 32-1541
Ro 31-9790
Ro 32-0526

The assay was repeated using natural MMP inhibitors TIMP-1, 2 and 3 in place of the synthetic hydroxamate based inhibitors. Ro 31-9790 was included in the assays as a positive control.

As previously seen with reconstituted $RAG^{-/-}$ mice, there was little or no surface basal shedding seen. However, release of soluble L-selectin was seen from both $tace^{WT}$ and $tace^{\Delta Zn/\Delta Zn}$ cells. Ro 31-9790 completely blocked TACE independent shedding, with some soluble L-selectin, possibly derived from TACE dependent shedding, being present in the supernatant of $tace^{WT}$ cells. There was no effect of TIMP-1, 2 and 3 on soluble levels of L-selectin due to basal shedding. As described previously, Ro 31-9790 completely inhibited the release of soluble L-selectin due to basal shedding from $tace^{\Delta Zn/\Delta Zn}$ cells (table 5.4 and figure 5.8 d).

The inhibitory effects of TIMP-1, 2, and 3 on surface levels of L-selectin on PMA stimulated $tace^{WT}$ and $tace^{\Delta Zn/\Delta Zn}$ PLN T lymphocytes were measured as a positive control (figure 5.9). As described previously (Borland et al., 1999) TIMP-1 and 2 did not inhibit PMA stimulated shedding of L-selectin. There was partial inhibition of PMA stimulated L-selectin shedding from $tace^{WT}$ T lymphocytes by TIMP-3. This experiment was only performed once during the course of these studies to ensure that the results obtained were consistent to those described by Borland et al (1999). These results have been plotted in figure 5.9 to illustrate this response.

Figure 5.8: Surface and soluble levels of L-selectin on PLN cells from $RAG^{-/-}$ chimeric mice following inhibition of basal shedding by TIMP-1, 2, for 3 for 2 hours at 37°C. a) Inhibition of basal shedding from $tace^{WT}$ PLN T lymphocytes with TIMP-1, 2 and 3 (1μM). b) Inhibition of basal shedding from $tace^{\Delta Zn/\Delta Zn}$ PLN T lymphocytes with TIMP-1, 2 and 3 (1μM). c) Soluble levels (determined by ELISA) of L-selectin in the supernatant of $tace^{WT}$ cells incubated in the presence of TIMP-1, 2 and 3 (1 μM). d) Soluble levels (determined by ELISA) of L-selectin in the supernatant of $tace^{\Delta Zn/\Delta Zn}$ cells incubated in the presence of TIMP-1, 2 and 3 (1 μM). Soluble results are a mean of two experiments with the exception of 4°C, absence of inhibitor and Ro 31-9790 samples, which are a mean of four experiments.

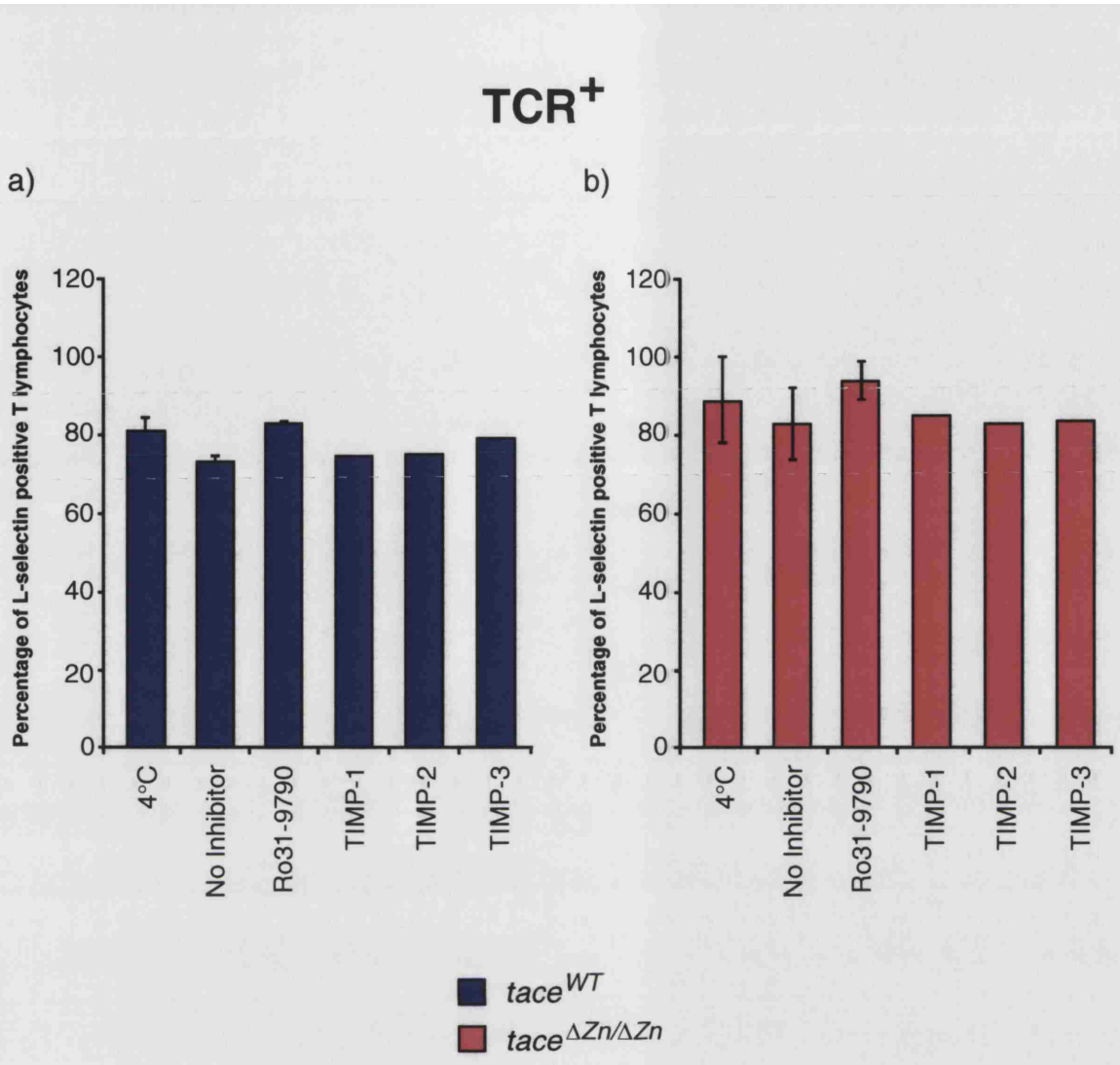
TCR+
a)
b)
Percentage of L-selectin positive T lymphocytes
120
100
80
60
40
20
0
4°C
No Inhibitor
Ro31-9790
TIMP-1
TIMP-2
TIMP-3
tace WT
tace ΔZn/ΔZn

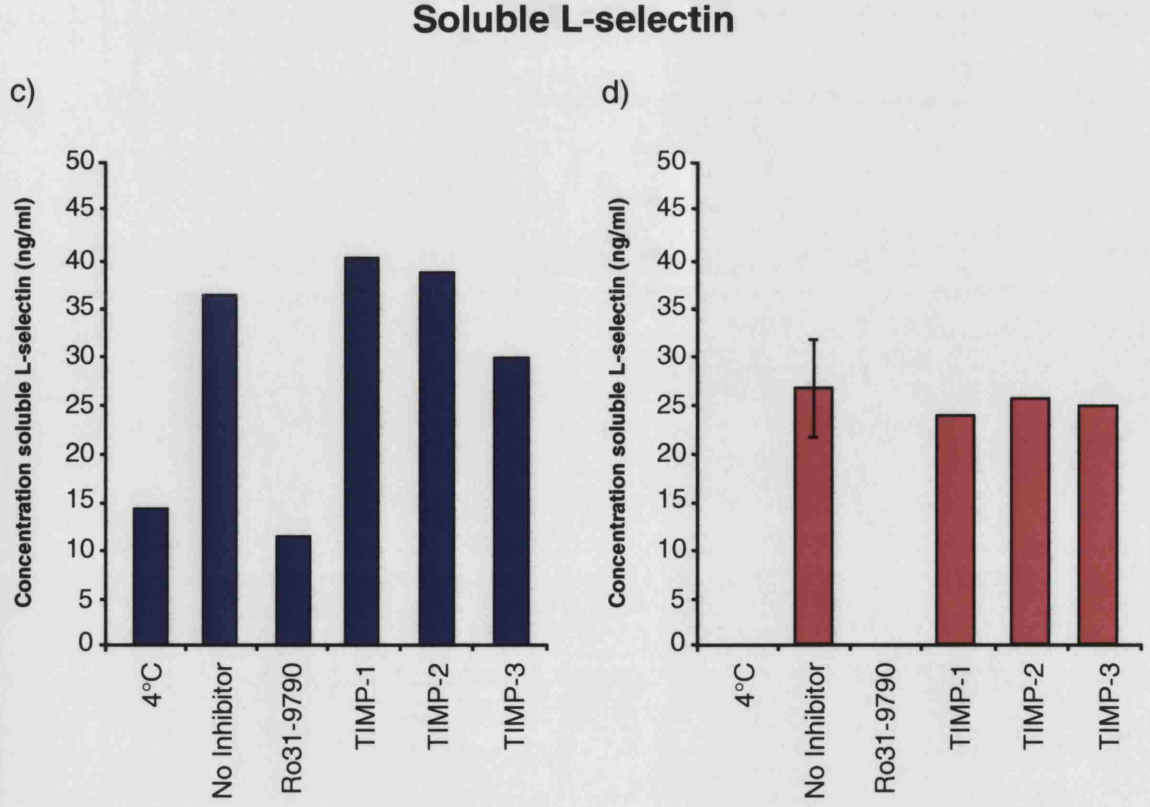
Soluble L-selectin
c)
d)
Concentration soluble L-selectin (ng/ml)
50
45
40
35
30
25
20
15
10
5
0
4°C
No Inhibitor
Ro31-9790
TIMP-1
TIMP-2
TIMP-3

Figure 5.9: Cell surface expression of L-selectin on *tace*^{WT} and *tace*$^{\Delta Zn/\Delta Zn}$ PLN T lymphocytes from RAG$^{-/-}$ chimeric mice, following incubation with PMA (100nM) and TIMP-1, 2 and 3 for 3 for 2 hours at 37°C. a) Percentage of *tace*^{WT} T lymphocytes positive for L-selectin following stimulation with PMA in the absence of inhibitor or presence of Ro 31-9790, TIMP-1, 2 or 3. TIMP-1 and 2 failed to inhibit PMA induced shedding of L-selectin. There was partial inhibition of shedding by TIMP-3. b) Percentage of *tace*$^{\Delta Zn/\Delta Zn}$ T lymphocytes positive for L-selectin following stimulation with PMA in the absence of inhibitor or presence of Ro 31-9790, TIMP-1, 2 or 3. As shown previously, *tace*$^{\Delta Zn/\Delta Zn}$ T lymphocytes do not shed L-selectin in response to PMA. Results are from a single experiment.

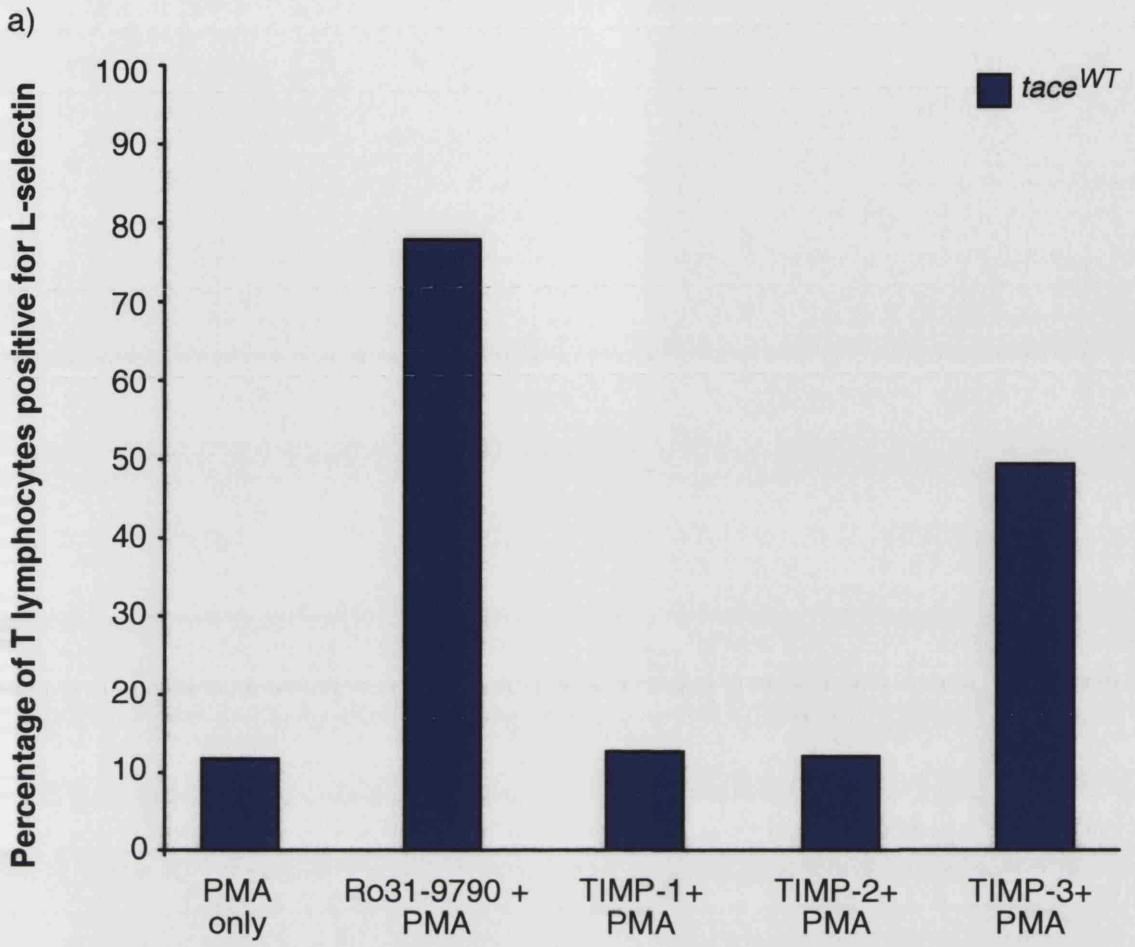
a)
Percentage of T lymphocytes positive for L-selectin
100
90
80
70
60
50
40
30
20
10
0
tace^WT
PMA only
Ro31-9790 + PMA
TIMP-1+ PMA
TIMP-2+ PMA
TIMP-3+ PMA

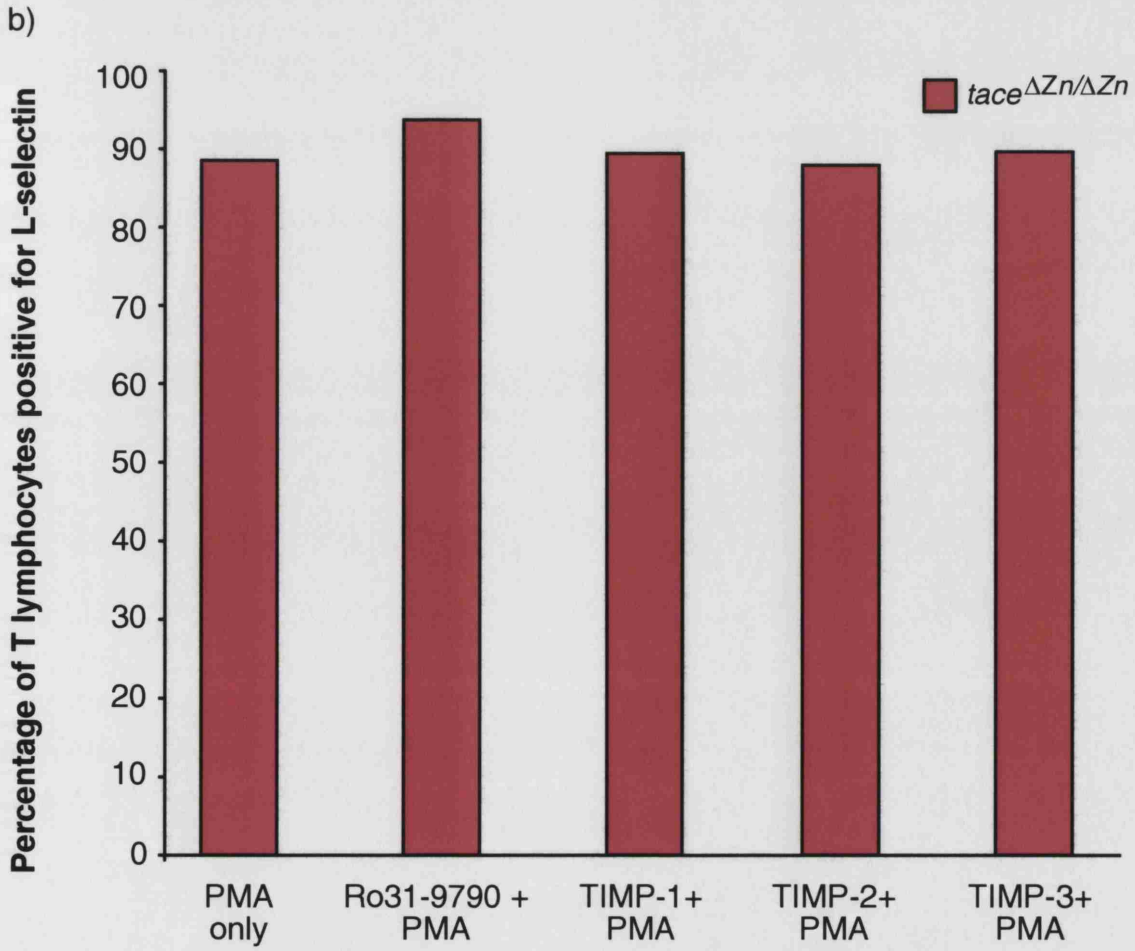
b)
Percentage of T lymphocytes positive for L-selectin
100
90
80
70
60
50
40
30
20
10
0
tace^ΔZn/ΔZn
PMA only
Ro31-9790 + PMA
TIMP-1+ PMA
TIMP-2+ PMA
TIMP-3+ PMA

	$tace^{WT}$	$tace^{\Delta Zn/\Delta Zn}$
4℃	81.2	89.0
No Inhibitor	75.2	70.3
Ro 32-1541	71.4	63.7
Ro 31-9790	83.0	87.1
Ro 32-0526	90.5	92.1
TIMP-1	74.7	85.0
TIMP-2	75.1	83.0
TIMP-3	78.9	83.5

Table 5.3: Percentage of L-selectin positive $RAG^{-/-}$ chimeric mice PLN T lymphocytes following inhibition of basal shedding for 2 hours at 37°C. Results are from a single experiment.

	$tace^{WT}$	$tace^{\Delta Zn/\Delta Zn}$
4℃	16	0
No Inhibitor	41	34
Ro 32-1541	26	23
Ro 31-9790	13	0
Ro 32-0526	24	0
TIMP-1	45	25
TIMP-2	43	28
TIMP-3	33	24

Table 5.4: Concentration of soluble L-selectin the supernatant of $RAG^{-/-}$ chimeric mice PLN cells following inhibition of basal shedding for 2 hours at 37°C. $tace^{WT}$ results are from a single experiment. $tace^{\Delta Zn/\Delta Zn}$ results are from a single experiment but are representative of two separate experiments.

5.7: Summary

Peripheral lymph node *tace*$^{\Delta Zn/\Delta Zn}$ T and B lymphocytes and non-lymphoid cells do not down-regulate L-selectin in response to PMA, while there is complete loss of L-selectin from the surface of *tace*^{WT} cells. There is a possible up-regulation of L-selectin levels in on the surface of *tace*$^{\Delta Zn/\Delta Zn}$ cells stimulated with PMA. PMA titration on *tace*^{WT} and *tace*$^{\Delta Zn/\Delta Zn}$ splenocytes confirmed that *tace*$^{\Delta Zn/\Delta Zn}$ cells do not undergo PMA induced cleavage of L-selectin even at high concentrations of PMA. These observations determine that downregulation of L-selectin in response to PMA is TACE dependent.

The lack of PMA induced shedding in *tace*$^{\Delta Zn/\Delta Zn}$ lymphocytes, was not from an inability to respond to PMA, as expression of the activation antigen CD69 was upregulated normally in T and B lymphocytes and non-lymphoid cells.

Basal shedding was most readily detected by measuring levels of soluble L-selectin released into the supernatant. Basal shedding of L-selectin occurred in *tace*$^{\Delta Zn/\Delta Zn}$ T lymphocytes suggesting an alternative shedding pathway in these cells. Studies on cells from C57BL/10 RAG$^{-/-}$ chimeric mice determine that Ro 32-1541 had little effect on basal shedding from *tace*$^{\Delta Zn/\Delta Zn}$ T lymphocytes, whereas Ro 31-9790 and Ro 32-0526 completely blocked basal shedding. TIMP-3 is known to inhibit PMA induced L-selectin shedding, however, it and TIMP-1 and 2 failed to inhibit basal shedding from *tace*$^{\Delta Zn/\Delta Zn}$ T lymphocytes. As basal shedding from *tace*$^{\Delta Zn/\Delta Zn}$ T lymphocytes is inhibited by Ro 31-9790 but not TIMP-3, shedding appears to be metalloproteinase dependent but TACE independent.

Basal shedding from the cell surface (i.e. changes in percentage of cells positive for L-selectin) is not always significant, however, levels of soluble L-selectin present in the supernatant of these cells show greater changes. It is not clear why this is the case. It maybe that some soluble L-selectin generated by the metalloproteinase is not released via the cell surface.

Chapter 6: Circulating Soluble L-selectin in Mice

Proteolytic cleavage releases the extracellular domain of L-selectin into the blood as a soluble form. Soluble L-selectin exists in two forms, one of 62 kDa and the other 75-100 kDa (Schleiffenbaum et al., 1992). The two isoforms are thought to consist of the same fragment of the L-selectin molecule (same cleavage site), however the 75-100 kDa isoform is thought to originate from neutrophils and be differentially glycosylated from that expressed and released from lymphocytes (Gearing and Newman, 1993). The shed form of L-selectin has been shown to be biologically active and will block L-selectin mediated adhesion (Gearing and Newman, 1993; Schleiffenbaum et al., 1992) Soluble L-selectin is found in the plasma of healthy individuals (Schleiffenbaum et al., 1992) but levels have shown to be affected in certain diseases. Patients with sepsis and HIV have been shown to have raised levels of soluble L-selectin. In patients at risk of developing adult respiratory distress syndrome (ARDS), there are significantly lower levels of soluble L-selectin in those who subsequently progress to disease (Donnelly et al., 1994).

The amount of soluble L-selectin in plasma can be quantified by a sandwich ELISA using MEL-14 mAb (Gallatin et al., 1983) recognising an epitope in the lectin domain as a capture antibody and biotinylated T28 mAb, recognising the Ly 22 epitope in the EGF domain (Siegelman et al., 1990) as a detecting antibody.

As with the previous two chapters, the control mouse samples that were used in the analyses in this chapter were chimeric mice where it was not known whether the foetal liver cells used to reconstitute them were of a $tace^{+/+}$ genotype or a $tace^{+/-}$ genotype. Therefore, the term $tace^{WT}$, referring to the normal L-selectin shedding response seen in lymphocytes from these mice, was used to describe these samples.

6.1: LEC-Ig

A known concentration of LEC-Ig fusion protein, comprising the extracellular portion of L-selectin fused to the Fc domain of human IgG was previously provided by Genentech (figure 6.1) for use as a standard in the ELISA. To provide the quantities of LEC-Ig used in this report a cDNA construct encoding LEC-Ig was generated and transfected into a mammalian expression system.

Previously, DNA encoding full length murine L-selectin had been cloned into the pEE6CMV/neo (CellTech) plasmid between *Hind III* and *Sal I* restriction sites by Dr. Kiki Tanousis. Primers had also been designed (by Dr. Kiki Tanousis) to amplify a truncated form of L-selectin termed MPΔ from full length L-selectin DNA. The MPΔ mutation primers amplify the extracellular region of L-selectin, including the Mel 14 and Ly 22 epitopes, however as they amplify the DNA from the beginning of the SCR sequence the membrane proximal region is not included in the amplification (figure 6.2).

Figure 6.1: LEC-Ig fusion protein consisting of the extracellular portion of L-selectin fused to the Fc domain of human IgG.

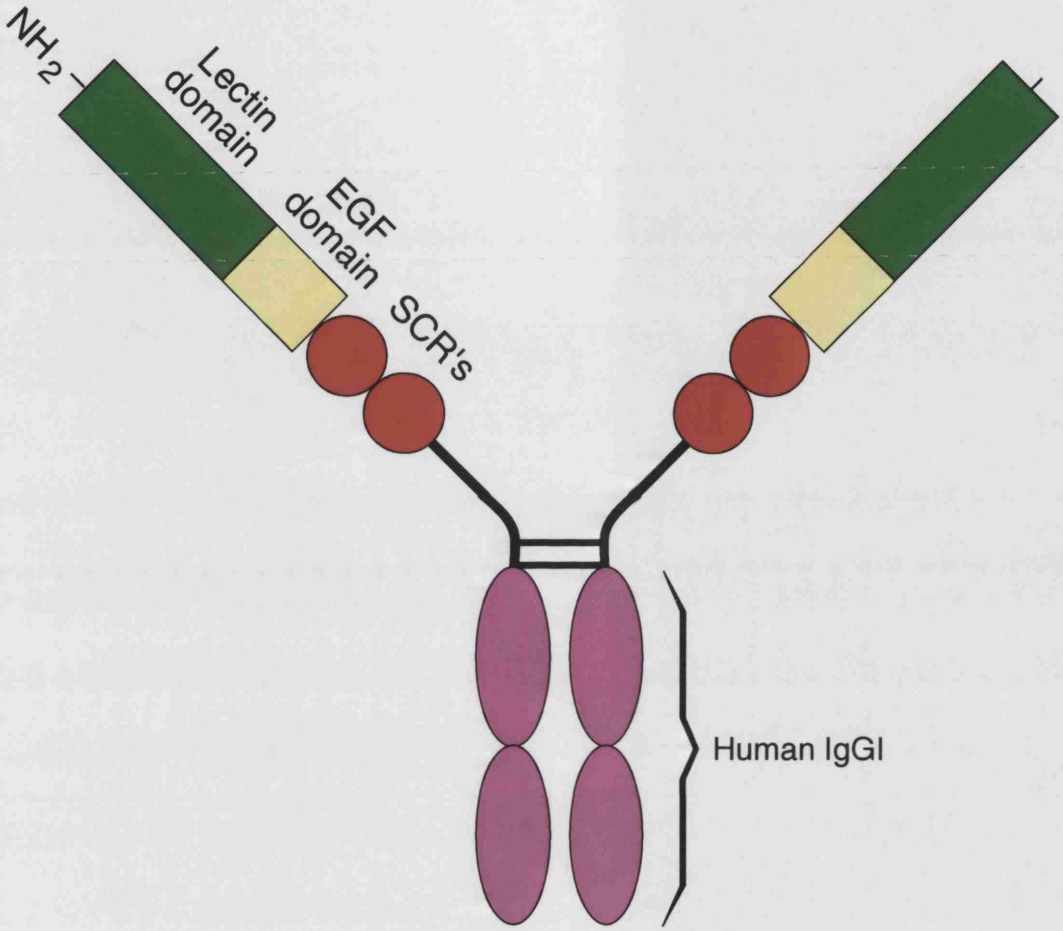
NH2
Lectin domain
EGF domain
SCR's
Human IgGI

Figure 6.2: Amplification of a truncated form of L-selectin, MPΔ. Reverse PCR primer recognises the sequence at the start of either SCR. Expected product sizes for the reverse primer amplifying both SCR or only one SCR are shown in red and green respectively.

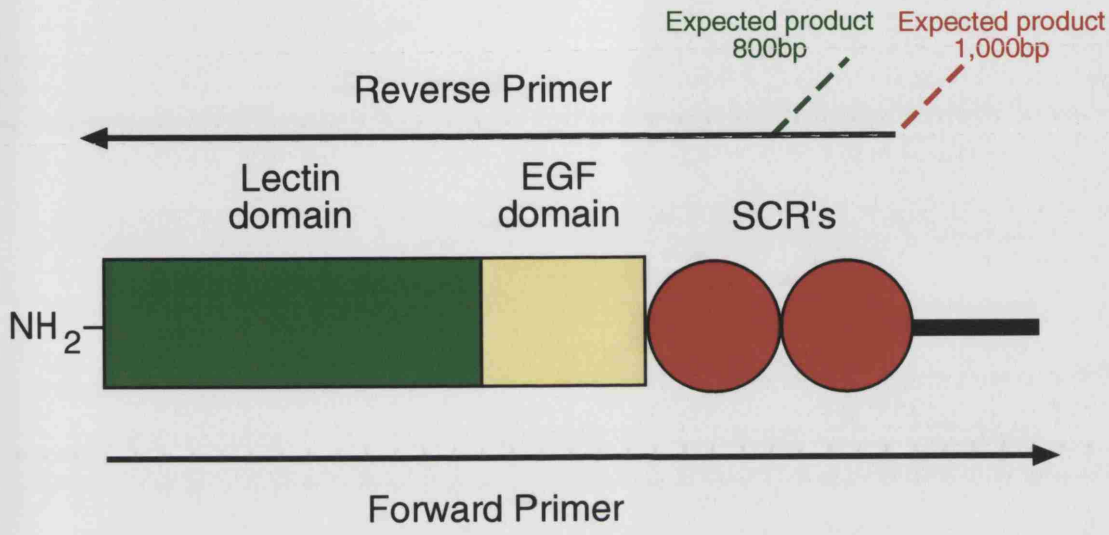
Expected product
800bp
Expected product
1,000bp
Reverse Primer
Lectin
domain
EGF
domain
SCR's
NH2
Forward Primer

6.2: Cloning of MPΔ

Prior to amplification of MPΔ by PCR the pEE6CMV/neo plasmid containing the full length L-selectin DNA was linerised using the restriction endonucleases *Hind III* and *Ecor I.* DNA encoding L-selectin was amplified by PCR using forward primer, 5' GGCC**AAGCTT**CTAGACCGCCATGGTGTTTCCATGG 3' (sequence in bold is a *Hind III* restriction site), and reverse primer 5' GGTCTCGGTTAGACGGTTCA GCTGCCGG 3'. The reverse primer reads from the start of the short consensus repeat (SCR) regions, thus producing a mutated form of the L-selectin DNA coding for the SCR, EGF and lectin domains of L-selectin only. When the PCR products were run on a 1% agarose gel a band at ~800 bp (figure 6.3) was seen. The size of the insert suggested that the polymerase had mainly read one SCR region only as opposed to both. The MPΔ PCR products were digested using the restriction enzymes, *Hind III* and *Sal I.*

To produce the fusion protein MPΔ-Ig, MPΔ DNA was spliced into the pEE12FcG1 plasmid (supplied by CellTech) encoding the Fc region of human IgG (figure 6.4). Two bacterial colonies (6 and 7) containing the neomycin resistant pEE12FcG1 plasmid were chosen for further growth and transfection into a mammalian expression system and were checked for the presence of an insert encoding to MPΔ-Ig (figure 6.5). Primers reading along the L-selectin DNA sequence were designed. The harvested insert DNA was sequenced and the sequence confirmed that the MPΔ insert comprised murine L-selectin with only one of the SCR regions.

Figure 6.3: PCR products following amplification of a truncated form of L-selectin. The reverse primer amplifies from the beginning of either SCR repeat. As the PCR product was ~800bp in size (lane 1), it was probable that only one SCR had been amplified. The expected product for amplification of both SCR was 1,000bp.

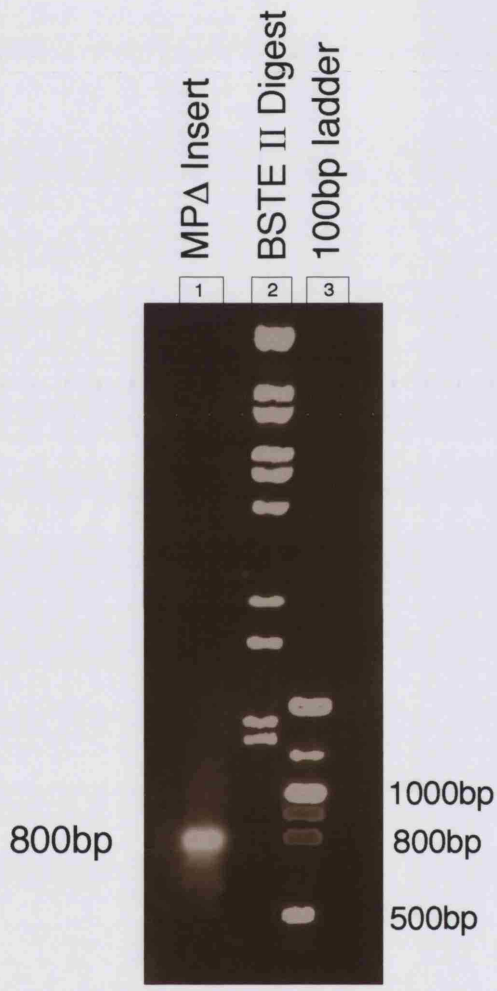
MPΔ Insert
BSTE II Digest
100bp ladder
1
2
3
800bp
1000bp
800bp
500bp

Figure 6.4: pEE12FcG1 plasmid (CellTech) containing the Fc region of human IgG (blue). The site of the MPΔ insert is shown in red.

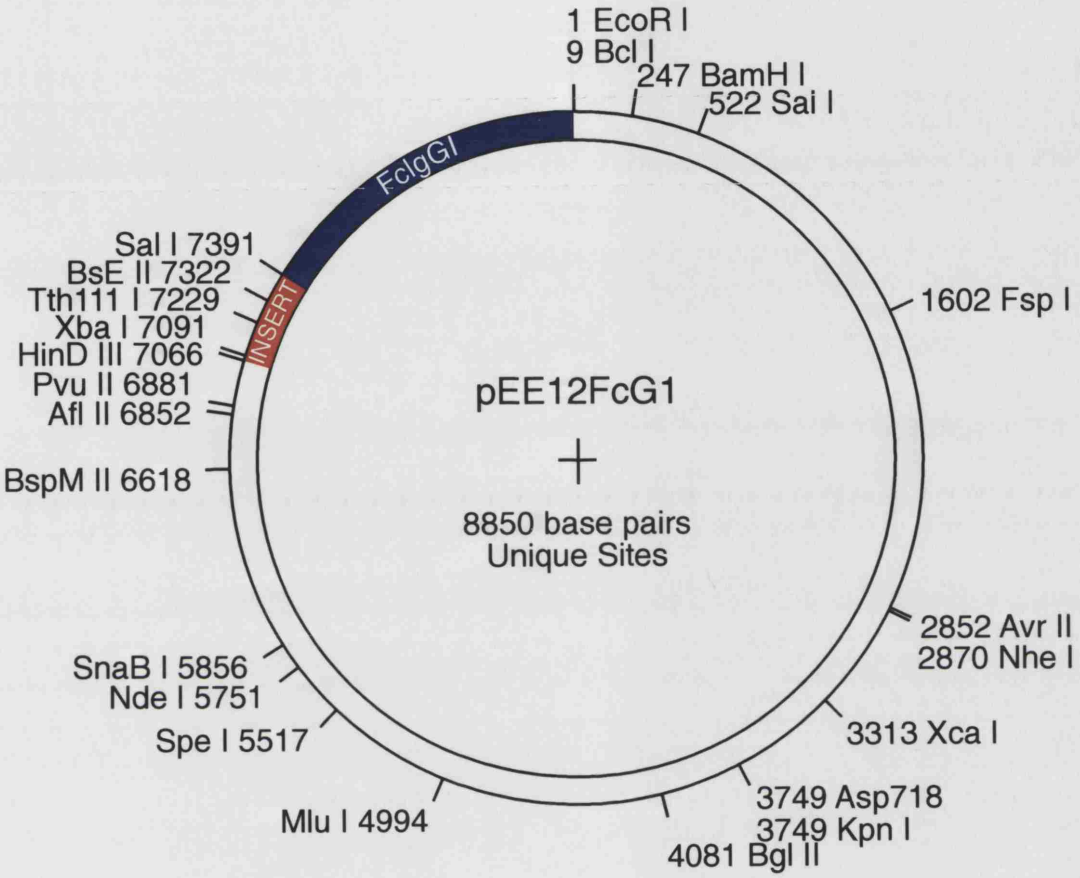
1 EcoR I
9 Bcl I
247 BamH I
522 Sal I
FcIgGI
Sal I 7391
BsE II 7322
Tth111 I 7229
Xba I 7091
HinD III 7066
Pvu II 6881
Afl II 6852
INSERT
BspM II 6618
1602 Fsp I
pEE12FcG1
8850 base pairs
Unique Sites
2852 Avr II
2870 Nhe I
SnaB I 5856
Nde I 5751
Spe I 5517
3313 Xca I
Mlu I 4994
3749 Asp718
3749 Kpn I
4081 Bgl II

Figure 6.5: DNA harvested from bacterial colonies 6 and 7 (lanes 1 and 2). Bands present at 7391bp relating to the pEE12FcG1 vector and 800bp relating to the MPΔ insert.

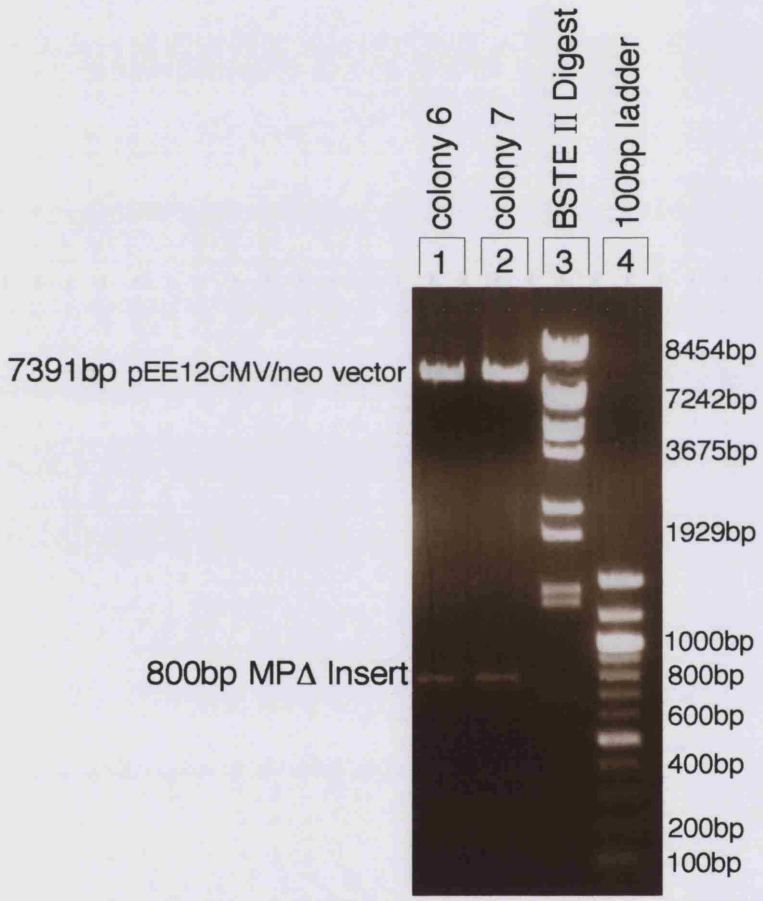
colony 6
colony 7
BSTE II Digest
100bp ladder
1
2
3
4
7391bp pEE12CMV/neo vector
800bp MPΔ Insert
8454bp
7242bp
3675bp
1929bp
1000bp
800bp
600bp
400bp
200bp
100bp

6.3: Transfection of NSϕ cells

NSϕ were cultured according to the CellTech protocol (chapter 2). The cells were checked for greater than 90% viability, then electroplated with linearised insert DNA with 2 consecutive pulses of 1500 volts, 3μF and selected for GS-gene expression (glutamine-independent growth). Cell colonies were tested by ELISA for the concentration of LEC-Ig present in the supernatant. High yield stable transfectants were selected. Supernatant from these colonies was collected and LEC-Ig purified (chapter 2) and tested against stock from Genentech.

Using the new stock of LEC-Ig various plasma samples were tested for levels of soluble L-selectin present.

6.4: Circulating Soluble L-selectin in 129/Sv Chimeric Mice

Serum samples from the 129/Sv mice reconstituted with *tace*$^{+/+}$ and *tace*$^{\Delta Zn/\Delta Zn}$ foetal liver cells were collected by exsanguination under anaesthetic. Although there would have been soluble L-selectin originating from residual host cells, sera were tested using an ELISA method for the presence of a general increase or decrease in the levels of soluble L-selectin due to the TACE mutation.

There was a large variation in soluble L-selectin levels between individual mouse serum samples (figure 6.6). The average levels of soluble L-selectin in serum from *tace*$^{+/+}$ and *tace*$^{\Delta Zn/\Delta Zn}$ chimeric mice were 2.4 μg/ml and 2.0 μg/ml, respectively. There was no significant effect of the TACE mutation in 129/Sv chimeric mice ($p=0.6$).

Figure 6.6: Circulating soluble L-selectin in 129/Sv chimeric mice reconstituted with *tace*$^{+/+}$ or *tace*$^{\Delta Zn/\Delta Zn}$ foetal liver cells. Levels of soluble L-selectin (μg/ml) as measured by ELISA in the sera from *tace*$^{+/+}$ and *tace*$^{\Delta Zn/\Delta Zn}$ chimeric mice (n=5). There was no significant effect of the TACE mutation on serum levels of soluble L-selectin. Means and SD are also shown.

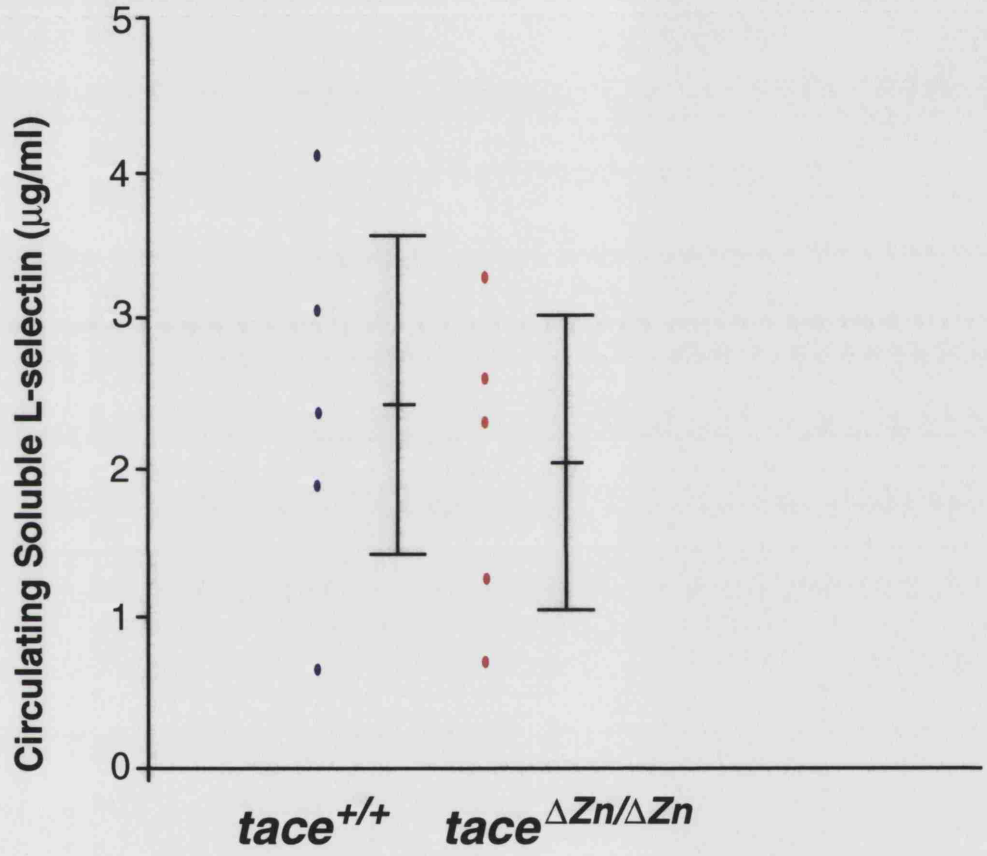
Circulating Soluble L-selectin (μg/ml)
5
4
3
2
1
0
tace+/+
taceΔZn/ΔZn

6.5: Circulating soluble L-selectin in *tace*$^{\Delta Zn/\Delta Zn}$ mice

As well as collecting blood from reconstituted (chimeric) mice, serum samples from the few *tace*$^{\Delta Zn/\Delta Zn}$ mice that survive up to two weeks following birth were generously provided by Dr. Roy Black, Immunex. These samples were tested for soluble L-selectin levels. However, *tace*$^{\Delta Zn/\Delta Zn}$ knockouts are of the mouse strain DBA-1, rather than C57BL/6. The DBA-1 mouse strain does not express the Ly 22 epitope, thus, the T28 antibody cannot be used to detect soluble L-selectin. An attempt was made to raise a polyclonal antiserum to a peptide, termed Lectin-1 (amino acid sequence, WTYHYSEKPMNWENARK), from the lectin domain of murine L-selectin.

6.6: Raising a Polyclonal Antiserum Against Lectin-1.

Rabbits (R3421, R3422, R3426, and R3427) were injected with 1ml of 0.5mg/ml Lectin-1 conjugated to ovalbumin in complete Freunds adjuvant (CFA) into four separate sites on the back of each rabbit. 28 days later the same rabbits were injected with the same amounts of Lectin-1 conjugated to keyhole limpet haemocyanin (KLH) in incomplete Freunds adjuvant (IFA). Further injections (as described above) of Lectin-1/KLH in IFA were carried out 28 days later. Antibodies recognizing Lectin-1 peptide were present in sera from all four rabbits. The rabbits were culled and the sera collected after boosts. Rabbit anti-Lectin-1 immunoglobulin was purified from whole sera by affinity chromatography and used instead of T28 mAb in the ELISA for soluble L-selectin, however it did not detect native L-selectin in the assay (data not shown).

As it was not possible to raise a polysera against DBA-1 soluble L-selectin, antibodies to L-selectin from alternative species were tested for cross reactivity to murine L-selectin.

Anti-human L-selectin antibodies were tested for cross reactivity to murine L-selectin (Figure 6.7). Two possible antibodies were tested; LAM-1.16, which recognizes an epitope in the lectin domain of human L-selectin, and LAM-1 18, which recognizes an epitope in the SCR. As expected, Mel-14

recognises L-selectin on both C57BL/6 and DBA-1 cells (figure 6.7a) whereas T28 recognises C57BL/6 L-selectin positive cells but not DBA-1 cells (figure 6.7b). LAM-1 16 cross-reacted with L-selectin on cells from both C57Bl/6 and DBA-1 mice. LAM-1 18 showed some cross-reaction but not all L-selectin positive cells were stained.

LAM-1 16 was substituted into the ELISA as a replacement for T28. As LAM-1 16 was not biotinylated, it was used to coat the ELISA plate and act as a capture antibody, while biotinylated MEL-14 was used to detect bound soluble L-selectin (figure 6.8).

Figure 6.7: Anti-human L-selectin antibodies cross-react with murine L-selectin. FACs analysis of PLN cells labelled with murine or human anti L-selectin antibodies. a) Staining of L-selectin on C57BL/6 and DBA-1 cells with MEL 14. Both strains stained positively for MEL 14. b) Staining of L-selectin on C57BL/6 and DBA-1 cells with T28. C57BL/6 mice stained positively for T28, however, DBA-1 mice were negative for the Ly 22 epitope that is recognised by T28. c) Staining of L-selectin on C57BL/6 and DBA-1 cells with anti-human L-selectin antibody, LAM-1 16. Both strains stained positively for LAM-1.16. d) Staining of L-selectin on C57BL/6 and DBA-1 cells anti-human L-selectin antibody, LAM-1 18. In both strains, only a small proportion of cells stained positively using LAM-1 18.

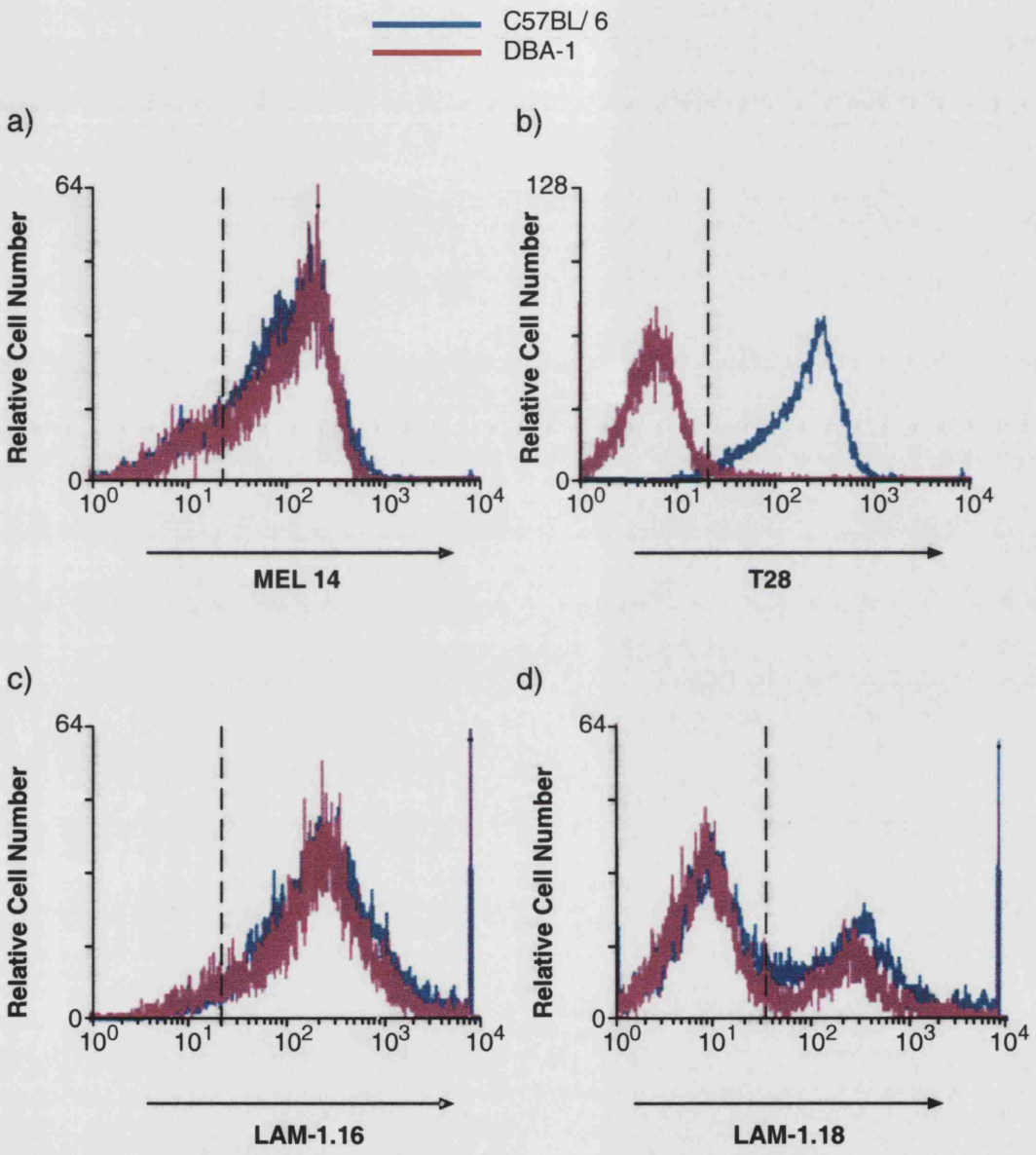
C57BL/ 6
DBA-1
a)
b)
c)
d)
Relative Cell Number
64
128
0
10^0
10^1
10^2
10^3
10^4
MEL 14
T28
LAM-1.16
LAM-1.18

Figure 6.8: ELISA protocols for detecting soluble L-selectin. a) ELISA method used to detect soluble L-selectin from Ly 22 positive mice. The protocol uses MEL 14 and T28 to detect L-selectin. b) ELISA method used to detect soluble L-selectin from Ly 22 negative mice. The protocol uses MEL 14 and LAM-1 16 to detect L-selectin.

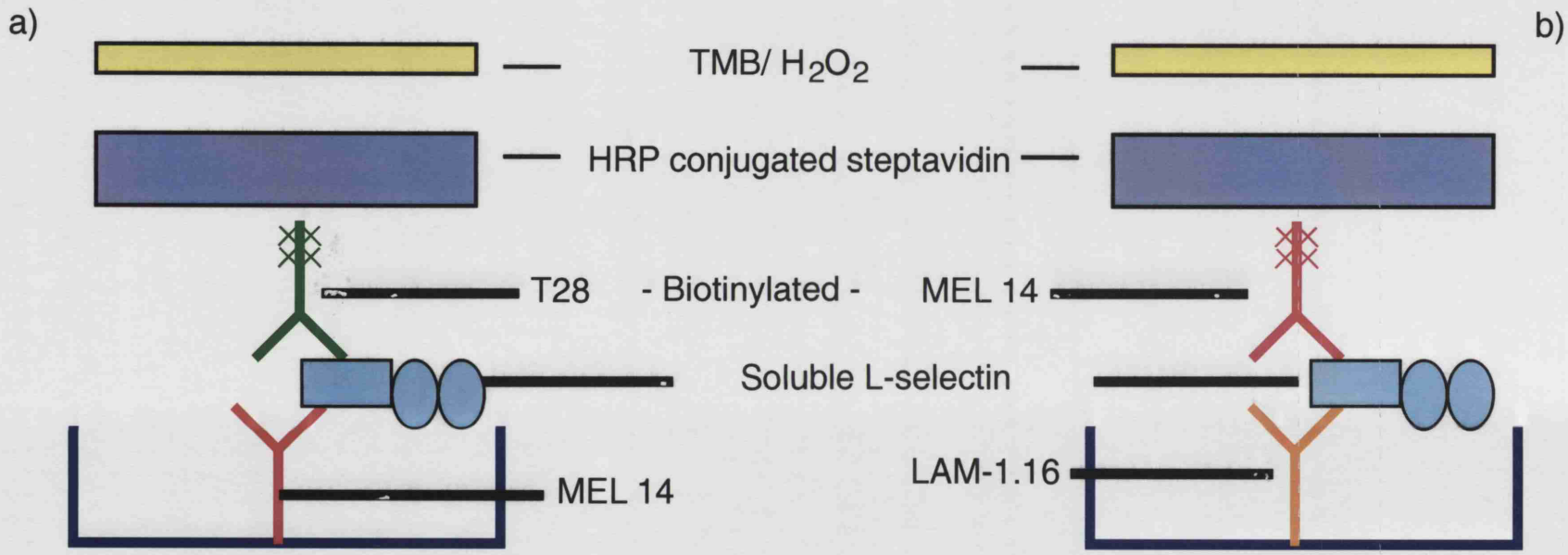
a)
b)
TMB/ H_2O_2
HRP conjugated steptavidin
T28
- Biotinylated -
MEL 14
Soluble L-selectin
MEL 14
LAM-1.16

The LAM-1 16 ELISA protocol was used to measure L-selectin levels in *tace*$^{\Delta Zn/\Delta Zn}$ mice of the DBA-1 strain(Figure 6.9). Unexpectedly, rather than there being a decrease of soluble L-selectin levels in the surviving *tace*$^{\Delta Zn/\Delta Zn}$ mice, there was an increase in the average concentration. The average concentration of soluble L-selectin in sera of *tace*$^{+/+}$ mice was 0.5 μg/ml, whereas the average was 0.75 μg/ml in sera *tace*$^{\Delta Zn/\Delta Zn}$ mice. However, there were only 3 mice in the *tace*$^{\Delta Zn/\Delta Zn}$ group and this increase was not significant (p=0.2).

Figure 6.9: Circulating soluble L-selectin in DBA-1 *tace*$^{\Delta Zn/\Delta Zn}$ mice. Concentration (μg/ml) – measured by ELISA – of soluble L-selectin in the sera from 7 *tace*^{WT} and 3 *tace*$^{\Delta Zn/\Delta Zn}$ mice. There was no statistically significant difference between these mice. Means and SD are also shown.

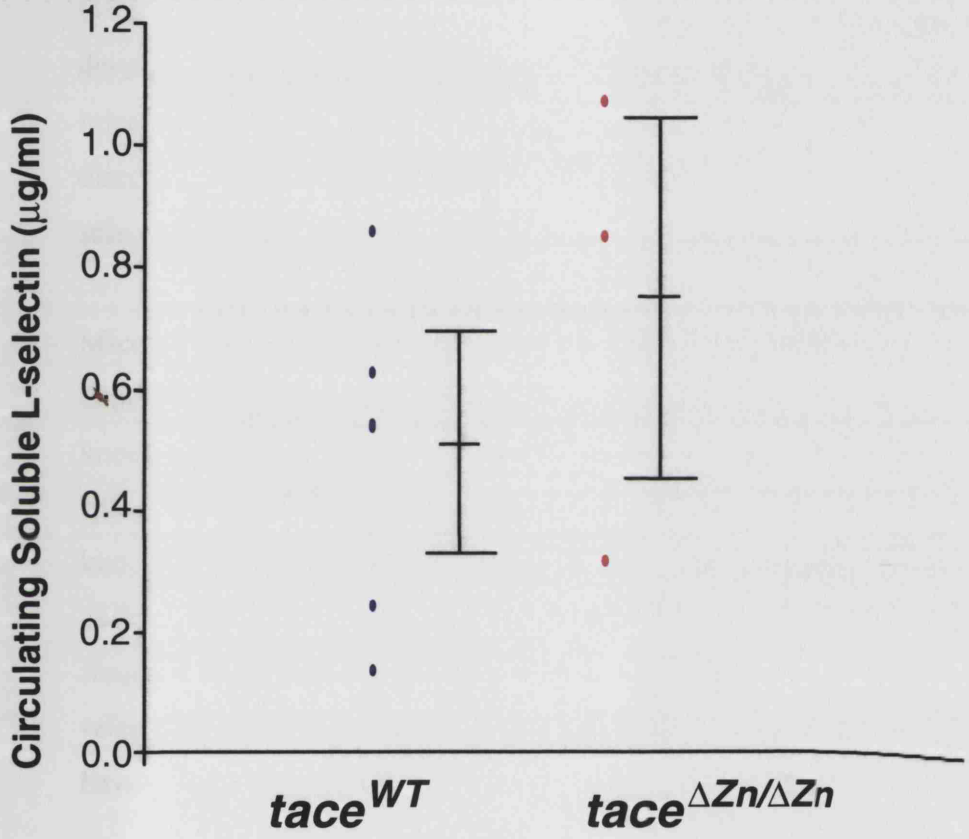
Circulating Soluble L-selectin (μg/ml)
1.2
1.0
0.8
0.6
0.4
0.2
0.0
tace^WT
tace^ΔZn/ΔZn

6.7: Circulating Soluble L-selectin in L-selectin Knockout Mice Reconstituted with *tace*$^{\Delta Zn/\Delta Zn}$ Foetal Liver Cells

The previous results suggested that there was no effect of the TACE mutation on serum levels of soluble L-selectin. However, in the case of the 129/Sv chimeric mice, the ELISA would have also detected soluble L-selectin derived from host derived cells and in their paper Peschon et al, (1998) show that the TACE mutation has an essential role in many areas of development suggesting that the levels of soluble L-selectin in *tace*$^{\Delta Zn/\Delta Zn}$ mice may be affected by other factors. In an attempt to develop a model that directly measures the effect of the TACE mutation on serum soluble L-selectin, L-selectin knockout mice were reconstituted with foetal liver cells.

Mice with a mutant L-selectin gene resulting in complete loss of cell surface expression were originally generated by Arbonés et al, 1994. L-selectin knockouts have smaller lymph nodes, lower lymph node cell yields, larger spleens and fewer HEV than their control littermates. Studies with L-selectin knockout lymphocytes have shown an inability to bind to HEV, a 99% decrease in migration to peripheral lymph nodes and a reduction in rolling frequency (Arbonés et al., 1994). Due to the complete lack of endogenous L-selectin, soluble L-selectin present in the reconstituted mice sera could only have originated from donor leukocytes.

L-selectin knockout mice were irradiated with 6 Gys of irradiation and intravenously injected with foetal liver cells collected at day 16.5 of gestation (see chapter 3). Twelve weeks after irradiation, blood samples were screened for the presence of soluble L-selectin. *tace*^{WT} and *tace*$^{\Delta Zn/\Delta Zn}$ peripheral lymph node and spleen cell yields were measured.

	tace^{WT}	*tace*$^{\Delta Zn/\Delta Zn}$
Peripheral Lymph Nodes	12 ± 5	10 ± 2
Spleen	77 ± 29	114 ± 28

Table 6.1: Cell yields from pooled peripheral lymph nodes and spleen in reconstituted L-selectin knockout mice. Results are means ± SD x 10^6 (n=5).

Soluble L-selectin is present in the sera of L-selectin knockout mice reconstituted with *tace*$^{\Delta Zn/\Delta Zn}$ foetal liver cells (figure 6.10). This supports the data in chapter 5 suggesting that TACE is not the only enzyme involved in L-selectin cleavage. The average concentrations of soluble L-selectin in *tace*^{WT} and *tace*$^{\Delta Zn/\Delta Zn}$ reconstituted mice were 3.6 μg/ml and 2.7 μg/ml respectively. Unlike the result seen in the surviving DBA-1 *tace*$^{\Delta Zn/\Delta Zn}$ mice, there were significantly lower levels of L-selectin present in the sera of L-selectin$^{-/-}$ mice reconstituted with *tace*$^{\Delta Zn/\Delta Zn}$ foetal liver cells ($p=0.04$).

Figure 6.10: Circulating soluble L-selectin in L-selectin knockout mice reconstituted with *tace*$^{\Delta Zn/\Delta Zn}$ foetal liver cells. Levels of L-selectin (μg/ml) present in the sera – detected by ELISA – of 5 *tace*^{WT} and 5 *tace*$^{\Delta Zn/\Delta Zn}$ reconstituted L-selectin KO mice. There were significantly lower levels of L-selectin present in the sera of L-selectin$^{-/-}$ mice reconstituted with *tace*$^{\Delta Zn/\Delta Zn}$ foetal liver cells ($p=0.04$). Means and SD are shown.

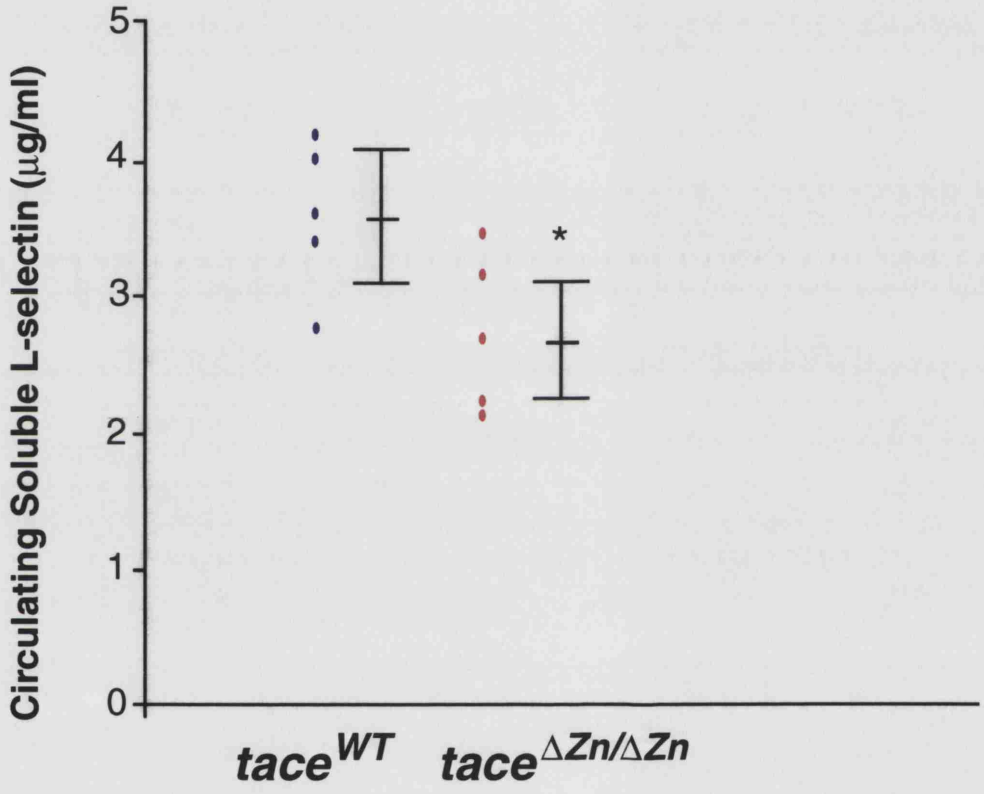
Circulating Soluble L-selectin (μg/ml)
5
4
3
2
1
0
*
tace^WT
tace^ΔZn/ΔZn

6.8: Intercellular cleavage of L-selectin by TACE

It is possible that TACE present on one cell may be able to cleave L-selectin expressed on a neighbouring cell. There was no evidence of this occurring in cell samples from 129/Sv chimeric mice where there are both $TACE^{+/+}$ host cells and TACE deficient donor cells, however a controlled experiment was performed where $tace^{WT}$ and $tace^{\Delta Zn/\Delta Zn}$ PLN cells from reconstituted $RAG^{-/-}$ host mice were mixed (at a ratio of 7:1 respectively) in the presence and absence of PMA. $tace^{\Delta Zn/\Delta Zn}$ cells were stained with the fluorescent marker CFSE to enable identification of the two cell populations. A control of CFSE labelled $tace^{WT}$ cells was also included to ensure no effect of CFSE on the results obtained.

There was no loss of L-selectin from $tace^{\Delta Zn/\Delta Zn}$ T or B lymphocytes incubated with excess $tace^{WT}$ cells in the presence of PMA (figure 6.11).

There was a slightly higher percentage of L-selectin positive $tace^{\Delta Zn/\Delta Zn}$ T cells incubated with PMA alone. However, it is not clear whether this is due to downregulation of L-selectin in the presence of excess $tace^{WT}$ cells or increased expression of L-selectin on the T lymphocytes incubated with PMA as seen in chapter 5 (figure 6.11a). Results in figure 6.11 are from a single experiment but are representative of two separate experiments.

Figure 6.11: Effect of *tace*^{WT} cells on L-selectin shedding by CFSE stained *tace*$^{\Delta Zn/\Delta Zn}$ lymphocytes. FACs analysis of *tace*$^{\Delta Zn/\Delta Zn}$ lymphocytes labelled with MEL 14 mAB following stimulation with PMA (300nM) in the presence and absence of excess of *tace*^{WT} cells for 1 hour at 37°C. a) Effect of PMA on L-selectin expression by *tace*$^{\Delta Zn/\Delta Zn}$ T lymphocytes, in the presence or absence of *tace*^{WT} cells. Cells were mixed in a *tace*^{WT} to *tace*$^{\Delta Zn/\Delta Zn}$ ratio of 7:1. L-selectin shedding in *tace*$^{\Delta Zn/\Delta Zn}$ in response to PMA stimulation was not induced by incubation with excess *tace*^{WT} cells. b) Effect of PMA on L-selectin expression by *tace*$^{\Delta Zn/\Delta Zn}$ B lymphocytes, in the presence or absence of *tace*^{WT} cells. Cells were mixed in a *tace*^{WT} to *tace*$^{\Delta Zn/\Delta Zn}$ ratio of 7:1. . L-selectin shedding in *tace*$^{\Delta Zn/\Delta Zn}$ in response to PMA stimulation was not induced by incubation with excess *tace*^{WT} cells. Results shown are from a single experiment.

a)

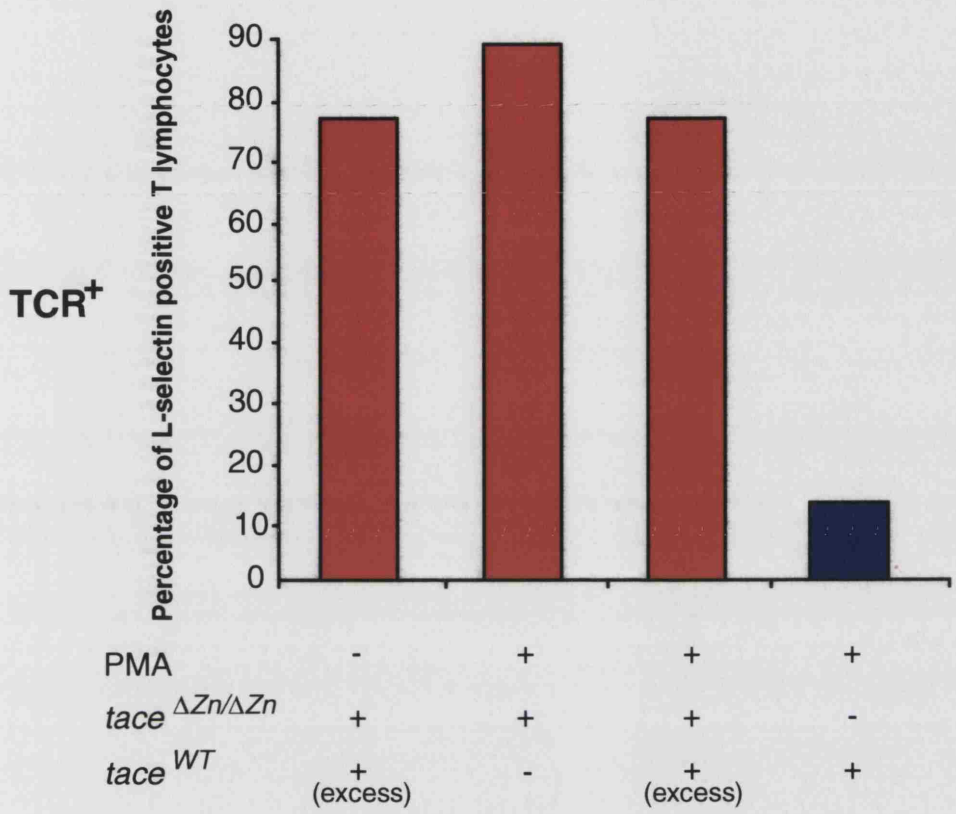
TCR+
Percentage of L-selectin positive T lymphocytes
90
80
70
60
50
40
30
20
10
0
PMA - + + +
tace ΔZn/ΔZn + + + -
tace WT + (excess) - + (excess) +

b)

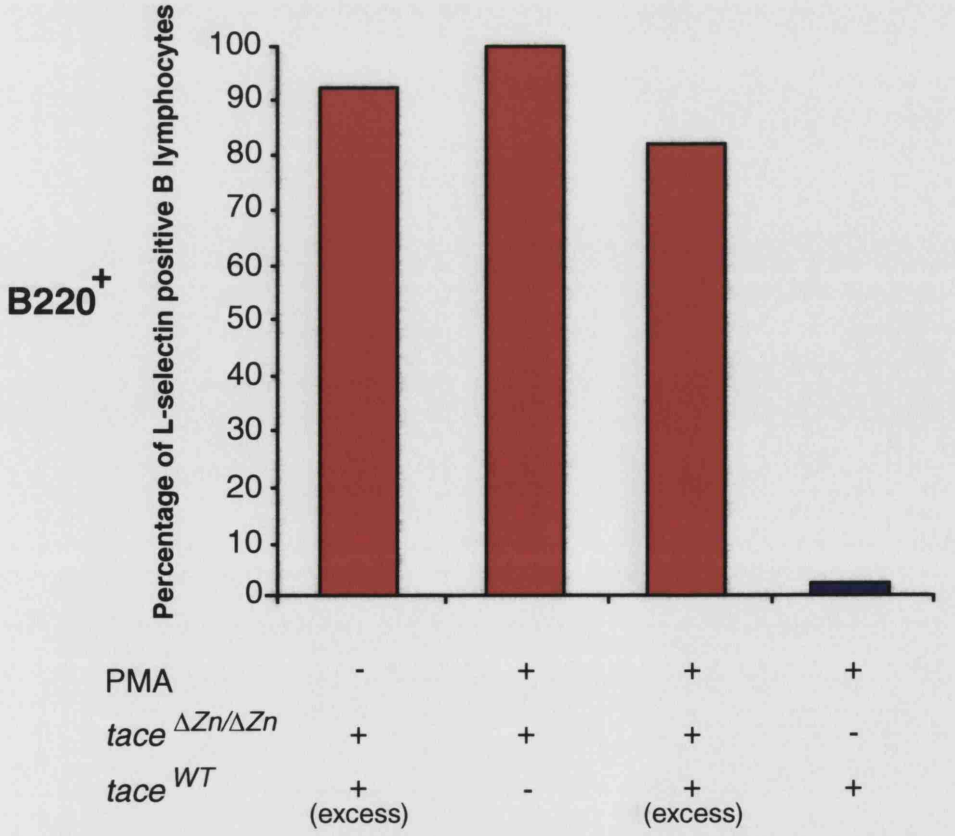
B220+
Percentage of L-selectin positive B lymphocytes
100
90
80
70
60
50
40
30
20
10
0
PMA - + + +
tace ΔZn/ΔZn + + + -
tace WT + (excess) - + (excess) +

6.9: Effect of Soluble TACE on L-Selectin Shedding by Lymphocytes

From the results obtained it was apparent that although TACE is not implicated in basal shedding, it is directly or indirectly responsible for PMA induced shedding of L-selectin. It was attempted to restore PMA induced downregulation in *tace*$^{\Delta Zn/\Delta Zn}$ cells from 129/Sv chimeric mice by incubation with soluble TACE (kindly donated by Dr. Gillian Murphy) in the presence and absence of PMA (figure 6.12).

There was normal downregulation of L-selectin from *tace*^{WT} T lymphocytes in response to PMA. PMA induced shedding was not restored in *tace*$^{\Delta Zn/\Delta Zn}$ T lymphocytes upon incubation with soluble TACE (figure 6.12a).

There was normal downregulation of L-selectin from *tace*^{WT} B lymphocytes following stimulation with PMA. Rapid downregulation of L-selectin due to PMA stimulation was not restored in *tace*$^{\Delta Zn/\Delta Zn}$ B lymphocytes by the addition of soluble TACE (figure 6.12b).

To ensure that the TACE that was used in this experiment was active, the sample was used in a TNF-α cleavage assay and found to be active (data not shown).

Figure 6.12: Effect of soluble TACE on L-selectin shedding by *tace*$^{\Delta Zn/\Delta Zn}$ lymphocytes. FACs analysis of lymphocytes stained with MEL 14 following stimulation with PMA (300nM) in the presence or absence of soluble TACE for 1 hour at 37°C. a) Effect of soluble TACE (0.1 μM) on *tace*$^{\Delta Zn/\Delta Zn}$ and *tace*^{WT} T lymphocytes in the presence and absence of PMA (300 nM). L-selectin shedding in response to PMA stimulation was not restored in *tace*$^{\Delta Zn/\Delta Zn}$ cells by incubation with soluble TACE. b) Effect of soluble TACE (0.1 μM) on *tace*$^{\Delta Zn/\Delta Zn}$ and *tace*^{WT} B lymphocytes in the presence and absence of PMA (300 nM). L-selectin shedding in response to PMA stimulation was not restored in *tace*$^{\Delta Zn/\Delta Zn}$ cells by incubation with soluble TACE. Results are from three experiments.

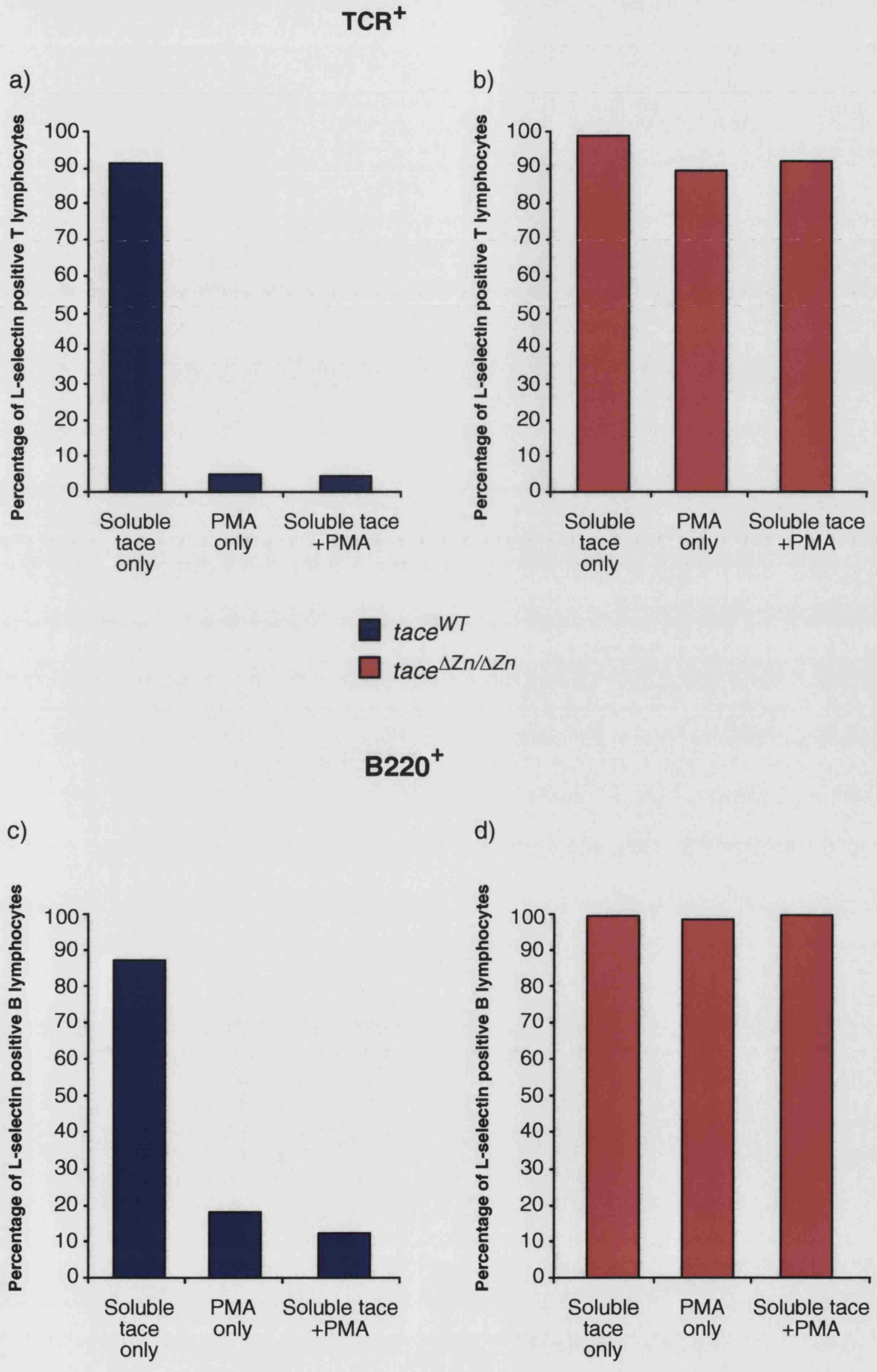
TCR+
a)
b)
Percentage of L-selectin positive T lymphocytes
100
90
80
70
60
50
40
30
20
10
0
Soluble tace only
PMA only
Soluble tace +PMA
tace^WT
tace^ΔZn/ΔZn
B220+
c)
d)
Percentage of L-selectin positive B lymphocytes

6.10: Circulating Soluble L-selectin in MMP-9 Knockout Mice

As the TACE mutation had shown little effect on serum levels of L-selectin, other ADAMs/MMPs started to be tested as having a possible role in L-selectin shedding. Matrix Metalloproteinase-9 (MMP-9), also known as gelatinase B, is thought to be involved in the degradation of the extracellular matrix during the extravasation of leukocytes. Its' substrates include collagens, gelatin, elastin and fibronectin. MMP-9 has been implicated in a variety of different cancers, including breast and colon. MMP-9 cleaves and inactivates IL-1β (Ito et al., 1996). The role of MMP-9 in L-selectin cleavage was investigated by measuring the levels of soluble L-selectin present in the plasma of MMP-9 knockout mice (kindly donated by Dr Steve Shapiro and Dr Susan Noursharh).

The average concentration of soluble L-selectin in the wild type (WT) mice was 4 μg/ml in comparison to 3.4 μg/ml in the MMP-9 knock out plasma (figure 6.13). There was no significance due to the MMP-9 mutation on soluble L-selectin levels ($p=0.4$).

Figure 6.13: Circulating soluble L-selectin in MMP-9 knockout mice. Levels of soluble L-selectin (μg/ml) as measured by ELISA from 4 WT plasma samples and 5 MMP-9 knockout plasma samples. There was no effect on L-selectin shedding from the MMP-9 mutation. Means and SD are shown.

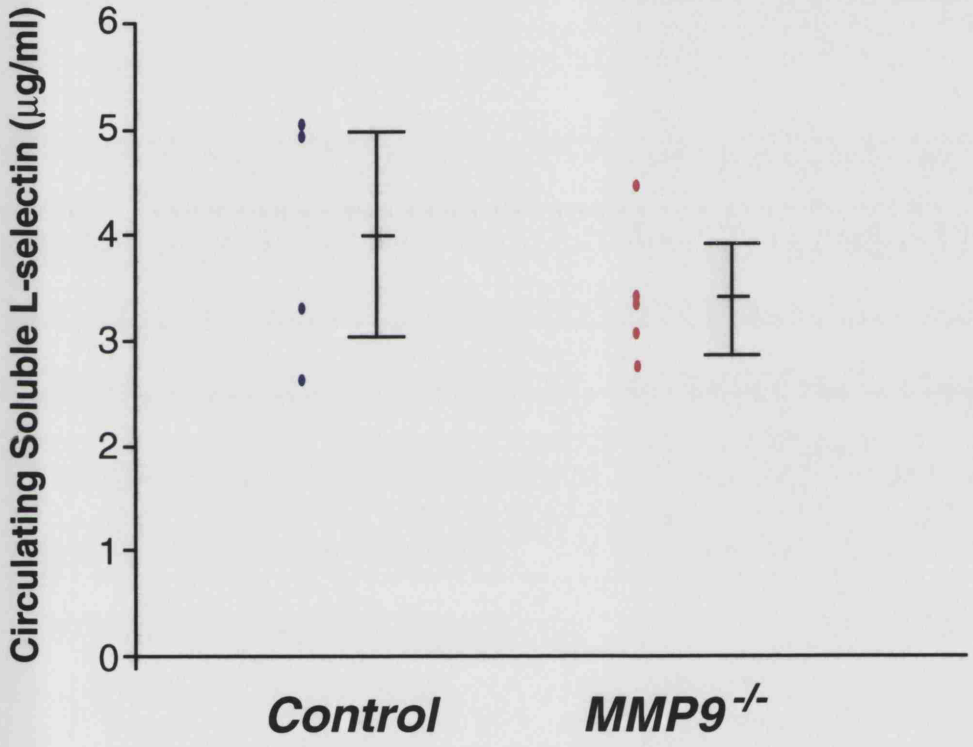
Circulating Soluble L-selectin (μg/ml)
6
5
4
3
2
1
0
Control
MMP9-/-

6.11: Summary

The aim of these studies was to measure circulating soluble L-selectin in mice. To achieve this a stock of a fusion protein, LEC-Ig, was established for use as a standard in an ELISA assay. A truncated form of L-selectin, consisting of the lectin domain, EGF region and one SCR, was fused to the Fc domain of human IgG and transfected into a mammalian expression system. Transfected colonies were selected for GS-gene expression and high yield of LEC-Ig.

In addition to stocks of LEC-Ig being generated, an ELISA protocol enabling detection of Ly 22^{-} soluble L-selectin was also established. Anti-human L-selectin antibody, LAM-1 16, was substituted for T28 in the ELISA protocol to determine the concentration of soluble L-selectin present in the plasma of surviving $tace^{\Delta Zn/\Delta Zn}$ DBA-1 mice.

Soluble L-selectin levels in sera of $tace^{\Delta Zn/\Delta Zn}$ mice and 129/Sv chimeric mice reconstituted with $tace^{\Delta Zn/\Delta Zn}$ foetal liver cells were measured. No significant effect of the TACE mutation was detected.

L-selectin knockout mice were reconstituted with $tace^{\Delta Zn/\Delta Zn}$ foetal liver cells. Sera from reconstituted mice were analysed for the presence of L-selectin. L-selectin levels were significantly lower in the $tace^{\Delta Zn/\Delta Zn}$ reconstituted mice in comparison to those reconstituted with $tace^{WT}$ cells, however, the levels of L-selectin present were significant providing further evidence for a TACE independent pathway of L-selectin cleavage. As it was possible that TACE on the host L-selectin$^{-/-}$ cells may be cleaving L-selectin on the donor cells, the ability of excess $tace^{WT}$ cells to restore PMA induced shedding in $tace^{\Delta Zn/\Delta Zn}$ cells was investigated. TACE appears not to cleave L-selectin on the surface of neighbouring cells since PMA induced shedding was not restored in $tace^{\Delta Zn/\Delta Zn}$ cells even in the presence of an excess of $tace^{WT}$ cells.

It was also attempted to restore PMA induced shedding of L-selectin in *tace*$^{\Delta Zn/\Delta Zn}$ by the addition of soluble TACE. However, incubation with soluble TACE did not restore rapid down-regulation of L-selectin in response to PMA in *tace*$^{\Delta Zn/\Delta Zn}$ T or B lymphocytes.

As it is probable that TACE is not the only enzyme involved in L-selectin downregulation, we started to investigate alternative enzymes. Circulating levels of soluble L-selectin in MMP-9 knockout mice were measured. There was no effect of the MMP-9 mutation on soluble L-selectin levels.

Chapter 7: The Role of TACE in Lymphocyte Migration

L-selectin is essential for lymphocyte migration into peripheral lymph nodes (Xu et al., 1996). Studies blocking L-selectin shedding show a decreased leucocyte rolling velocity (Hafezi-Moghadam and Ley, 1999) and possibly an inability of lymphocytes to effectively migrate through the endothelial lining (Faveeuw et al., 2001). As TACE has been shown to be responsible for PMA induced shedding, *tace*$^{\Delta Zn/\Delta Zn}$ cells were put into migration assays to determine the effect of the TACE mutation on migration.

Two migration assays were used; an *in vitro* model of migration through a high endothelial cell (HEC) monolayer and an *in vivo* trafficking assay. Cultured rat HECs express lymphocyte adhesion ligands and bind lymphocytes as efficiently as high endothelium in lymphoid tissue (Ager, 1987). The lymphocyte-HEC adhesion assay used in this study (figure 7.1) was a variation of that described by Ager and Mistry (Ager and Mistry, 1988).

7.1:Migration of *tace*$^{\Delta Zn/\Delta Zn}$ Cells through an HEC layer

tace$^{\Delta Zn/\Delta Zn}$ cells from RAG$^{-/-}$ chimeric mice were incubated with an IFNγ stimulated HEC monolayer. Phase contrast images of the adherent cells were collected and non-adherent and adherent cell populations analysed by flow cytometry. Type I cells are phase-light, round cells attached to the HEC surface and type II cells are phase-dark, flattened cells which have transmigrated and are underneath the monolayer.

There were type I and type II cells present in both *tace*^{WT} and *tace*$^{\Delta Zn/\Delta Zn}$ endothelial assays (Figure 7.2). Although, as this was a preliminary experiment, the number of wells analysed did not generate quantitative data, the presence of type II transmigrated *tace*$^{\Delta Zn/\Delta Zn}$ lymphocytes, suggests there is no effect of the TACE mutation on migration through HEV.

Figure 7.1: *In vitro* endothelial migration assay. A monolayer of rat HECs was cultured (~3 days). Peripheral lymph node cells from *tace*^{WT} and *tace*$^{\Delta Zn/\Delta Zn}$ RAG$^{-/-}$ chimeric mice were incubated with the endothelium for I hour at 37°C. *tace*^{WT} cells incubated in the absence of HEC were used as controls.

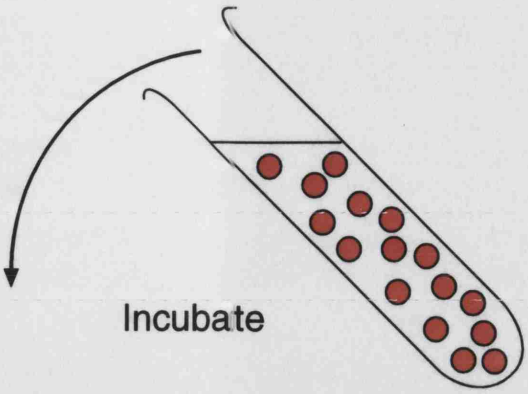

Cultured
HEC monolayer

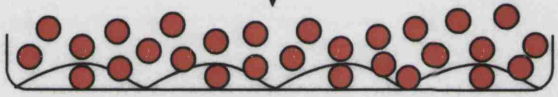

Non adherent cells collected

Phase contrast analysis of phase I, phase II cells

Incubation of adherent cells with 0.1% EDTA

Collect

Analyse non-adherent and adherent cell populations by flow cytometry

Figure 7.2: Phase contract images of HEC monolayer following incubation with *tace*^{WT} (a) and *tace*$^{\Delta Zn/\Delta Zn}$ (b) peripheral lymph node cells for 1 hour at 37°C. Non-migrated cells appear as phase light, whilst transmigrated cells appear phase dark. No effect of the TACE mutation on transmigration was seen.

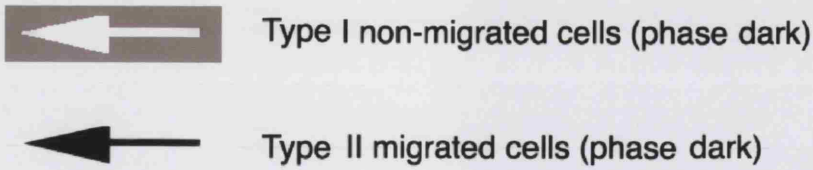

a) *tace*^{WT}

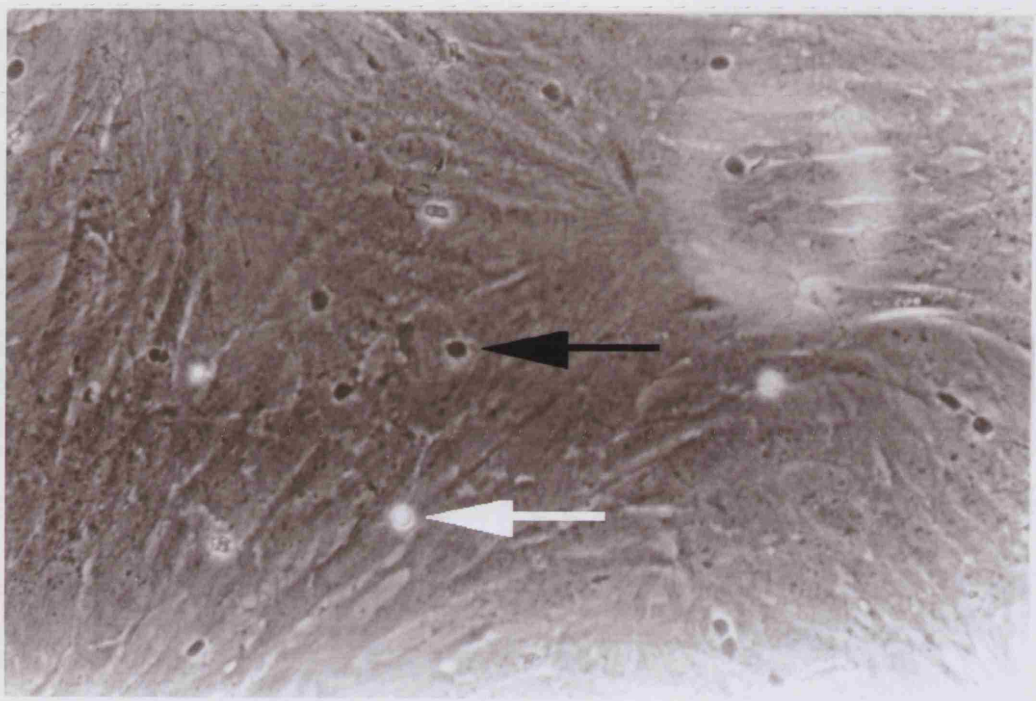

b) *tace*$^{\Delta Zn/\Delta Zn}$

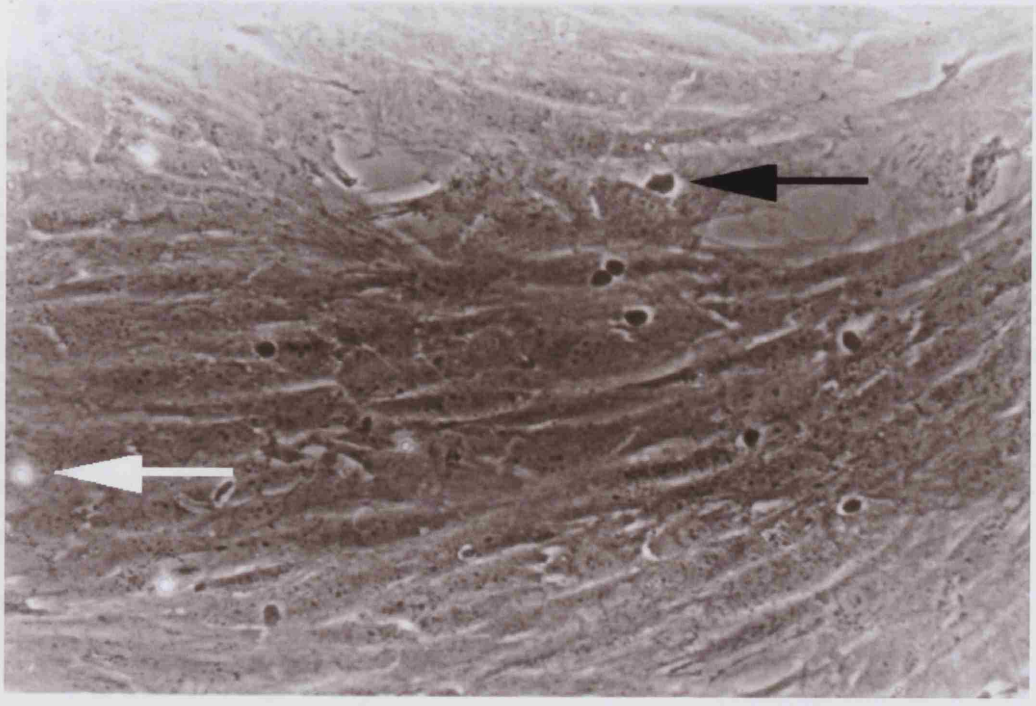

The non-adherent and adherent lymphocytes were analysed by flow cytometry. Control wells consisting of *tace*^{WT} cells incubated in the absence of endothelium were also analysed. As the endothelial cells were cultured in a medium containing 20% FCS, which blocks non-specific binding to tissue culture plastic, very few cells remained in the wells without endothelium following removal of non-adherent cells. Hence, only non-adherent cells from the control wells were analysed.

There was a decrease in the proportion of T lymphocytes present in the adherent population in comparison to the non-adherent cell population for both *tace*^{WT} (60% to 53%), and *tace*$^{\Delta Zn/\Delta Zn}$ (74% to 30%) lymphocytes (figure 7.3a). This was explained by increases in the proportion of B lymphocytes in the adherent populations of *tace*^{WT} (36% to 41%), and *tace*$^{\Delta Zn/\Delta Zn}$ (22% to 59%) cells (figure 7.3b). There seems to be enrichment of B lymphocytes following adhesion to HEC. This B lymphocyte enrichment was particularly marked using *tace*$^{\Delta Zn/\Delta Zn}$ lymphocytes in the adhesion assay.

L-selectin levels on non-adherent and adherent cell populations were also measured. There was downregulation of L-selectin from adherent T lymphocytes in both *tace*^{WT} (74% to 63%), and *tace*$^{\Delta Zn/\Delta Zn}$ (82% to 45%) populations (figure 7.4a). There were lower levels of downregulation in B lymphocytes in the *tace*^{WT} and *tace*$^{\Delta Zn/\Delta Zn}$ populations (74-70%, 98%-96%, respectively) (figure 7.4b). The down regulation on *tace*$^{\Delta Zn/\Delta Zn}$ T lymphocytes was particularly marked. The degree of downregulation (decrease in 37% from non-adherent levels) was larger than that seen in TACE independent basal shedding (decrease of between 10 and 15% from starting levels) suggesting that downregulation due to cross-linking of the L-selectin molecule by HEC is also TACE independent (and independent of basal shedding). Although results in figure 7.3 and 7.4 were from three separate wells, they were from the same preliminary experiment and are included here to demonstrate proposed future research.

Figure 7.3: Flow cytometric analysis of non-adherent and adherent cell populations in an endothelial assay. a) Proportion of T lymphocytes in the non-adherent and adherent cell populations from control, $tace^{WT}$, and $tace^{\Delta Zn/\Delta Zn}$ adhesion assay wells. b) Proportion of B lymphocytes in the non-adherent and adherent cell populations from control, $tace^{WT}$, and $tace^{\Delta Zn/\Delta Zn}$ adhesion assay wells. Results are means of three wells in a single experiment.

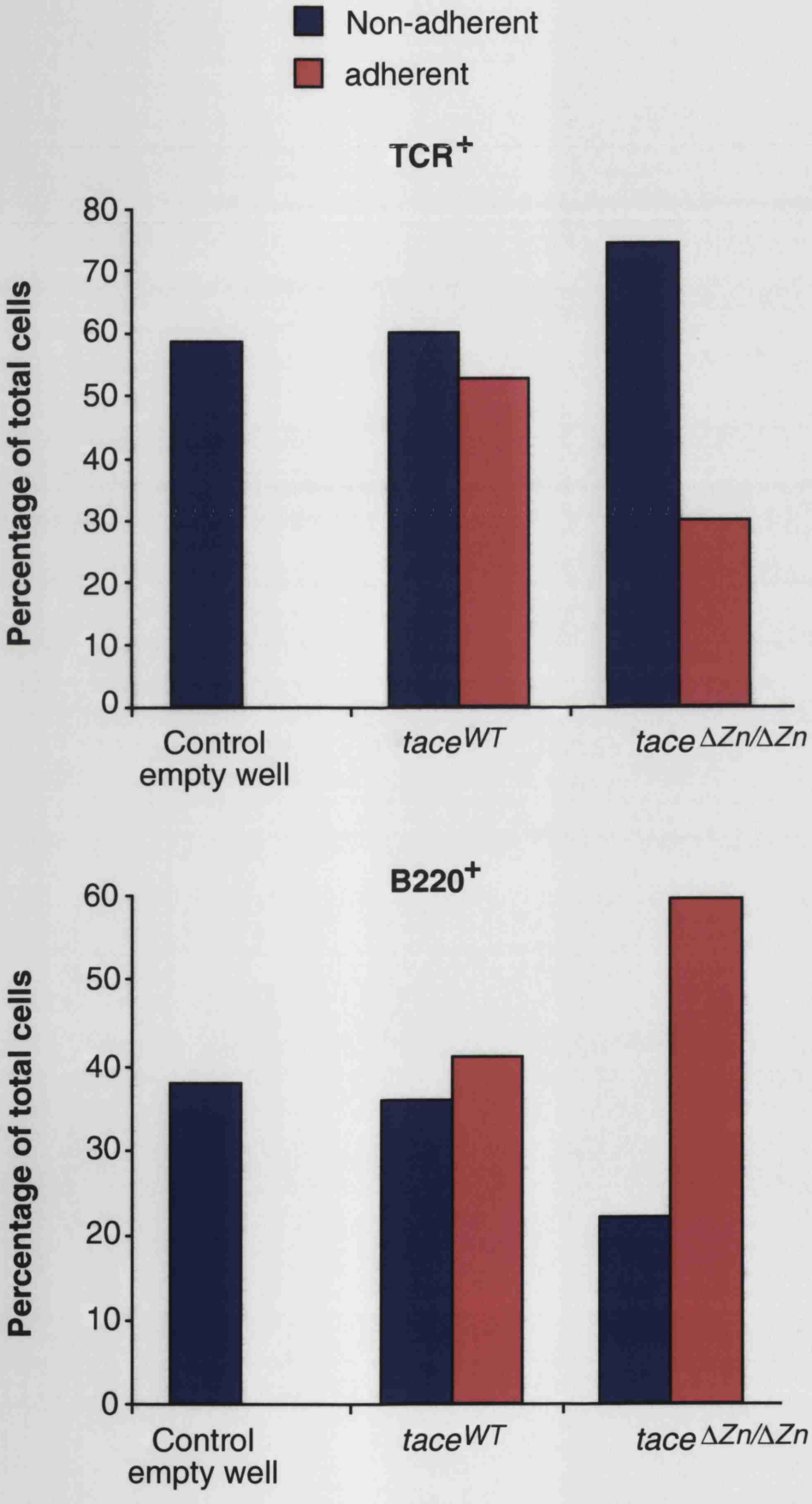
Non-adherent
adherent
TCR+
Percentage of total cells
80
70
60
50
40
30
20
10
0
Control
empty well
taceWT
taceΔZn/ΔZn
B220+
Percentage of total cells
60
50
40
30
20
10
0
Control
empty well
taceWT
taceΔZn/ΔZn

Figure 7.4: L-selectin levels, measured by FACs, on non-adherent and adherent cell populations in adhesion assays. a) L-selectin levels on T lymphocytes in the non-adherent and adherent cell populations from control, $tace^{WT}$, and $tace^{\Delta Zn/\Delta Zn}$ adhesion assay wells. There were decreased levels of L-selectin on the adherent populations of both the $tace^{WT}$ and $tace^{\Delta Zn/\Delta Zn}$ populations. b) L-selectin levels on B lymphocytes in the non-adherent and adherent cell populations from control, $tace^{WT}$, and $tace^{\Delta Zn/\Delta Zn}$ adhesion assay wells. There was no difference between L-selectin levels on the adherent and non-adherent cell populations. Results are means of three wells from a single experiment.

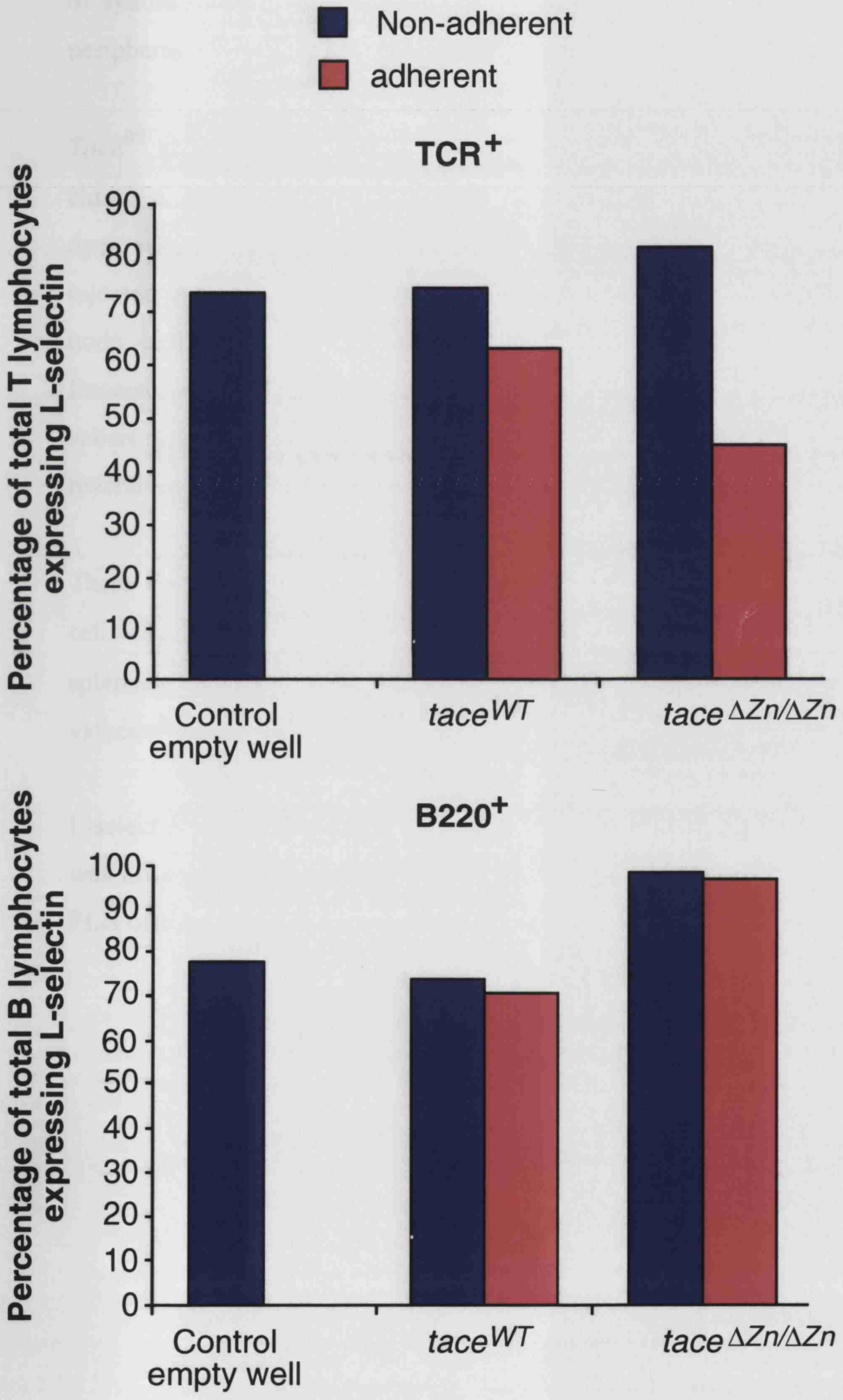
Non-adherent
adherent
TCR+
Percentage of total T lymphocytes expressing L-selectin
90
80
70
60
50
40
30
20
10
0
Control empty well
taceWT
taceΔZn/ΔZn
B220+
Percentage of total B lymphocytes expressing L-selectin
100
90
80
70
60
50
40
30
20
10
0
Control empty well
taceWT
taceΔZn/ΔZn

7.2: *In vivo* Migration of $tace^{\Delta Zn/\Delta Zn}$ Lymphocytes

Trafficking experiments have previously been used to determine the effect of synthetic L-selectin shedding inhibitors on migration of lymphocytes to peripheral lymph nodes (Faveeuw et al., 2001).

$Tace^{WT}$ and $tace^{\Delta Zn/\Delta Zn}$ peripheral lymph node cell populations from $RAG^{-/-}$ chimeric mice were stained with either Rhodamine or CFSE fluorescent dyes, respectively. The two cell populations were mixed and intravenously injected into $RAG^{-/-}$ mice. After, 1 hour blood, spleen and peripheral lymph node cell suspensions were made and analysed for the presence of fluorescently labelled cells. Cells were also stained with TCR and L-selectin subset markers. Prior to this experiment a small investigation was performed reversing the dyes to ensure there was no effect on migration.

There was no significant difference in migration of $tace^{WT}$ and $tace^{\Delta Zn/\Delta Zn}$ cells (figure 7.5a). Approximately 11% of total cells in PLN, 8% of total splenocytes and 3% of PBL were migrated $tace^{WT}$ or $tace^{\Delta Zn/\Delta Zn}$ cells (p values<0.05).

L-selectin levels on T lymphocytes were also measured (figure 7.5b). There was no significant effect of the TACE mutation on L-selectin levels in the PLN or blood.

Figure 7.5: Analysis of peripheral lymph node, spleen and blood of $RAG^{-/-}$ mice 1h after intravenous injection of fluorescently labelled $tace^{WT}$ and $tace^{\Delta Zn/\Delta Zn}$ cells. a) Percentage of total peripheral lymph node population that was migrated $tace^{WT}$ and $tace^{\Delta Zn/\Delta Zn}$ cells. b) L-selectin levels on migrated $tace^{WT}$ and $tace^{\Delta Zn/\Delta Zn}$ T lymphocytes. Results are means and SD of 5 recipient mice.

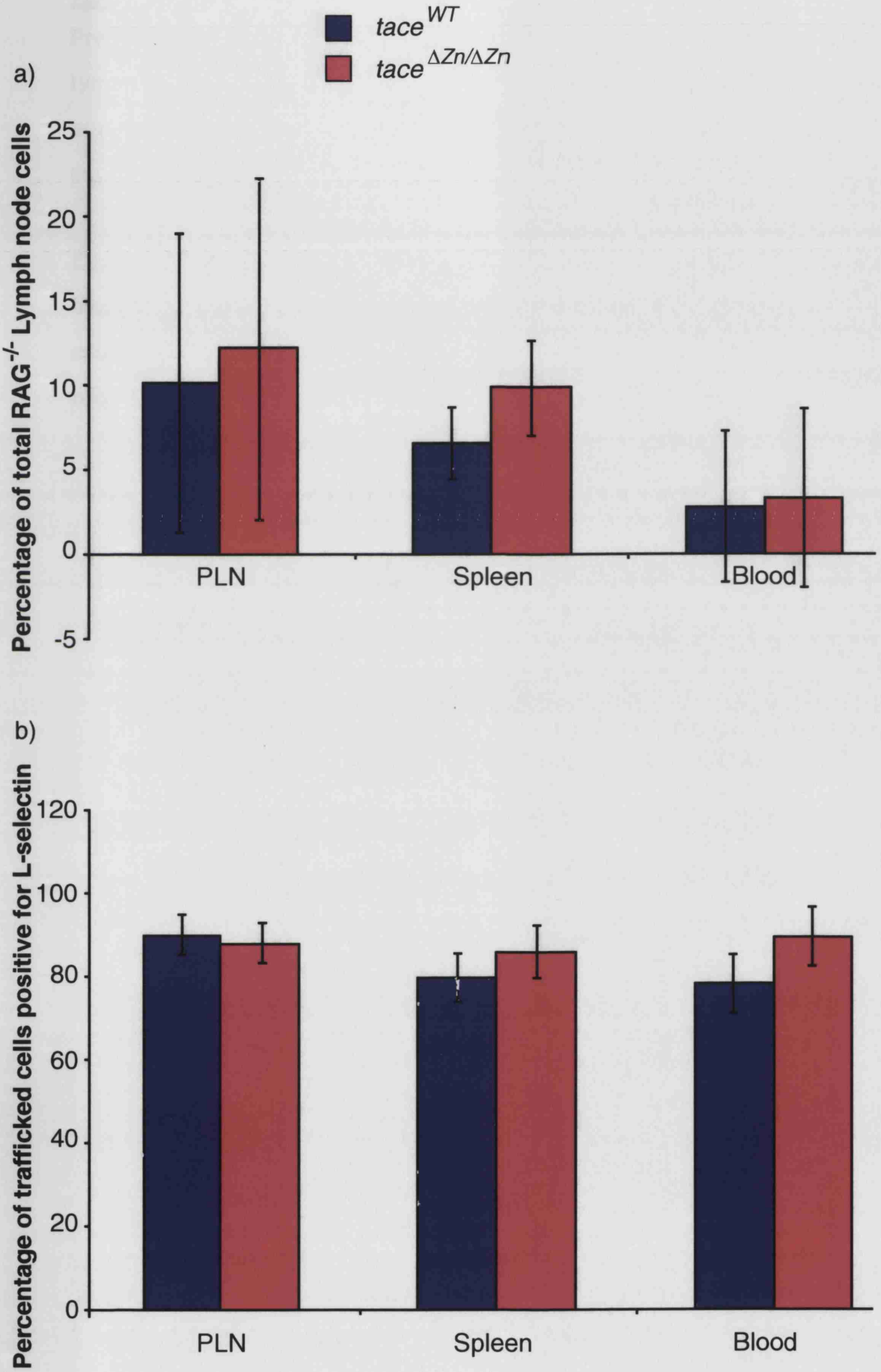
a)
tace WT
tace ΔZn/ΔZn
Percentage of total RAG-/- Lymph node cells
25
20
15
10
5
0
-5
PLN
Spleen
Blood
b)
Percentage of trafficked cells positive for L-selectin
120
100
80
60
40
20
0
PLN
Spleen
Blood

7.3: Summary

Preliminary experiments were performed to investigate the role of TACE in lymphocyte migration. No effect of the TACE mutation could be seen with normal migration of cells through a HEC monolayer. $tace^{\Delta Zn/\Delta Zn}$ migrated equally as well as $tace^{WT}$ cells in an *in vivo* trafficking assay.

Downregulation of L-selectin from $tace^{\Delta Zn/\Delta Zn}$ T lymphocytes following binding to HEC confirms a TACE independent shedding pathways in T cells. There was no effect on L-selectin levels on $tace^{\Delta Zn/\Delta Zn}$ cells following migration to PLN, spleen or in the blood *in vivo*.

Chapter 8: Discussion

8.1: Genotyping and Generation of Chimeric Mice

We were unable genotype the *tace*$^{\Delta Zn/\Delta Zn}$ colony using the primers suggested by Immunex. Although the method was followed accurately, when the products were run on an agarose gel, what was thought to be a product of 150bp relating to an intact zinc binding domain proved to be present when the reaction was run in the absence of genomic DNA. It was hypothesised that the presence of this band was the amplification of dimers formed between the primers themselves. To further investigate this, the primers were analysed by OLIGO software. This revealed that both the neomycin and the zinc oligonucleotide primers were indeed prone to forming hairpin structures and dimers. Hence, instead of amplifying the genomic DNA, the PCR reaction may have been amplifying the dimer structures themselves. It was decided to redesign the primers and, optimise the PCR conditions to increase the probability of getting a successful PCR reaction.

Once the new primers were designed and the optimum reaction conditions established, the need to establish a new method of DNA extraction became apparent following indistinct product bands. The PCR seemed to be particularly sensitive to inhibitors in the tissue biopsy as a protocol using only small amounts of tail biopsy was found to be the most consistent and successful method for genotyping the colony.

It must be stressed at this point, although the PCR reaction was proved to be successful in the genotyping of the TACE colony and enabled the establishment of *tace*$^{+/-}$/ *tace*$^{+/-}$ matings, it was apparent that the reaction conditions were not optimum. This is particularly illustrated by the presence of additional PCR products seen from reactions run with the zinc primers. The presence of these bands, which are smaller than the expected product of 360 bp, may be due to incomplete annealing or melting of the genomic DNA. There are larger bands present at the top of the well in the positive control (DNA from a known *tace*$^{+/+}$ mouse) as well. These bands also

demonstrate that the conditions of the PCR are not optimum and, again, suggest that the melting temperature of the DNA may need to be adjusted. For future studies the PCR reaction needs to be run at a range of different melting temperatures varying by a degree centigrade to establish the optimum temperature.

Although embryos collected from timed matings were initially genotyped using the revised PCR protocol on DNA extracted from brain tissue (fig 3.9), subsequent PCR often gave ambiguous results. It was because of this and time constraints on the project that the majority of embryos were selected by phenotypic analysis. Although, the reconstituted chimeric mice were all tested for response to PMA to ensure that the phenotypic analysis was effective, for future experiments all embryos should also be genotyped. By not genotyping the embryos in this project it was not possible to know whether the control littermates were of the genotype *tace*$^{+/\Delta Zn}$ or *tace*$^{+/+}$. Although, there has been no report of a heterozygous phenotype, either by Immunex or within the lab, this could not be tested within the scope of this project. By determining the optimum melting temperature for the PCR reaction, it is possible that the embryos could be quickly and successfully genotyped.

Embryos were phenotypically analysed by H and E staining of a cross section of the eye. *tace*$^{\Delta Zn/\Delta Zn}$ embryos were selected by the presence of open eyelid. Littermates, with fused eyelids were used as controls. Unlike the original studies on *tace*$^{\Delta Zn/\Delta Zn}$ embryos ($_e$17.5) (Peschon et al., 1998), we did not see an attenuated cornea in embryos ($_e$16.5-17) collected from timed matings at the NIMR. This may have been due to the slightly earlier time point that the embryos were collected.

A variety of mouse strains were used to generate stem cell chimeras in this study. 129/Sv, C57BL/10 RAG$^{-/-}$ (RAG-1 knockout) and L-selectin$^{-/-}$ mice were successful hosts. All three strains tolerated irradiation and successfully reconstituted a full immune system from donor stem cells. 129/Sv and L-

selectin$^{-/-}$ chimeric mice had residual host cell populations so could only be used in assays where results were independent of host cells. T and B cell populations in RAG$^{-/-}$ chimeric mice were solely derived from donor stem cells, however, there may have been residual myeloid cells even after irradiation. As host-derived cells cannot be distinguished from donor-derived cells in these mice, they cannot be used for studies on the myeloid cell population.

SCID and C57BL/6 (Ly 5.2^{+}) mice were found to be unsuitable for stem cell reconstitution. The SCID strain was too radiation sensitive for the purpose of this study. It is possible that irradiation causes damage to C57BL/6 megakaryocytes leading to platelet deficiency and, hence, haemorrhaging.

There is some discussion to whether the SCID and RAG1$^{-/-}$ mice need to receive any irradiation at all. It was decided to use irradiation in this study due to the experiences of other labs at the NIMR who failed to get reconsitution in immunodeficient mice that did not receive irradiation prior to the injection of stem cells. This observation is consistent with results published by Fulop and Phillips (1986), who compared irradiated SCID mice with unirradiated and found that unirradiated mice had few immunoglobulin positive cells in the spleen and bone marrow whereas the irradiated mice had normal levels by 4–6 weeks post irradiation; at 8 weeks only the irradiated mice had normal levels of cytotoxic T cell activity. It seems logical that although the immunodeficient mice do not have mature lymphocytes – as the mutation in both the RAG$^{-/-}$ and the SCID occur during antigen receptor rearrangement – the primary lymphoid organs will be full of stem cells and very early pro-B cells or double negative T-cells. Hence, it is probable that the irradiation destroys these cells and increases the chance of full reconstitution by providing niches, within these primary organs, for donor stem cell development. In addition the irradiation should destroy the SCID or RAG$^{-/-}$ innate immune cells – such as natural killer cells – which may respond to the foreign donor cells.

8.2: Generation and Analysis of Chimeric Mice.

The large percentage of host-derived T cells in the spleen and lymph nodes of 129/Sv chimeric mice presents problems for certain assays such as migration and soluble L-selectin assays. Increasing the dose of irradiation could reduce the number of host cells remaining after irradiation. However, this will obviously reduce the survival rate of the procedure, which in 129/Sv is very good (over 97% survival). The best way to eliminate the presence of host T splenocytes is to use empty mice such as the $RAG^{-/-}$ described above.

The significantly enlarged spleens in the 129/Sv chimeric mice were the first indication of the TACE mutation affecting lymphoid organs. This was substantiated by a lack of phenotypic effect of the TACE mutation in the lymph nodes and thymus. However, there was no effect of the mutation on TCR^{+} or $B220^{+}$ lymphocytes in the spleen.

An enlarged spleen is one of the first indications of graft versus host disease. However, this is unlikely to have been the cause of the enlarged spleens in this situation as the stem cells originated from the foetal liver. Unlike bone marrow transfers, no mature T cells were injected along with the stem cells. Thus, all cells must have matured in the host bone marrow, in the case of B cells and myeloid cells, or the thymus, in the case of T cells. Therefore, the developing cells would have been subjected to the same selection procedures as the hosts' own immune cells. Thus, any cells that were reactive towards the hosts own antigens should have been selected against in the primary organs and died or become anergic. It is, however, possible that the hosts own mature immune cells mounted a host versus graft response against the donor-derived cells. If this was the case you would expect to see very little reconstitution at all, as the injected cells would be cleared from the bloodstream and bone marrow stroma prior to maturation. In addition, if there were a response against the mature cells it would be expected that there would be a systemic reaction rather than a response located entirely in the spleen. No such reaction was seen in other organs. As the reconstituted 129/Sv mice survived for over a year, although all mice in this report were

analysed at 4 months, it is unlikely that there was any type of host versus graft response.

The increased splenic weight and the observation of higher L-selectin expression on total and $B220^+$ cells in bone marrow of $tace^{\Delta Zn/\Delta Zn}$ chimeras, encouraged further investigation of the total cell populations in both the spleen and the bone marrow. The fact that the increased expression of L-selectin on $B220^+$ cells in the bone marrow is not statistically significant does not correlate with the histogram profiles. This is shown in figure 4.5 where the profiles from all four experiments are shown. It is possible that with increased numbers of chimeras, as with the splenic weight data, this will also prove to be a statistically significant result.

The strain marker Ly 9.1, which was used for the phenotypic analysis of lymphoid cells, does not stain cells of the myeloid linage, a different marker had to be found to distinguish between residual host cells and donor-derived cells in the bone marrow. The S19/8 antibody, which recognises MHC-Class I associated β2-microglobulin, was the only commercially available antibody that fitted these criteria. It has, however, been shown that the MHC class I peptides, such as β2-microglobulin, can be directly, or via endocytic compartments, exchanged between cells (Horig et al., 1997). This exchange will dilute any differences between the two cell populations. However, in 129/Sv chimeras reconstituted with $tace^{\Delta Zn/\Delta Zn}$ foetal liver cells, lymphocytes identified as donor-derived ($tace^{\Delta Zn/\Delta Zn}$) did not shed L-selectin in response to PMA.

The increased proportion of cells with a large granular morphology in the spleen was also seen in the bone marrow. Although again this was not statistically significant, it is possible with increased numbers of chimeras this will also prove to be a significant result. Analysis of the large cells in these two organs using myeloid cell markers showed significant effects of the TACE mutation on L-selectin expression on myeloid subsets. Interestingly, the increase in L-selectin positive cells in the bone marrow of

tace$^{\Delta Zn/\Delta Zn}$ chimeras was confined to non-neutrophil granulocytes, possibly monocytes or developing neutrophils. However, in the spleen there was an increase in the number of L-selectin positive neutrophils. As both small, B220 positive cells and non-neutrophil granulocytes in the bone marrow have higher L-selectin expression in *tace*$^{\Delta Zn/\Delta Zn}$ chimeric mice, it may be that TACE is involved in regulating the adhesive interactions with the bone marrow stroma during immune cell development. As L-selectin is not required for migration to the spleen, it is unclear why neutrophils expressing high levels of L-selectin are found here whilst neutrophils have normal level of L-selectin in the bone marrow. Increased numbers of neutrophils are usually associated with inflammation. However, as previously discussed, there was no evidence of inflammation in any of these mice.

It is apparent that the effects of the TACE mutation on leucocyte differentiation are confined to cells of a myeloid linage. Further work should, therefore, involve detailed analysis of these cell populations including development in the bone marrow. It would also be interesting to challenge these mice with an infection to establish whether neutrophil and monocytes/macrophage mediated inflammatory responses are affected.

8.3: Regulation of L-selectin Shedding

Investigation of the role of TACE in L-selectin cleavage showed that TACE is responsible for PMA induced shedding. *tace*$^{\Delta Zn/\Delta Zn}$ splenocytes do not down regulate L-selectin even at high concentrations of PMA. The experiments conducted in this study do not address the question of whether TACE is the actual enzyme responsible for the cleavage or whether it is involved in a series of reactions that end in the cleavage of L-selectin by another enzyme. There is a suggestion that incubation of *tace*$^{\Delta Zn/\Delta Zn}$ T lymphocytes with PMA actually increases L-selectin expression on these cells. This suggests that upon stimulation with PMA there is actually upregulation of L-selectin synthesis and transport to the cell surface during L-selectin shedding. If this is the case then it is possible that L-selectin

shedding is necessary for migration into peripheral lymph nodes but L-selectin is re-expressed once inside the lymph node itself.

Upregulation of L-selectin and basal shedding in B lymphocytes is variable and, thus, has not been addressed in great depth in this report. It is likely that B cell migration is different to that of T cells as they have distinct roles and migrate to different areas within lymphoid organs. It is also known that B lymphocytes migrate in response to different chemokines suggesting that regulation of migration is achieved by a different method.

Quantifiable levels of soluble L-selectin in the supernatants of $tace^{\Delta Zn/\Delta Zn}$ cells incubated at 37°C were consistent with the observation of basal shedding from $tace^{\Delta Zn/\Delta Zn}$ T lymphocytes *in vitro*. Basal shedding has been well reported (Preece et al., 1996; Zhao et al., 2001), although the significance of its role *in vivo* has not been established.

In this study, small but measurable levels of soluble L-selectin were observed in the supernatant of $tace^{WT}$ cells, but not $tace^{\Delta Zn/\Delta Zn}$, incubated at 4°C. In addition, there was incomplete inhibition of release of soluble L-selectin from these cells by the hydroxamate based metalloproteinase inhibitors. These results are consistent with those obtained from normal C57BL/6 lymphocytes, where reduction of total cells positive for surface expression of L-selectin, following both PMA stimulation and incubation at 37°C, was completely inhibited by the presence of Ro 32-0526, even in very low concentrations, however, absence of soluble L-selectin was only seen at concentrations higher than 30 μM in the case of PMA stimulation and 100 μM for basal shedding. This further complicates the processes involved in L-selectin shedding. From the lower levels of soluble L-selectin present in the reconstituted L-selectin$^{-/-}$ chimeras in addition to the higher level of basal shedding from $tace^{WT}$ cells *in vitro*, it seems apparent that although the majority of basal shedding is TACE independent there is a degree of TACE dependent basal shedding occurring. TACE independent shedding is completely inhibited by synthetic hydroxamate based metalloproteinase

inhibitors although not by TIMPs. In contrast, TACE dependent basal shedding is only partially inhibited by synthetic hydroxamate based metalloproteinase inhibitors, although is partially inhibited by TIMP-3 (slight decrease in soluble L-selectin levels in the supernatant of cells incubated in the presence of TIMP-3 at 37°C). These experiments need further repeats to confirm these results.

Basal shedding of L-selectin, like that in response to PMA, is inhibited by hydroxamate inhibitors. It was also observed that the levels of soluble L-selectin in the supernatants of cells undergoing either basal or PMA stimulated L-selectin shedding do not correlate exactly with trends seen in the surface levels. This was seen in normal C57BL/6 mice where there was complete inhibition of shedding from the cell surface by Ro 32-0526 at concentrations from as low as 1μM, however, there was soluble L-selectin present in the supernatants of these assays up to a concentration of 10μM. It was found that $tace^{\Delta Zn/\Delta Zn}$ T lymphocytes basal shed L-selectin at levels comparable to those of the $tace^{WT}$ cells. It was interesting to observe that the inhibitors completely blocked L-selectin release into the supernatant from $tace^{\Delta Zn/\Delta Zn}$ cells (as reflected in the surface expression), however, there was release of L-selectin from $tace^{WT}$ even in the presence of inhibitors. This indicates that the mechanism for this shedding, although the quantities of soluble L-selectin were low, must be due to a TACE dependent pathway. It is also interesting to note that for both $tace^{WT}$ and $tace^{\Delta Zn/\Delta Zn}$ T lymphocytes, there was an increase in the percentage of L-selectin positive cells in the presence of Ro 31-9790 and Ro 32-0526. This again demonstrates that there is some form of upregulation at the cell surface. These results indicate that TACE dependent L-selectin shedding is not completely blocked by Ro 31-9790 or Ro 32-0526, but that the enzyme responsible for TACE independent shedding is completely blocked by these two inhibitors. It is possible that these two enzymes work in conjunction with each other, so that in the case of the $tace^{WT}$ cells there is some release of L-selectin in to the supernatant – mediated by TACE – however, complete inhibition of the second enzyme means that the cell cannot effectively clear L-selectin from its cell surface

leading to elevated expression of L-selectin. This would explain the complete ablation of soluble L-selectin in the supernatent of *tace*$^{\Delta Zn/\Delta Zn}$ cells inhibited with Ro 31-9790 and Ro 32-0526.

Previously published work (Preece et al., 1996, Borland et al.,1999) used the hydroxamate inhibitors at concentrations of 30μM. For the basal shedding assays in this report the inhibitors were used at concentrations of 100μM. This was due to the observation that Ro 31-9790 did not completely block the release of L-selectin from C57BL/6 cells into the supernatent at a concentration of 30μM.

It has been shown here that some basal shedding in T lymphocytes is TACE independent. This observation questions the relevance of TACE in *in vivo* regulation of L-selectin shedding. Most previous studies of L-selectin shedding use PMA as a stimulus, however, from our results it is difficult to establish the physiological relevance of using PMA. Basal shedding from *tace*$^{\Delta Zn/\Delta Zn}$ lymphocytes is inhibited by synthetic metalloproteinase inhibitors but, in contrast to PMA induced shedding, is not inhibited by TIMP-3. Although TACE appears not to be the enzyme responsible for most basal (and HEC induced) L-selectin shedding, the enzyme responsible is likely to be a Zinc dependent metalloproteinase as basal shedding is block by Ro 31-9790. A possible candidate for L-selectin shedding is MDC-L (ADAM 28). Like TACE, MDC-L is expressed on the surface of human lymphocytes and has proteolytic activity (Howard et al., 2001).

8.4: Soluble L-selectin

It is important to address the issue of soluble L-selectin in a *in vivo* model in addition to looking at L-selectin release in basal shedding assays. For, this reason it was decided to look at soluble L-selectin in the sera of mice reconstituted with *tace*$^{\Delta Zn/\Delta Zn}$ foetal liver cells. There was no effect of the TACE mutation on serum levels of soluble L-selectin. However, this was not the best model for this analysis as it has been shown that there are residual

host-derived TACE positive cells present within the reconstituted mice, which would shed L-selectin via the TACE dependent route.

As some *tace*$^{\Delta Zn/\Delta Zn}$ knockout mice survive for a few weeks following birth (Peschon et al., 1998), there was the opportunity to study soluble L-selectin in the sera of these mice. Unfortunately, as these samples were not generated in house the number of samples was not high. No significant effect of the TACE mutation was seen, however, analysis of a greater number of mice may show an effect.

Although useful, the surviving *tace*$^{\Delta Zn/\Delta Zn}$ knockout mice were not of the same strain as the *tace*$^{\Delta Zn/\Delta Zn}$ foetal liver cells that were used to reconstitute host mice in this study. In addition to this meaning that a different assay had to be used to quantify levels of L-selectin, there may be strain differences that would affect the results obtained. It was sought to develop an assay that would enable the analysis of L-selectin release from donor-derived *tace*$^{\Delta Zn/\Delta Zn}$ cells within an *in vivo* assay. It was decided to reconstitute L-selectin$^{-/-}$ mice with *tace*$^{\Delta Zn/\Delta Zn}$ foetal liver cells. This would enable the observation of L-selectin release entirely from the donor-derived cells as all soluble L-selectin present must have originated from these cells due to all host cells being L-selectin$^{-/-}$. Upon analysis of samples from these reconstituted mice L-selectin was found to be present in the sera. This proves inconclusively that there is release of L-selectin from *tace*$^{\Delta Zn/\Delta Zn}$ leucocytes. As the stem cells would have differentiated into both lymphocytes and cells of a myeloid linage, it is not possible to tell whether this release was from lymphocytes or myeloid cells such as neutrophils. However, it does prove that there is a TACE independent pathway for L-selectin shedding. To improve this model, the L-selectin$^{-/-}$ should be reconstituted with bone marrow lymphoid precursors, or naïve T lymphocytes.

As stated above, the presence of soluble L-selectin in the serum of L-selectin$^{-/-}$ mice reconstituted with *tace*$^{\Delta Zn/\Delta Zn}$ foetal liver cells, confirms that

there is a TACE independent L-selectin cleavage mechanism *in vivo*. Although the L-selectin$^{-/-}$ mouse cells have active TACE, further experiments found no evidence of a trans-cellular cleavage mechanism between TACE and L-selectin.

There were reduced amounts of soluble L-selectin in the $tace^{\Delta Zn/\Delta Zn}$ chimeric mice in comparison to $tace^{WT}$ chimeric mice. This suggests that TACE is responsible for some *in vivo* shedding of L-selectin or it is possible that the reduced amounts are due to a deficiency in B lymphocyte shedding. It is possible that L-selectin shedding from B lymphocytes is TACE dependent. To determine if this is the case, further work on the migration and L-selectin expression of B lymphocytes should be performed.

8.5: The role of TACE in Lymphocyte Migration

Our results from endothelial cell adhesion and trafficking assays suggest no effect of the TACE mutation on lymphocyte migration. However, as we have determined that there is a TACE independent pathway of L-selectin shedding we cannot determine whether shedding of L-selectin is necessary for migration. This is further demonstrated by the observation that induction of L-selectin shedding by binding to HEC is also TACE independent in T lymphocytes. Hence, TACE independent shedding of L-selectin may be required for successful migration and it was this, and not a TACE dependent pathway that was blocked in studies suggesting a role for shedding in migration (Faveeuw et al., 2001). To determine if this is the case, it would be interesting to carry out trafficking assays in the presence of TIMP-3. If the cells migrate as normal then it can be determined that the synthetic metalloproteinase inhibitors used in these studies was blocking TACE independent shedding. By treating the HEC monolayer in the endothelial assay with Ro 31-9790, confirmation that it is not a metalloproteinase on the HEC that is cleaving L-selectin, could be established.

As L-selectin adhesion, and possibly shedding, occur under flow *in vivo*, the static adhesion assay can only be used for preliminary experiments. Future

studies should examine the role of L-selectin shedding under flow. It is under these conditions that it could be determined whether TACE dependent shedding is required for successful adhesion and rolling. From the results of this study, it could be hypothesised that there will be no difference between the adhesion and rolling of *tace*$^{\Delta Zn/\Delta Zn}$ to that of TACE wild-type leucocytes. To fully examine the role of L-selectin shedding in adhesion and rolling, both TACE and the enzyme(s) responsible for TACE independent shedding would need to be inactivated. Again from the observations made in this study, that may be possible by incubation of *tace*$^{\Delta Zn/\Delta Zn}$ cells with Ro 32-0526 or Ro 31-9790 before use in the assay.

8.6: Further investigation of L-selectin shedding

There has been some question over whether the mutated form of TACE is being transcribed and having a dominant negative effect over other metalloproteinases such as ADAM-10. Hence, the suggestion was that the deficiency in L-selectin shedding seen here may be due to inhibition of cleavage by other enzymes. However, from our study it is clear that there are other enzymes actively cleaving L-selectin without being effected by mutant TACE.

It has been shown that there are at least two separate pathways for L-selectin shedding. Neither were inhibited by TIMP-1. This dismisses the claim that ADAM-10 may be the enzyme responsible for L-selectin cleavage, but is being negatively dominated by mutant TACE, as ADAM-10 is inhibited by TIMP-1 (Amour et al., 2000). As we know that MMPs cannot be responsible for shedding (as they are inhibited by the TIMPs), there is the possibility that there may be other ADAMs involved in the cleavage. As WT shedding is partially inhibited by TIMP-3, it is possible that ADAMs that can be inhibited by TIMP-3 may have a role in L-selection shedding. Possible L-selectin sheddases include ADAM-9, which is widely expressed and is known to cleave HB-EGF (see introduction).

It seems likely that future investigations into L-selectin shedding may involve cells with multiple enzymes mutated as TACE seems to play only a minor role in basal shedding of L-selectin.

8.7: Proof of Hypothesis

The aim of this thesis was to investigate the role of TACE in L-selectin shedding using phenotypic and shedding assay analyses. Shedding assays demonstrated that deficiency in TACE does not inhibit basal shedding from T lymphocytes. Therefore, it was concluded, TACE is not the sole enzyme responsible for L-selectin cleavage. No effect of the TACE mutation on migration, in preliminary endothelial assays, was observed. However, this may be due to the presence of other enzyme(s) involved in T lymphocyte basal shedding.

Bibliography

Ager, A. (1987). Isolation and culture of high endothelial cells from rat lymph nodes. J Cell Sci ***87***, 133-144.

Ager, A. (1994). Lymphocyte recirculation and homing: Roles of adhesion molecules and chemoattractants. Trends Cell Biol ***4***, 326-333.

Ager, A. (1997). Regulation of lymphocyte migration into lymph nodes by high endothelial venules. Biochem Soc Trans ***25***, 421-428.

Ager, A., and Mistry, S. (1988). Interaction between lymphocytes and cultured high endothelial cells: an in vitro model of lymphocyte migration across high endothelial venule endothelium. Eur J Immunol ***18***, 1265-1274.

Allport, J. R., Ding, H. T., Ager, A., Steeber, D. A., Tedder, T. F., and Luscinskas, F. W. (1997). L-selectin shedding does not regulate human neutrophil attachment, rolling, or transmigration across human vascular endothelium in vitro. J Immunol ***158***, 4365-4372.

Alon, R., Chen, S., Fuhlbrigge, R., Puri, K. D., and Springer, T. A. (1998). The kinetics and shear threshold of transient and rolling interactions of L-selectin with its ligand on leukocytes. Proc Natl Acad Sci U S A ***95***, 11631-11636.

Alon, R., Fuhlbrigge, R. C., Finger, E. B., and Springer, T. A. (1996). Interactions through L-selectin between leukocytes and adherent leukocytes nucleate rolling adhesions on selectins and VCAM-1 in shear flow. J Cell Biol ***135***, 849-865.

Althoff, K., Reddy, P., Voltz, N., Rose-John, S., and Müllberg, J. (2000). Shedding of interleukin-6 receptor and tumour necrosis factor α. Eur J Biochem ***267***, 2624-2631.

Amour, A., Knight, C. G., Webster, A., Slocombe, P. M., Stephens, P. E., Knäuper, V., Docherty, A. J. P., and Murphy, G. (2000). The in vitro activity of ADAM-10 is inhibited by TIMP-1 and TIMP-3. FEBS Letters *473*, 275-279.

Amour, A., Slocombe, P. M., Webster, A., Butler, M., Knight, C. G., Smith, B. J., Stephens, P. E., Shelley, C., Hutton, M., Knäuper, V., Docherty, A. J. P., and Murphy, G. (1998). TNF-α converting enzyme (TACE) is inhibited by TIMP-3. FEBS Lett *435*, 39-44.

Anderson, A. O., and Shaw, S. (1993). T cell adhesion to endothelium: The FRC conduit system and other anatomic and molecular features which facilitate the adhesion cascade in lymph node. Semin Immunol *5*, 271-282.

Andersson, P., Perry, V. H., and Gordon, S. (1992). Intracerebral injection of proinflammatory cytokines or leukocyte chemotaxins induces minimal myelomonocytic cell recruitment to the parenchyma of the central nervous system. J Exp Med *176*, 255-259.

Apte, S. S., Olsen, B. R., and Murphy, G. (1996). The gene structure of tissue inhibitor of metalloproteinases (TIMP)-3 and its inhibitory activities define the distinct TIMP gene family. J Biol Chem *271*, 2874 -2874.

Arbonés, M. L., Ord, D. C., Ley, K., Ratech, H., Maynard-Curry, C., Otten, G., Capon, D. J., and Tedder, T. F. (1994). Lymphocyte homing and leucocyte rolling and migration are impaired in L-selectin deficient mice. Immunity *1*, 247-260.

Arribas, J., Coodly, L., Vollmer, P., Kishimoto, T. K., Rose-John, S., and Massague, J. (1996). Diverse cell surface protein ectodomains are shed by a system sensitive to metalloprotease inhibitors. J Biol Chem *271*, 11376-11382.

Asakura, M., Kitakaze, M., Takasima, S., Liao, Y., Ishikura, F., Yoshinaka, T., Ohmoto, H., Node, K., Yoshino, K., Ishiguro, H., Asanuma, H., Sanada, S., Matsumura, Y., Takeda, H., Beppu, S., Tada, M., Hori, M., and Higashiyama, S. (2002). Cardiac hypertrophy is inhibited by antagonism of ADAM 12 processing of HB-EGF: Metalloproteinase inhibitors as a new therapy. Nature Med ***8,*** 35-40.

Bartholdy, C., Marker, O., and Thomsen, A. R. (2000). Migration of activated CD8+ T lymphocytes to sites of viral infection does not require endothelial selectins. Blood ***95***, 1362-1369.

Baumheter, S., Singer, M. S., Henzel, W., Hemmerich, S., Renz, M., Rosen, S. D., and Lasky, L. A. (1993). Binding of L-selectin to the vascular sialomucin CD34. Science ***262***, 436-438.

Berg, E. L., McEvoy, L. M., Berlin, C., Bargatze, R. F., and Butcher, E. C. (1993). L-selectin-mediated lymphocyte rolling on MAdCAM-1. Nature ***366***, 695-698.

Berg, E. L., Robinson, M. K., Warnock, R. A., and Butcher, E. C. (1991). The human peripheral lymph node vascular addressin is a ligand for LECAM-1, the peripheral lymph node homing receptor. J Cell Sci ***114***, 343-349.

Berlin-Rufenach, C., Otto, F., Mathies, M., Westermann, J., Owen, M. J., Hamann, A., and Hogg, N. (1999). Lymphocyte migration in lymphocyte function-associates antigen (LFA) -1-deficient Mice. J Exp Med ***189***, 1467-1478.

Bevan, M. J., Hogquist, K. A., and Jameson, S. C. (1994). Selecting the T cell receptor repertoire. Science ***264***, 796-797.

Bianchi, E., Bender, J. R., Blasi, F., and Pardi, R. (1997). Through and beyond the wall: Late steps in leucocyte transendothelial migration. Immunol Today ***18***, 586-590.

Bjornberg, F., and Lantz, M. (1998). Endothelial cell contact potentates release of soluble tumour necrosis factor (TNF) receptors from the monocyte-like cell line THP-1. J Interferon Cytokine Res ***18***, 167-174.

Black, R. A., Rauch, C. T., Kozlosky, C. J., Peschon, J. J., Slack, J. L., Wolfson, M. F., Castner, B. J., Stocking, K. L., Reddy, P., Srinivasan, S., Nelson, N., Boiani, N., Schooley, K. A., Gerhart, M., Davis, R., Fitzner, J. N., Johnson, R. S., Paxton, R. J., March, C. J., and Cerretti, D. P. (1997). A metalloproteinase disintegrin that releases tumour-necrosis factor-alpha from cells. Nature ***385***, 729-733.

Black, R. A., and White, J. M. (1998). ADAMs: Focus on the protease domain. Curr Opin Cell Biol ***10***, 654-659.

Bleul, C. C., Fuhlbrigge, R. C., Casasnovas, J. M., Aiuti, A., and Springer, T. A. (1996). A highly efficacious lymphocyte chemoattractant, stromal cell-derived factor 1 (SDF-1). J Exp Med ***184***, 1101-1109.

Blobel, C. P. (1997). Metalloprotease-disintegrins: Links to cell adhesion and cleavage of TNFα and Notch. Cell ***90***, 589-592.

Blobel, C. P., Wolfsberg, T. G., Turck, C. W., Myles, D. G., Primakoff, P., and White, J. M. (1992). A potential fusion peptide and an integrin ligand domain in a protein active in sperm-egg fusion. Nature ***356***, 248-252.

Bode, U., Duda, C., Weidner, F., Rodriguez-Palmero, M., Wonigeit, K., Pabst, R., and Westermann, J. (1999). Activated T cells enter rat lymph nodes and Peyer's patches via high endothelial venules: Survival by tissue-specific proliferation and preferential exit of $CD8^+$ T cell progeny. Eur J Immunol ***29***, 1487-1495.

Bode, W., Gomis-Ruth, F. X., and Stocker, W. (1993). Astacins, serralysins, snake venom and matrix metalloproteinases exhibit identical zinc-binding environments (HEXXHXXGXXH and Met-turn) and topologies and should be grouped into a common family, the 'metzincins'. FEBS Lett ***331***, 134-140.

Borland, G., Murphy, G., and Ager, A. (1999). Tissue inhibitor of metalloproteinases-3 inhibits shedding of L- selectin from leukocytes. J Biol Chem ***274***, 2810-2815.

Borrell-Pagés, M., Rojo, F., Albanell, J., Baselga, J., and Arribas, J. (2003) TACE is required for the activation of the EGFR by TGF-α in tumours. EMBO ***22,*** 1114-1124.

Bosma, G. C., Custer, R. P., and Bosma, M. J. (1983). A severe combined immunodeficiency mutation in the mouse. Nature ***301***, 527-530.

Bradley, L. M., Harbertson, J., and Watson, S. R. (1999). Memory CD4 cells do not migrate into peripheral lymph nodes in the absence of antigen. Eur J Immunol ***29***, 3273-3284.

Bradley, L. M., Watson, S. R., and Swain, S. L. (1994). Entry of naive CD4 T cells into peripheral lymph nodes requires L- selectin. J Exp Med ***180***, 2401-2406.

Brown, E. J. (1997). Adhesive interactions in the immune system. Trends in Cell Biology *7*, 289-295.

Brustein, M., Kraal, G., Mebius, R. E., and Watson, S. R. (1992). Identification of a soluble form of a ligand for the lymphocyte homing receptor. J Exp Med ***176***, 1415-1419.

Bührer, C., Berlin, C., Jablonski-Westrich, D., Holzmann, B., Thiele, H. G., and Hamann, A. (1992). Lymphocyte activation and regulation of three adhesion molecules with supposed function in homing: LECAM-1 (MEL-14 Antigen), LPAM-1/2 (α_4-Integrin) and CD44 (Pgp-1). Scand J Immunol ***35***, 107-120.

Butcher, E. C., and Picker, L. J. (1996). Lymphocyte homing and homeostasis. Science ***272***, 60-66.

Butcher, E. C., Scollay, R. G., and Weissman, I. L. (1980). Organ specificity of lymphocyte migration: mediation by highly selective lymphocyte interaction with organ-specific determinants on high endothelial venules. Eur J Immunol ***10***, 556-561.

Chao, C. C., Jensen, R., and Dailey, M. O. (1997). Mechanisms of L-selectin regulation by activated T cells. J Immunol ***159***, 1686-1694.

Chen, A., Engel, P., and Tedder, T. F. (1995). Structural requirements regulate endoproteolytic release of the L- selectin (CD62L) adhesion receptor from the cell surface of leukocytes. J Exp Med ***182***, 519-530.

Condon, T. P., Flournoy, S., Sawyer, G. J., Baker, B. F., Kishimoto, T. K., and Bennett, C. F. (2001). ADAM17 but not ADAM10 mediates tumour necrosis factor-α and L-selectin shedding from leucocyte membranes. Antisense Nucleic Acid Drug Dev ***11***, 107-116.

Coebella, P., Moskophidis, D., Spanopoulou, E., Mamalaki, C., Tolaini, M., Itano, A., Lans, D., Baltimore, D., Robey, E., and Kioussis, D. (1994). Functional commitment to helper T cell linage precedes positive selection and is independent of T receptor MHC specificity. Immunity ***1,*** 269-276.

Coussens, L. M., Fingleton, B., and Matrisian, L. M. (2002). Matrix metalloproteinase inhibitors and cancer: trials and tribulations. Science ***295,*** 2387-2392.

Ding, Z., Issekutz, T. B., Downey, G.P., and Waddell, T.K. (2003). L-selectin stimulation enhances functional expression of surface CXCR4 in lymphocytes: Implications for cellular activation, adhesion and migration. Blood ***101,*** 4245-4252.

Doedens, J. R., and Black, R. A. (2000). Stimulation-induced down-regulation of tumour necrosis factor-α converting enzyme. J Biol Chem ***275,*** 14598-14607.

Donnelly, S. C., Haslett, C., Dransfield, I., Robertson, C. E., Carter, D. C., Ross, J. A., Grant, I. S., and Tedder, T. F. (1994). Role of selectins in development of adult respiratory distress syndrome. Lancet ***344,*** 215-219.

Dri, P., Gasparini, C., Menegazzi, R., Cramer, R., Albéri, L., Presani, G., Garbisa, S., and Patriarca, P. (2000). TNF-induced shedding of TNF receptors in human polymorphonuclear leucocytes: role of the 55-kDa TNF receptor and involvement of a membrane-bound non-matrix metalloproteinase. J Immunol ***165,*** 2165-2172.

Dwir, O., Kansas, G. S., and Alon, R. (2001). Cytoplasmic anchorage of L-selectin controls leukocyte capture and rolling by increasing the mechanical stability of the selectin tether. J Cell Biol ***155,*** 145-156.

Faveeuw, C., Di Mauro, M. E., Price, A. A., and Ager, A. (2000). Roles of α_4 integrins/VCAM-1 and LFA-1/ICAM-1 in the binding and transendothelial migration of T lymphocytes and T lymphoblasts across high endothelial venules. Int Immunol ***12***, 241-251.

Faveeuw, C., Preece, G., and Ager, A. (2001). Transendothelial migration of lymphocytes across high endothelial venules into lymph nodes is affected by metalloproteinases. Blood ***98***, 688-695.

Fehling, H. J., and von Boehmer, H. (1997). Early T cell development in the thymus of normal and genetically altered mice. Curr Opin Immunol ***9***, 263-275.

Finger, E. B., Puri, K. D., Alon, R., Lawrence, M. B., von Andrian, U. H., and Springer, T. A. (1996). Adhesion through L-selectin requires a threshold hydrodynamic shear. Nature ***379***, 266-269.

Fitzgerald, M. L., Wang, Z., Park, P. W., Murphy, G., and Bernfield, M. (2000). Shedding of syndecan-1 and -4 ectodomains is regulated by multiple signalling pathways and mediated by a TIMP-3-sensitive metalloproteinase. J Cell Biol ***148***, 811-824.

Forster, R., Schubel, A., Breitfield, D., Kremmer, E., Renner-Muller, I., Wolf, E., and Lipp, L. M. (1999). CCR7 coordinates the primary immune response by establishing functional microenvironments in secondary lymphoid organs. Cell ***99,*** 23-33.

Foxman, E. F., Campbell, J. J., and Butcher, E. C. (1997). Multistep navigation and the combinatorial control of leukocyte chemotaxis. J Cell Biol **139**, 1349-1360.

Frenette, P. S., Mayadas, T. N., Rayburn, H., Hynes, R. O., and Wagner, D. D. (1996). Susceptibility to infection and altered hematopoiesis in mice deficient in both P- and E-selectins. Cell ***84***, 563-574.

Fulop, G. M., and Phillips, R. A. (1986). Full reconstitution of the immune deficiency in SCID mice with normal stem cells requires low-dose irradiation of the recipient. J Immunol ***136***, 4438-4443

Gallatin, W. M., Weissman, I. L., and Butcher, E. C. (1983). A cell-surface molecule involved in organ-specific homing of lymphocytes. Nature ***304***, 30-34.

Gearing, A. J. H., and Newman, W. (1993). Circulating adhesion molecules in disease. Immunol Today ***14***, 506-512.

Giblin, P. A., Hwang, S. T., Katsumoto, T. R., and Rosen, S. D. (1997). Ligation of L-selectin on T lymphocytes activates β_1 integrins and promotes adhesion to fibronectin. J Immunol ***159***, 3498-3507.

Girard, J.-P., and Springer, T. A. (1995). High endothelial venules (HEVs): Specialized endothelium for lymphocyte migration. Immunology Today ***16***, 449-457.

Gowans, J. L., and Knight, E. J. (1964). The route of re-circulation of lymphocytes in the rat. Proc Roy Soc ***159***, 257-282.

Gu, B., Bendall, L. J., and Wiley, J. S. (1998). Adenosine triphospate-induced shedding of CD23 and L-selectin (CD62L) from lymphocytes is mediated by the same receptor but different metalloproteases. Blood ***92***, 946-951.

Gunn, M. D., Kyuwa, S., Tam, C., Kakiuchi, T., Matsuzawa, A., Williams, L. T., and Nakano, H. (1999). Mice lacking expression of secondary lymphoid organ chemokine have defects in lymphocyte homing and dendritic cell localization. J Exp Med ***189***, 451-460.

Gutman, G. A., and Weissman, I. L. (1972). Lymphoid tissue architecture. Experimental analysis of the origin and distribution of T and B cells. Immunology ***23***, 465-479.

Hafezi-Moghadam, A., and Ley, K. (1999). Relevance of L-selectin shedding for leukocyte rolling in vivo. J Exp Med ***189***, 939-948.

Hafezi-Moghadam, A., Thomas, K. L., Prorock, A. J., Huo, Y., and Ley, K. (2001). L-selectin shedding regulates leukocyte recruitment. J Exp Med ***193***, 863-872.

Haig, D. M., Hopkins , J., and Miller, H. R. P. (1999). Local immune resposes in afferent and efferent lymph. Immunology ***96***, 155-163.

Harris, H. (1991). The stimulation of lymphocyte motility by cultered high endothelial cells and its inhibition by pertussis toxin. Int Immunol ***3***, 535-542.

Harris, H., and Miyasaka, M. (1995). Reversible stimulation of lymphocyte motility by cultured high endothelial cells: Mediation by L-selectin. Immunology ***85***, 47-54.

Hattori, S., Nishimura, H., Tsurui, H., Kato, M., Endo, N., Abe, M., Akakura, S., Mitsui, K., Ishikawa, S., Hirose, S., and Shirai, T. (1998). L-selectin specific autoantibodies in murine lupus: possible involvement in abnormal homing and polarization of CD4+ T cell subsets. J Immunol ***161***, 1231-1238.

Hemmerich, S., Butcher, E. C., and Rosen, S. D. (1994). Sulphation-dependent recognition of high endothelial venules (HEV)- ligands by L-selectin and MECA 79, and adhesion-blocking monoclonal antibody. J Exp Med ***180***, 2219-2226.

Hemmerich, S., Leffler, H., and Rosen, S. D. (1995). Structure of the O-glycans in GlyCAM-1, an endothelial-derived ligand for L-selectin. J Biol Chem **270,** 12035-12047.

Hoke, D., Mebius, R. E., Dybdal, N., Dowbenko, D., Gribling, P., Kyle, C., Baumhueter, S., and Watson, S. R. (1995). Selective modulation of the expression of L-selectin ligands by an immune response. Curr Biol ***5***, 670-678.

Hooper, N. M. (1994). Families of zinc metalloproteases. FEBS Lett ***354***, 1-6.

Hooper, N. M., Karran, E. H., and Turner, A. J. (1997). Membrane protein secretases. Biochem J ***321***, 265-79.

Horig, H., Papadopoulos, N. J., Vegh, Z., Palmieri, E., Angeleeti, H. H., and Nathen, S. G. (1997). An in vitro study of the dynamic features of the major histocompatibility complex class I complex relevant to its role as a versatile peptide-receptor molecule. Proc Natl Acad Sci USA ***94***, 13826-31.

Howard, L., Zheng, Y., Horrocks, M., Maciewicz, R. A., and Blobel, C. (2001). Catalytic activity of ADAM28. FEBS Lett ***498***, 82-86.

Huang, T. F., Holt, J. C., Kirby, E. P., and Niewiarowski, S. (1989). Trigramin: primary structure and its inhibition of von Willebrand factor binding to glycoprotein IIb/IIIa complex on human platelets. Biochemistry ***28***, 661-666.

Hwang, S.T., Singer, M.S., Giblin, P.A., Yednock, T.A., Bacon, K.B., Simon, S.I., and Rosen, S.D. (1996). GlyCAM-1, a physiologic ligand for L-selectin, activates beta 2 integrins on naive peripheral lymphocytes. J Exp Med ***184,*** 1343-1348.

Iba, K., Albrechtsen,. R., Gilpin, B. J., Loechel, F., and Wewer, U. M. (1999) Cysteine-rich domain of human ADAM 12 (meltrin alpha) supports tumor cell adhesion. Am J Pathol ***154,*** 1489-1501

Iba, K., Albrechtsen, R., Gilpin, B., Frohlich, C., Loechel, F., Zolkiewska, A., Ishiguro, K., Kojima, T., Liu, W., Langford, J. K., Sanderson, R. D., Brakebusch, C., Fassler, R., Wewer, U. M. (2000) The cysteine-rich domain of human ADAM 12 supports cell adhesion through syndecans and triggers signaling events that lead to beta 1 integrin-dependent cell spreading. J Cell Biol ***149,*** 1143-1156

Imai, Y., Lasky, L. A., and Rosen, S. D. (1992). Further characterization of the interaction between L-selectin and its endothelial ligands. Glycobiol ***2,*** 373-381.

Imai, Y., Lasky, L. A., and Rosen, S. D. (1993). Sulphation requirement for GlyCAM-1, an endothelial ligand for L- selectin. Nature ***361,*** 555-557.

Imai, Y., Singer, M. S., Fennie, C., Lasky, L. A., and Rosen, S. D. (1991). Identification of a carbohydrate-based endothelial ligand for a lymphocyte homing receptor. J Cell Biol ***113,*** 1213-1221.

Imai, Y., True, D. D., Singer, M. S., and Rosen, S. D. (1990). Direct demonstration of the lectin activity of gp90MEL, a lymphocyte homing receptor. J Cell Biol ***111,*** 1225-1232.

Ito, A., Mukaiyama, A., Itoh, Y., Nagase, H., Thogersen, I. B., Enghild, J. J., Sasaguri, Y., and Mori, Y. (1996). Degradation of interleukin 1beta by matrix metalloproteinases. J Biol Chem ***271,*** 14657-14660.

Izumi, Y., Hirata, M., Hasuwa, H., Iwamoto, R., Umata, T., Miyado, K., Kurisaki, T., Sehara-Fujisawa, A., Ohno, S., and Mekada, E. (1998). A metalloprotease-disintegrin, MCD9/meltrin-gamma/ADAM9 and PKCdelta are involved in TPA-induced ectodomain shedding of membrane-anchored heparin-binding EGF-like growth factor. EMBO *17,* 7260-7272.

Johnson, R. C., Mayadas, T. N., Frenette, P. S., Mebius, R. E., Subramanium, M., Lacasce, A., Hynes, R. O., and Wagner, D. D. (1995). Blood cell dynamics in P-selectin deficient mice. Blood *86*, 1106-1114.

Kadono, T., Venturi, G. M. Steeber, D. A., and Tedder, T.F. (2002). Leukocyte rolling velocities and migration are optimized by cooperative L-selectin and intercellular adhesion molecule-1 functions. J Immunol *169,* 4542-4550.

Kahn, J., Ingraham, R. H., Shirley, F., Migaki, G. I., and Kishimoto, T. K. (1994). Membrane proximal cleavage of L-selectin: Identifiction of the cleavage site and a 6-KD transmembrane peptide fragment of L-selectin. J Cell Biol *125*, 461-470.

Kahn, J., Walcheck, B., Migaki, G. I., and Jutila, M. A. (1998). Calmodulin regulates L-selectin adhesion molecule expression and function through a protease-dependent mechanism. Cell *92*, 809-818.

Kansas, G. S. (1996). Selectins and their ligands: Current concepts and controversies. Blood *88*, 3259-3287.

Kansas, G. S., Ley, K., Munro, M., and Tedder, T. F. (1993). Regulation of leukocyte rolling and adhesion to high endothelial venules through the cytoplasmic domain of L-selectin. J Exp Med *177*, 833-838.

Kaushal, g. P., and Shah, S. V. (2000). The new kids on the block: ADAMTSs potentially multifunctional metalloproteinases of the ADAM family. J Clin Invest *105*, 1335-1337.

Kim, Y. S., Gum, J., and Brockhausen, I. (1996). Mucin glycoproteins in neoplasia. Glycoconj J *13*, 693-707.

Kishimoto, T. K., Jutila, M. A., Berg, E. L., and Butcher, E. C. (1989). Neutrophil Mac-1 and MEL-14 adhesion proteins inversely regulated by chemotactic factors. Science *245*, 1238-1241.

Knight, S. C., and Stagg, A. J. (1993). Antigen-presenting cell types. Curr Opin Immunol *5*, 374-382.

Kraal, G., Weissman, I. L., and Butcher, E. C. (1983). Differences in in vivo distribution and homing of T cell subsets to mucosal *vs* nonmucosal lymphoid organs. J Immunol *130*, 1097-1102.

Kurtz, M. E., Graff, R. J., Adelman, A., Martin-Morgan, D., and Click, R. E. (1985). CTL and serologically defined antigens of B2m, H-3 region. J Immunol *135*, 2847-2852.

Labow, M. A., Norton, C. R., Rumberger, J. M., Lombard-Gilloly, K. M., Shuster, D. J., Hubbard, J., Bertko, R., Knaack, P. A., Terry, R. W., Harbison, M. L., Kontgen, F., Stewart, C. L., McIntyre, K. W., Will, P. C., Burns, D. K., and Wolitzky, B. A. (1994). Characterization of E-selectin -deficient mice: Demonstration of overlapping function of the endothelial selectins. Immunity *1*, 709-720.

Leco, K. J., Khokha, R., Parloff, N., Hawkes, S. P., and Edwards, D. R. (1994). Tissue inhibitor of metalloprotienases-3 (TIMP-3) is an extracellular matrix associated protein with a distinctive pattern of expression in mouse cells and tissues. J. Biol Chem **269,** 9352-9360.

Ledbetter, J. A., Goding, J. W., Tsu, T. T., and Herzenberg, L. A. (1979). A new mouse lymphoid alloantigen (Lpg100) recognized by a monoclonal rat antibody. Immunogenetics *8*, 347-360.

Ledbetter, J. A., and Herzenberg, L. A. (1979). Xenogenic monoclonal antibodies to mouse lymphoid differentiation antigens. Immunol Rev ***47***, 63-90.

Leeuwenberg, J. F., Smeets, E. F., Neefjes, J. J., Shaffer, M. A., Cinek, T., Jeunhomme, T. M., Ahern, T. J., and Buurman, W. A. (1992). E-selectin and intercellular adhesion molecule-1 are released by activated human endothelial cells in vitro. Immunology *77*, 543-549.

Lepault, F., Gagnerault, M. C., Faveeuw, C., and Boitard, C. (1994). Recirculation, phenotype and functions of lymphocytes in mice treated with monoclonal antibody MEL-14. Eur J Immunol ***24***, 3106-3112.

Ley, K., Gaehtgens, P., Fennie, C., Singer, M. S., Lasky, L. A., and Rosen, S. D. (1991). Lectin-like cell adhesion molecule-1 mediates leukocyte rolling in mesenteric venules in vivo. Blood ***12***, 2553-2555.

Ley, K., Tedder, T. F., and Kansas, G. S. (1993). L-selectin can mediate leukocyte rolling in untreated mesenteric venules in vivo independent of E- or P- selectin. Blood ***82***, 1632-1638.

Li, L., Yang, Y., Wang, Z., and Gong, F. (2002a). Study of the effects of LPS on the TACE gene expression and function. J Huanhong Univ Sci Technolog Med Sci ***22,*** 5-8.

Li, Q., Park, P. W., Wilson, C. L., and Parks, W. C. (2002b) Matrilysin shedding of syndecan-1 regulates chemokine mobilization and transepithelial efflux of neutrophils in acute lung injury. Cell ***111,*** 635-646.

Liu, Y.-J., de Bouteiller, O., and Fugier-Vivier, I. (1997). Mechanisms of selection and differentiation in germinal centers. Curr Opin Immunol ***9***, 256-262.

Lunn, C. A., Fan, X., Dalie, B., Millar, K., Zavodny, P. J., Narula, S. K., and Lundell, D. (1997). Purification of ADAM 10 from bovine spleen as a TNFα convertase. FEBS Lett ***400***, 333-335.

MacLennan, I. C. M. (1994). Germinal Centers. Ann Rev Immunol ***12***, 117-139.

Madri, J. A., Graesser, D., and Haas, T. (1996). The roles of adhesion molecules and proteinases in lymphocyte transendothelial migration. Biochem Cell Biol ***74***, 749-757.

Martìn-Padura, I., Lostaglio, S., Schneemann, M., Williams, L., Romano, M., Fruscella, P., Panzeri, C., Stoppacciaro, A., Ruco, L., Villa, A., Simmons, D., and Dejana, E. (1998). Junctional adhesion molecule, a novel member of the immunoglobulin superfamily that distributes at intercellular junctions and modulates monocyte transmigration. J Cell Biol ***142***, 117-127.

Maskos, K., Fernandez-Catalan, C., Huber, R., Bourenkov, G. P., Bartunik, H., Ellestad, G. A., Reddy, P., Wolfson, M. F., Rauch, C. T., Castner, B. J., Davis, R., Clarke, H. R., Petersen, M., Fitzner, J. N., Cerretti, D. P., March, C. J., Paxton, R. J., Black, R. A., and Bode, W. (1998). Crystal structure of the catalytic domain of human tumor necrosis factor-alpha-converting enzyme. Proc Natl Acad Sci U S A ***95***, 3408-3412.

May, M. J., and Ager, A. (1992). ICAM-1-independent lymphocyte transmigration across high endothelium : diffferential up-regulation by interferon γ, tumour necrosis factor-α and interleukin 1β. Eur J Immunol ***22***, 219-226.

Mayadas, T. N., Johnson, R. C., Rayburn, H., Hynes, R. O., and Wagner, D. D. (1993). Leukocyte rolling and extravasation are severely compromised in P-selectin deficient mice. Cell ***74***, 541-554.

McEver, R. P. (1994). Selectins. Curr Opin Immunol ***6***, 75-84.

Medzhitov, R., and Janeway Jr, C. A. (1998). Innate immune recognition and control of adaptive immune responses. Semin Immunol ***10***, 351-353.

Miller, B. A., Antognetti, G., and Springer, T. A. (1985). Identification of cell surface antigens present on murine haematopoietic stem cells. J Immunol ***134***, 3286-3290.

Moore, K. L., Patel, K. D., Breuhl, R. E., Fugang, L., Johnson, D. L., Lichenstein, H. S., Cummings, R. D., Bainton, D. F., and McEver, R. P. (1995). P-selectin glycoprotein ligand-1 mediates rolling of human neutrophils on P-selectin. J Cell Biol ***128***, 661.

Moss, M. L., Jin, S. L., Milla, M. E., Bickett, D. M., Burkhart, W., Carter, H. L., Chen, W. J., Clay, W. C., Didsbury, J. R., Hassler, D., Hoffman, C. R., Kost, T. A., Lambert, M. H., Leesnitzer, M. A., McCauley, P., McGeehan, G., Mitchell, J., Moyer, M., Pahel, G., Rocque, W., Overton, L. K., Schoenen, F., Seaton, T., Su, J. L., Becherer, J. D., and et al. (1997). Cloning of a disintegrin metalloproteinase that processes precursor tumour-necrosis factor-alpha. Nature ***385***, 733-736.

Müllberg, J., Rauch, C. T., Wolfson, M. F., Castner, B., Fitzner, J. N., Otten-Evans, C., Mohler, K. M., Cosman, D., and Black, R. A. (1997). Futher evidence for a common mechanism for shedding of cell surface proteins. FEBS Lett ***401***, 235-238.

Muller, W. A., Weigl, S. A., Deng, X., and Phillips, D. M. (1993). PECAM-1 is required for transendothelial migration of leukocytes. J Exp Med ***178***, 449-460.

Murai, M., Yoneyama, H., Ezaki, T., Suematsu, M., Terashima, Y., Harada, H., Hamada, H., Asakura, H., Ishikawa, H., and Matsushima,

K. (2003). Peyer's patch is the essential site in initiating murine acute and lethal graft-versus-host reaction. Nat Immunol ***4,*** 154-160.

Nath, D., Slocombe, P. M., Stephens, P. E., Warn, A., Hucthinson, G. R., Yanada, K. M., Docherty, A. J., and Murphy, G. (1999). Interaction of metargidin (ADAM-15) with $\alpha v\beta_3$ and $\alpha_5\beta_1$ integrins on different haemopoietic cells. J Cell Sci ***112,*** 579-587.

Nath, D., Slocombe, P. M., Webster, A., Stephens, P. E., Docherty, A. J., and Murphy, G. (2000). Meltrin λ/ADAM-9 mediates cellular adhesion through α/6/β/1 integrin, leading to a marked induction of fibroblast cell motility. J Cell Sci ***133,*** 2319-2328.

Nelson, K. K., Schlöndorff, J., and Blobel, C. P. (1999). Evidence of an interaction of the metalloprotease-disintegrin tumour necrosis factor α convertase (TACE) with mitotic arrest deficient 2 (MAD2), and of the metalloprotease-disintegrin MDC9 with a novel MAD2-related protein, MAD2β. Biochem J ***343***, 673-680.

Okada, T., Ngo, V. N., Ekland, E. H., Forster, R., Lipp, M., Littman, D. R., Cyster, J. G. (2002). Chemokine requirements for B cell entry to lymph nodes and Peyer's patches. J Exp Med ***196,*** 65-75.

Paavonen, T., and Renkonen, R. (1992). Selective expression of sialyl-Lewis X and Lewis Am epitopes, putative ligands for L-selectin, on peripheral lymph-node high endothelial venules. Am J Pathol ***141***, 1259-1264.

Pan, D., and Rubin, G. M. (1997). Kuzbanian controls proteolytic processing of notch and mediates lateral inhibition during Drosophila and vertebrate neurogenesis. Cell ***90***, 271-280.

Panès, J., Perry, M., and Granger, D. N. (1999). Leukcoyte-endothelial cell adhesion: Avenues for theraputic intervention. British J Pharm ***126***, 537-550.

Park, A. J., Matrisian, L. M., Kells, A. F., Pearson, R., Yuan, Z., and Navre, M. (1991). Mutational analysis of the transin (rat stromelysin) autoinhibitor region demonstrates a role for residues surrounding the "cysteine switch". J Biol Chem ***266***, 1584-1590.

Patel, I. R., Attur, M. G., Patel, R. N., Stuchin, S. A., Abagyan, R. A., Abramson, S. B., and Amin, A. R. (1998). TNF-α convertase enzyme from human arthritis-affected cartilage: isolation of cDNA by differential display, expression of the active enzyme, and regulation of TNF-α. J Immunol ***160***, 4570-4579.

Peiretti, F., Depez-Beauclair, P., Bonardo, B., Abert, H., Juhan-Vague, I., and Nalbone, G. (2003). Identification of SAP97 as an intracellular binding partner of TACE. J Cell Sci ***116***, 1949-1957.

Peschon, J. J., Slack, J. L., Reddy, P., Stocking, K. L., Sunnarborg, S. W., Lee, D. C., Russell, W. E., Castner, B. J., Johnson, R. S., Fitzner, J. N., Boyce, R. W., Nelson, N., Kozlosky, C. J., Wolfson, M. F., Rauch, C. T., Cerretti, D. P., Paxton, R. J., March, C. J., and Black, R. A. (1998). An essential role for ectodomain shedding in mammalian development. Science ***282***, 1281-1284.

Preece, G., Murphy, G., and Ager, A. (1996). Metalloproteinase-mediated regulation of L-selectin levels on leucocytes. J Biol Chem ***271***, 11634-11640.

Puri, K. D., Chen, S., and Springer, T. A. (1998). Modifying the mechanical property and shear threshold of L-selectin adhesion independently of equilibrium properties. Nature ***392***, 930-933.

Puri, K. D., Finger, E. B., Gaudernack, G., and Springer, T. A. (1995). Sialomucin CD34 is the major L-selectin ligand in human tonsil high endothelial venules. J Cell Biol ***131***, 261-270

Rajagopalan, S., Ping Meng, X., Ramasamy, S., Harrison, D. G., and Galis, Z. S. (1996). Reactive oxygen species produced by macrophage-derived foam cells regulate the activity of vascular matrix metalloproteinases in vitro. J Clin Invest ***98***, 2572-2579.

Reddy, P., Slack, J. L., Davis, R., Cerretti, D. P., Kozlosky, C. J., Blanton, R. A., Shows, D., Peschon, J. J., and Black, R. A. (2000). Functional analysis of the domain structure of tumour necrosis factor-α converting enzyme. J Biol Chem ***275***, 14608-14614.

Roghani, M., Becherer, J. D., Moss, M. L., Atherton, R. E., Erdjument-Bromage, H., Arribas, J., Blackburn, R. K., Weskamp, G., Tempst, P., and Blobel, C. P. (1999). Metalloprotease disintegrin MDC9: Intercellular maturation and catalytic activity. J Biol Chem ***274***, 3531-3540.

Rosen, S. D. (1999). Endothelial ligands for L-selectin: From lymphocyte recirculation to allograft rejection. Am J Pathol ***155***, 1013-1020.

Rosen, S. D., and Bertozzi, C. R. (1994). The selectins and their ligands. Curr Opin Cell Biol ***6***, 663-673.

Rosendahl, M. S., Ko, S. C., Long, D. L., Brewer, M. T., Rosenzweig, B., Hedl, E., Anderson, L., Pyle, S. M., Moreland, J., Meyers, M. A., Kohno, T., Lyons, D., and Lichenstein, H. S. (1997). Identification and characterization of a pro-tumor necrosis factor-α-processing enzyme from the ADAM family of zinc metalloproteases. J Biol Chem ***39***, 24588-24593.

Rovida, E., Paccagnini, A., Del Rosso, M., Peschon, J., and Sbarba, P. D. (2001). TNF-α–converting enzyme cleaves the macrophage colony-stimulating factor receptor in macrophages undergoing activation. J Biol Chem ***166***, 1583-1589.

Sadhukhan, R., Santhamma, K. R., Reddy, P., Peschon, J. J., Black, R. A., and Sen, I. (1999). Unaltered cleavage and secretion of angiotensin-converting enzyme in tumour necrosis factor-α-converting enzyme deficient mice. J Biol Chem ***274***, 10511-10516.

Sallusto, F., Lenig, D., Forster, R., Lipp, M., and Lanzavecchia, A. (1999). Two subsets of memory T lymphocytes with distinct homing potentials and effector functions. Nature ***401***, 708-712.

Sánchez-Madrid, F., and del Pozo, M. A. (1999). Leucocyte polarisation in cell migration and immune interactions. EMBO ***18***, 501-511.

Sassetti, C., Tangemann, K., Singer, M. S., Kershaw, D. B., and Rosen, S. D. (1998). Identification of podocalyxin-like protein as a high endothelial venule ligand for L-selectin: parallels to CD34. J Exp Med ***187***, 1965-1975.

Sawada, M., Takada, A., Ohwaki, I., Takahashi, N., Tateno, H., Sakamoto, J., and Kannagi, R. (1993). Specific expression of a sialyl Lewis X antigen on high endothelial venules of human lymph nodes: possible candidate for L-selectin ligand. Biochem Biophys Res Commun ***193***, 337-347.

Schenk, B. I., Petersen, F., Flad, H. D., and Brandt, E. (2002). Platelet-derived chemokines CXC chemokine ligand (CXCL), connective tissue-activating peptide III, and CXCL4 differently effect and cross-regulate neutrophil adhesion and transendothelial migration. J Immunol ***169,*** 2602-2610.

Schleiffenbaum, B., Spertini, O., and Tedder, T. F. (1992). Soluble L-selectin is present in human plasma at high levels and retains functional activity. J Cell Biol ***119***, 229-238.

Schlöndorff, J., Becherer, J. D., and Blobel, C. P. (2000). Intracellular maturation and localization of the tumour necrosis factor α convertase (TACE). Biochem J ***347***, 131-138.

Schmidt, W., Festenstein, H., Ward, P. J., and Sanderson, A. R. (1981). Interspecies exchange of beta 2- microglobulin and associated MHC and differentiation antigens. Immunogenetics ***13,*** 483-491.

Seals, D. F., and Courtneidge, S. A. (2003) The ADAMs family of metalloproteases: Multidomain proteins with multiple functions. Genes Dev ***17,*** 7-30.

Serrador, J. M., Nieto, M., Alonso-Lebrero, J. L., del Pozo, M. A., Calvo, J., Furthmayr, H., Schwartz-Albiez, R., Lozano, F., González-Amaro, R., Sánchez-Mateos, P., and Sánchez-Madrid, F. (1998). CD43 interacts with moesin and ezrin and regulates its redistribution to the uropods of T lymphocytes at the cell-cell contacts. Blood ***91***, 4632-4644.

Shaw, T., Nixon, J. S., and Bottomley, K. M. (2000). Metalloproteinase inhibitors: new opportunities for the treatment of rheumatoid arthritis and osteoarthritis. Exp Opin Invest Drugs ***9***, 1469-1478.

Shields, M. J., Moffat, L. E., and Ribaudo, R. K. (1998). Functional comparison of bovine, murine, and human beta 2-microglobulin: Interactions with murine MHC I molecules. Mol Immunol ***35,*** 919-928.

Siegelman, M. H., Cheng, I. C., Weissman, I. L., and Wakeland, E. K. (1990). The mouse lymph node homing receptor is identical with the lymphocyte cell surface marker Ly-22: Role of the EGF domain in endothelial binding. Cell ***61***, 611-622.

Soede, R. D. M., Zeelenberg, I. S., Wijnands, Y. M., Kamp, M., and Roos, E. (2001). Stromal cell-derived factor-1-induced LFA-1 activation in vivo migration of T cell hybridoma cells requires $G_{q/11}$, RhoA, and Myosin, as well as G_i and Cdc42. J Immunol ***166***, 4293-4301.

Springer, T. A. (1994). Traffic signals for lymphocyte recirculation and leukocyte emigration: the multistep paradigm. Cell ***76***, 301-314.

Springman, E. B., Angleton, E. L., Birken-Hansen, H., and Van Wart, H. E. (1990). Multiple modes of activation of latent fibroblast collagenase: Evidence for the role of Cys73 active-site zinc complex in latency and a "cysteine switch" mechanism for activation. Proc Natl Acad Sci U S A ***87***, 364-368.

Stamper, H. B., Jr., and Woodruff, J. J. (1976). Lymphocyte homing into lymph nodes: In vitro demonstration of the selective affinity of recirculating lymphocytes for high-endothelial venules. J Exp Med ***144***, 828-833.

Steeber, D. A., Engel, P., Miller, A. S., Sheetz, M. P., and Tedder, T. F. (1997). Ligation of L-selectin through conserved regions within the lectin domain activates signal transduction pathways and integrin function in human, mouse and rat leukocytes. J Immunol ***159***, 952-963.

Stein, J. V., Cheng, G., Stockton, B. M., Fors, B. P., Butcher, E. C., and von Andrian, U. H. (1999). L-selectin-mediated leukocyte adhesion in vivo: microvillous distribution determines tethering efficiency, but not rolling velocity. J Exp Med ***189***, 37-49.

Steinman, R. M. (1991). The dendritic cell system and its role in immunogenicity. Annu Rev Immunol ***9***, 271-296.

Stoddart, J. H. Jr., Jasuja, R. R., Sikorski, M, A., von Andrian, U. H., Mier, J. W. (1996). Protease-resistant L-selectin mutants. Down-modulation by cross-linking but not cellular activation. J Immunol ***157,*** 5653-5659.

Stoolman, L. M., and Rosen, S. D. (1983). Possible role for cell-surface carbohydrate-binding molecules in lymphocyte recirculation. J Cell Biol ***96***, 722-729.

Tada, N., Kimura, S., Hatzfeld, A., and Hammerling, U. (1980). Ly-m11: the H-3 region of mouse chromosome 2 controls a new surface alloantigen. Immunogenetics ***11***, 441-449.

Tamatani, T., Kuida, K., Watanabe, T., Koike, S., and Miyasaka, M. (1993). Molecular mechanisms underlying lymphocyte recirculation. III. Characterization of the LECAM-1 (L-selectin)-dependent adhesion pathway in rats. J Immunol ***150***, 1735-1745.

Tang, M. L., Hale, L. P., Steeber, D. A., and Tedder, T. F. (1997). L-selectin is involved in lymphocyte migration to sites of inflammation in the skin: delayed rejection of allografts in L-selectin-deficient mice. J Immunol ***158***, 5191-5199.

Tang, M. L., Steeber, D. A., Zhang, X. Q., and Tedder, T. F. (1998). Intrinsic differences in L-selectin expression levels affect T and B lymphocyte subset-specific recirculation pathways. J Immunol ***160***, 5113-5121.

Tedder, T. F., Steeber, D. A., Chen, A., and Engel, P. (1995). The selectins: vascular adhesion molecules. FASEB J ***9***, 866-873.

Toppila, S., Paavonen, T., Nieminen, M. S., Hayry, P., and Renkonen, R. (1999). Endothelial L-selectin ligands are likely to recruit lymphocytes into rejecting human heart transplants. Am J Pathol ***155***, 1303-1310.

Trachtman, H., Futterweit, S., Garg, P., Reddy, K., and Singhal, P. C. (1996). Nitric oxide stimulates the activity of a 72-kDa neutral matrix metalloproteinase in cultered rat mesangial cells. Biochem Biophys Res Commun ***218***, 704-708.

Tu, L., Poe, J. C., Kadono, T., Venturi, G. M., Bullard, D. C., Tedder, T. F., and Steeber, D. A. (2000). A functional role for circulating mouse L-selectin in regulating leukocyte/endothelial interactions in vivo. J Immunol ***169***, 2034-2043.

Varki, A. (1997). Selectin ligands: will the real ones please stand up? J Clin Invest ***100***, S31-35.

Von Andrian, U. H., Hansell, P., Chambers, J. D., Berger, E. M., Torres Filho, I., Butcher, E. C., and Arfors, K. E. (1992). L-selectin function is required for beta 2-integrin-mediated neutrophil adhesion at physiological shear rates in vivo. Am J Physiol ***263***, H1034-1044.

von Andrian, U. H., and M'Rini, C. (1998). In situ analysis of lymphocyte migration to lymph nodes. Cell Adhes Commun ***6***, 85-96.

von Asmuth, E. J., Smeets, E. F., Ginsel, L. A., Onderwater, J. J., Leeuwenberg, J. F., and Buurman, W. A. (1992). Evidence for endocytosis of E-selectin in human endothelial cells. Eur J Immunol ***22***, 2519-2526.

von Boehmer, H. (1994). Positive selection of lymphocytes. Cell ***76***, 219-228.

von Boehmer, H. (1988). The developmental biology of T lymphocytes. Ann Rev Immunol *6*, 309-326.

Wagner, N., Löhler, J., Kunkel, E. J., Leung, E., Krissansen, G., Rajewsky, K., and Müller, W. (1996). Critical Role for β7 integrins in formation of gut-associated lymphoid tissue. Nature *382*, 366-370.

Walcheck, B., Kahn, J., Fisher, J. M., Wang, B. B., Fisk, R. S., Payan, D. G., Feehan, C., Betageri, R., Darlak, K., Spatola, A. F., and Kishimoto, T. K. (1996). Neutrophil rolling altered by inhibition of L-selectin shedding in vitro. Nature *380*, 720-723.

Wang, J., Al-Lamki, R. S., Zhang, H., Kirkiles-Smith, N., Gaeta, M. L., Thirt-Pober, J. S., and Bradley, J. R. (2003). Histamine antagonizes TNF signalling by stimulating from the cell surface and Golgi storage pool. J Biol Chem *278*, 21751-21760.

Warnock, R. A., Askari, S., Butcher, E. C., and von Andrian, U. H. (1998). Molecular mechanisms of lymphocyte homing to peripheral lymph nodes. J Exp Med *187*, 205-216.

Warnock, R. A., Campbell, J. J., Dorf, M. E., Matsuzawa, A., McEvoy, L. M., and Butcher, E. C. (2000). The role of chemokines in the microenvironmental control of T versus B cell arrest in Peyer's patch high endothelial venules. J Exp Med *191*, 77-88.

Weskamp, G., and Blobel, C. P. (1994). A family of cellular proteins related to snake venom disintegrins. Proc Natl Acad Sci U S A *91*, 2748-2751.

Westermann, J., Nagahori, Y., Walter, S., Heerwagen, C., Miyasaka, M., and Pabst, R. (1994). B and T lymphocyte subsets enter peripheral lymph nodes and Peyer's patches without preference in vivo: No correlation occurs between their localization in different types of high endothelial venules and the expression of CD44, VLA-4, LFA-1, ICAM-1, CD2 or L-selectin. Eur J Immunol ***24***, 2312-2316.

Westermann, J., Ronneberg, S., Fritz, F. J., and Pabst, R. (1989). Proliferation of lymphocyte subsets in the adult rat: A comparison of different lymphoid organs. Eur J Immunol ***19***, 1087-1093.

Westermann, J., Walter, S., Nagahori, Y., Heerwagen, C., Miyasaka, M., and Pabst, R. (1996). Blood leucocyte subsets of the rat: Expression of adhesion molecules and localisation within high endothelial venules. Scand J Immunol ***43***, 297-303.

Wolfsberg, T. G., and White, J. M. (1996). ADAMs in fertilisation and development. Dev Biol ***180***, 389-401.

Wroblewski, M., and Hamann, A. (1997). CD45-mediated signals can trigger shedding of lymphocyte L-selectin. Int Immunol ***9***, 555-562.

Xu, J., Grewal, I. S., Geba, G. P., and Flavell, R. A. (1996). Impaired primary T cell responses in L-selectin-deficient mice. J Exp Med ***183***, 589-598.

Yarden, Y., and Sliwkowski, M. X. (2003) Untangling the ErbB signalling network. Nat Rev Mol Cell Biol ***2,*** 127-137

Yuan, R., Primakoff, P., and Myles, D. G. (1997). A role for the disintegrin domain of cyritestin, a sperm surface protein belonging to the ADAM family, in mouse sperm-egg plasma membrane adhesion and fusion. J Cell Biol ***137***, 105-112.

Zhang, Y., Jiang, J., Black, R. A., Baumann, G., and Frank, S. J. (2000a). Tumour necrosis factor-α converting enzyme (TACE) is a growth hormone binding protein (GHBP) sheddase: The metalloprotease TACE/ADAM-17 is critical for (PMA-induced) GH receptor proteolysis and GHBP generation. Endocrinol ***141***, 4342-4348.

Zhang, Z., Kolls, J. K., Oliver, P., Good, D., Schwarzenberger, P. O., Joshi, M. S., Ponthier, J. L., and Lancaster, J. R. (2000). Activation of tumour necrosis factor-α-converting enzyme-mediated ectodomain shedding by nitric oxide. J Biol Chem ***275***, 15839-15844.

Zhang, Z., Oliver, P., Lancaster, J. R., Schwarzenberger, P. O., Joshi, M. S., Cork, J., and Kolls, J. K. (2001). Reactive oxygen species mediate tumor necrosis factor alpha-converting, enzyme-dependent ectodomain shedding induced by phorbol myristate acetate. FASEB ***15,*** 303-305.

Zhao, L. C., Edgar, J. B., and Dailey, M. O. (2001). Characterisation of the rapid proteolytic shedding of murine selectin. Dev Immunol ***8,*** 267-277.

Zhao, L., Shey, M., Farnsworth, M., and Dailey, M. O. (2001). Regulation of membrane metalloproteolytic cleavage of L-selectin (CD62l) by the epidermal growth factor domain. J Biol Chem ***276***, 30631-30640.

Zimmerman, G. A., Prescott, S. M., and McIntyre, T. M. (1992). Endothelial cell interactions with granulocytes: tethering and signalling molecules. Immunol Today ***13***, 93-99.

Zocchi, M. R., Ferrero, E., Leone, B. E., Rovere, P., Bianchi, E., Toninelli, E., and Pardi, R. (1996). CD31/PECAM-1 driven chemokine-independent transmigration of human T-lymphocytes. Eur J Immunol ***26***, 759-767.